Title: Particle-Phase Accretion Forms Dimer Esters in Pinene Secondary Organic Aerosol

Authors: Christopher M. Kenseth[1]*†, Nicholas J. Hafeman[1], Samir P. Rezgui[1], Jing Chen[2], Yuanlong Huang[3], Nathan F. Dalleska[3], Henrik G. Kjaergaard[2], Brian M. Stoltz[1], John H. Seinfeld[1,4], and Paul O. Wennberg[3,4]

Affiliations:

[1]Division of Chemistry and Chemical Engineering, California Institute of Technology, Pasadena, CA 91125, USA.

[2]Department of Chemistry, University of Copenhagen, DK-2100 Copenhagen, Denmark.

[3]Division of Geological and Planetary Sciences, California Institute of Technology, Pasadena, CA 91125, USA.

[4]Division of Engineering and Applied Science, California Institute of Technology, Pasadena, CA 91125, USA.

*Corresponding author. Email: ckenseth@caltech.edu

[†]Present address: Department of Atmospheric Sciences, University of Washington, Seattle, WA 98195, USA.

Abstract: Secondary organic aerosol (SOA) is ubiquitous in the atmosphere and plays a pivotal role in climate, air quality, and health. The production of low-volatility dimeric compounds via accretion reactions is a key aspect of SOA formation. However, despite extensive study, the structures and thus formation mechanisms of dimers in SOA remain largely uncharacterized. Here, we elucidate the structures of several major dimer esters in SOA from ozonolysis of α-pinene and β-pinene, substantial global SOA sources, through independent synthesis of authentic standards. We show that these dimer esters are formed in the particle phase and propose a mechanism of nucleophilic addition of alcohols to a cyclic acylperoxyhemiacetal. This chemistry likely represents a general pathway to dimeric compounds in ambient SOA.

One-Sentence Summary: Reaction of alcohols with acylperoxyhemiacetals forms low-volatility organic compounds in atmospheric aerosols.

Main Text:

Secondary organic aerosol (SOA) contributes substantially (15–80% by mass) to the global burden of atmospheric fine particulate matter ($PM_{2.5}$) (*1*), which exerts large but uncertain effects on climate (*2*) as well as adverse impacts on air quality and human health (*3*, *4*). The oxidation of monoterpenes ($C_{10}H_{16}$), emitted in appreciable quantities from forested regions (~150 Tg y^{-1}) (*5*), represents a dominant source of SOA (*6*–*8*). For over two decades, high-molecular-weight dimeric compounds, notably those proposed to contain ester linkages, have been identified using advanced mass spectrometric techniques as significant components of both laboratory-derived and ambient monoterpene SOA, and have been implicated as key players in particle formation and growth, volatility, viscosity, and cloud condensation nuclei (CCN) activity (*9*–*39*). Particle-phase reactions of closed-shell monomers (e.g., esterification and peroxyhemiacetal/diacyl peroxide decomposition) and gas-phase reactions involving early-stage oxidation products and/or reactive intermediates [e.g., stabilized Criegee intermediates (SCIs), carboxylic acids, and organic peroxy radicals (RO_2)] have been advanced as possible dimer ester formation pathways (Fig. S1). Due to a lack of authentic standards (*40*), however, the structures of the dimer esters are not known but only inferred from accurate mass/fragmentation data. As a result, mechanistic understanding of dimer ester formation, in particular the relevance of gas- vs. particle-phase chemistry, remains unconstrained (Fig. 1).

In this work, informed by detailed structural analyses, we synthesize the first authentic standards of several major dimer esters identified in SOA from ozonolysis of α-pinene and β-pinene, which together account for over 50% of total monoterpene emissions (*5*). Based on targeted experiments in the Caltech dual 24 m^3 Teflon Environmental Chambers (CTEC) using ultra-performance liquid chromatography/negative electrospray ionization quadrupole time-of-flight mass spectrometry [UPLC/(−)ESI-Q-TOF-MS] for analysis of SOA molecular composition (*41*), we demonstrate that these dimer esters are formed through particle-phase chemistry and propose a unifying mechanism that accounts for the observed regioselectivity, dynamics, and environmental dependencies (e.g., oxidant type and RO_2 fate) of ester formation. Identification of the chemistry underlying dimer ester production provides a missing link tying the atmospheric degradation of monoterpenes to the formation of low-volatility accretion products capable of driving aerosol formation and growth.

Dimer Esters in Pinene SOA

Guided by our previous work on dimers formed from synergistic O_3 + OH oxidation (*33*), the structure of one of the major dimers identified in SOA from β-pinene ozonolysis (Fig. 2A, dimer ester **I**) was proposed to consist of an ester of *cis*-pinic acid, the most abundant carboxylic acid measured in pinene SOA (*34*) and a commonly reported dimer subunit (*15*, *17*, *27*, *30*, *33*), and β-pinanediol (βPdiol) (Fig. S2). CTEC experiments featuring synthesized *cis*-pinic acid and synthesized βPdiol (Fig. S3) did not, however, result in detectable production of dimer ester **I**, suggesting, in line with past studies (*27*, *30*, *33*), that dimer formation does not occur via conventional esterification (i.e., carboxylic acid + alcohol) in either the gas or particle phase. To constrain the potential involvement of βPdiol in forming dimer ester **I**, β-pinene ozonolysis experiments were carried out in the absence of cyclohexane (CHX) as a scavenger for OH, which is formed as a byproduct of ozonolysis, presence of CHX, and presence of both CHX and βPdiol (Fig. 2A). As dimer ester **I** is one of several dimers shown to form from accretion of O_3- and OH-derived products/intermediates (*33*), its production was significantly inhibited by CHX. Unlike the other synergistic O_3 + OH dimers, however, dimer ester **I** was observed to form on addition of βPdiol, demonstrating that it is produced from reaction of βPdiol and a derivative of *cis*-pinic acid.

Based on the formation of dimer ester **I** in β-pinene photooxidation experiments performed in the presence of commercial *cis*-pinic acid, we previously suggested that dimer ester **I** is produced via reaction of an OH-derived product, tentatively identified as either βPdiol or a derivative, and *cis*-pinic acid (*33*). However, the above findings, together with unsuccessful attempts to replicate the β-pinene photooxidation experiments using synthesized *cis*-pinic acid, exclude *cis*-pinic acid as the dimer ester source. We hypothesize that dimer ester **I** was formed in the earlier photooxidation experiments due to the presence of an impurity in the commercial *cis*-pinic acid, likely the *cis*-pinic acid derivative or an oxidizable precursor. These insights were made possible only through the synthesis of high-purity *cis*-pinic acid and βPdiol standards.

β-Pinene ozonolysis experiments conducted in the presence of CHX and alcohols of varying structure and volatility (Fig. S4) clarify that the *cis*-pinic acid derivative forms dimer esters only with alcohols of sufficiently low volatility to undergo gas-particle partitioning (*42*) and, therefore, that the accretion reaction occurs in the particle phase. Motivated by MS/MS analysis suggesting that the major dimer only present in SOA from β-pinene ozonolysis with CHX (Fig. 2A, dimer ester **II**) is an ester of *cis*-pinic acid and 6-hydroxyhexanoic acid, an OH oxidation product of CHX, 6-hydroxyhexanoic acid was added to a β-pinene ozonolysis experiment performed without CHX (Fig. S5) and led to appreciable formation of dimer ester **II.** Together with production of dimer ester **I** from βPdiol, this result illustrates the generality of the particle-phase reaction between the *cis*-pinic acid derivative and semi/low-volatility alcohols.

The currently accepted mechanism for production of *cis*-pinic acid from ozonolysis of both α-pinene and β-pinene proceeds through a common acyl peroxy radical (Fig. S6). This commonality suggests that dimer esters proposed to contain *cis*-pinic acid subunits in each SOA system may be formed from the same *cis*-pinic acid derivative. α-Pinene ozonolysis experiments without CHX, with CHX, and with both CHX and either βPdiol or α-pinanediol (αPdiol) (Fig. 2B) confirm that the *cis*-pinic acid derivative is produced from both α-pinene and β-pinene ozonolysis, as evidenced by the formation of dimer ester **I,** the analogous ester of *cis*-pinic acid and αPdiol (Fig. 2B, dimer ester **III)**, and dimer ester **II**. These experiments also underscore the role of alcohol volatility in dimer ester production, as the less volatile βPdiol yielded a higher abundance of dimer ester **I** than αPdiol did dimer ester **III**, although the impact of structural differences between the diols cannot be discounted.

The two most abundant dimers identified in SOA from α-pinene ozonolysis (Fig. 2, dashed boxes) (*34*) have been the subject of extensive study (*9*, *12*, *13*, *15–18*, *21*, *25–30*, *37*, *38*, *43*, *44*) and are both proposed to consist of esters with *cis*-pinic acid subunits. Together with dimer ester **II**, their abundances were impacted by the formation of dimer esters **I** and **III** in α-pinene and β-pinene ozonolysis experiments with CHX and either βPdiol or αPdiol (Fig. 2A and B). This behavior implies that the two dimers are also formed from the *cis*-pinic acid derivative, the particle-phase abundance of which limits ester production. Consistent with expectations, β-pinene ozonolysis with CHX carried out in the presence of synthesized *cis*-10-hydroxypinonic acid (OH-pinonic) (Fig. 2C), an abundant constituent of SOA from α-pinene ozonolysis (*34*) not produced by ozonolysis of β-pinene, was observed to yield the corresponding major dimer (Fig. 2C, dimer ester **IV**). Conversely, detected amounts of dimer ester **IV** were negligible in CTEC experiments featuring *cis*-pinic acid and OH-pinonic acid (Fig. S7). These results establish that the well-

characterized dimer ester **IV** is not formed through conventional esterification but via particle-phase accretion of OH-pinonic acid and the *cis*-pinic acid derivative.

Structures of Dimer Esters

The CTEC experiments conclusively demonstrate that dimer esters **I–IV** are formed through particle-phase reaction of a *cis*-pinic acid derivative and the corresponding semivolatile alcohol. As *cis*-pinic acid is an asymmetric dicarboxylic acid, however, structures containing either a primary or secondary ester are possible for each dimer ester (Fig. 3) and cannot be definitively resolved by MS/MS analysis. To address this ambiguity, primary and secondary esters of *cis*-pinic acid and the identified alcohol subunits of dimer esters **I–IV** were prepared using modular synthetic strategies in 10–13% yield [8 steps, longest linear sequence (LLS)] and 5–17% yield (6–8 steps, LLS), respectively (Fig. S8). Comparison of the LC retention times and MS/MS fragmentation patterns of dimer esters **I–IV** to those of the synthesized primary and secondary esters (Fig. 3) reveals that dimer ester production from the *cis*-pinic acid derivative is regioselective and forms the more sterically hindered secondary ester in each case. To our knowledge, this represents the first synthesis of authentic standards of dimer esters identified in SOA from ozonolysis of α-pinene and β-pinene, including the extensively studied dimer ester **IV**.

Formation Mechanism of Dimer Esters

To assess the reactivity of the *cis*-pinic acid derivative, α-pinene ozonolysis experiments with CHX were conducted in which βPdiol was added either prior to or 10 h following the onset of ozonolysis (Fig. S9). As before (Fig. 2B), significant formation of dimer ester **I** was observed in the former experiment, whereas only trace amounts of dimer ester **I** were detected in the latter. The small but nonnegligible yield of dimer ester **I** with delayed βPdiol addition indicates that the *cis*-pinic acid derivative is a short-lived, most likely closed-shell species, which had largely reacted away over the 10-h interval but was still present in trace quantities to react with βPdiol.

As a means of elucidating a central feature of the dimerization reaction, namely which monomeric species contributes the O atom in the ester linkage, β-pinene ozonolysis with CHX was carried out in the presence of synthesized ^{18}OH-pinonic acid, labeled at the hydroxy group (Fig. S10). Formation of ^{18}O-labeled dimer ester **IV** at the same retention time as its ^{16}O isotopologue establishes that the ester O atom in dimer ester **IV**, and by extension dimer esters **I–III,** originates from the alcohol and suggests that the particle-phase accretion reaction proceeds via nucleophilic addition of the semi/low-volatility alcohol to the reactive *cis*-pinic acid derivative.

Additional mechanistic evidence is provided by ozonolysis experiments with CHX and βPdiol featuring one of two synthesized unsaturated carbonyl isomers ($C_{11}H_{18}O$), an enone or enal, that respectively produce only one of the two CIs on ozonolysis that form concurrently from ozonolysis of α-pinene (Fig. S11). As anticipated, dimer esters **I**, **II**, and **IV**, as well as the major $C_{17}H_{26}O_8$ dimer, were observed to form only from ozonolysis of the enal, given that only the CI arising from the enal is understood to yield the acyl peroxy radical common to α-pinene and β-pinene ozonolysis (Fig. S6) from which the *cis*-pinic acid derivative is hypothesized to stem. In light of the inferred short lifetime of the *cis*-pinic acid derivative, of the same order as those measured for organic peroxides in SOA from α-pinene ozonolysis (*45*), *cis*-peroxypinic acid was investigated as a likely candidate. CTEC experiments with synthesized *cis*-peroxypinic acid and either βPdiol or OH-pinonic acid proved inconclusive due to the instability of the peracid standard. However, detection of *cis*-peroxypinic acid in SOA from ozonolysis of the enone but not enal, confirmed via

comparison with the authentic standard (Fig. S11), implies that *cis*-peroxypinic acid is not involved in dimer ester formation.

The key insight into the chemistry underlying dimer ester production comes from α-pinene ozonolysis experiments in which the ratio of RO_2 to HO_2 concentrations ($[RO_2]$:$[HO_2]$) was modulated through the use of either CHX or methanol (MeOH) as an OH scavenger (Fig. 4A) (*46–48*). In the presence of MeOH, under reduced $[RO_2]$:$[HO_2]$ relative to CHX, higher abundances of dimer ester **IV**, together with three additional dimers also proposed to consist of esters with *cis*-pinic acid subunits based on MS/MS analysis, were observed. As elevated HO_2 concentrations shift the fate of the common acyl peroxy radical and increase the fraction that forms *cis*-3-peroxypinalic acid (Fig. S6), the corresponding enhancement in dimer ester abundance indicates that *cis*-3-peroxypinalic acid is either the *cis*-pinic acid derivative or a direct precursor.

We propose that dimer esters **I–IV** and, by extension, dimer esters in α-pinene and β-pinene SOA that contain *cis*-pinic acid subunits are formed via particle-phase nucleophilic addition of the requisite semi/low-volatility alcohol to the cyclic acylperoxyhemiacetal derived from particle-phase tautomerization of *cis*-3-peroxypinalic acid, with subsequent decomposition of the addition product yielding the primary carboxylic acid and water (Fig. 4B). This mechanism accounts for the observed regioselectivity, dynamics, isotopic labeling, alcohol volatility, and $[RO_2]$:$[HO_2]$ dependence of ester production. Acylperoxyhemiacetal formation is known to occur readily in solution (*49*), and it has recently been shown that *cis*-3-peroxypinalic acid is a significant gas-phase product of α-pinene ozonolysis (*50*). Moreover, quantum chemical calculations evaluating the reactivity of a series of carboxylic acid derivatives [$CH_3C(=O)–X$] toward esterification with MeOH (Fig. S12) reveal that the acylperoxyhemiacetal reaction is the most energetically favorable (i.e., lowest reaction barrier). Given the ubiquity of peracid, aldehyde, and alcohol functionalities in SOA from both biogenic and anthropogenic sources, it is expected that ester formation via condensed-phase reaction of alcohols with acylperoxyhemiacetals followed by Baeyer-Villiger decomposition of the resulting peroxyhemiacetals (Fig. 4C) represents a general route to the production of low-volatility dimeric compounds in ambient SOA.

Atmospheric Implications

The formation of dimer esters **I–IV**, shown through synthesis of authentic standards to be secondary esters of *cis*-pinic acid, via particle-phase accretion of alcohols with an acylperoxyhemiacetal resolves a longstanding puzzle in atmospheric aerosol chemistry and rationalizes a number of experimental and ambient observations from past studies (Supplementary, S2). This chemistry incorporates otherwise semivolatile oxidation products into the particle phase as low-volatility dimeric compounds, providing an important source of irreversibly condensed mass for SOA growth. As alcohols, aldehydes, and, in turn, peracids, are formed from oxidation of almost all biogenic and anthropogenic SOA precursors (*49*), this chemistry is likely a general feature of SOA formation. Notably, the production of dimer esters of *cis*-pinic acid and *meso*-erythritol in α-pinene and β-pinene ozonolysis experiments with CHX featuring *meso*-erythritol as a surrogate for semivolatile isoprene tetrols (Fig. S13) establishes this chemistry as a synergistic pathway between major oxidation products of pinene and isoprene, the most abundant nonmethane hydrocarbons emitted to the atmosphere (*5*). Longer aerosol residence times in the real atmosphere as compared to CTEC experiments are expected to increase the importance of this particle-phase reactivity in ambient SOA. Further investigation is needed to determine the dependence of this chemistry on aerosol physicochemical properties (e.g., pH, chemical composition, and phase state)

and environmental conditions (e.g., temperature and relative humidity). Quantitative understanding of these complex interactions is essential to assessing the effects of dimer ester formation on the abundance, composition, properties, and associated impacts of SOA.

References and Notes

1. J. L. Jimenez, M. R. Canagaratna, N. M. Donahue, A. S. H. Prevot, Q. Zhang, J. H. Kroll, P. F. DeCarlo, J. D. Allan, H. Coe, N. L. Ng, A. C. Aiken, K. S. Docherty, I. M. Ulbrich, A. P. Grieshop, A. L. Robinson, J. Duplissy, J. D. Smith, K. R. Wilson, V. A. Lanz, C. Hueglin, Y. L. Sun, J. Tian, A. Laaksonen, T. Raatikainen, J. Rautiainen, P. Vaattovaara, M. Ehn, M. Kulmala, J. M. Tomlinson, D. R. Collins, M. J. Cubison, E., J. Dunlea, J. A. Huffman, T. B. Onasch, M. R. Alfarra, P. I. Williams, K. Bower, Y. Kondo, J. Schneider, F. Drewnick, S. Borrmann, S. Weimer, K. Demerjian, D. Salcedo, L. Cottrell, R. Griffin, A. Takami, T. Miyoshi, S. Hatakeyama, A. Shimono, J. Y. Sun, Y. M. Zhang, K. Dzepina, J. R. Kimmel, D. Sueper, J. T. Jayne, S. C. Herndon, A. M. Trimborn, L. R. Williams, E. C. Wood, A. M. Middlebrook, C. E. Kolb, U. Baltensperger, D. R. Worsnop, Evolution of Organic Aerosols in the Atmosphere. *Science*. **326**, 1525–1529 (2009).

2. Intergovernmental Panel on Climate Change, *Climate Change 2013: The Physical Science Basis* (Cambridge University Press, Cambridge, United Kingdom, 2013).

3. A. J. Cohen, M. Brauer, R. Burnett, H. R. Anderson, J. Frostad, K. Estep, K. Balakrishnan, B. Brunekreef, L. Dandona, R. Dandona, V. Feigin, G. Freedman, B. Hubbell, A. Jobling, H. Kan, L. Knibbs, Y. Liu, R. Martin, L. Morawska, C. A. Pope, H. Shin, K. Straif, G. Shaddick, M. Thomas, R. van Dingenen, A. van Donkelaar, T. Vos, C. J. L. Murray, M. H. Forouzanfar, Estimates and 25-year trends of the global burden of disease attributable to ambient air pollution: an analysis of data from the Global Burden of Diseases Study 2015. *Lancet*. **389**, 1907–1918 (2017).

4. R. Burnett, H. Chen, M. Szyszkowicz, N. Fann, B. Hubbell, C. A. Pope, J. S. Apte, M. Brauer, A. Cohen, S. Weichenthal, J. Coggins, Q. Di, B. Brunekreef, J. Frostad, S. S. Lim, H. Kan, K. D. Walker, G. D. Thurston, R. B. Hayes, C. C. Lim, M. C. Turner, M. Jerrett, D. Krewski, S. M. Gapstur, W. R. Diver, B. Ostro, D. Goldberg, D. L. Crouse, R. V. Martin, P. Peters, L. Pinault, M. Tjepkema, A. van Donkelaar, P. J. Villeneuve, A. B. Miller, P. Yin, M. Zhou, L. Wang, N. A. H. Janssen, M. Marra, R. W. Atkinson, H. Tsang, T. Quoc Thach, J. B. Cannon, R. T. Allen, J. E. Hart, F. Laden, G. Cesaroni, F. Forastiere, G. Weinmayr, A. Jaensch, G. Nagel, H. Concin, J. V. Spadaro, Global estimates of mortality associated with long-term exposure to outdoor fine particulate matter. *Proc. Natl. Acad. Sci. U.S.A.* **115**, 9592–9597 (2018).

5. A. B. Guenther, X. Jiang, C. L. Heald, T. Sakulyanontvittaya, T. Duhl, L. K. Emmons, X. Wang, The Model of Emissions of Gases and Aerosols from Nature version 2.1 (MEGAN2.1): an extended and updated framework for modeling biogenic emissions. *Geosci. Model Dev.* **5**, 1471–1492 (2012).

6. M. Hallquist, J. C. Wenger, U. Baltensperger, Y. Rudich, D. Simpson, M. Claeys, J. Dommen, N. M. Donahue, C. George, A. H. Goldstein, J. F. Hamilton, H. Herrmann, T. Hoffmann, Y. Iinuma, M. Jang, M. E. Jenkin, J. L. Jimenez, A. Kiendler-Scharr, W. Maenhaut, G. McFiggans, Th. F. Mentel, A. Monod, A. S. H. Prévôt, J. H. Seinfeld, J. D.

Surratt, R. Szmigielski, J. Wildt, The formation, properties and impact of secondary organic aerosol: current and emerging issues. *Atmos. Chem. Phys.* **9**, 5155–5236 (2009).

7. C. L. Heald, D. K. Henze, L. W. Horowitz, J. Feddema, J.-F. Lamarque, A. Guenther, P. G. Hess, F. Vitt, J. H. Seinfeld, A. H. Goldstein, I. Fung, Predicted change in global secondary organic aerosol concentrations in response to future climate, emissions, and land use change. *J. Geophys. Res.* **113**, D05211 (2008).

8. H. Zhang, L. D. Yee, B. H. Lee, M. P. Curtis, D. R. Worton, G. Isaacman-VanWertz, J. H. Offenberg, M. Lewandowski, T. E. Kleindienst, M. R. Beaver, A. L. Holder, W. A. Lonneman, K. S. Docherty, M. Jaoui, H. O. T. Pye, W. Hu, D. A. Day, P. Campuzano-Jost, J. L. Jimenez, H. Guo, R. J. Weber, J. de Gouw, A. R. Koss, E. S. Edgerton, W. Brune, C. Mohr, F. D. Lopez-Hilfiker, A. Lutz, N. M. Kreisberg, S. R. Spielman, S. V. Hering, K. R. Wilson, J. A. Thornton, A. H. Goldstein, Monoterpenes are the largest source of summertime organic aerosol in the southeastern United States. *Proc. Natl. Acad. Sci. U.S.A.* **115**, 2038–2043 (2018).

9. T. Hoffmann, R. Bandur, U. Marggraf, M. Linscheid, Molecular composition of organic aerosols formed in the α-pinene/O_3 reaction: Implications for new particle formation processes. *J. Geophys. Res.* **103**, 25569–25578 (1998).

10. M. P. Tolocka, M. Jang, J. M. Ginter, F. J. Cox, R. M. Kamens, M. V. Johnston, Formation of Oligomers in Secondary Organic Aerosol. *Environ. Sci. Technol.* **38**, 1428–1434 (2004).

11. A. Reinhardt, C. Emmenegger, B. Gerrits, C. Panse, J. Dommen, U. Baltensperger, R. Zenobi, M. Kalberer, Ultrahigh Mass Resolution and Accurate Mass Measurements as a Tool To Characterize Oligomers in Secondary Organic Aerosols. *Anal. Chem.* **79**, 4074–4082 (2007).

12. L. Müller, M.-C. Reinnig, J. Warnke, Th. Hoffmann, Unambiguous identification of esters as oligomers in secondary organic aerosol formed from cyclohexene and cyclohexene/α-pinene ozonolysis. *Atmos. Chem. Phys.* **8**, 1423–1433 (2008).

13. L. Müller, M.-C. Reinnig, H. Hayen, T. Hoffmann, Characterization of oligomeric compounds in secondary organic aerosol using liquid chromatography coupled to electrospray ionization Fourier transform ion cyclotron resonance mass spectrometry. *Rapid Commun. Mass Spectrom.* **23**, 971–979 (2009).

14. M. Camredon, J. F. Hamilton, M. S. Alam, K. P. Wyche, T. Carr, I. R. White, P. S. Monks, A. R. Rickard, W. J. Bloss, Distribution of gaseous and particulate organic composition during dark α-pinene ozonolysis. *Atmos. Chem. Phys.* **10**, 2893–2917 (2010).

15. F. Yasmeen, R. Vermeylen, R. Szmigielski, Y. Iinuma, O. Böge, H. Herrmann, W. Maenhaut, M. Claeys, Terpenylic acid and related compounds: precursors for dimers in secondary organic aerosol from the ozonolysis of α- and β-pinene. *Atmos. Chem. Phys.* **10**, 9383–9392 (2010).

16. F. Yasmeen, R. Szmigielski, R. Vermeylen, Y. Gómez-González, J. D. Surratt, A. W. H. Chan, J. H. Seinfeld, W. Maenhaut, M. Claeys, Mass spectrometric characterization of

isomeric terpenoic acids from the oxidation of α-pinene, β-pinene, *d*-limonene, and Δ^3-carene in fine forest aerosol. *J. Mass Spectrom.* **46**, 425–442 (2011).

17. F. Yasmeen, R. Vermeylen, N. Maurin, E. Perraudin, J.-F. Doussin, M. Claeys, Characterisation of tracers for aging of α-pinene secondary organic aerosol using liquid chromatography/negative ion electrospray ionisation mass spectrometry. *Environ. Chem.* **9**, 236–246 (2012).

18. Y. Gao, W. A. Hall, M. V. Johnston, Molecular Composition of Monoterpene Secondary Organic Aerosol at Low Mass Loading. *Environ. Sci. Technol.* **44**, 7897–7902 (2010).

19. W. A. Hall, M. V. Johnston, Oligomer Content of α-Pinene Secondary Organic Aerosol. *Aerosol Sci. Technol.* **45**, 37–45 (2011).

20. A. L. Putman, J. H. Offenberg, R. Fisseha, S. Kundu, T. A. Rahn, L. R. Mazzoleni, Ultrahigh-resolution FT-ICR mass spectrometry characterization of α-pinene ozonolysis SOA. *Atmos. Environ.* **46**, 164–172 (2012).

21. B. Witkowski, T. Gierczak, Early stage composition of SOA produced by α-pinene/ozone reaction: α-Acyloxyhydroperoxy aldehydes and acidic dimers. *Atmos. Environ.* **95**, 59–70 (2014).

22. I. Kourtchev, S. J. Fuller, C. Giorio, R. M. Healy, E. Wilson, I. O'Connor, I., J. C. Wenger, M. McLeod, J. Aalto, T. M. Ruuskanen, W. Maenhaut, R. Jones, D. S. Venables, J. R. Sodeau, M. Kulmala, M. Kalberer, Molecular composition of biogenic secondary organic aerosols using ultrahigh-resolution mass spectrometry: comparing laboratory and field studies. *Atmos. Chem. Phys.* **14**, 2155–2167 (2014).

23. I. Kourtchev, J.-F. Doussin, C. Giorio, B. Mahon, E. M. Wilson, N. Maurin, E. Pangui, D. S. Venables, J. C. Wenger, M. Kalberer, Molecular composition of fresh and aged secondary organic aerosol from a mixture of biogenic volatile compounds: a high-resolution mass spectrometry study. *Atmos. Chem. Phys.* **15**, 5683–5695 (2015).

24. I. Kourtchev, C. Giorio, A. Manninen, E. Wilson, B. Mahon, J. Aalto, M. Kajos, D. Venables, T. Ruuskanen, J. Levula, M. Loponen, S. Connors, N. Harris, D. Zhao, A. Kiendler-Scharr, T. Mentel, Y. Rudich, M. Hallquist, J.-F. Doussin, W. Maenhaut, J. Bäck, T. Petäjä, J. Wenger, M. Kulmala, M. Kalberer, Enhanced Volatile Organic Compounds emissions and organic aerosol mass increase the oligomer content of atmospheric aerosols. *Sci. Rep.* **6**, 35038 (2016).

25. K. Kristensen, K. L. Enggrob, S. M. King, D. R. Worton, S. M. Platt, R. Mortensen, T. Rosenoern, J. D. Surratt, M. Bilde, A. H. Goldstein, M. Glasius, Formation and occurrence of dimer esters of pinene oxidation products in atmospheric aerosols. *Atmos. Chem. Phys.* **13**, 3763–3776 (2013).

26. K. Kristensen, T. Cui, H. Zhang, A. Gold, M. Glasius, J. D. Surratt, Dimers in α-pinene secondary organic aerosol: effect of hydroxyl radical, ozone, relative humidity and aerosol acidity. *Atmos. Chem. Phys.* **14**, 4201–4218 (2014).

27. K. Kristensen, Å. K. Watne, J. Hammes, A. Lutz, T. Petäjä, M. Hallquist, M. Bilde, M. Glasius, High-Molecular Weight Dimer Esters Are Major Products in Aerosols from α-Pinene Ozonolysis and the Boreal Forest. *Environ. Sci. Technol. Lett.* **3**, 280–285 (2016).

28. K. Kristensen, L. N. Jensen, M. Glasius, M. Bilde, The effect of sub-zero temperature on the formation and composition of secondary organic aerosol from ozonolysis of alpha-pinene. *Environ. Sci.: Processes Impacts*. **19**, 1220–1234 (2017).

29. K. Kristensen, L. N. Jensen, L. L. J. Quéléver, S. Christiansen, B. Rosati, J. Elm, R. Teiwes, H. B. Pedersen, M. Glasius, M. Ehn, M. Bilde, The Aarhus Chamber Campaign on Highly Oxygenated Organic Molecules and Aerosols (ACCHA): particle formation, organic acids, and dimer esters from <i>α</i>-pinene ozonolysis at different temperatures. *Atmos. Chem. Phys.* **20**, 12549–12567 (2020).

30. X. Zhang, R. C. McVay, D. D. Huang, N. F. Dalleska, B. Aumont, R. C. Flagan, J. H. Seinfeld, Formation and evolution of molecular products in α-pinene secondary organic aerosol. *Proc. Natl. Acad. Sci. U.S.A.* **112**, 14168–14173 (2015).

31. K. Sato, T. Jia, K. Tanabe, Y. Morino, Y. Kajii, T. Imamura, Terpenylic acid and nine-carbon multifunctional compounds formed during the aging of β-pinene ozonolysis secondary organic aerosol. *Atmos. Environ.* **130**, 127–135 (2016).

32. A. Mutzel, M. Rodigast, Y. Iinuma, O. Böge, H. Herrmann, Monoterpene SOA – Contribution of first-generation oxidation products to formation and chemical composition. *Atmos. Environ.* **130**, 136–144 (2016).

33. C. M. Kenseth, Y. Huang, R. Zhao, N. F. Dalleska, J. C. Hethcox, B. M. Stoltz, J. H. Seinfeld, Synergistic O_3 + OH oxidation pathway to extremely low-volatility dimers revealed in β-pinene secondary organic aerosol. *Proc. Natl. Acad. Sci. U.S.A.* **115**, 8301–8306 (2018).

34. C. M. Kenseth, N. J. Hafeman, Y. Huang, N. F. Dalleska, B. M. Stoltz, J. H. Seinfeld, Synthesis of Carboxylic Acid and Dimer Ester Surrogates to Constrain the Abundance and Distribution of Molecular Products in α-Pinene and β-Pinene Secondary Organic Aerosol. *Environ. Sci. Technol.* **54**, 12829–12839 (2020).

35. R. Zhao, C. M. Kenseth, Y. Huang, N. F. Dalleska, J. H. Seinfeld, Iodometry-Assisted Liquid Chromatography Electrospray Ionization Mass Spectrometry for Analysis of Organic Peroxides: An Application to Atmospheric Secondary Organic Aerosol. *Environ. Sci. Technol.* **52**, 2108–2117 (2018).

36. Y. Huang, C. M. Kenseth, N. F. Dalleska, J. H. Seinfeld, Coupling Filter-Based Thermal Desorption Chemical Ionization Mass Spectrometry with Liquid Chromatography/Electrospray Ionization Mass Spectrometry for Molecular Analysis of Secondary Organic Aerosol. *Environ. Sci. Technol.* **54**, 13238–13248 (2020).

37. A. Kahnt, R. Vermeylen, Y. Iinuma, M. Safi Shalamzari, W. Maenhaut, M. Claeys, High-molecular-weight esters in α-pinene ozonolysis secondary organic aerosol: structural

characterization and mechanistic proposal for their formation from highly oxygenated molecules. *Atmos. Chem. Phys.* **18**, 8453–8467 (2018).

38. Y. Zhao, M. Yao, Y. Wang, Z. Li, S. Wang, C. Li, H. Xiao, Acylperoxy Radicals as Key Intermediates in the Formation of Dimeric Compounds in α-Pinene Secondary Organic Aerosol. *Environ. Sci. Technol.* **56**, 14249–14261 (2022).

39. O. Peräkylä, T. Berndt, L. Franzon, G. Hasan, M. Meder, R. R. Valiev, C. D. Daub, J. G. Varelas, F. M. Geiger, R. J. Thomson, M. Rissanen, T. Kurtén, M. Ehn, Large Gas-Phase Source of Esters and Other Accretion Products in the Atmosphere. *J. Am. Chem. Soc.* **145**, 7780–7790 (2023).

40. M. A. Upshur, A. G. Bé, J. Luo, J. G. Varelas, F. M. Geiger, R. J. Thomson, Organic synthesis in the study of terpene-derived oxidation products in the atmosphere. *Nat. Prod. Rep.* **40**, 890–921 (2023).

41. Materials and methods are available as supplementary materials at the Science website.

42. J. F. Pankow, An absorption model of gas/particle partitioning of organic compounds in the atmosphere. *Atmos. Environ.* **28**, 185–188 (1994).

43. Y. Iinuma, S. Ramasamy, K. Sato, A. Kołodziejczyk, R. Szmigielski, Structural Characterisation of Dimeric Esters in α-Pinene Secondary Organic Aerosol Using N_2 and CO_2 Ion Mobility Mass Spectrometry. *Atmosphere*. **12**, 17 (2020).

44. M. Beck, T. Hoffmann, A detailed MSn study for the molecular identification of a dimer formed from oxidation of pinene. *Atmos. Environ.* **130**, 120–126 (2016).

45. M. Krapf, I. El Haddad, E. A. Bruns, U. Molteni, K. R. Daellenbach, A. S. H. Prévôt, U. Baltensperger, J. Dommen, Labile Peroxides in Secondary Organic Aerosol. *Chem*. **1**, 603–616 (2016).

46. K. S. Docherty, P. J. Ziemann, Effects of Stabilized Criegee Intermediate and OH Radical Scavengers on Aerosol Formation from Reactions of β-Pinene with O 3. *Aerosol Science and Technology*. **37**, 877–891 (2003).

47. M. D. Keywood, J. H. Kroll, V. Varutbangkul, R. Bahreini, R. C. Flagan, J. H. Seinfeld, Secondary Organic Aerosol Formation from Cyclohexene Ozonolysis: Effect of OH Scavenger and the Role of Radical Chemistry. *Environ. Sci. Technol.* **38**, 3343–3350 (2004).

48. D. M. Bell, V. Pospisilova, F. Lopez-Hilfiker, A. Bertrand, M. Xiao, X. Zhou, W. Huang, D. S. Wang, C. P. Lee, J. Dommen, U. Baltensperger, A. S. H. Prevot, I. El Haddad, J. G. Slowik, Effect of OH scavengers on the chemical composition of α-pinene secondary organic aerosol. *Environ. Sci.: Atmos.* **3**, 115–123 (2023).

49. P. J. Ziemann, R. Atkinson, Kinetics, products, and mechanisms of secondary organic aerosol formation. *Chem. Soc. Rev.* **41**, 6582 (2012).

50. W. Zhang, H. Zhang, Secondary Ion Chemistry Mediated by Ozone and Acidic Organic Molecules in Iodide-Adduct Chemical Ionization Mass Spectrometry. *Anal. Chem.* **93**, 8595–8602 (2021).

51. R. H. Schwantes, R. C. McVay, X. Zhang, M. M. Coggon, H. Lignell, R. C. Flagan, P. O. Wennberg, J. H. Seinfeld, "Science of the Environmental Chamber" in *Advances in Atmospheric Chemistry*, J. R. Barker, A. L. Steiner, T. J. Wallington, Eds. (World Scientific, Singapore, 2017; http://www.worldscientific.com/doi/abs/10.1142/9789813147355_0001), pp. 1–93.

52. S. M. Aschmann, J. Arey, R. Atkinson, OH radical formation from the gas-phase reactions of O_3 with a series of terpenes. *Atmos. Environ.* **36**, 4347–4355 (2002).

53. A. A. Presto, N. M. Donahue, Ozonolysis Fragment Quenching by Nitrate Formation: The Pressure Dependence of Prompt OH Radical Formation. *J. Phys. Chem. A*. **108**, 9096–9104 (2004).

54. Y. Ma, G. Marston, Multifunctional acid formation from the gas-phase ozonolysis of β-pinene. *Phys. Chem. Chem. Phys.* **10**, 6115 (2008).

55. T. L. Nguyen, J. Peeters, L. Vereecken, Theoretical study of the gas-phase ozonolysis of β-pinene ($C_{10}H_{16}$). *Phys. Chem. Chem. Phys.* **11**, 5643 (2009).

56. R. Atkinson, J. Arey, Atmospheric Degradation of Volatile Organic Compounds. *Chem. Rev.* **103**, 4605–4638 (2003).

57. E. Kwok, R. Atkinson, Estimation of hydroxyl radical reaction rate constants for gas-phase organic compounds using a structure-reactivity relationship: An update. *Atmospheric Environment*. **29**, 1685–1695 (1995).

58. J. D. Crounse, K. A. McKinney, A. J. Kwan, P. O. Wennberg, Measurement of Gas-Phase Hydroperoxides by Chemical Ionization Mass Spectrometry. *Anal. Chem.* **78**, 6726–6732 (2006).

59. J. M. St. Clair, D. C. McCabe, J. D. Crounse, U. Steiner, P. O. Wennberg, Chemical ionization tandem mass spectrometer for the *in situ* measurement of methyl hydrogen peroxide. *Review of Scientific Instruments*. **81**, 094102 (2010).

60. R. H. Schwantes, S. M. Charan, K. H. Bates, Y. Huang, T. B. Nguyen, H. Mai, W. Kong, R. C. Flagan, J. H. Seinfeld, Low-volatility compounds contribute significantly to isoprene secondary organic aerosol (SOA) under high-NO_x conditions. *Atmos. Chem. Phys.* **19**, 7255–7278 (2019).

61. R. Bahreini, M. D. Keywood, N. L. Ng, V. Varutbangkul, S. Gao, R. C. Flagan, J. H. Seinfeld, D. R. Worsnop, J. L. Jimenez, Measurements of Secondary Organic Aerosol from Oxidation of Cycloalkenes, Terpenes, and *m*-Xylene Using an Aerodyne Aerosol Mass Spectrometer. *Environ. Sci. Technol.* **39**, 5674–5688 (2005).

62. Q. G. J. Malloy, S. Nakao, L. Qi, R. Austin, C. Stothers, H. Hagino, D. R. Cocker, Real-Time Aerosol Density Determination Utilizing a Modified Scanning Mobility Particle Sizer—Aerosol Particle Mass Analyzer System. *Aerosol Sci. Technol.* **43**, 673–678 (2009).

63. J. E. Shilling, Q. Chen, S. M. King, T. Rosenoern, J. H. Kroll, D. R. Worsnop, P. F. DeCarlo, A. C. Aiken, D. Sueper, J. L. Jimenez, S. T. Martin, Loading-dependent elemental composition of α-pinene SOA particles. *Atmos. Chem. Phys.* **9**, 771–782 (2009).

64. H. Saathoff, K.-H. Naumann, O. Möhler, Å. M. Jonsson, M. Hallquist, A. Kiendler-Scharr, Th. F. Mentel, R. Tillmann, U. Schurath, Temperature dependence of yields of secondary organic aerosols from the ozonolysis of α-pinene and limonene. *Atmos. Chem. Phys.* **9**, 1551–1577 (2009).

65. P. Mikuška, Z. Večeřa, A. Bartošíková, W. Maenhaut, Annular diffusion denuder for simultaneous removal of gaseous organic compounds and air oxidants during sampling of carbonaceous aerosols. *Anal. Chim. Acta*. **714**, 68–75 (2012).

66. A. Mutzel, M. Rodigast, Y. Iinuma, O. Böge, H. Herrmann, An improved method for the quantification of SOA bound peroxides. *Atmos. Environ.* **67**, 365–369 (2013).

67. K. H. Møller, R. V. Otkjær, N. Hyttinen, T. Kurtén, H. G. Kjaergaard, Cost-Effective Implementation of Multiconformer Transition State Theory for Peroxy Radical Hydrogen Shift Reactions. *J. Phys. Chem. A*. **120**, 10072–10087 (2016).

68. T. A. Halgren, R. B. Nachbar, Merck molecular force field. IV. conformational energies and geometries for MMFF94. *J. Comput. Chem.* **17**, 587–615 (1996).

69. T. A. Halgren, Merck molecular force field. V. Extension of MMFF94 using experimental data, additional computational data, and empirical rules. *J. Comput. Chem.* **17**, 616–641 (1996).

70. Spartan'18 (2018), (available at https://www.wavefun.com/spartan).

71. M. J. Frisch, G. W. Trucks, H. B. Schlegel, G. E. Scuseria, M. A. Robb, J. R. Cheeseman, G. Scalmani, V. Barone, G. A. Petersson, H. Nakatsuji, X. Li, M. Caricato, A. V. Marenich, J. Bloino, B. G. Janesko, R. Gomperts, B. Mennucci, H. P. Hratchian, J. V. Ortiz, A. F. Izmaylov, J. L. Sonnenberg, Williams, F. Ding, F. Lipparini, F. Egidi, J. Goings, B. Peng, A. Petrone, T. Henderson, D. Ranasinghe, V. G. Zakrzewski, J. Gao, N. Rega, G. Zheng, W. Liang, M. Hada, M. Ehara, K. Toyota, R. Fukuda, J. Hasegawa, M. Ishida, T. Nakajima, Y. Honda, O. Kitao, H. Nakai, T. Vreven, K. Throssell, J. A. Montgomery Jr., J. E. Peralta, F. Ogliaro, M. J. Bearpark, J. J. Heyd, E. N. Brothers, K. N. Kudin, V. N. Staroverov, T. A. Keith, R. Kobayashi, J. Normand, K. Raghavachari, A. P. Rendell, J. C. Burant, S. S. Iyengar, J. Tomasi, M. Cossi, J. M. Millam, M. Klene, C. Adamo, R. Cammi, J. W. Ochterski, R. L. Martin, K. Morokuma, O. Farkas, J. B. Foresman, D. J. Fox, Gaussian 16 Rev. C.01 (2016).

72. A. J. Stone, Distributed multipole analysis, or how to describe a molecular charge distribution. *Chemical Physics Letters*. **83**, 233–239 (1981).

73. C. M. Breneman, K. B. Wiberg, Determining atom-centered monopoles from molecular electrostatic potentials. The need for high sampling density in formamide conformational analysis. *J. Comput. Chem.* **11**, 361–373 (1990).

74. T. Lu, F. Chen, Multiwfn: A multifunctional wavefunction analyzer. *J. Comput. Chem.* **33**, 580–592 (2012).

75. K. Fukui, The path of chemical reactions - the IRC approach. *Acc. Chem. Res.* **14**, 363–368 (1981).

76. S. M. Saunders, M. E. Jenkin, R. G. Derwent, M. J. Pilling, Protocol for the development of the Master Chemical Mechanism, MCM v3 (Part A): tropospheric degradation of non-aromatic volatile organic compounds. *Atmos. Chem. Phys.* **3**, 161–180 (2003).

77. L. Vereecken, J. Peeters, A theoretical study of the OH-initiated gas-phase oxidation mechanism of β-pinene ($C_{10}H_{16}$): first generation products. *Phys. Chem. Chem. Phys.* **14**, 3802 (2012).

78. J. Peeters, L. Vereecken, G. Fantechi, The detailed mechanism of the OH-initiated atmospheric oxidation of α-pinene: a theoretical study. *Phys. Chem. Chem. Phys.* **3**, 5489–5504 (2001).

79. M. S. Claflin, J. E. Krechmer, W. Hu, J. L. Jimenez, P. J. Ziemann, Functional Group Composition of Secondary Organic Aerosol Formed from Ozonolysis of α-Pinene Under High VOC and Autoxidation Conditions. *ACS Earth Space Chem.* **2**, 1196–1210 (2018).

80. L. Renbaum-Wolff, J. W. Grayson, A. P. Bateman, M. Kuwata, M. Sellier, B. J. Murray, J. E. Shilling, S. T. Martin, A. K. Bertram, Viscosity of *α*-pinene secondary organic material and implications for particle growth and reactivity. *Proc. Natl. Acad. Sci. U.S.A.* **110**, 8014–8019 (2013).

81. C. Kidd, V. Perraud, L. M. Wingen, B. J. Finlayson-Pitts, Integrating phase and composition of secondary organic aerosol from the ozonolysis of α-pinene. *Proc. Natl. Acad. Sci. U.S.A.* **111**, 7552–7557 (2014).

82. D. Thomsen, J. Elm, B. Rosati, J. T. Skønager, M. Bilde, M. Glasius, Large Discrepancy in the Formation of Secondary Organic Aerosols from Structurally Similar Monoterpenes. *ACS Earth Space Chem.* **5**, 632–644 (2021).

83. J. F. Hamilton, A. C. Lewis, J. C. Reynolds, L. J. Carpenter, A. Lubben, Investigating the composition of organic aerosol resulting from cyclohexene ozonolysis: low molecular weight and heterogeneous reaction products. *Atmos. Chem. Phys.* **6**, 4973–4984 (2006).

84. L. Xu, K. H. Møller, J. D. Crounse, R. V. Otkjær, H. G. Kjaergaard, P. O. Wennberg, Unimolecular Reactions of Peroxy Radicals Formed in the Oxidation of α-Pinene and β-Pinene by Hydroxyl Radicals. *J. Phys. Chem. A*. **123**, 1661–1674 (2019).

85. L. Müller, M.-C. Reinnig, K. H. Naumann, H. Saathoff, T. F. Mentel, N. M. Donahue, T. Hoffmann, Formation of 3-methyl-1,2,3-butanetricarboxylic acid via gas phase oxidation of

pinonic acid – a mass spectrometric study of SOA aging. *Atmos. Chem. Phys.* **12**, 1483–1496 (2012).

86. S. Compernolle, K. Ceulemans, J.-F. Müller, EVAPORATION: a new vapour pressure estimation methodfor organic molecules including non-additivity and intramolecular interactions. *Atmos. Chem. Phys.* **11**, 9431–9450 (2011).

87. J. H. Kroll, J. H. Seinfeld, Chemistry of secondary organic aerosol: Formation and evolution of low-volatility organics in the atmosphere. *Atmospheric Environment*. **42**, 3593–3624 (2008).

88. Y. Ma, T. R. Willcox, A. T. Russell, G. Marston, Pinic and pinonic acid formation in the reaction of ozone with α-pinene. *Chem. Commun.*, 1328–1330 (2007).

89. Y. Ma, A. T. Russell, G. Marston, Mechanisms for the formation of secondary organic aerosol components from the gas-phase ozonolysis of α-pinene. *Phys. Chem. Chem. Phys.* **10**, 4294 (2008).

90. M. E. Jenkin, D. E. Shallcross, J. N. Harvey, Development and application of a possible mechanism for the generation of cis-pinic acid from the ozonolysis of α- and β-pinene. *Atmos. Environ.* **34**, 2837–2850 (2000).

91. S. Koch, R. Winterhalter, E. Uherek, A. Kolloff, P. Neeb, G. K. Moortgat, Formation of new particles in the gas-phase ozonolysis of monoterpenes. *Atmospheric Environment*. **34**, 4031–4042 (2000).

92. A. D. Castañeda, Z. Li, T. Joo, K. Benham, B. T. Burcar, R. Krishnamurthy, C. L. Liotta, N. L. Ng, T. M. Orlando, Prebiotic Phosphorylation of Uridine using Diamidophosphate in Aerosols. *Sci Rep*. **9**, 13527 (2019).

93. A. Bellcross, A. G. Bé, F. M. Geiger, R. J. Thomson, Molecular Chirality and Cloud Activation Potentials of Dimeric α-Pinene Oxidation Products. *J. Am. Chem. Soc.* **143**, 16653–16662 (2021).

94. Z. Zhao, W. Zhang, T. Alexander, X. Zhang, D. B. C. Martin, H. Zhang, Isolating α-Pinene Ozonolysis Pathways Reveals New Insights into Peroxy Radical Chemistry and Secondary Organic Aerosol Formation. *Environ. Sci. Technol.* **55**, 6700–6709 (2021).

95. K. S. Docherty, W. Wu, Y. B. Lim, P. J. Ziemann, Contributions of Organic Peroxides to Secondary Aerosol Formed from Reactions of Monoterpenes with O_3. *Environ. Sci. Technol.* **39**, 4049–4059 (2005).

96. G. McFiggans, T. F. Mentel, J. Wildt, I. Pullinen, S. Kang, E. Kleist, S. Schmitt, M. Springer, R. Tillmann, C. Wu, D. Zhao, M. Hallquist, C. Faxon, M. Le Breton, Å. M. Hallquist, D. Simpson, R. Bergström, M. E. Jenkin, M. Ehn, J. A. Thornton, M. R. Alfarra, T. J. Bannan, C. J. Percival, M. Priestley, D. Topping, A. Kiendler-Scharr, Secondary organic aerosol reduced by mixture of atmospheric vapours. *Nature*. **565**, 587–593 (2019).

97. J. N. Moorthy, N. Singhal, K. Senapati, Oxidative cleavage of vicinal diols: IBX can do what Dess–Martin periodinane (DMP) can. *Org. Biomol. Chem.* **5**, 767–771 (2007).

98. M. Gomes, O. A. C. Antunes, Upjohn catalytic osmium tetroxide oxidation process: Diastereoselective dihydroxylation of monoterpenes. *Catalysis Communications*. **2**, 225–227 (2001).

99. C. Samorì, H. Ali-Boucetta, R. Sainz, C. Guo, F. M. Toma, C. Fabbro, T. da Ros, M. Prato, K. Kostarelos, A. Bianco, Enhanced anticancer activity of multi-walled carbon nanotube–methotrexate conjugates using cleavable linkers. *Chem. Commun.* **46**, 1494–1496 (2010).

100. H.-X. Liu, H.-B. Tan, M.-T. He, L. Li, Y.-H. Wang, C.-L. Long, Isolation and synthesis of two hydroxychavicol heterodimers from Piper nudibaccatum. *Tetrahedron*. **71**, 2369–2375 (2015).

101. F. Fache, O. Piva, P. Mirabel, First synthesis of hydroxy-pinonaldehyde and hydroxy-pinonic acid, monoterpene degradation products present in atmosphere. *Tetrahedron Letters*. **43**, 2511–2513 (2002).

102. P. A. Procopiou, S. P. D. Baugh, S. S. Flack, G. G. A. Inglis, An Extremely Powerful Acylation Reaction of Alcohols with Acid Anhydrides Catalyzed by Trimethylsilyl Trifluoromethanesulfonate. *J. Org. Chem.* **63**, 2342–2347 (1998).

103. R. H. Beddoe, D. C. Edwards, L. Goodman, H. F. Sneddon, R. M. Denton, Synthesis of ^{18}O-labelled alcohols from unlabelled alcohols. *Chem. Commun.* **56**, 6480–6483 (2020).

104. S. S. Steimer, A. Delvaux, S. J. Campbell, P. J. Gallimore, P. Grice, D. J. Howe, D. Pitton, M. Claeys, T. Hoffmann, M. Kalberer, Synthesis and characterisation of peroxypinic acids as proxies for highly oxygenated molecules (HOMs) in secondary organic aerosol. *Atmos. Chem. Phys.* **18**, 10973–10983 (2018).

Acknowledgments: We thank John Crounse and Joel Thornton for useful discussions and the Thomson Group at Northwestern University for providing one of the dimer ester standards. UPLC/(−)ESI-Q-TOF-MS was performed in the Resnick Sustainability Institute Water and Environment Lab at the California Institute of Technology.

Funding: This work was supported by the National Science Foundation (AGS-1523500, CHE-1800511, and CHE-1905340), the Independent Research Fund Denmark (9040-00142B), the Villum Fonden (VIL50443), and the Alfred P. Sloan Foundation (G-2019-12281). C.M.K. acknowledges support from a National Science Foundation Atmospheric and Geospace Sciences Postdoctoral Research Fellowship (AGS-2132296).

Author contributions: C.M.K. designed research; C.M.K. and Y.H. performed research; C.M.K., N.J.H., S.P.R., and B.M.S. contributed new reagents; J.C. and H.G.K. performed theoretical calculations; C.M.K., J.C., Y.H., N.F.D., and P.O.W. analyzed data; and C.M.K., J.H.S., and P.O.W. wrote the paper.

Competing interests: The authors declare no competing interests.

Data and materials availability: All data are available in the main text or Supplementary Materials.

Supplementary Materials

Materials and Methods
Supplementary Text
References (*51–104*)
Figs. S1 to S17
Table S1
Synthetic Procedures
NMR and IR Spectra

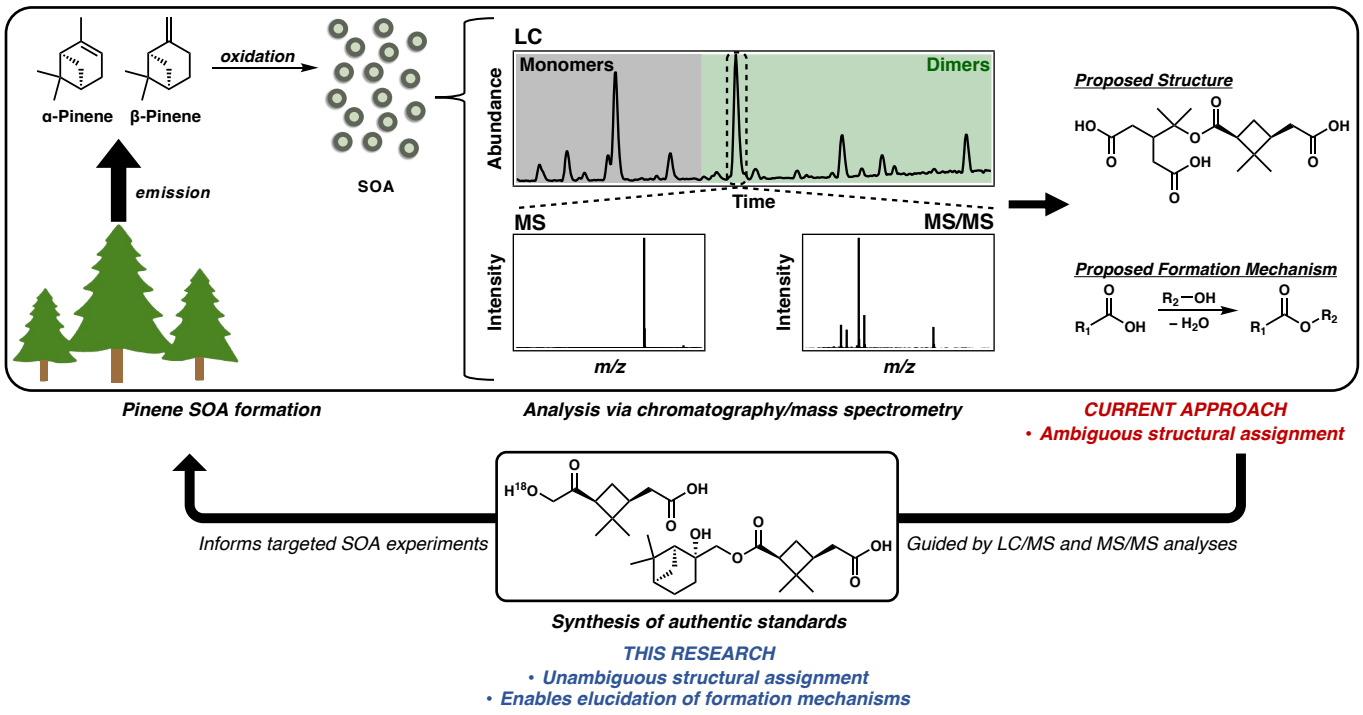

Fig. 1. Characterization of dimeric compounds in pinene SOA. Currently proposed structures, and by extension formation mechanisms, of dimeric compounds identified in pinene SOA using advanced mass spectrometric techniques are inferred from accurate mass/fragmentation data and are thus uncertain. Independent synthesis of authentic standards, guided by mass spectrometric analysis, affords unambiguous structural assignment and enables elucidation of formation mechanisms by informing targeted SOA experiments.

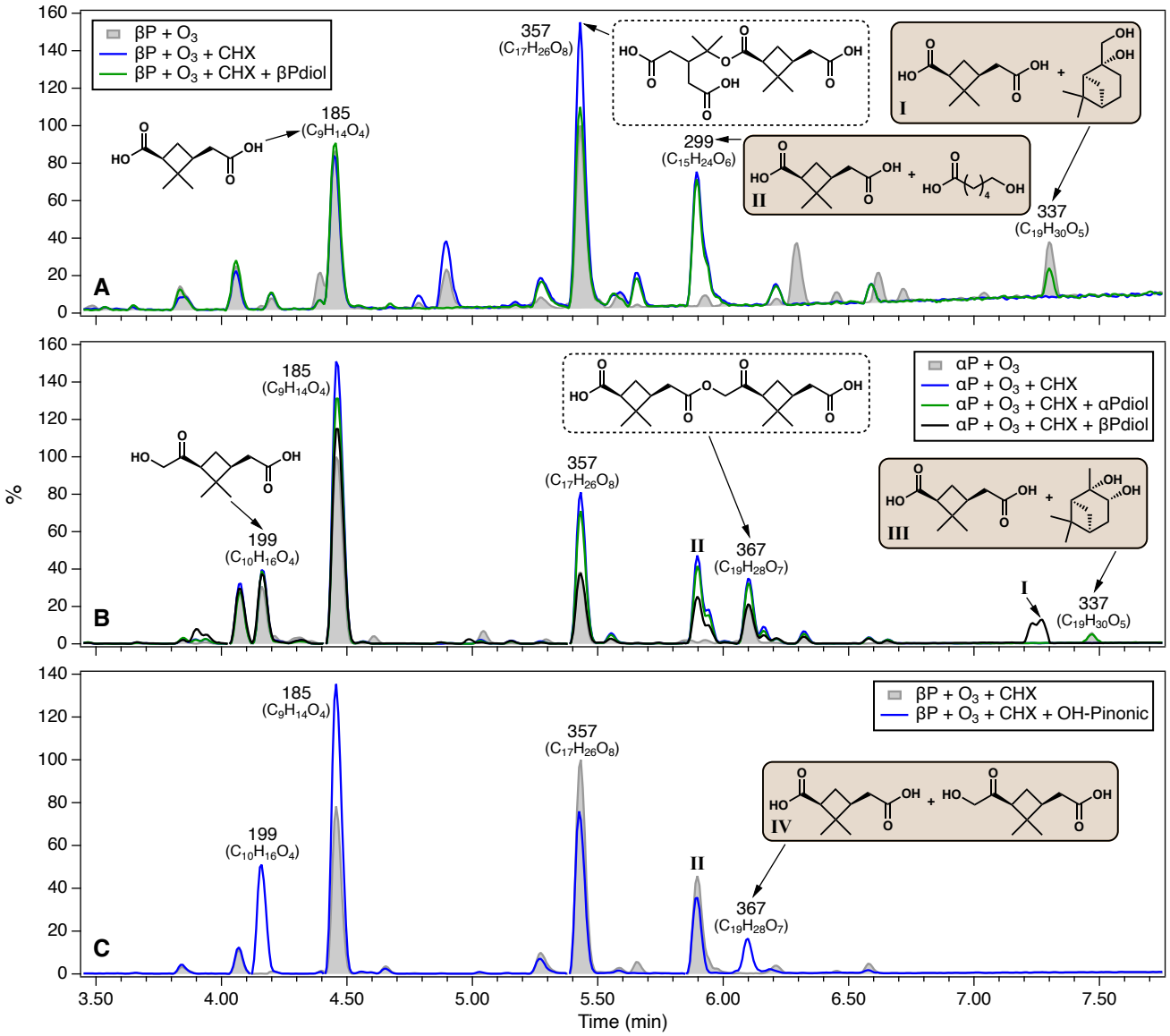

Fig. 2. Formation of dimer esters in pinene SOA. Base peak ion (BPI) chromatograms of SOA formed from ozonolysis of (**A** and **C**) β-pinene (βP) and (**B**) α-pinene (αP) after ~4 h of reaction in the CTEC. Experiments were conducted in the absence of cyclohexane (CHX) as an OH scavenger, presence of CHX, and presence of both CHX and α-pinanediol (αPdiol), β-pinanediol (βPdiol), or *cis*-10-hydroxypinonic acid (OH-pinonic). Numbers correspond to nominal *m/z* values of $[M-H]^-$ ions; molecular formulas are given in parentheses. Chromatograms are normalized to the total organic carbon (TOC) content of the corresponding SOA filter samples, reported as averages of duplicate samples collected in parallel for each experiment, and scaled such that the largest peak in the control experiments (gray shading) is 100%. *cis*-Pinic acid ($C_9H_{14}O_4$) and OH-pinonic acid ($C_{10}H_{16}O_4$) were identified via comparison with authentic standards. Structures in dashed boxes denote those proposed in past studies (*12*, *15*). Structures in shaded boxes are of monomeric subunits identified for dimer esters **I–IV**. For clarity, all structures are drawn as the (+) enantiomers despite experiments being carried out with (+)-αP, (−)-βP, (+)-αPdiol, (−)-βPdiol, and (−)-OH-pinonic acid.

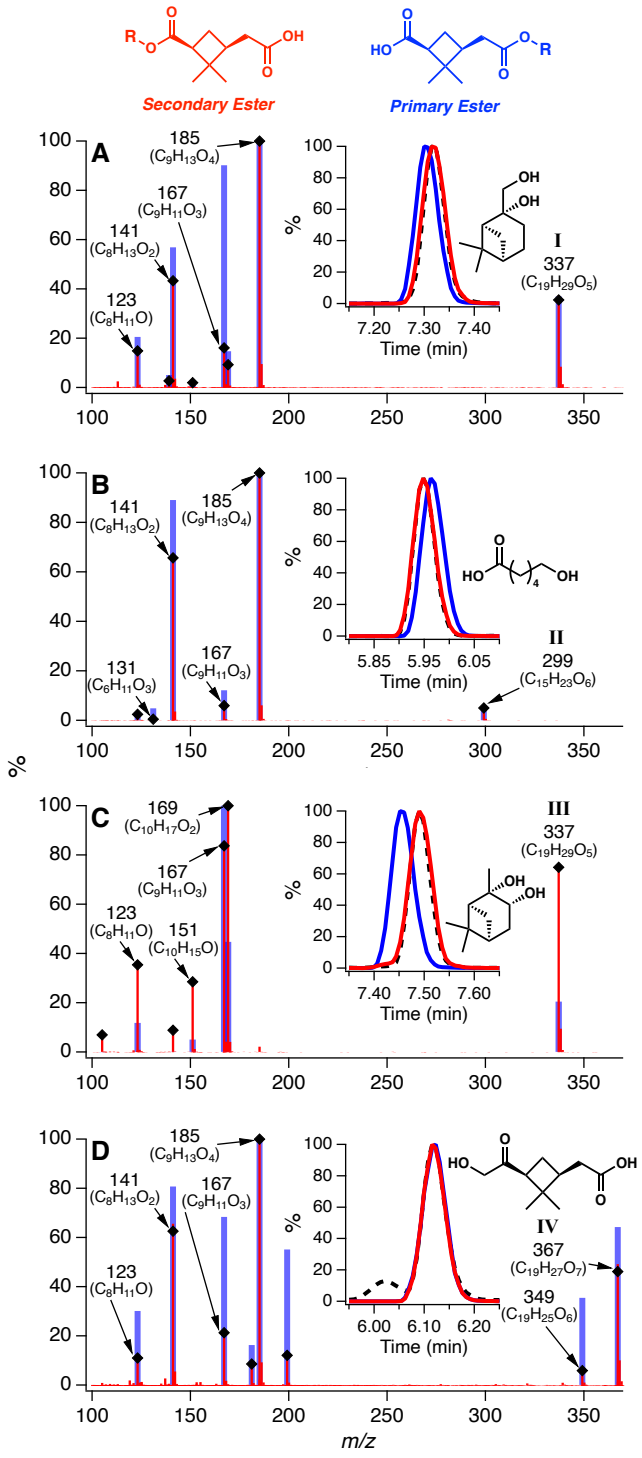

Fig. 3. Determination of dimer ester structures. Extracted ion chromatograms (EIC) and MS/MS spectra of synthesized secondary (red) and primary (blue) dimer esters of (+)-*cis*-pinic acid and (**A**) (+)-β-pinanediol, (**B**) 6-hydroxyhexanoic acid, (**C**) (+)-α-pinanediol, and (**D**) (+)-*cis*-10-hydroxypinonic acid as well as of dimer esters identified in SOA formed from ozonolysis of α-pinene and/or β-pinene (black diamonds and dashed lines): (**A**) dimer ester **I** ($C_{19}H_{30}O_5$), (**B**) dimer ester **II** ($C_{15}H_{24}O_6$), (**C**) dimer ester

III ($C_{19}H_{30}O_5$), and (**D**) dimer ester **IV** ($C_{19}H_{28}O_7$). Numbers in MS/MS spectra correspond to nominal *m/z* values of $[M-H]^-$ ions; ionic formulas $[C_xH_yO_z]^-$ are given in parentheses.

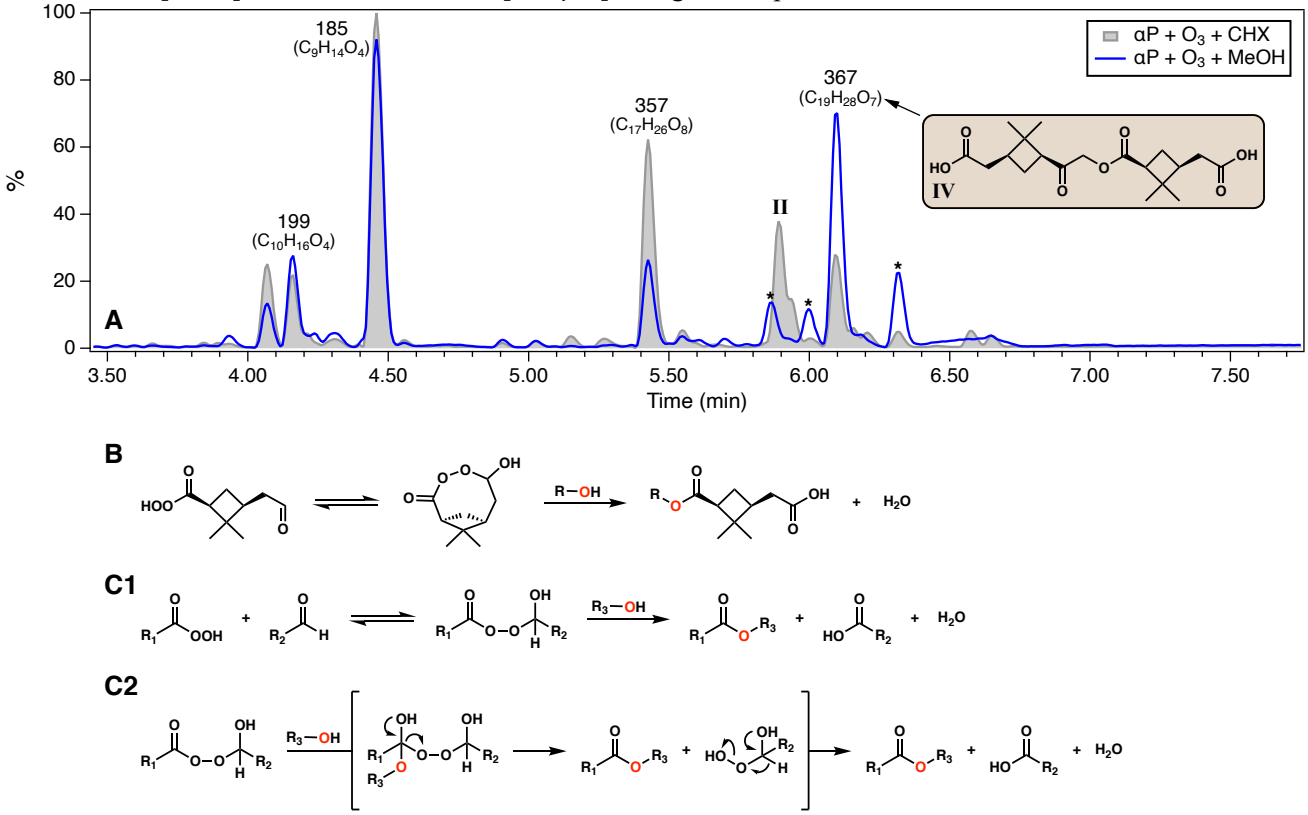

Fig. 4. Formation mechanism of dimer esters. (**A**) Base peak ion (BPI) chromatograms of SOA formed from ozonolysis of α-pinene (αP) after ~4 h of reaction in the CTEC in the presence of either cyclohexane (CHX) or methanol (MeOH) as an OH scavenger. Numbers correspond to nominal *m/z* values of $[M-H]^-$ ions; molecular formulas are given in parentheses. Chromatograms are normalized to the total organic carbon (TOC) content of the corresponding SOA filter samples, reported as averages of duplicate samples collected in parallel for each experiment, and scaled such that the largest peak in the control experiments (gray shading) is 100%. *cis*-Pinic acid ($C_9H_{14}O_4$), *cis*-10-hydroxypinonic acid ($C_{10}H_{16}O_4$), dimer ester **II**, and dimer ester **IV** were identified via comparison with authentic standards. *Indicates dimers ($C_{19}H_{28}O_9$ and $C_{18}H_{26}O_6$) proposed to consist of esters with *cis*-pinic acid subunits based on MS/MS analysis. (**B**) Proposed formation mechanism of dimer esters in pinene SOA via particle-phase nucleophilic addition of a semi/low-volatility alcohol to the cyclic acylperoxyhemiacetal derived from particle-phase tautomerization of *cis*-3-peroxypinalic acid. (**C**) General mechanism of dimer ester formation via condensed-phase reaction of an alcohol with an acylperoxyhemiacetal.

Science
AAAS

Supplementary Materials for

Particle-Phase Accretion Forms Dimer Esters in Pinene Secondary Organic Aerosol

Christopher M. Kenseth*, Nicholas J. Hafeman, Samir P. Rezgui, Jing Chen, Yuanlong Huang, Nathan F. Dalleska, Henrik G. Kjaergaard, Brian M. Stoltz, John H. Seinfeld, and Paul O. Wennberg

*Corresponding author. Email: ckenseth@caltech.edu

This PDF file includes:

Table of Contents

S1. Materials and Methods

S1.1 Secondary Organic Aerosol (SOA) Formation Experiments. Ozonolysis experiments were carried out in the Caltech dual 24 m^3 Teflon Environmental Chambers (CTEC) (*51*) at ~295 K and ~1 atm under dry [<5% relative humidity (RH)], low-NO_x (<0.5 ppb) conditions. Representative experimental conditions are reported in Table S1. Prior to each experiment, the chamber was flushed with dry, purified air for 24 h such that the particle number and volume concentrations were less than 10 cm^{-3} and 0.01 μm^3 cm^{-3}, respectively. α-Pinene, β-pinene, synthesized enone, or synthesized enal (~100 ppb) was added to the chamber by passing dry, purified air through a glass cylinder, warmed to 50 °C with electrical heat tape, containing a volumetric injection of liquid (+)-α-pinene (15.5 μL, ≥99%, Sigma-Aldrich), (−)-β-pinene (15.5 μL, ≥99%, Sigma-Aldrich), (+)-enone (16.4 μL), or (+)-enal (16.4 μL). In certain experiments, alcohols (~100 ppb) of varying structure and volatility, cyclohexanol (CHXOH, 10.3 μL, 99%, Sigma-Aldrich), benzyl alcohol (BnOH, 10.2 μL, ≥99%, Sigma-Aldrich), *cis*-1,2-cyclohexanediol (CHXdiol, 11.5 mg, 99%, Sigma-Aldrich), (+)-α-pinanediol (αPdiol, 16.8 mg, 99%, Sigma-Aldrich), synthesized (−)-β-pinanediol (βPdiol, 16.8 mg), or 6-hydroxyhexanoic acid (OH-hexanoic, 13.1 mg, 95%, AmBeed), were added to the chamber using a modified version of a custom-built, filter-based thermal desorption system (*36*).

Polydisperse seed aerosol (~50–230 μm^3 cm^{-3}, $\overline{D}_p \approx 145 \pm 19$ nm) was generated via atomization of a dilute (0.06 M) solution of $(NH_4)_2SO_4$ (Macron Fine Chemicals) in ultra-pure water (18.2 MΩ cm, <3 ppb TOC, Millipore Milli-Q), followed by diffusive drying and neutralization. In select experiments, seed aerosol was produced from solutions of $(NH_4)_2SO_4$ (0.06 M) and synthesized (+)-*cis*-pinic acid (0.02 M), synthesized (−)-*cis*-10-hydroxypinonic acid (OH-pinonic) (0.02 M), synthesized (−)-^{18}OH-pinonic acid (0.02 M), or *meso*-erythritol (0.02 M, ≥99%, Sigma-Aldrich) in ultra-pure water. Experiments were also conducted that featured only seed aerosol, generated from a solution of (+)-*cis*-pinic acid (0.005 M) and (−)-OH-pinonic acid (0.005 M) in ultra-pure water. Synthesized compounds used in the CTEC experiments were prepared in 9–90% yield (1–6 steps) from commercial precursors (Fig. S14).

O_3 (~150 ppb) was produced by flowing dry, purified air through a custom-built UV O_3 generator. Ozonolysis experiments were carried out both in the absence of an OH scavenger, resulting in initial OH molar yields for α-pinene and β-pinene of 77–89% (*52*, *53*) and 28–44% (*54*, *55*), respectively, as well as in the presence of either cyclohexane (CHX, ~25 ppm) or methanol (MeOH, ~185 ppm). Volumetric injections of liquid CHX (2.7 mL, 99.5%, Sigma-Aldrich) and MeOH (7.4 mL, Optima™ LC/MS, Fisher Scientific) were added to the chamber in the same manner as the hydrocarbon precursors. Given recommended values of k_{OH} (cm^3 $molecules^{-1}$ s^{-1})

for CHX (7.0×10^{-12}), MeOH (9.4×10^{-13}), α-pinene (5.2×10^{-11}), and β-pinene (7.4×10^{-11}) (*56*), and estimated values for the enone (3.3×10^{-11}) and enal (7.6×10^{-11}) (*57*), OH scavenging efficiencies of both CHX and MeOH were >95%.

S1.2 Gas-Phase Measurements. α-Pinene and β-pinene mixing ratios were quantified with an Agilent 6890N gas chromatograph equipped with a flame ionization detector (GC/FID) and operated with an Agilent HP-5 column (30 m × 0.32 mm, 0.25 μm). The GC/FID was calibrated as described in Kenseth et al. (*33*). Enone and enal abundances were also measured via GC/FID, but were not calibrated. O_3 and NO_x mixing ratios were quantified by a Horiba APOA-360 O_3 monitor and a Teledyne T200 NO_x analyzer, respectively. Temperature and RH were monitored with a Vaisala HMM211 probe.

Chemical Ionization Mass Spectrometer (CIMS). CHXOH, CHXdiol, αPdiol, βPdiol, OH-hexanoic acid, and select gas-phase α-pinene and β-pinene oxidation products were monitored using a custom-modified triple-quadrupole CIMS employing CF_3O^- as the reagent ion, which is sensitive to multifunctional organic compounds. CF_3O^- selectively interacts with analytes to form either $[M{\cdot}CF_3O]^-$ cluster ions or $[(M–H){\cdot}HF]^-$ fluoride-transfer ions for acidic species. The triple-quadrupole MS (unit-mass resolution) was operated in a scanning mode (*m/z* 50–300, ~145 s per scan). Analyte ion signals were normalized to the sum of isotopes of the reagent ion ($^{13}CF_3O^- + {}^{13}CF_3O^-{\cdot}H_2O$) to account for variations in total ion signal, but were not calibrated. Detailed descriptions of the CF_3O^- CIMS are presented elsewhere (*58*, *59*).

S1.3 Particle-Phase Measurements. *Scanning Mobility Particle Sizer (SMPS).* Aerosol size distributions and number concentrations ($D_p \approx 15–800$ nm) were measured with a custom-built SMPS consisting of a TSI 3081 differential mobility analyzer (DMA) coupled to a TSI 3010 condensation particle counter (CPC). Details of the SMPS operation are provided elsewhere (*33*, *60*). Suspended SOA volume concentrations were derived using the approach of Kenseth et al. (*33*), and were not corrected for particle wall loss to enable direct comparison with the concentrations of individual molecular products detected in suspended SOA using off-line mass spectrometry. SOA mass concentrations were calculated assuming an effective density of 1.25 g mL^{-1} for α-pinene and β-pinene SOA (*61–64*).

Teflon Filter Samples. Chamber-generated SOA was collected on Pall Life Sciences Teflon membrane disc filters (2 μm pore size, 47 mm diameter) for off-line, molecular-level characterization. Duplicate samples were collected for 2 h in parallel after ~4 h, or in select cases ~14 h, of ozonolysis for each experiment, such that the mass of SOA on each filter pair was approximately equivalent. A cylindrical diffusion denuder packed with activated charcoal (Sigma-Aldrich) was placed upstream of the dual filter holder to remove O_3 and gas-phase species, thereby preventing on-filter reactions and further partitioning of gas-phase compounds to collected particles; particle loss through the denuder was assumed to be negligible (*65*). Filters were stored at −16 °C immediately after collection. Filter samples were extracted into 6 mL of ultra-pure water for 1 h using an orbital shaker, as extraction via sonication has been shown to cause degradation of α-pinene SOA molecular products (e.g., *cis*-pinic acid) and elevated concentrations of particle-bound peroxides (*66*). To account for variations in filter collection and extraction efficiency, the total organic carbon (TOC) content of the filter extracts was quantified using an OI-Analytical Aurora 1030W TOC Analyzer following the method in Kenseth et al. (*33*).

Ultra-Performance Liquid Chromatography/Negative Electrospray Ionization Quadrupole Time-of-Flight Mass Spectrometry [UPLC/(–)ESI-Q-TOF-MS]. SOA filter samples were analyzed by a Waters ACQUITY UPLC I-Class system coupled to a Xevo G2-S Q-TOF-MS equipped with an ESI source and operated in (–) ion mode. An ACQUITY BEH C_{18} column (1.7 μm, 2.1 mm × 50 mm) fitted with an ACQUITY BEH C_{18} VanGaurd pre-column (1.7 μm, 2.1 mm × 5 mm) was used to separate SOA molecular constituents. Instrument specifications, acquisition parameters (e.g., gradient-elution and MS/MS methods), and calibration procedures are detailed in Kenseth et al. (*33*). Note that due to the addition of the guard column, retention times of SOA molecular products in this study and our previous work (*34*) are shifted by +0.11–0.15 min compared to those reported in Kenseth et al. (*33*). All analytes were detected as $[M–H]^-$ ions, generated via deprotonation of parent molecules during (–)ESI. Instrument stability [i.e., extracted ion chromatogram (EIC) peak area reproducibility] was verified to within 4% using an equimolar (1.00 μM) solution of synthesized, pinene-derived carboxylic acid and dimer ester homologues (*34*) in ultra-pure water, run twice every 10 samples during routine analysis. Data were acquired and processed using MassLynx v4.1 software. Molecular formulas ($C_xH_yO_z$) of $[M–H]^-$ ions were assigned with mass tolerances of <7 ppm and supported by the associated ^{13}C isotope distributions. Prior separation of analytes from the complex SOA matrix via UPLC precludes potential ion-source artifacts (e.g., signal suppression and noncovalent clustering), ensuring the quantitative nature of the method. Abundances of molecular products measurable by LC/(–)ESI-MS in SOA from ozonolysis of α-pinene and β-pinene, including dimer esters **I**, **III**, and **IV**, were quantified in our previous work (*34*) using the calibrated (–)ESI efficiencies of the carboxylic acid and dimer ester homologues as surrogates. Molecular formulas, retention times, SOA mass fractions, and physicochemical properties of the 40 identified monomers ($C_{7–10}H_{10–18}O_{3–6}$) and 87 identified dimers ($C_{15–19}H_{24–32}O_{4–11}$) are presented therein, together with select proposed structures assigned based on comparison with authentic standards and/or previously reported LC/(–)ESI-MS data.

S1.4 Quantum Chemical Calculations. Charge distributions and one-step reaction potentials for esterification with methanol in vacuum were calculated for a series of carboxylic acid derivatives [$CH_3C(=O)–X$] (Fig. S12). A conformer sampling process based on a previously developed approach (*67*) was carried out to ensure that the lowest-energy conformers of the reactants, transition states, and products were used in the calculations. Briefly, conformers were generated by rotating each dihedral angle in a structure three times in 120° intervals and preoptimized to remove unphysical structures from the dihedral angle torsions using MMFF (Merck Molecular Force Field) (*68*, *69*) in Spartan'18 (*70*). Obtained conformers were optimized at the B3LYP/6-31+G(d) level in Gaussian 16, Rev. C.01 (*71*). Conformers with a zero-point-vibrational-corrected electronic energy (E+ZPVE) difference of <0.03 kcal mol^{-1} and dipole moment difference of <0.015 Debye were treated as the same conformers (*67*). The unique conformers were subsequently reoptimized at the M06-2X/aug-cc-pVTZ and ωB97X-D/aug-cc-pVTZ levels in Gaussian 16, Rev. C.01. Conformers with the lowest E+ZPVE were used in subsequent calculations. For the transition states of the one-step esterification reactions, the conformer sampling process was modified. The transition state of the esterification consists of a four-membered ring with six diastereomers. Given that MMFF fails to flip the functional groups on the four-membered ring, different isomers of the transition states were first manually generated and optimized in Gaussian 16, Rev. C.01. The ring structures were then fixed and all dihedral angles outside the rings were rotated using MMFF to produce conformers that were reoptimized in Gaussian 16, Rev. C.01.

Mulliken (*72*) and electrostatic potential (ESP) charges were calculated at the B3LYP/6-31+G(d) level on the lowest E+ZPVE conformers. Mulliken charges were calculated as implemented in Gaussian 16, Rev. C.01, wherein the electron density between two atoms is separated at the midpoint of nucleus positions. ESP charges were fitted using the CHELPG (CHarges from ELectrostatic Potentials using a Grid-based method) scheme (*73*) in Multiwfn (*74*). Enthalpies of reactants, transition states, and products for the one-step esterification reaction potentials were calculated using the lowest E+ZPVE conformers. Enthalpies of reactant and product complexes were derived from optimized end-point geometries obtained from intrinsic reaction coordinate (IRC) (*75*) calculations carried out for each lowest E+ZPVE transition state conformer. All energies were calculated at the B3LYP/6-31+G(d) level in Gaussian 16, Rev. C.01.

S2. Implications of Dimer Ester Formation Mechanism

The formation of dimer esters in α-pinene and β-pinene SOA via particle-phase accretion of semi/low-volatility alcohols with the cyclic acylperoxyhemiacetal derived from *cis*-3-peroxypinalic acid rationalizes a number of notable experimental and ambient observations. Accumulating studies (*26–28*, *30*, *33*) have shown that dimers in α-pinene and β-pinene SOA measurable by LC/(–)ESI-MS are formed only from O_3 and not OH oxidation, despite the apparent monomeric subunits (e.g., *cis*-pinic acid) being produced in both oxidative systems. For dimer esters **I**–**IV**, as well as dimer esters proposed to contain *cis*-pinic acid subunits (e.g., major $C_{17}H_{26}O_8$ dimer), these findings are consistent with the lack of a direct pathway to *cis*-3-peroxypinalic acid from OH oxidation of either α-pinene or β-pinene (*76–78*). More generally, peracids (acylperoxyhemiacetal precursors) are understood to be major first-generation products of α-pinene and β-pinene ozonolysis via the vinyl hydroperoxide (VHP) channel, but comparatively minor species in OH oxidation (*30*, *50*, *76*). The proposed centrality of peracids in dimer ester formation is also in line with results from α-pinene ozonolysis experiments with added NO_2 that implicate acyl peroxy radicals (peracid precursors) as key intermediates in the production of dimeric compounds in α-pinene SOA (*38*).

Recent time-resolved measurements of SOA molecular composition from α-pinene ozonolysis (*30*) reveal a continued growth of *cis*-pinic acid after >99% of α-pinene has been consumed, which cannot be explained solely by gas-phase photochemical production coupled with gas-particle partitioning. Although other potential reaction pathways (e.g., diacyl peroxide decomposition) may contribute, particle-phase Baeyer-Villiger decomposition of the cyclic acylperoxyhemiacetal derived from *cis*-3-peroxypinalic acid (Fig. S6) provides a probable mechanism for the observed *cis*-pinic acid behavior congruent with the proposed mechanism of dimer ester formation. The particle-phase conversion of peracids to nonperoxidic species via both accretion and Baeyer-Villiger decomposition of acylperoxyhemiacetals is also in line with results from our novel iodometry-assisted LC/(–)ESI-MS assay (*35*), which found that only one compound identified in SOA from α-pinene ozonolysis ($C_8H_{14}O_6$) contains (hydro)peroxide functionalities, as well as a recent functional group analysis of SOA from α-pinene ozonolysis (*79*), which determined that measured peroxide, carbonyl, and hydroxy groups were considerably overpredicted by an explicit chemical model whereas carboxyl and ester groups were markedly underpredicted.

MS/MS analysis indicates that the major $C_{17}H_{26}O_8$ dimer is the secondary ester of *cis*-pinic acid and diaterpenylic acid (*15*, *37*). This regioselectivity is consistent with formation via particle-phase nucleophilic addition of diaterpenylic acid to the cyclic acylperoxyhemiacetal derived from *cis*-3-

peroxypinalic acid. Positive and negative temperature dependences respectively observed for the abundances of the $C_{17}H_{26}O_8$ dimer and dimer ester **IV** in SOA from α-pinene ozonolysis have prompted suggestions of dissimilar formation pathways (*29*). However, the particle-phase abundances of the corresponding precursor alcohols, diaterpenylic acid and OH-pinonic acid, also exhibit opposite temperature dependences (*28*, *29*), in line with the proposed mechanism of dimer ester production. Correlated ($R^2 > 0.78$) particle-phase abundances of the $C_{17}H_{26}O_8$ dimer and dimer ester **IV** during two field campaigns in forested regions with appreciable monoterpene emissions, the Blodgett Forest Research Station in Georgetown, CA (*25*) and the Station for Measuring Forest Ecosystem-Atmosphere Relations in Hyytiälä, Finland (*27*), further imply similar formation chemistry from a common precursor.

Multiple studies have reported increases in the mass fractions of dimers in SOA from α-pinene and β-pinene ozonolysis measured using LC/(−)ESI-MS with increasing RH (*27*, *30*, *33*), which have been cited as evidence against production via conventional esterification (i.e., carboxylic acid + alcohol). Although the proposed mechanism of dimer ester formation is also a net condensation reaction (Fig. 4B) and, therefore, subject to the same equilibrium considerations (i.e., Le Chatelier), it is likely that the unfavorable thermodynamics at elevated RH are offset, at least partially, by the reduced viscosity of pinene SOA (*80*, *81*) and resultant increase in gas-particle partitioning of the semivolatile dimer ester precursors.

Two of the most abundant dimers identified in SOA from ozonolysis of Δ^3-carene are proposed based on MS/MS analysis to be analogs of dimer esters **III** and **IV** (*82*). As per the chemistry elucidated here, these dimer esters are likely produced via particle-phase nucleophilic addition of Δ^3-caranediol and *cis*-10-hydroxycaronic acid, respectively, to the cyclic acylperoxyhemiacetal derived from *cis*-peroxycaralic acid (Fig. S15). Similarly, the major dimers identified in SOA from cyclohexene ozonolysis proposed to consist of esters with adipic acid and glutaric acid subunits (*12*, *83*) are likely formed from particle-phase accretion of alcohols with the cyclic acylperoxyhemiacetals derived from 6-oxohexaneperoxoic acid and 5-oxopentaneperoxoic acid, respectively (Fig. S16).

As additional evidence for the generality of dimer ester formation via condensed-phase reaction of alcohols with acylperoxyhemiacetals, three major dimers, proposed based on MS/MS analysis to be homologues of dimer esters **I**, **II**, and **IV** with *cis*-10-carboxypinonic acid subunits, were identified in SOA from α-pinene ozonolysis with CHX and βPdiol (Fig. S17). We propose that these homologues are formed via particle-phase nucleophilic addition of βPdiol, OH-hexanoic acid, and OH-pinonic acid, respectively, to the cyclic acylperoxyhemiacetal derived from *cis*-10-oxoperoxypinonic acid (Fig. S17). Due to the structure of *cis*-10-oxoperoxypinonic acid, nucleophilic addition of alcohols to the corresponding cyclic acylperoxyhemiacetal will yield regioselective primary esters, on the opposite side of the dimethylcyclobutyl ring as the secondary esters formed from the cyclic acylperoxyhemiacetal derived from *cis*-3-peroxypinalic acid. Additionally, given the lack of an established route to *cis*-10-carboxypinonic acid from ozonolysis of α-pinene (*76*), we suggest that, similar to *cis*-pinic acid, particle-phase Baeyer-Villiger decomposition of the cyclic acylperoxyhemiacetal derived from *cis*-10-oxoperoxypinonic acid represents a likely formation pathway.

S3. Figs. S1 to S17

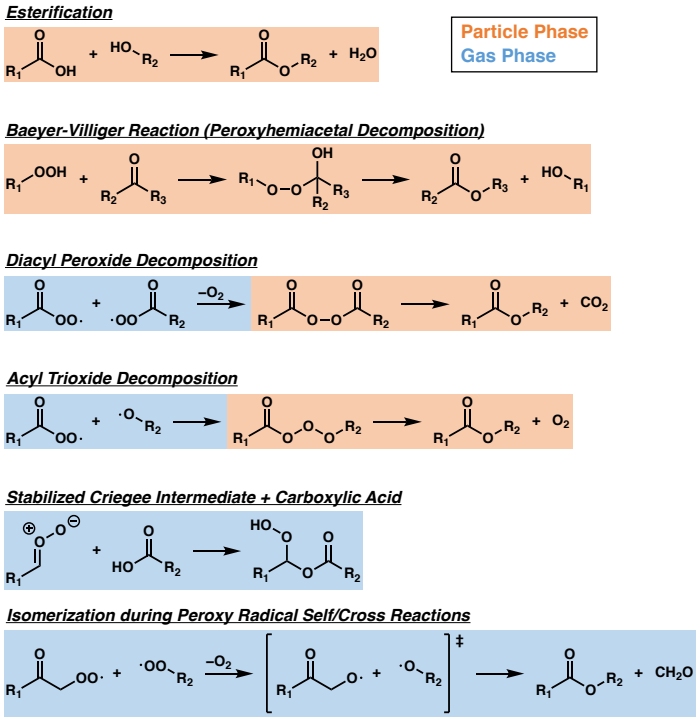

Fig. S1. Proposed formation mechanisms of dimer esters in pinene SOA. Conventional esterification (*12*, *15*), Baeyer-Villiger decomposition of peroxyhemiacetals (*79*), diacyl peroxide decomposition (*30*, *38*), acyl trioxide decomposition (*37*), reaction of stabilized Criegee intermediates with carboxylic acids (*27*), and isomerization during self/cross reactions of organic peroxy radicals (RO_2) (*39*).

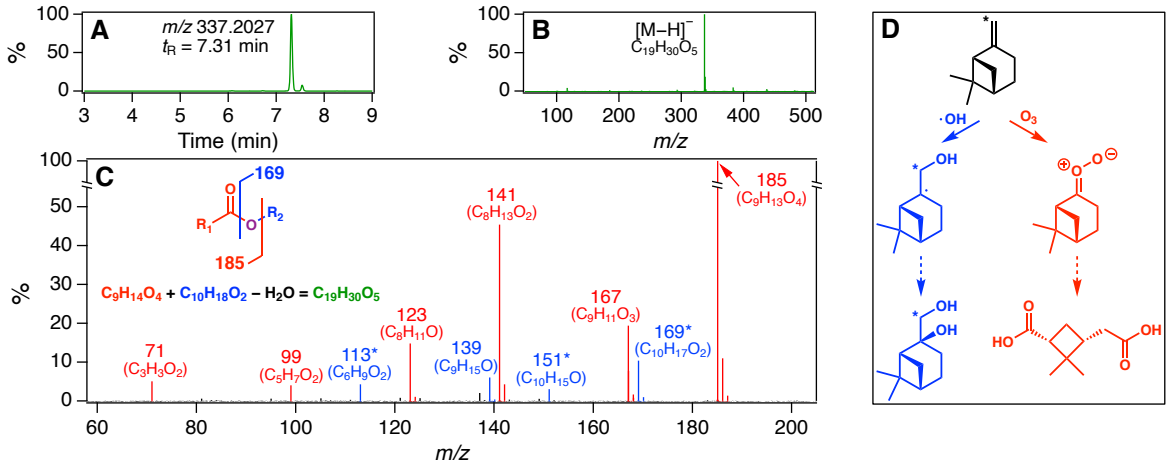

Fig. S2. Structural characterization of dimer ester I. (**A**) EIC, (**B**) MS spectrum, (**C**) MS/MS spectrum, and (**D**) proposed monomeric subunits, *cis*-pinic acid and βPdiol, of major dimer in SOA from β-pinene ozonolysis (Fig. 2A, dimer ester **I**) shown to form from accretion of O_3- and OH-derived products/intermediates (*33*). Colors denote O_3-derived (red) and OH-derived (blue) MS/MS fragment ions and oxidation pathways/products. Numbers in MS/MS spectrum correspond to nominal *m/z* values of $[M–H]^-$ ions; ionic formulas $[C_xH_yO_z]^-$ are given in parentheses. *Indicates peaks that underwent a one-unit mass shift on formation from ^{13}C-β-pinene (*33*).

The structure of dimer ester **I** was proposed based on detailed analysis from our previous work on dimers formed via synergistic O_3 + OH oxidation (*33*). Briefly, application of our novel iodometry-assisted LC/(–)ESI-MS assay (*35*) to SOA from ozonolysis of α-pinene and β-pinene demonstrated that detectable dimers do not contain (hydro)peroxide functionalities. Analysis of SOA from β-pinene ozonolysis using hydrogen/deuterium exchange (HDX) LC/(–)ESI-MS enabled quantification of the number of labile hydrogens (e.g., –OH and –COOH) in the structures of identified monomers and dimers; dimer ester **I** was determined to contain two labile hydrogens. MS/MS spectra of the synergistic O_3 + OH dimers formed from ozonolysis of ^{13}C-β-pinene, labeled at the terminal vinylic carbon, revealed distinct OH-derived (^{13}C-mass-shifted) and O_3-derived (unshifted) fragmentation patterns, given that reaction of ^{13}C-β-pinene with O_3 will cleave the ^{13}C label whereas reaction with OH, formed as a byproduct of ozonolysis, will retain the label. The fragmentation patterns of certain synergistic dimers, including dimer ester **I**, were found to be characteristic of covalent dimer esters; the elemental composition of the dimers is given by condensation of the O_3- and OH-derived monomeric subunits ($M_1 + M_2 - M_{H_2O} = M_D$). The O_3-derived monomeric subunit of dimer ester **I** was assigned to *cis*-pinic acid based on comparison of its fragmentation pattern to that of an authentic standard. The OH-derived monomeric subunit was assigned to βPdiol on the basis of its molecular formula ($C_{10}H_{18}O_2$), fragmentation pattern, and the prevailing mechanism of β-pinene photooxidation (*76*, *77*). Recent experimental estimates (*84*) of the ratios of (*i*) ring-retained vs. ring-opened $C_{10}H_{17}O_3$ RO_2 formed following the major OH addition to β-pinene (83% of total OH reactivity) at the terminal vinylic carbon (2:1) and (*ii*) *syn* vs. *anti* diastereomers of the ring-retained $C_{10}H_{17}O_3$ RO_2 (4:1) provided additional evidence for the βPdiol assignment.

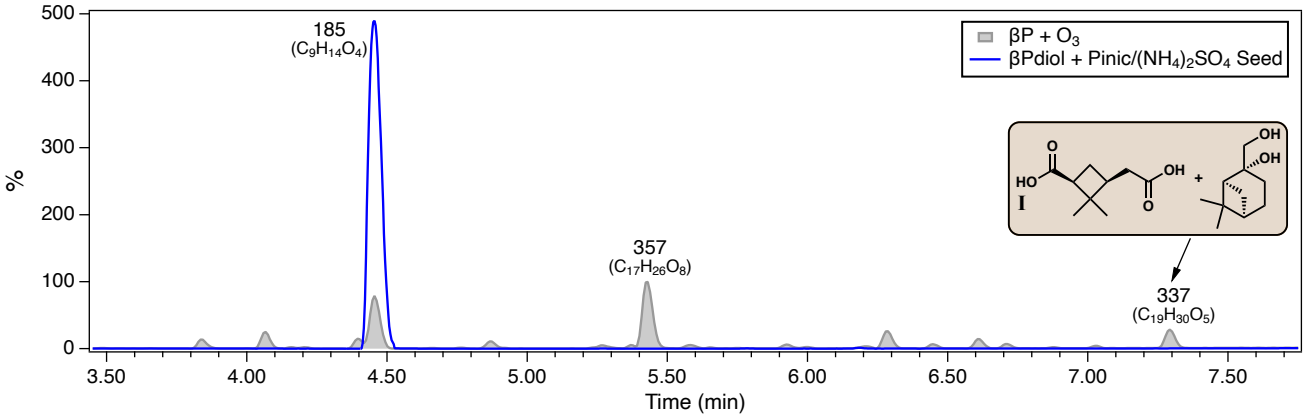

Fig. S3. Lack of dimer ester I formation via conventional esterification. Base peak ion (BPI) chromatograms of SOA formed from ozonolysis of β-pinene (βP) after ~4 h of reaction in the CTEC and aerosol from a CTEC experiment featuring ~100 ppb gas-phase βPdiol and 175 μm^3 cm^{-3} of seed aerosol generated from an aqueous solution of $(NH_4)_2SO_4$ (0.06 M) and *cis*-pinic acid ($C_9H_{14}O_4$) (0.02 M) after ~4 h. Numbers correspond to nominal *m/z* values of $[M–H]^-$ ions; molecular formulas are given in parentheses. Chromatograms are reported as averages of duplicate aerosol filter samples collected in parallel for each experiment and scaled such that the largest peak in the control experiment (gray shading) is 100%. Structures in shaded box are of monomeric subunits identified for dimer ester **I**.

Consistent with the relative particle-phase abundances of *cis*-pinic acid, gas-phase concentrations of *cis*-pinic acid, partitioned from the seed aerosol, were roughly five times larger than those in the β-pinene ozonolysis experiment. For βPdiol, gas-phase concentrations were over 30 times larger than those in the β-pinene ozonolysis experiment. Due to equilibrium partitioning, the 3:1 mole ratio of $(NH_4)_2SO_4$ to *cis*-pinic acid in the aqueous solution cannot be preserved in the seed aerosol. However, assuming an evaporative loss for *cis*-pinic acid of 15% [i.e., gas-phase fraction of *cis*-pinic acid predicted for OA mass loading of 16 μg^3 m^{-3} (*85*)] and taking the density of *cis*-pinic acid to be that assumed for α-pinene and β-pinene SOA (1.25 g mL^{-1}) (*61–64*), estimated suspended OA mass loadings after ~4 h (74 μg^3 m^{-3}) were comparable to those in the β-pinene ozonolysis experiment (96 μg^3 m^{-3}).

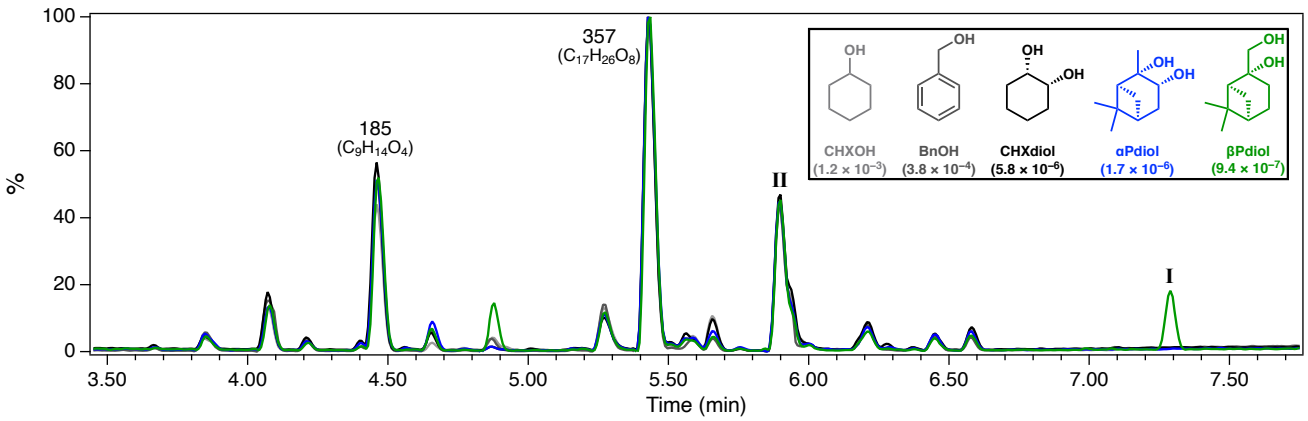

Fig. S4. Role of alcohol volatility in dimer ester formation. BPI chromatograms of SOA formed from ozonolysis of β-pinene after ~4 h of reaction in the CTEC in the presence of CHX as an OH scavenger and alcohols of varying structure and volatility: CHXOH, BnOH, CHXdiol, αPdiol, or βPdiol. Numbers correspond to nominal *m/z* values of $[M–H]^-$ ions; molecular formulas are given in parentheses. Chromatograms are reported as averages of duplicate SOA filter samples collected in parallel for each experiment and are normalized to the area of the $C_{17}H_{26}O_8$ dimer peak. Vapor pressures at 295 K (atm) in legend were estimated using the EVAPORATION model (*86*).

Given suspended SOA mass loadings after ~4 h of ozonolysis of 31 ± 6 μg m^{-3}, equilibrium partitioning theory predicts that only CHXdiol, αPdiol, and βPdiol will be present in the particle phase, with particle-phase fractions of 0.11%, 0.25% and 0.47%, respectively (*87*). Due to the high viscosity of pinene SOA at low RH, however, it has been suggested that particle-phase fractions of semivolatile organic compounds may be overestimated by an order of magnitude or more if equilibrium partitioning is assumed (*80*). Although structural differences (e.g., functionalization and degree of substitution) likely affect the alcohol reactivity, formation only of dimer ester **I** from the least-volatile βPdiol indicates that such factors are second order and that the accretion reaction occurs in the particle not gas phase, otherwise similarly functionalized (CHXdiol and αPdiol) or substituted (BnOH) alcohols should also have produced dimer esters with the *cis*-pinic acid derivative. For the experiments presented in this work, the accretion reaction was likely confined to the particle surface owing to the high viscosity of pinene SOA at low RH (*80*, *81*).

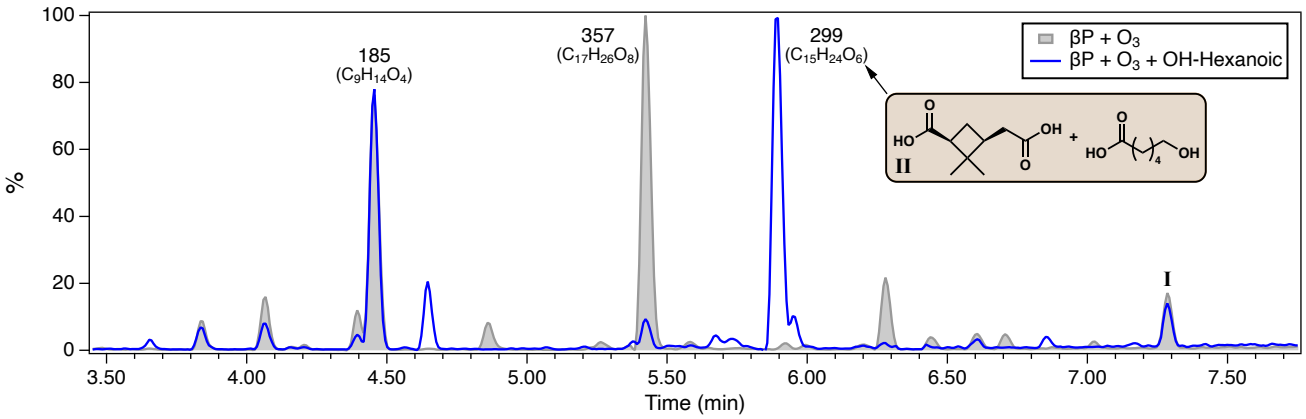

Fig. S5. Formation of dimer ester II. BPI chromatograms of SOA formed from ozonolysis of βP after ~4 h of reaction in the CTEC in the presence and absence of OH-hexanoic acid. Numbers correspond to nominal *m/z* values of $[M–H]^-$ ions; molecular formulas are given in parentheses. Chromatograms are reported as averages of duplicate SOA filter samples collected in parallel for each experiment and scaled such that the largest peak in each experiment is 100%. Structures in shaded box are of monomeric subunits identified for dimer ester **II**.

Formation of dimer ester **II** from reaction of OH-hexanoic acid and the *cis*-pinic acid derivative underscores that volatility not structure is the main determinant of alcohol reactivity. Like BnOH, which did not yield dimer esters (Fig. S4), OH-hexanoic acid is a primary monoalcohol. However, the vapor pressure at 295 K of OH-hexanoic acid estimated using the EVAPORTATION model (7.1×10^{-8} atm) (*86*) is almost an order of magnitude lower than that of βPdiol, resulting in a larger particle-phase fraction and, therefore, efficient dimer ester formation due to effective competition for reaction with the *cis*-pinic acid derivative.

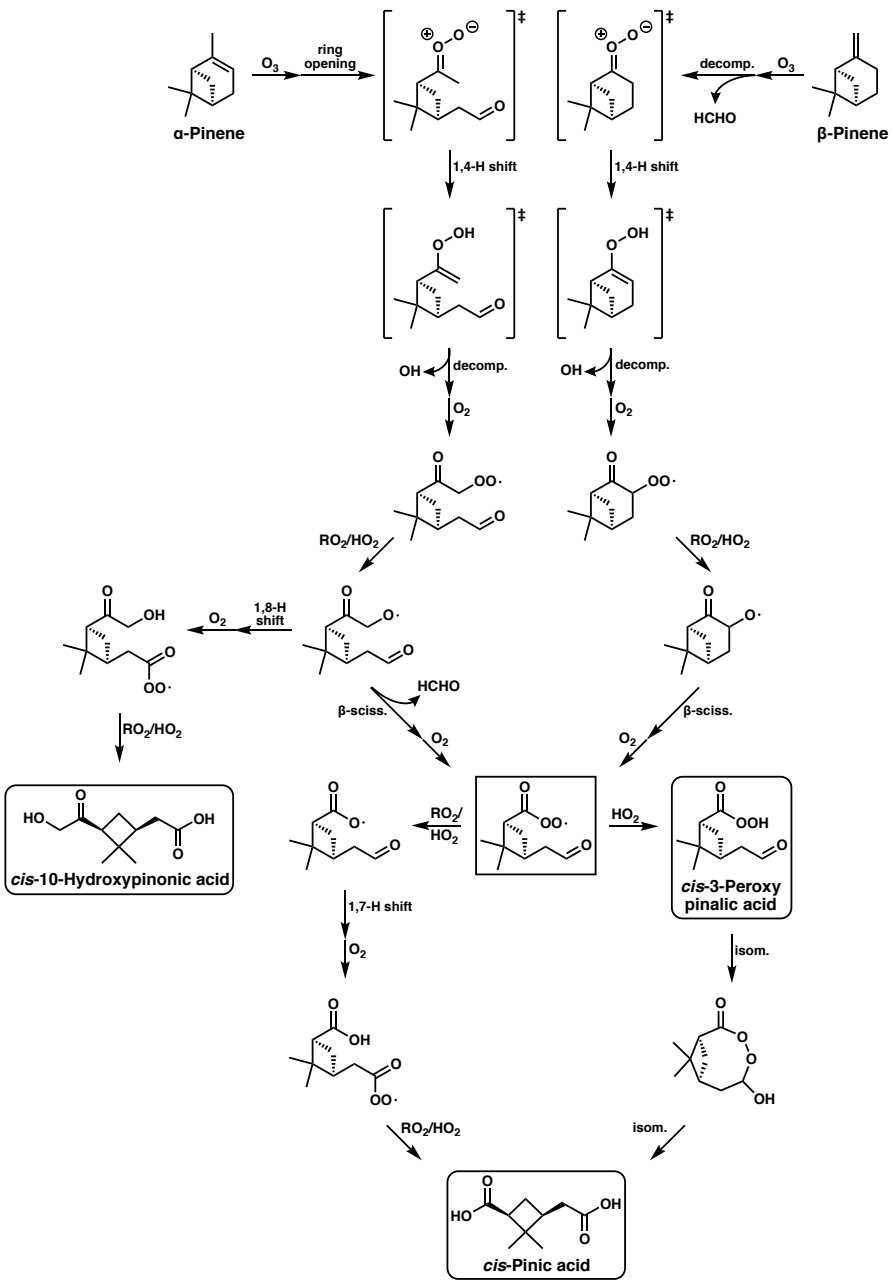

Fig. S6. α-Pinene and β-pinene ozonolysis mechanisms. Production of *cis*-pinic acid is understood to proceed through a common acyl peroxy radical (square box) formed from ozonolysis of both α-pinene and β-pinene (*54*, *88*, *89*). Both RO_2 (*90*) and HO_2 (*91*) channels from the common acyl peroxy radical to *cis*-pinic acid have been proposed. Rounded boxes denote closed-shell products. With the exception of isomerization of *cis*-3-peroxypinalic acid to *cis*-pinic acid via Baeyer-Villiger decomposition of the corresponding cyclic acylperoxyhemiacetal, which is understood to occur in the particle phase (*49*, *79*), all reactions represent gas-phase transformations.

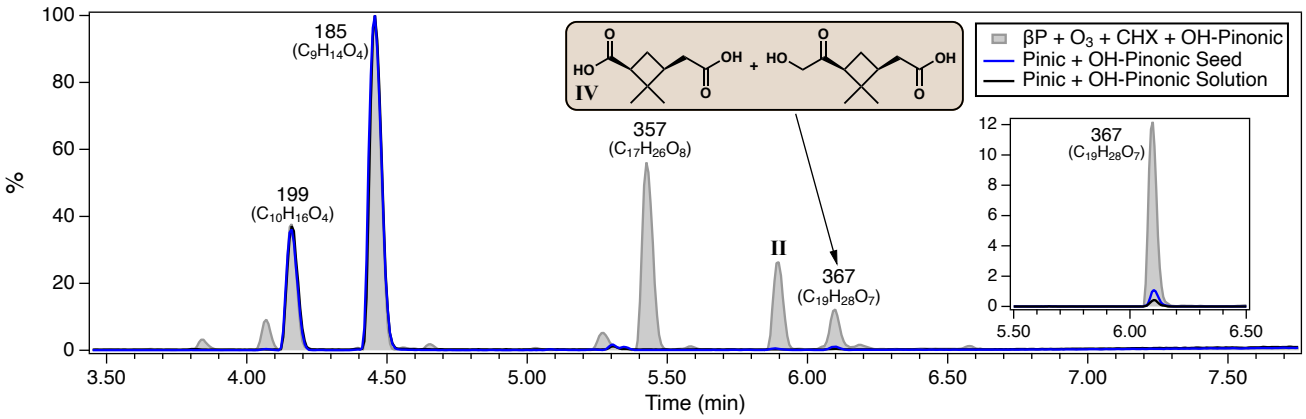

Fig. S7. Lack of dimer ester IV formation via conventional esterification. BPI chromatograms of SOA formed from ozonolysis of βP after ~4 h of reaction in the CTEC in the presence of CHX as an OH scavenger and OH-pinonic acid ($C_{10}H_{16}O_4$), aerosol from a CTEC experiment featuring 80 μm^3 cm^{-3} of seed aerosol generated from an equimolar (0.005 M) aqueous solution of *cis*-pinic acid ($C_9H_{14}O_4$) and OH-pinonic acid after ~4 h, and the aqueous solution of *cis*-pinic acid and OH-pinonic acid after ~4 h. Numbers correspond to nominal *m/z* values of $[M–H]^-$ ions; molecular formulas are given in parentheses. Chromatograms are reported as averages of either duplicate aerosol filter samples collected in parallel for each experiment or solution aliquots and are normalized to the area of the *cis*-pinic acid peak. Structures in shaded box are of monomeric subunits identified for dimer ester **IV**.

Acid-catalyzed esterification of *cis*-pinic acid and OH-pinonic acid in the bulk aqueous solution resulted in negligible production of dimer ester **IV**. Consistent with a recent study (*92*) demonstrating that phosphorylation in atomized aerosol particles occurs at accelerated rates compared to bulk solution, atomization of the aqueous solution and collection of the resulting aerosol yielded a factor-of-two enhancement in the formation of dimer ester **IV**, likely due to rapid water evaporation, increased reactant concentrations, and decreased pH. Nonetheless, the amount of dimer ester **IV**, normalized by the abundance of *cis*-pinic acid, produced in the atomized aerosol was an order of magnitude smaller than that formed from β-pinene ozonolysis with CHX in the presence of OH-pinonic acid.

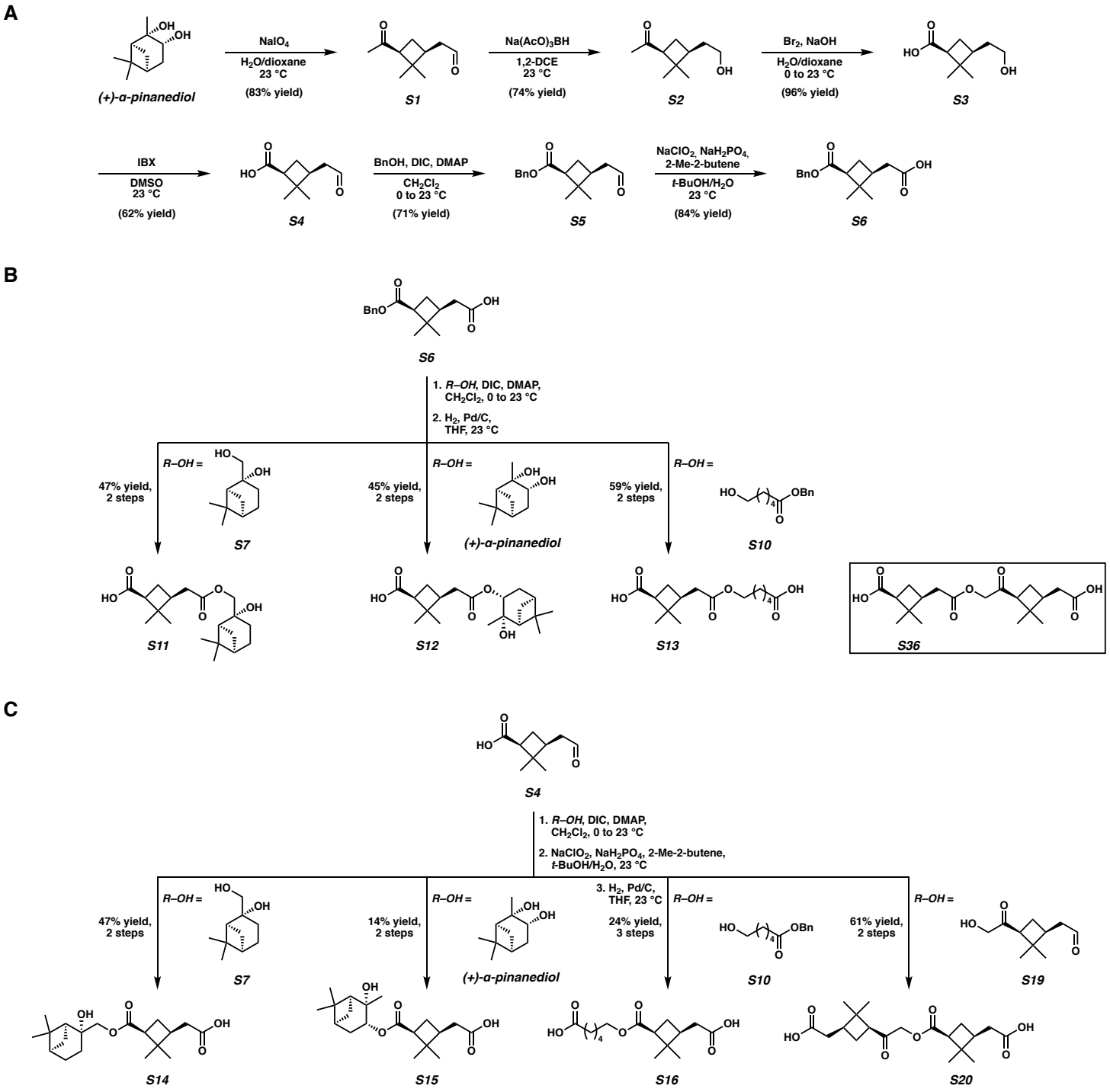

Fig. S8. Synthesis of dimer ester standards. (**A**) Synthesis of (+)-*cis*-3-pinalic acid (**S4**) and (+)-*cis*-pinic acid monobenzyl ester (**S6**) from commercial (+)-αPdiol. (**B** and **C**) Modular synthesis of primary (B) and secondary (C) esters of (+)-*cis*-pinic acid and (+)-βPdiol, OH-hexanoic acid, (+)-αPdiol, and (+)-OH-pinonic acid. Dimer ester **S36** was provided courtesy of the Thomson Group at Northwestern University (*93*). Structure numbering corresponds to that used in Supplementary, S5.

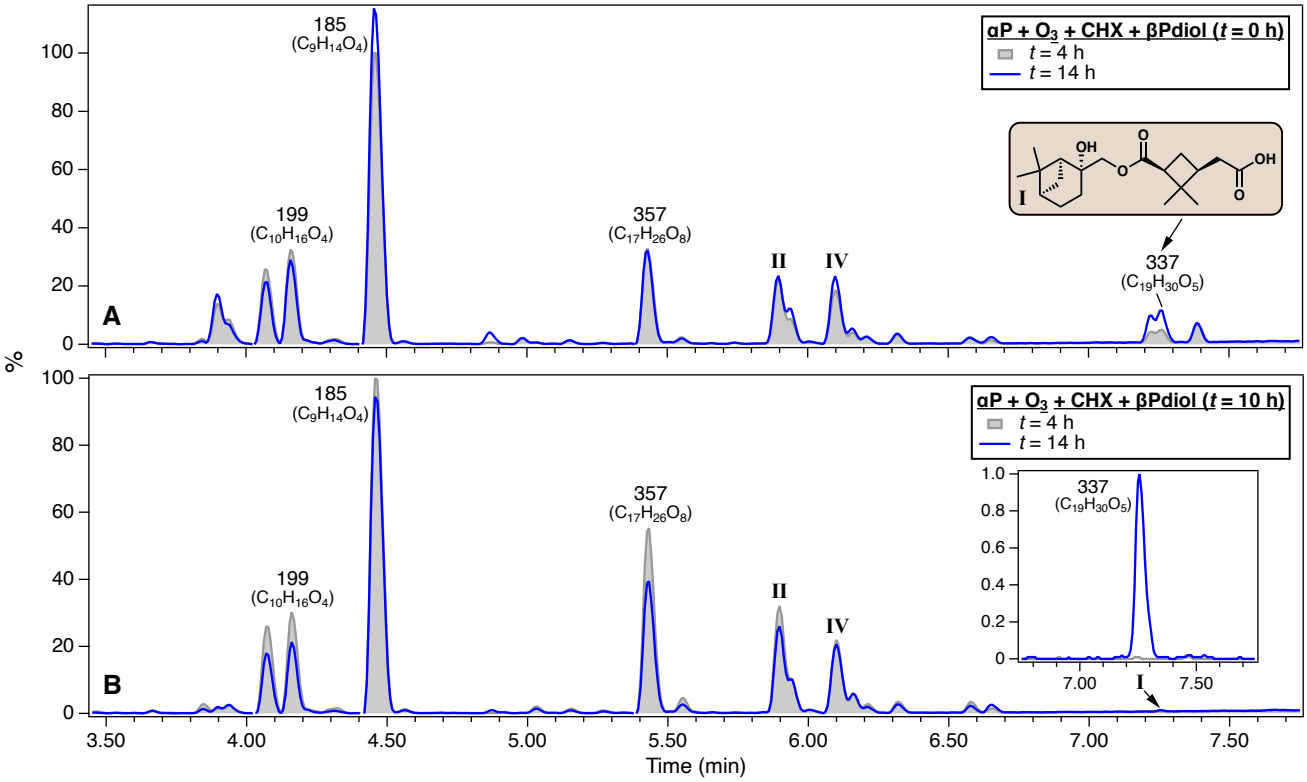

Fig. S9. Dynamics of dimer ester I formation. (**A** and **B**) BPI chromatograms of SOA formed from ozonolysis of α-pinene (αP) after ~4 and ~14 h of reaction in the CTEC in the presence of CHX as an OH scavenger and βPdiol added either prior to (A) or 10 h following (B) the onset of ozonolysis. Numbers correspond to nominal *m/z* values of $[M–H]^-$ ions; molecular formulas are given in parentheses. Chromatograms are normalized to the TOC content of the corresponding SOA filter samples, reported as averages of duplicate samples collected in parallel for each experiment timepoint, and scaled such that the largest peak in the control experiments (gray shading) is 100%.

One set of filter samples in each experiment was collected after ~4 h of potential reaction between βPdiol and the *cis*-pinic acid derivative, initiated by injection of either O_3 in (A) or βPdiol in (B). Although βPdiol exposure (concentration × time) was lower in (B) due to addition during the reaction period, βPdiol concentrations were never limiting; gas-phase βPdiol concentrations in (A) and (B) were both a factor of two larger than those in typical β-pinene ozonolysis experiments after less than 10 min of injection and within 10% of one another at the start of filter collection [t = 4 in (A) and t = 14 h in (B)].

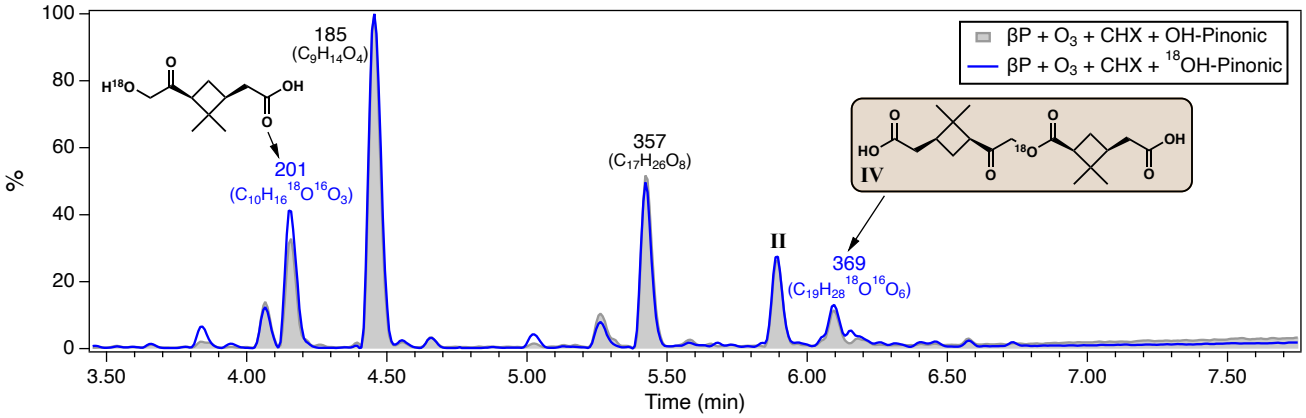

Fig. S10. Formation of ^{18}O-labeled dimer ester IV. BPI chromatograms of SOA formed from ozonolysis of βP after ~4 h of reaction in the CTEC in the presence of CHX as an OH scavenger and either OH-pinonic acid or ^{18}OH-pinonic acid. Numbers correspond to nominal *m/z* values of $[M-H]^-$ ions; molecular formulas are given in parentheses. Chromatograms are reported as averages of duplicate SOA filter samples collected in parallel for each experiment and are normalized to the area of the *cis*-pinic acid ($C_9H_{14}O_4$) peak.

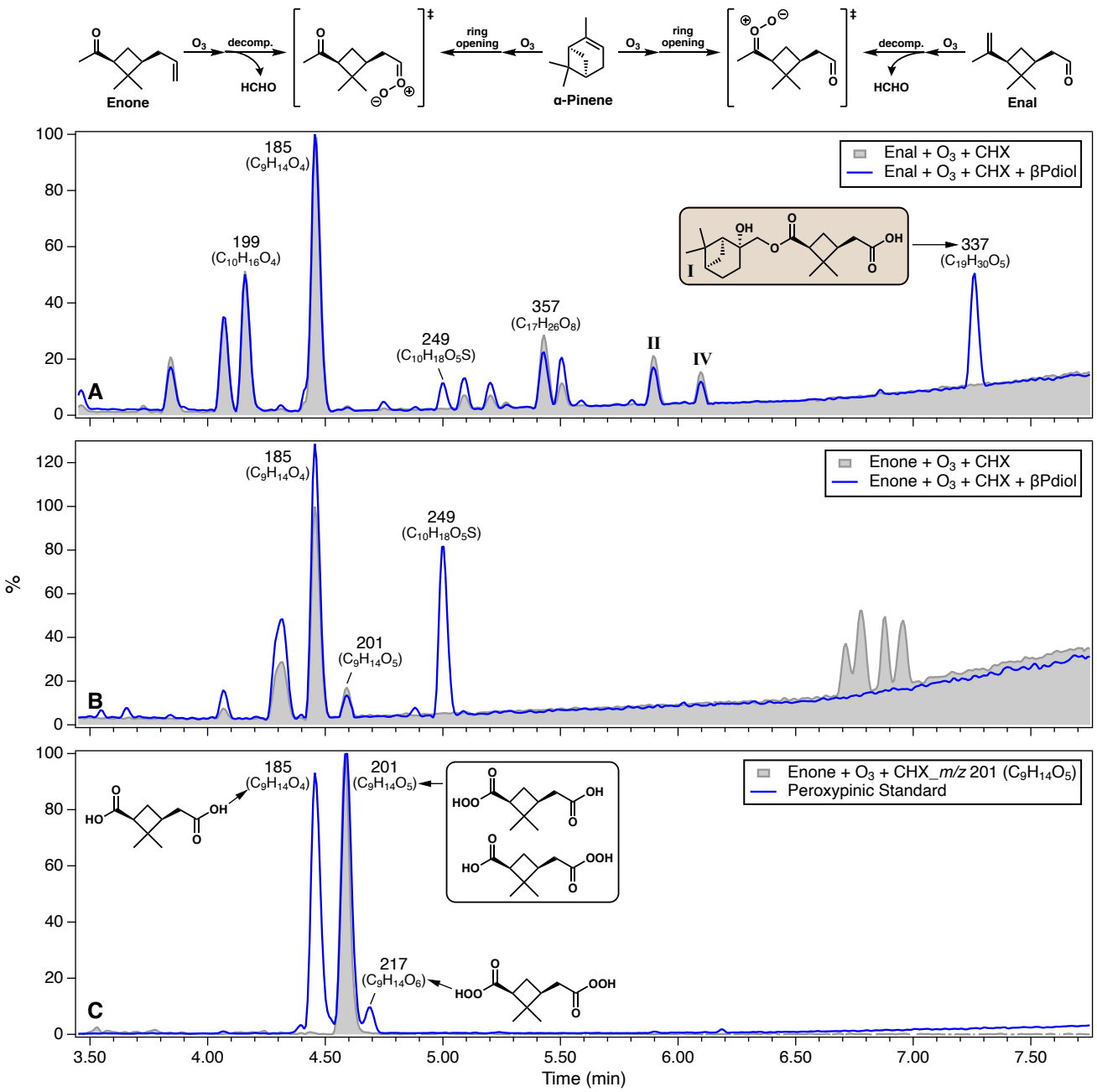

Fig. S11. Enone and enal ozonolysis. (**A** and **B**) BPI chromatograms of SOA formed from ozonolysis of the enal (A) and enone (B) after ~4 h of reaction in the CTEC in the presence of CHX as an OH scavenger with and without addition of βPdiol. (**C**) EIC of $C_9H_{14}O_5$ in SOA from enone ozonolysis and BPI chromatogram of a synthesized mixture of *cis*-pinic acid ($C_9H_{14}O_4$), *cis*-monoperoxypinic acid isomers ($C_9H_{14}O_5$), and *cis*-diperoxypinic acid ($C_9H_{14}O_6$). Numbers in (A)–(C) correspond to nominal *m/z* values of $[M–H]^-$ ions; molecular formulas are given in parentheses. Chromatograms in (A) and (B) are normalized to the TOC content of the corresponding SOA filter samples, reported as averages of duplicate samples collected in parallel for each experiment, and scaled such that the largest peak in the control experiments (gray shading) is 100%. Chromatograms in (C) are normalized to the area of the $C_9H_{14}O_5$ peak.

Although dimer esters **I**, **II**, and **IV**, as well as the major $C_{17}H_{26}O_8$ dimer and OH-pinonic acid ($C_{10}H_{16}O_4$) were detected only in SOA from ozonolysis of the enal, consistent with current understanding that the acyl peroxy radical common to α-pinene and β-pinene ozonolysis (Fig. S6) stems only from the enal-derived Criegee intermediate, *cis*-pinic acid was observed in SOA from ozonolysis of both the enal and enone, as recently reported (*94*). Additionally, *cis*-monoperoxypinic acid, which is also presumed to form from the common acyl peroxy radical (*95*), was detected in SOA from ozonolysis of the enone but not enal. These compositional differences indicate that unidentified pathways not involving the common acyl peroxy radical are operative in forming *cis*-pinic acid and *cis*-monoperoxypinic acid from ozonolysis of the enone and, by extension, α-pinene.

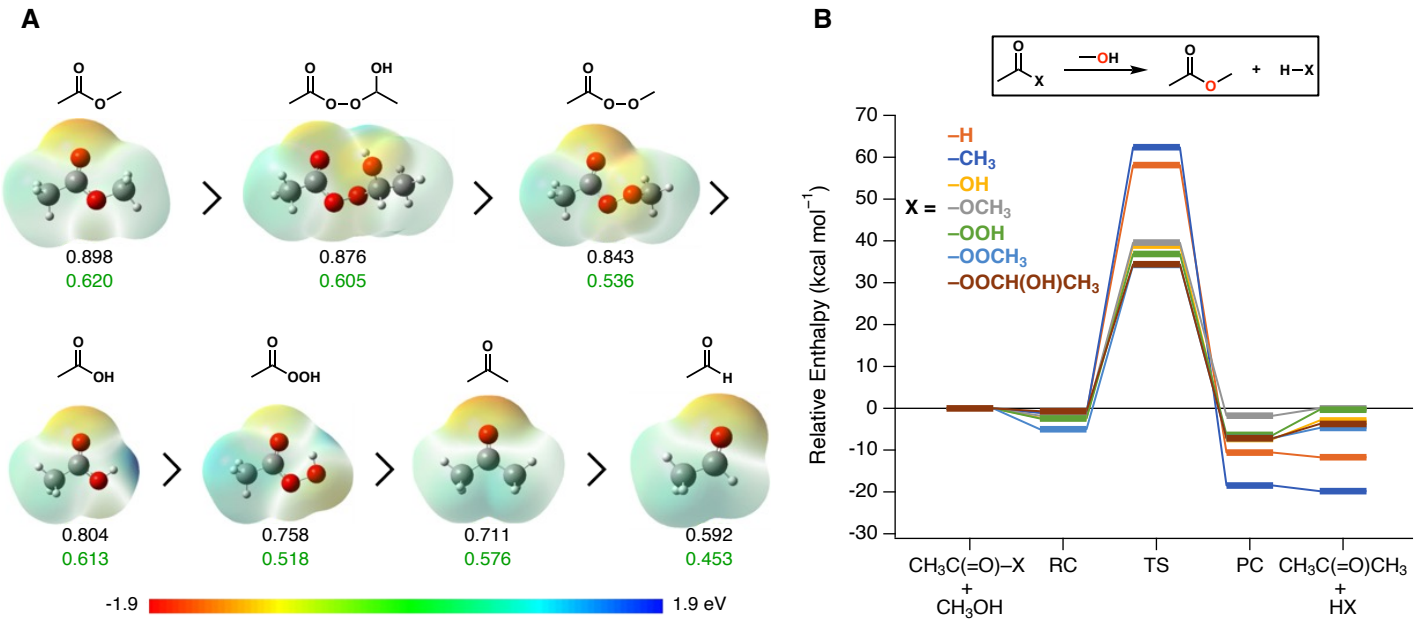

Fig. S12. Quantum chemical calculations for carboxylic acid derivatives [$CH_3C(=O)–X$]. (**A**) Electrostatic potential (ESP) contoured on the electron density isosurface (isovalue = 0.0027 e Å^{-3}). Numbers correspond to ESP charge (black) and Mulliken charge (green) of the carbonyl carbon atom ([e]). (**B**) One-step reaction potential for esterification with methanol (CH_3OH) in vacuum. The reactants [$CH_3C(=O)–X$ + CH_3OH] first form a reactant complex [RC, $CH_3C(=O)–X•CH_3OH$], the RC proceeds through a transition state (TS) forming a product complex [PC, $CH_3C(=O)OCH_3•HX$], and the PC dissociates to the final products [$CH_3C(=O)OCH_3$ + HX]. All charges, ESP surfaces, and reaction potentials were calculated at the B3LYP/6-31+G(d) level on the lowest zero-point-vibrational-corrected electronic energy (E+ZPVE) conformers. Reaction potentials calculated at the M06-2X/aug-cc-pVTZ and ωB97X-D/aug-cc-pVTZ levels yielded similar results in relative reactivity.

Esterification of the acylperoxyhemiacetal (X = $–OOCH(OH)CH_3$) with CH_3OH was found to have the lowest reaction barrier of the carboxylic acid derivatives, calculated from either the reactants to TS (34.4 kcal mol^{-1}) or RC to TS (35.1 kcal mol^{-1}). The carbonyl carbon of the acylperoxyhemiacetal was also calculated to have the second-highest ESP charge (0.876 e).

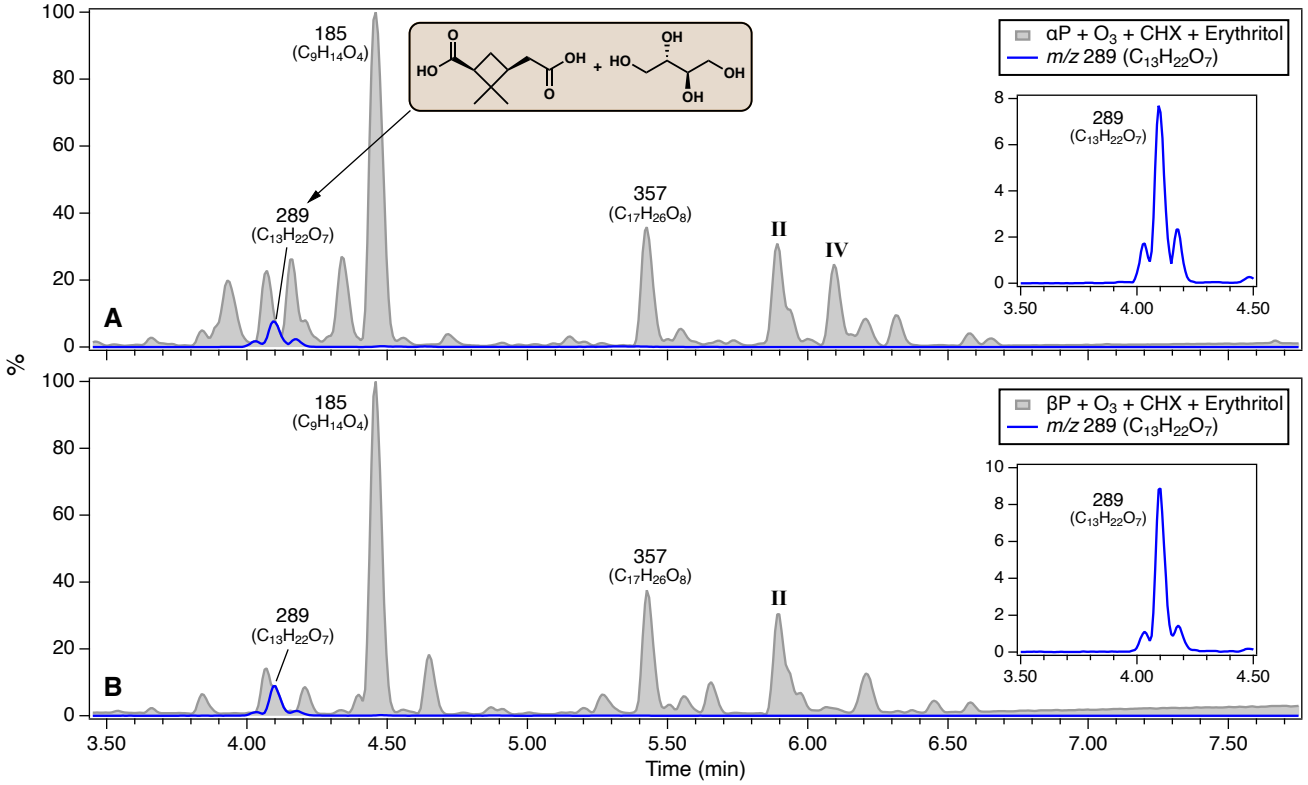

Fig. S13. Formation of dimer esters from *meso*-erythritol. (**A** and **B**) BPI chromatograms of SOA formed from ozonolysis of αP (A) and βP (B) after ~4 h of reaction in the CTEC in the presence of CHX as an OH scavenger and *meso*-erythritol, and EICs of $C_{13}H_{22}O_7$. Numbers correspond to nominal *m/z* values of $[M–H]^-$ ions; molecular formulas are given in parentheses. Chromatograms are reported as averages of duplicate SOA filter samples collected in parallel for each experiment. Structures in shaded box are of monomeric subunits identified for $C_{13}H_{22}O_7$ dimer ester isomers.

MS/MS analysis indicates that the $C_{13}H_{22}O_7$ dimers formed on addition of *meso*-erythritol to α-pinene and β-pinene ozonolysis experiments with CHX are esters of *cis*-pinic acid and *meso*-erythritol. The distribution of $C_{13}H_{22}O_7$ dimer esters is consistent with the expected impact of steric hindrance on the efficiency of nucleophilic addition of the primary vs. secondary alcohols of *meso*-erythritol to the cyclic acylperoxyhemiacetal derived from *cis*-3-peroxypinalic acid. Although the total peak area of the $C_{13}H_{22}O_7$ dimer esters is only ~25–35% that of either dimer ester **II** or **IV**, given the strong dependence of (–)ESI efficiency on both molecular size [$(–)ESI_{dimer} \gtrsim 10(–)ESI_{monomer}$] and the number of ionizable carboxyl groups [$(–)ESI_{diacid} \gtrsim 2(–)ESI_{monoacid}$] (*34*) it is likely that the smaller, monocarboxylic $C_{13}H_{22}O_7$ dimer esters are more abundant SOA constituents than the larger, dicarboxylic dimer esters **II** and **IV**. In contrast to gas-phase reactions between isoprene- and pinene-derived RO_2 that have been shown to suppress the formation of low-volatility products and SOA mass (*96*), production of the $C_{13}H_{22}O_7$ dimer esters illustrates that particle-phase reactions of semivolatile isoprene- and pinene-derived oxidation products can serve as a source of low-volatility dimeric compounds for SOA growth.

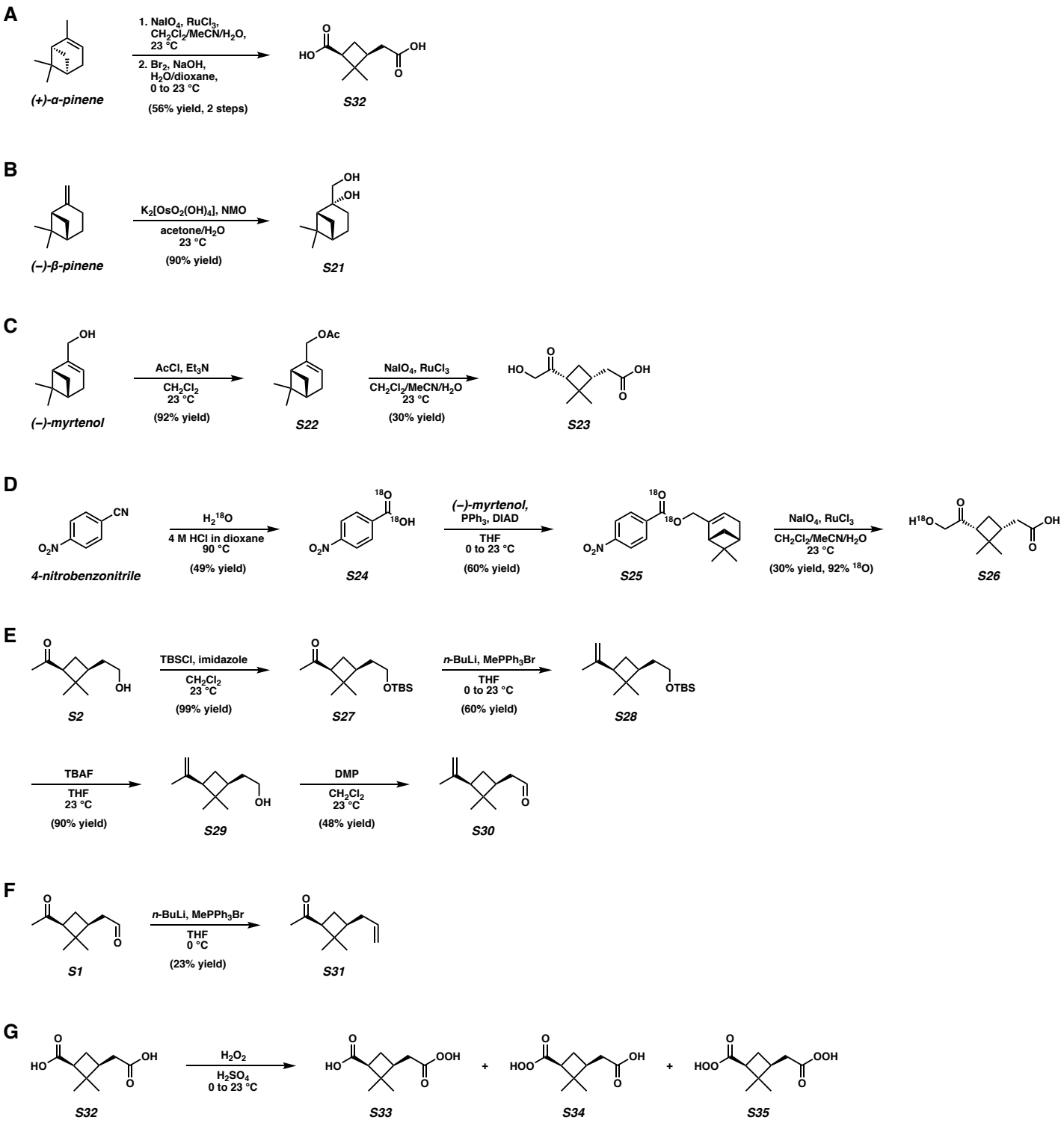

Fig. S14. Synthesis of compounds used in CTEC experiments. (**A**) (+)-*cis*-Pinic acid (**S32**), (**B**) (–)-βPdiol (**S21**), (**C**) (–)-OH-pinonic acid (**S23**), (**D**) (–)-^{18}OH-pinonic acid (**S26**), (**E**) (+)-enal (**S30**), (**F**) (+)-enone (**S31**), and (**G**) (+)-*cis*-monoperoxypinic acid isomers (**S33** and **S34**) and (+)-*cis*-diperoxypinic acid (**S35**). Structure numbering corresponds to that used in Supplementary, S5.

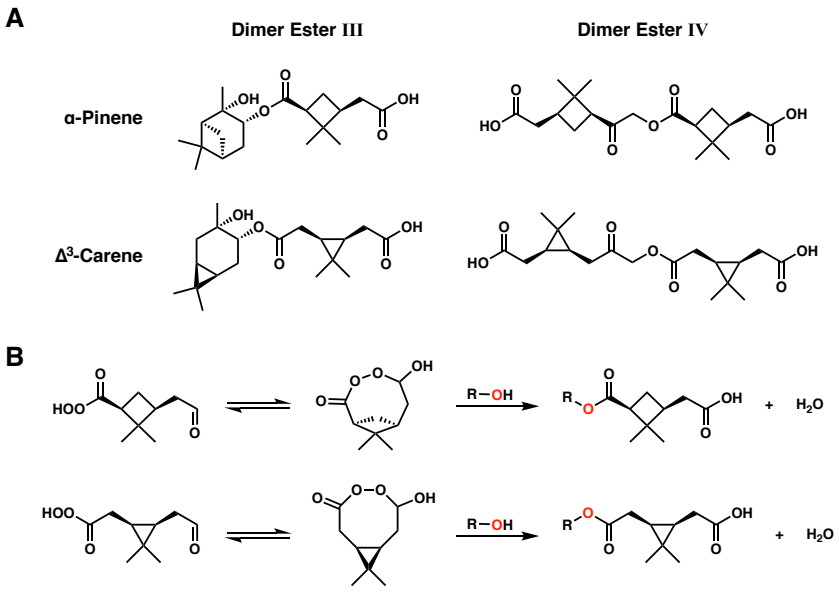

Fig. S15. Formation of dimer esters in Δ³-carene SOA. (**A**) Structures of dimer esters **III** and **IV** as well as of proposed analogs identified in SOA formed from ozonolysis of Δ³-carene (*82*). (**B**) Proposed formation mechanism of dimer esters in pinene and Δ³-carene SOA via particle-phase nucleophilic addition of semi/low-volatility alcohols to the cyclic acylperoxyhemiacetals derived from *cis*-3-peroxypinalic acid and *cis*-peroxycaralic acid, respectively.

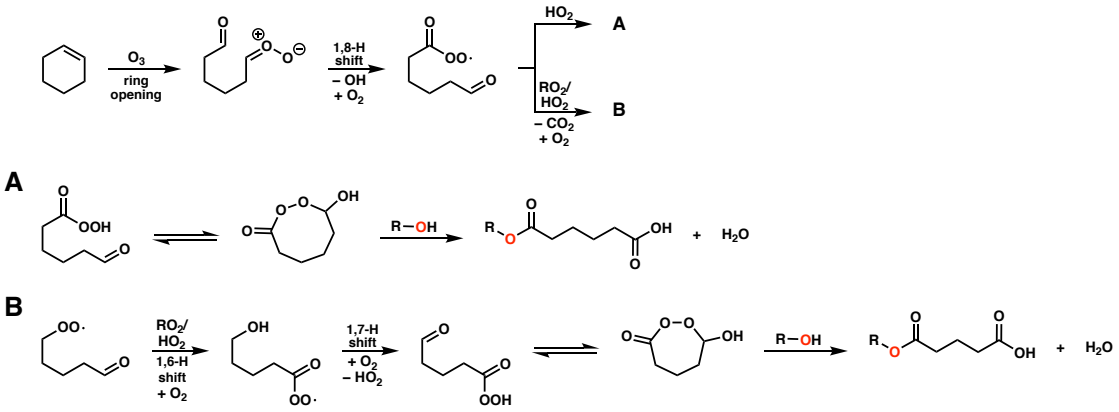

Fig. S16. Formation of dimer esters in cyclohexene SOA. (**A** and **B**) Proposed formation mechanism of dimer esters in SOA from cyclohexene ozonolysis with adipic acid (A) and glutaric acid (B) subunits (*12*, *83*) via particle-phase nucleophilic addition of semi/low-volatility alcohols to the cyclic acylperoxyhemiacetals derived from 6-oxohexaneperoxoic acid and 5-oxopentaneperoxoic acid, respectively.

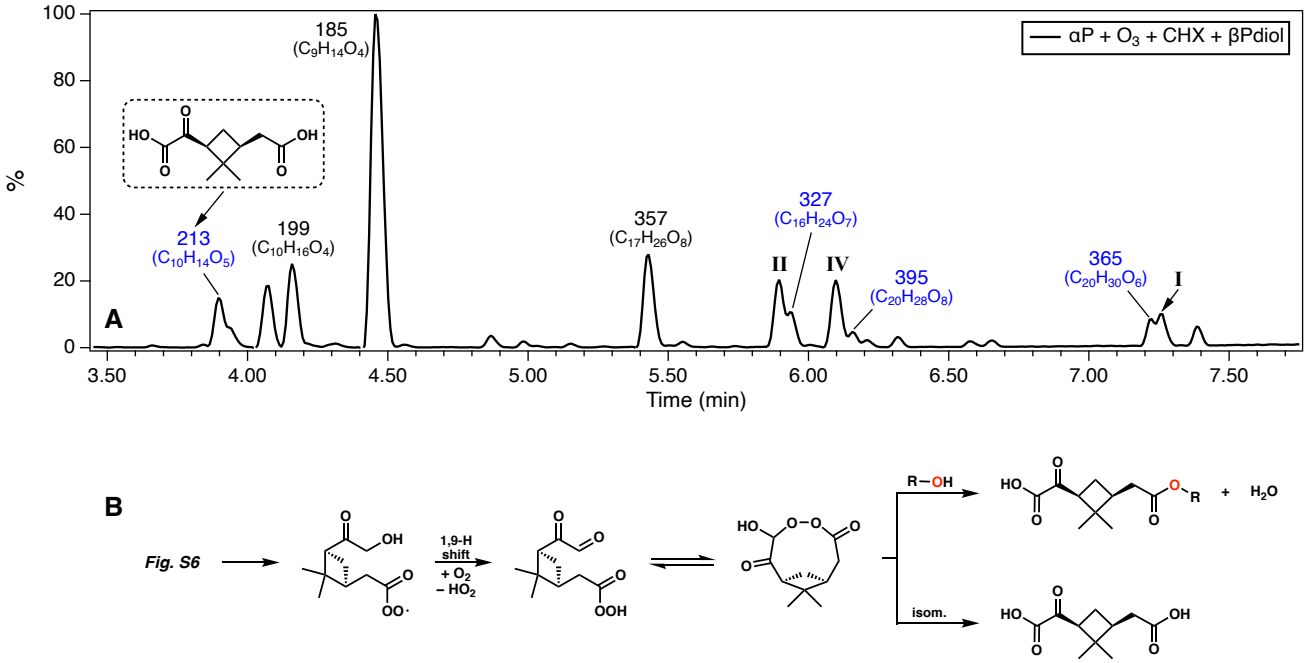

Fig. S17. Formation of dimer ester I–IV homologues. (**A**) BPI chromatogram of SOA formed from ozonolysis of αP after ~4 h of reaction in the CTEC in the presence of CHX as an OH scavenger and βPdiol. Numbers correspond to nominal *m/z* values of $[M–H]^-$ ions; molecular formulas are given in parentheses. Chromatogram is reported as an average of duplicate SOA filter samples collected in parallel for the experiment. Structure in dashed box denotes that of *cis*-10-carboxypinonic acid ($C_{10}H_{14}O_5$) proposed in a past study (*30*). Homologues of dimer esters **I** ($C_{20}H_{30}O_6$), **II** ($C_{16}H_{24}O_7$), and **IV** ($C_{20}H_{28}O_8$), suggested to contain *cis*-10-carboxypinonic acid subunits based on MS/MS analysis, are indicated by blue font. (**B**) Proposed formation mechanism of dimer ester homologues via particle-phase nucleophilic addition of a semivolatile alcohol (i.e., βPdiol, OH-hexanoic acid, or OH-pinonic acid) to the cyclic acylperoxyhemiacetal derived from *cis*-10-oxoperoxypinonic acid, as well as of *cis*-10-carboxypinonic acid via Baeyer-Villiger decomposition of the cyclic acylperoxyhemiacetal.

S4. Table S1

Table S1. Representative initial conditions for ozonolysis experiments in the CTEC.[a]

Exp. Type	$[VOC]_0$ (ppb)[b]	$[O_3]_0$ (ppb)	$[OH\ Scavenger]_0$ (ppm)	$[ROH]_0$ (ppb)[c]	Seed Aerosol[c]
A	100	150	–	–	$(NH_4)_2SO_4$
B	100	150	25 (CHX) or 185 (MeOH)	–	$(NH_4)_2SO_4$
C1	100	150	25 (CHX)	100	$(NH_4)_2SO_4$
C2	100	150	–	100	$(NH_4)_2SO_4$
C3	100	150	25 (CHX)	–	$(NH_4)_2SO_4$ + ROH (2:1)

[a]~6-h or ~16-h duration; $T_0 = 295 \pm 2$ K; P = 1 atm; RH < 5%; $[NO_x]_0 < 0.5$ ppb.
[b]Volatile organic compound (VOC): (+)-α-pinene, (–)-β-pinene, (+)-enone, or (+)-enal.
[c]Alcohol (ROH) added via thermal desorption [CHXOH, BnOH, CHXdiol, (+)-αPdiol, (–)-βPdiol, or OH-hexanoic acid] or atomization of aqueous solution of $(NH_4)_2SO_4$ and ROH [(–)-OH-pinonic acid, (–)-^{18}OH-pinonic acid, or *meso*-erythritol] in 2:1 mass ratio.

S5. Synthetic Procedures and Characterization Data

General Information

Unless otherwise stated, reactions were performed in flame-dried glassware under ambient conditions using dry, deoxygenated solvents. Solvents were dried by passage through an activated alumina column under Ar. Reagents were purchased from commercial sources and used as received. Reaction temperatures were controlled by an IKAmag temperature modulator. Thin-layer chromatography (TLC) was performed using E. Merck silica gel 60 F254 pre-coated plates (250 μm) and visualized by UV fluorescence quenching, potassium permanganate staining, or *p*-anisaldehyde staining. Silicycle Silia*Flash* P60 Academic Silica gel (particle size 40–63 μm) was used for flash chromatography. ^{1}H and ^{13}C NMR spectra were recorded on Varian Inova 500 (500 and 125 MHz, respectively), Varian Inova 600 (600 and 150 MHz, respectively), and Bruker 400 (400 and 100 MHz, respectively) spectrometers and are reported in terms of chemical shift relative to $CHCl_3$ (δ 7.26 and 77.16 ppm, respectively) or CH_3OH (δ 3.31 and 49.01 ppm, respectively). Data for ^{1}H NMR are reported as follows: chemical shift (δ ppm) (multiplicity, coupling constant, integration). Abbreviations are used as follows: s = singlet, d = doublet, t = triplet, q = quartet, m = multiplet. IR spectra were obtained from thin films deposited on NaCl plates using a Perkin Elmer Spectrum BXII spectrometer and are reported in frequency of absorption (cm^{-1}). Optical rotations were measured with a Jasco P-2000 polarimeter operating on the sodium D-line (589 nm) using a 100 mm path-length cell. High-resolution mass spectra (HRMS) were acquired using a Waters ACQUITY UPLC I-Class system coupled to a Xevo G2-S ESI-Q-TOF-MS, an Agilent 6200 Series TOF-MS with an Agilent G1978A multimode ESI-atmospheric pressure chemical ionization (MM:ESI-APCI) source, or a JEOL JMS-T2000GC AccuTOF GC-Alpha equipped with a field ionization (FI) source.

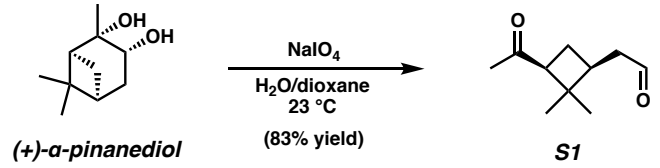

2-((1*S*,3*S*)-3-acetyl-2,2-dimethylcyclobutyl)acetaldehyde ((+)-*cis*-pinonaldehyde, S1)

(+)-*cis*-Pinonaldehyde (**S1**) was prepared according to a modified literature procedure (*94*) from commercial (+)-α-pinanediol (99%, 99% ee, Sigma-Aldrich). To a stirred solution of (+)-α-pinanediol (4.05 g, 23.8 mmol, 1.0 equiv) in H_2O/dioxane (1:2, 120 mL) at 23 °C was added $NaIO_4$ (12.2 g, 57.1 mmol, 2.4 equiv) in one portion. The mixture was stirred for 6 h at 23 °C, at which point TLC indicated complete consumption of the starting material. The solution was diluted with Et_2O (200 mL) and H_2O (200 mL). The layers were separated and the aqueous layer was extracted with Et_2O (3 × 200 mL). The combined organic phases were washed with brine, dried over $MgSO_4$, and concentrated to afford the title compound as a colorless oil (3.31 g, 19.7 mmol, 83% yield) in sufficient purity by NMR for use in the subsequent reaction. ^{1}H NMR (400 MHz, $CDCl_3$) δ 9.74 (t, *J* = 1.5 Hz, 1H), 2.92 (dd, *J* = 10.0, 7.7 Hz, 1H), 2.55 – 2.35 (m, 3H), 2.04 (s, 3H), 2.02 – 1.90 (m, 2H), 1.34 (s, 3H), 0.84 (s, 3H); ^{13}C NMR (100 MHz, $CDCl_3$) δ 207.5, 201.6, 54.5, 45.3, 43.4, 35.9, 30.5, 30.3, 22.9, 17.8. Spectral data are in good accordance with previously reported values (*94*, *97*).

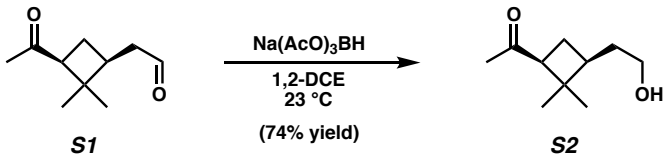

1-((1*S*,3*S*)-3-(2-hydroxyethyl)-2,2-dimethylcyclobutyl)ethan-1-one (S2)

To a stirred solution of (+)-*cis*-pinonaldehyde (**S1**) (2.50 g, 14.9 mmol, 1.0 equiv) in 1,2-DCE (25 mL) at 23 °C was added $Na(OAc)_3BH$ (7.25 g, 34.2 mmol, 2.3 equiv) in one portion. The resulting suspension was stirred for 24 h at 23 °C, at which point TLC indicated complete consumption of **S1**. The mixture was quenched by addition of H_2O (25 mL) and diluted with Et_2O (100 mL) and H_2O (100 mL). The layers were separated and the aqueous layer was extracted with Et_2O (3 × 100 mL). The combined organic phases were washed with brine, dried over $MgSO_4$, and concentrated. The crude product was purified by flash chromatography (30–60% EtOAc/hexanes) to afford the title compound as a colorless oil (1.88 g, 11.0 mmol, 74% yield). $[\alpha]_D^{25}$ +65.5° (*c* 1.0, $CHCl_3$); ^1H NMR (600 MHz, $CDCl_3$) δ 3.61 – 3.45 (m, 2H), 2.80 (dd, *J* = 10.2, 7.5 Hz, 1H), 2.02 – 1.97 (m, 4H), 1.92 – 1.78 (m, 2H), 1.58 (dq, *J* = 13.5, 6.8 Hz, 1H), 1.46 – 1.38 (m, 1H), 1.26 (s, 3H), 0.83 (s, 3H); ^{13}C NMR (150 MHz, $CDCl_3$) δ 208.3, 61.2, 54.5, 43.4, 38.7, 33.2, 30.5, 30.2, 23.1, 17.3; IR (thin film, NaCl) 3413, 2948, 2872, 1702, 1461, 1384, 1367, 1357, 1224, 1181, 1157, 1181, 1053 cm^{-1}; HRMS (MM:ESI-APCI+) *m/z* calc'd for $[M+Na]^+$ $C_{10}H_{18}O_2Na$ = 193.1204, found 193.1205.

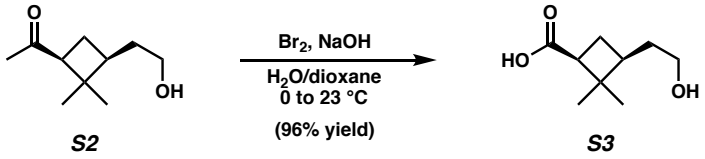

(1*S*,3*S*)-3-(2-hydroxyethyl)-2,2-dimethylcyclobutane-1-carboxylic acid (S3)

To a stirred solution of alcohol S2 (750 mg, 4.40 mmol, 1.0 equiv) in H_2O/dioxane (1:5, 65 mL) at 0 °C was added dropwise an aqueous solution of NaOBr, prepared via addition of Br_2 (745 µL, 14.5 mmol, 3.3 equiv) to a solution of NaOH (2.29 g, 57.2 mmol, 13.0 equiv) in H_2O (22 mL) at 0 °C. The mixture was stirred for 2 h and gradually allowed to warm to 23 °C, at which point TLC indicated complete consumption of **S2**. The mixture was diluted with H_2O (100 mL) and washed with Et_2O (2 × 100 mL). The aqueous phase was acidified to pH 2 with concentrated HCl and extracted with EtOAc (3 × 100 mL). The combined organic phases were washed with brine, dried over $MgSO_4$, and concentrated to afford the title compound as a colorless oil (729 mg, 4.23 mmol, 96% yield) in sufficient purity by NMR for use in the subsequent reaction. $[\alpha]_D^{25}$ = –9.4° (*c* 1.0, $CHCl_3$); ^1H NMR (400 MHz, $CDCl_3$) δ 3.62 – 3.51 (m, 2H), 2.72 (dd, *J* = 10.2, 7.3 Hz, 1H), 2.08 – 1.95 (m, 2H), 1.93 – 1.78 (m, 1H), 1.64 (dq, *J* = 13.4, 6.9 Hz, 1H), 1.55 – 1.44 (m, 1H), 1.20 (s, 3H), 0.98 (s, 3H); ^{13}C NMR (100 MHz, $CDCl_3$) δ 178.5, 61.2, 46.2, 43.0, 39.0, 33.3, 30.3, 24.5, 17.6; IR (thin film, NaCl) 3373, 2952, 2885, 2730, 1699, 1460, 1417, 1369, 1332, 1244, 1203, 1050, 1029 cm^{-1}; HRMS (MM:ESI-APCI–) *m/z* calc'd for $[M–H]^-$ $C_9H_{15}O_3$ = 171.1021, found 171.1021.

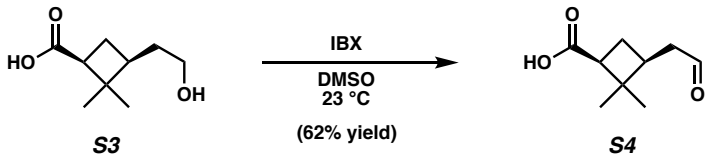

S3 *S4*

(1*S*,3*S*)-2,2-dimethyl-3-(2-oxoethyl)cyclobutane-1-carboxylic acid ((+)-cis-3-pinalic acid, S4)
To a stirred solution of acid **S3** (729 mg, 4.23 mmol, 1.0 equiv) in DMSO (42 mL) at 23 °C was added IBX (1.78 g, 6.35 mmol, 1.5 equiv) in one portion. The mixture was stirred for 16 h at 23 °C, at which point TLC indicated complete consumption of **S3**. The solution was diluted with EtOAc (100 mL) and H_2O (100 mL). The layers were separated and the aqueous layer was extracted with EtOAc (3 × 100 mL). The combined organic phases were washed with brine, dried over $MgSO_4$, and concentrated. The crude product was purified by flash chromatography (20–50% EtOAc/hexanes) to afford the title compound as a colorless oil (443 mg, 2.60 mmol, 62% yield). $[\alpha]_D^{25} = -0.80°$ (*c* 1.0, $CHCl_3$); ^{1}H NMR (600 MHz, $CDCl_3$) δ 9.72 (t, *J* = 1.5 Hz, 1H), 2.81 (dd, *J* = 10.2, 7.9 Hz, 1H), 2.56 – 2.49 (m, 1H), 2.48 – 2.40 (m, 2H), 2.13 (dt, *J* = 11.4, 7.8 Hz, 1H), 1.92 (dt, *J* = 11.3, 10.0 Hz, 1H), 1.25 (s, 3H), 0.97 (s, 3H); ^{13}C NMR (100 MHz, $CDCl_3$) δ 201.6, 179.0, 46.4, 45.4, 43.1, 36.1, 30.2, 24.2, 18.0; IR (thin film, NaCl) 2960, 1873, 1733, 1705, 1698, 1650, 1425, 1247, 1216, 1161, 935 cm^{-1}; HRMS (ESI-TOF) *m/z* calc'd for $[M-H]^-$ $C_9H_{13}O_3$ = 169.0865, found 169.0864.

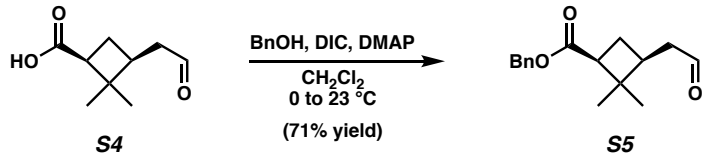

S4 *S5*

benzyl (1*S*,3*S*)-2,2-dimethyl-3-(2-oxoethyl)cyclobutane-1-carboxylate (S5)
To a stirred solution of aldehyde **S4** (200 mg, 1.18 mmol, 1.0 equiv), benzyl alcohol (245 µL, 2.36 mmol, 2.0 equiv), and DMAP (7.2 mg, 0.0590 mmol, 0.05 equiv) in CH_2Cl_2 (12 mL) at 0 °C was added DIC (370 µL, 2.36 mmol, 2.0 equiv) dropwise. The mixture was stirred for 2 h and gradually allowed to warm to 23 °C, at which point TLC indicated complete consumption of **S4**. The solution was diluted with Et_2O (50 mL) and H_2O (50 mL). The layers were separated and the aqueous layer was extracted with Et_2O (3 × 50 mL). The combined organic phases were washed with brine, dried over $MgSO_4$, and concentrated. The crude product was purified by flash chromatography (10–20% EtOAc/hexanes) to afford the title compound as a colorless oil (219 mg, 0.841 mmol, 71% yield). $[\alpha]_D^{25} = -5.1°$ (*c* 0.83, $CHCl_3$); ^{1}H NMR (400 MHz, $CDCl_3$) δ 9.68 (t, *J* = 1.7 Hz, 1H), 7.38 – 7.21 (m, 5H), 5.13 – 5.02 (m, 2H), 2.79 (dd, *J* = 10.2, 7.9 Hz, 1H), 2.53 – 2.33 (m, 3H), 2.14 – 2.06 (m, 1H), 2.02 – 1.88 (m, 1H), 1.20 (s, 3H), 0.83 (s, 3H); ^{13}C NMR (100 MHz, $CDCl_3$) δ 201.4, 172.6, 136.2, 128.6, 128.3, 128.2, 66.0, 46.4, 45.4, 42.9, 36.1, 30.2, 24.4, 18.0; IR (thin film, NaCl) 2954, 2880, 2718, 1726, 1455, 1383, 1336, 1231, 1173, 1130, 1023, 749, 735, 696 cm^{-1}; HRMS (ESI-TOF) *m/z* calc'd for $[M+Na]^+$ $C_{16}H_{20}O_3Na$ = 283.1310, found 283.1307.

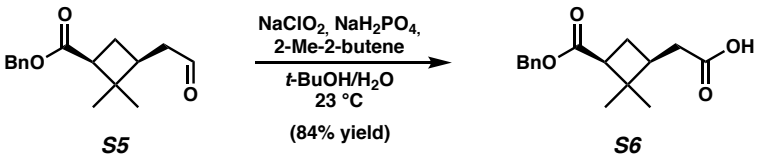

2-((1*S*,3*S*)-3-((benzyloxy)carbonyl)-2,2-dimethylcyclobutyl)acetic acid (S6)
To a stirred solution of benzyl ester **S5** (397 mg, 1.52 mmol, 1.0 equiv), NaH_2PO_4 (1.09 g, 9.12 mmol, 6.0 equiv), and 2-Me-2-butene (12.9 mL, 122 mmol, 80.0 equiv) in t-BuOH/H_2O (5:1, 180 mL) at 23 °C was added $NaClO_2$ (413 mg, 4.56 mmol, 3.0 equiv) in one portion. The mixture was stirred for 2 h at 23 °C, at which point TLC indicated complete consumption of **S5**. The t-BuOH was removed by rotary evaporation, and the remaining solution was diluted with EtOAc (50 mL) and H_2O (50 mL). The layers were separated and the aqueous layer was extracted with EtOAc (3 × 50 mL). The combined organic phases were washed with brine, dried over $MgSO_4$, and concentrated. The crude product was purified by flash chromatography (50–60% EtOAc/hexanes) to afford the title compound as a colorless oil (353 mg, 1.28 mmol, 84% yield). $[\alpha]_D^{25} = -9.4°$ (*c* 1.0, $CHCl_3$); ^{1}H NMR (400 MHz, $CDCl_3$) δ 7.38 – 7.29 (m, 5H), 5.17 – 5.05 (m, 2H), 2.80 (dd, *J* = 10.3, 7.8 Hz, 1H), 2.46 – 2.28 (m, 2H), 2.20 – 2.07 (m, 1H), 2.06 – 1.92 (m, 1H), 1.30 – 1.15 (m, 4H), 0.90 (s, 3H); ^{13}C NMR (100 MHz, $CDCl_3$) δ 179.0, 172.7, 136.3, 128.6, 128.4, 128.3, 66.1, 46.3, 43.0, 38.2, 35.2, 30.1, 24.6, 17.8; IR (thin film, NaCl) 3064, 3032, 2956, 1731, 1705, 1455, 1385, 1234, 1170, 747, 697 cm^{-1}; HRMS (MM:ESI-APCI–) *m/z* calc'd for $[M-H]^-$ $C_{16}H_{19}O_4$ = 275.1283, found 275.1290.

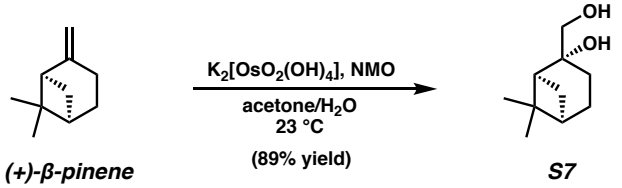

(1*S*,2*R*,5*R*)-2-(hydroxymethyl)-6,6-dimethylbicyclo[3.1.1]heptan-2-ol ((+)-β-pinanediol, S7)
(+)-β-Pinanediol (**S7**) was prepared from commercial (+)-β-pinene (≥98%, 97% ee, Sigma-Aldrich). To a stirred solution of (+)-β-pinene (1.00 mL, 6.36 mmol, 1.0 equiv) and NMO (1.12 g, 9.54 mmol, 1.5 equiv) in acetone/H_2O (4:1, 15 mL) at 23 °C was added $K_2[OsO_2(OH)_4]$ (117 mg, 0.318 mmol, 0.05 equiv) in one portion. The mixture was stirred for 24 h at 23 °C, at which point TLC indicated complete consumption of the starting material. The mixture was quenched by addition of saturated aqueous $NaHSO_3$ (25 mL), stirred for an additional 30 min, then diluted with EtOAc (30 mL) and H_2O (30 mL). The layers were separated and the aqueous layer was extracted with EtOAc (3 × 30 mL). The combined organic phases were washed with brine, dried over $MgSO_4$, and concentrated. The crude product was purified by flash chromatography (65% EtOAc/hexanes) to afford the title compound as a white solid (962 mg, 5.65 mmol, 89% yield). ^{1}H NMR (400 MHz, $CDCl_3$) δ 3.52 – 3.46 (m, 2H), 2.25 – 2.17 (m, 1H), 2.05 (t, *J* = 4.9 Hz, 1H), 1.98 – 1.88 (m, 2H), 1.83 – 1.66 (m, 3H), 1.46 (d, *J* = 10.2 Hz, 1H), 1.24 (s, 3H), 0.92 (s, 3H); ^{13}C NMR (100 MHz, $CDCl_3$) δ 77.2, 69.9, 48.5, 41.2, 38.3, 27.6, 27.4, 27.0, 24.8, 23.5. Spectral data are in good accordance with previously reported values (*98*).

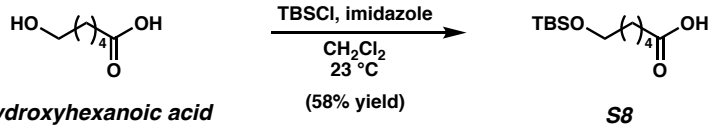

6-hydroxyhexanoic acid *S8*

6-((*tert*-butyldimethylsilyl)oxy)hexanoic acid (S8)

Silyl ether **S8** was prepared from commercial 6-hydroxyhexanoic acid (95%, AmBeed). To a stirred solution of 6-hydroxyhexanoic acid (150 mg, 1.14 mmol, 1.0 equiv) and imidazole (310 mg, 4.56 mmol, 4.0 equiv) in CH_2Cl_2 (12 mL) at 23 °C was added TBSCl (344 mg, 2.28 mmol, 2.0 equiv) in one portion. The mixture was stirred for 16 h at 23 °C, at which point TLC indicated complete consumption of the starting material. The solution was diluted with Et_2O (30 mL) and H_2O (30 mL). The layers were separated and the aqueous layer was extracted with Et_2O (3 × 30 mL). The combined organic phases were washed with brine, dried over $MgSO_4$, and concentrated. The crude product was purified by flash chromatography (30% Et_2O/hexanes) to afford the title compound as a colorless oil (163 mg, 0.661 mmol, 58% yield). ^{1}H NMR (500 MHz, $CDCl_3$) δ 3.61 (t, J = 6.4 Hz, 2H), 2.37 (t, J = 7.5 Hz, 2H), 1.70 – 1.64 (m, 2H), 1.57 – 1.52 (m, 2H), 1.44 – 1.37 (m, 2H), 0.90 (s, 9H), 0.05 (s, 6H); ^{13}C NMR (125 MHz, $CDCl_3$) δ 180.3, 63.0, 34.2, 32.5, 26.1, 25.5, 24.6, 18.5, -5.2. Spectral data are in good accordance with previously reported values (*99*).

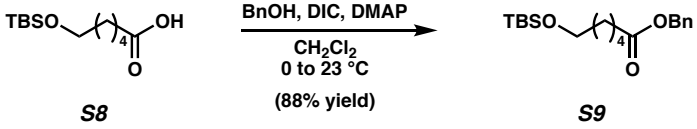

S8 *S9*

benzyl 6-((*tert*-butyldimethylsilyl)oxy)hexanoate (S9)

To a stirred solution of silyl ether **S8** (150 mg, 0.609 mmol, 1.0 equiv), benzyl alcohol (127 µL, 1.22 mmol, 2.0 equiv), and DMAP (3.7 mg, 0.0305 mmol, 0.05 equiv) in CH_2Cl_2 (6.1 mL) at 0 °C was added DIC (191 µL, 1.22 mmol, 2.0 equiv) dropwise. The mixture was stirred for 16 h and gradually allowed to warm to 23 °C, at which point TLC indicated complete consumption of **S8**. The solution was diluted with Et_2O (30 mL) and H_2O (30 mL). The layers were separated and the aqueous layer was extracted with Et_2O (3 × 30 mL). The combined organic phases were washed with brine, dried over $MgSO_4$, and concentrated. The crude product was purified by flash chromatography (10% Et_2O/hexanes) to afford the title compound as a colorless oil (181 mg, 0.538 mmol, 88% yield). ^{1}H NMR (400 MHz, $CDCl_3$) δ 7.39 – 7.31 (m, 5H), 5.11 (s, 2H), 3.59 (t, J = 6.5 Hz, 2H), 2.37 (t, J = 7.6 Hz, 2H), 1.67 (p, J = 7.6 Hz, 2H), 1.60 – 1.47 (m, 2H), 1.42 – 1.30 (m, 2H), 0.89 (s, 9H), 0.04 (s, 6H); ^{13}C NMR (100 MHz, $CDCl_3$) δ 173.7, 136.3, 128.7, 128.6, 128.3, 66.2, 63.1, 34.5, 32.6, 26.1, 25.6, 24.9, 18.5, -5.1. Spectral data are in good accordance with previously reported values (*99*).

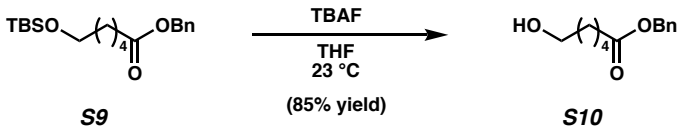

S9 *S10*

benzyl 6-hydroxyhexanoate (S10)

To a stirred solution of benzyl ester S9 (175 mg, 0.520 mmol, 1.0 equiv) in THF (5.2 mL) at 23 °C was added TBAF (1.0 M in THF, 1.56 mL, 1.56 mmol, 3.0 equiv) in one portion. The mixture was stirred for 3 h at 23 °C, at which point TLC indicated complete consumption of **S9**. The

solution was diluted with Et_2O (30 mL) and H_2O (30 mL). The layers were separated and the aqueous layer was extracted with Et_2O (3 × 30 mL). The combined organic phases were washed with brine, dried over $MgSO_4$, and concentrated. The crude product was purified by flash chromatography (60% Et_2O/hexanes) to afford the title compound as a colorless oil (98.3 mg, 0.442 mmol, 85% yield). ^{1}H NMR (400 MHz, $CDCl_3$) δ 7.41 – 7.29 (m, 5H), 5.11 (s, 2H), 3.62 (t, *J* = 6.5 Hz, 2H), 2.37 (t, *J* = 7.5 Hz, 2H), 1.74 – 1.62 (m, 2H), 1.60-1.53 (m, 2H), 1.44 – 1.34 (m, 2H); ^{13}C NMR (100 MHz, $CDCl_3$) δ 173.7, 136.1, 128.7, 128.3 (2C), 66.3, 62.7, 34.3, 32.4, 25.3, 24.7. Spectral data are in good accordance with previously reported values (*99*).

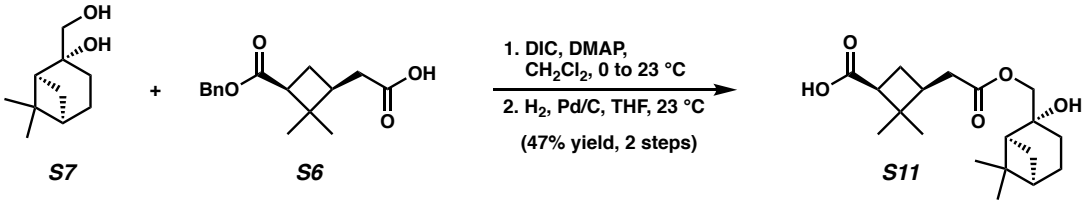

(1*S*,3*S*)-3-(2-(((1*S*,2*R*,5*R*)-2-hydroxy-6,6-dimethylbicyclo[3.1.1]heptan-2-yl)methoxy)-2-oxoethyl)-2,2-dimethylcyclobutane-1-carboxylic acid (S11)

To a stirred solution of acid **S6** (40.0 mg, 0.145 mmol, 1.0 equiv), (+)-β-pinanediol (**S7**) (24.7 mg, 0.145 mmol, 1.0 equiv), and DMAP (0.9 mg, 0.00725 mmol, 0.05 equiv) in CH_2Cl_2 (1.5 mL) at 0 °C was added DIC (23 μL, 0.145 mmol, 1.0 equiv) dropwise. The mixture was stirred for 16 h and gradually allowed to warm to 23 °C, at which point TLC indicated complete consumption of **S6**. The solution was diluted with EtOAc (10 mL) and H_2O (10 mL). The layers were separated and the aqueous layer was extracted with Et_2O (3 × 10 mL). The combined organic phases were washed with brine, dried over $MgSO_4$, and concentrated. The crude product was purified by flash chromatography (20–40% EtOAc/hexanes) to afford an intermediate diester as a colorless oil (30.4 mg, 0.0709 mmol, 49% yield).

In a 2-necked round bottom flask equipped with a 3-way valve at 23 °C, the intermediate diester (30.4 mg, 0.0709 mmol, 1.0 equiv) was dissolved in THF (3.5 mL) and to this solution was added Pd/C (10% w/w, 15 mg). The flask was evacuated and backfilled with N_2 (3×), then purged and backfilled with H_2 (3×). The suspension was stirred for 3 h at 23 °C under H_2 (1 atm, balloon), at which point TLC indicated complete consumption of the diester. The flask was evacuated and backfilled with N_2 (3×), then the suspension was diluted with EtOAc (10 mL), filtered through celite, and concentrated. The crude product was purified by flash chromatography (50–60% EtOAc/hexanes) to afford the title compound as a colorless oil (23.0 mg, 0.0680 mmol, 96% yield, 47% yield over two steps). $[\alpha]_D^{25}$ = +6.2° (*c* 1.0, $CHCl_3$); ^{1}H NMR (400 MHz, $CDCl_3$) δ 4.11 (d, *J* = 11.3 Hz, 1H), 4.04 (d, *J* = 11.3 Hz, 1H), 2.79 (dd, *J* = 10.3, 7.8 Hz, 1H), 2.46 – 2.30 (m, 3H), 2.26 – 2.19 (m, 1H), 2.17 – 2.09 (m, 1H), 2.01 – 1.90 (m, 4H), 1.86 – 1.72 (m, 3H), 1.54 (d, *J* = 10.3 Hz, 1H), 1.25 (s, 3H), 1.24 (s, 3H), 1.01 (s, 3H), 0.94 (s, 3H); ^{13}C NMR (100 MHz, $CDCl_3$) δ 178.0, 173.0, 75.7, 71.4, 49.0, 46.1, 43.0, 41.0, 38.5, 38.4, 35.4, 30.1, 27.6, 27.4, 26.9, 24.7, 24.6, 23.3, 17.8; IR (thin film, NaCl) 2922, 2872, 1711, 1233, 1204, 757 cm^{-1}; HRMS (ESI-TOF) *m/z* calc'd for $[M–H]^-$ $C_{19}H_{29}O_5$ = 337.2015, found 337.2013.

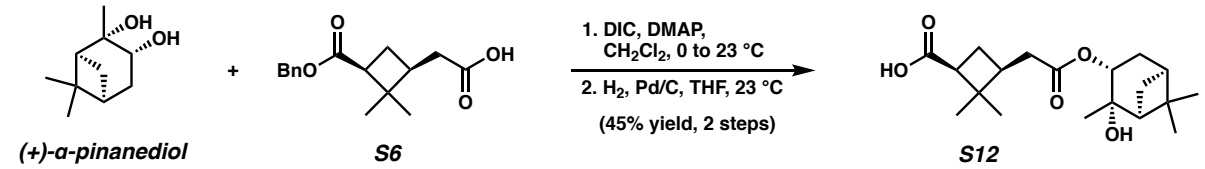

(+)-α-pinanediol *S6* *S12*

(1*S*,3*S*)-3-(2-(((1*S*,2*S*,3*R*,5*S*)-2-hydroxy-2,6,6-trimethylbicyclo[3.1.1]heptan-3-yl)oxy)-2-oxoethyl)-2,2-dimethylcyclobutane-1-carboxylic acid (S12)

Dimer ester **S12** was prepared from commercial (+)-α-pinanediol (99%, 99% ee, Sigma-Aldrich). To a stirred solution of acid **S6** (40.0 mg, 0.145 mmol, 1.0 equiv), (+)-α-pinanediol (24.7 mg, 0.145 mmol, 1.0 equiv), and DMAP (0.9 mg, 0.00725 mmol, 0.05 equiv) in CH_2Cl_2 (1.5 mL) at 0 °C was added DIC (23 μL, 0.145 mmol, 1.0 equiv) dropwise. The mixture was stirred for 16 h and gradually allowed to warm to 23 °C, at which point TLC indicated complete consumption of **S6**. The solution was diluted with EtOAc (10 mL) and H_2O (10 mL). The layers were separated and the aqueous layer was extracted with Et_2O (3 × 10 mL). The combined organic phases were washed with brine, dried over $MgSO_4$, and concentrated. The crude product was purified by flash chromatography (50–60% EtOAc/hexanes) to afford an intermediate diester as a colorless oil (44.1 mg, 0.103 mmol, 71% yield).

In a 2-necked round bottom flask equipped with a 3-way valve at 23 °C, the intermediate diester (22.0 mg, 0.0513 mmol, 1.0 equiv) was dissolved in THF (2.6 mL) and to this solution was added Pd/C (10% w/w, 11 mg). The flask was evacuated and backfilled with N_2 (3×), then purged and backfilled with H_2 (3×). The suspension was stirred for 3 h at 23 °C under H_2 (1 atm, balloon), at which point TLC indicated complete consumption of the diester. The flask was evacuated and backfilled with N_2 (3×), then the suspension was diluted with EtOAc (10 mL), filtered through celite, and concentrated. The crude product was purified by flash chromatography (50–60% EtOAc/hexanes) to afford the title compound as a colorless oil (11.0 mg, 0.0325 mmol, 63% yield, 45% yield over two steps). $[\alpha]_D^{25} = -2.6°$ (*c* 1.0, $CHCl_3$); ^{1}H NMR (400 MHz, $CDCl_3$) δ 5.12 (dd, *J* = 9.6, 5.4 Hz, 1H), 2.80 (dd, *J* = 10.2, 7.9 Hz, 1H), 2.54 – 2.34 (m, 4H), 2.24 (dtd, *J* = 10.6, 6.1, 2.5 Hz, 1H), 2.19 – 2.11 (m, 1H), 2.04 – 1.89 (m, 3H), 1.62 (ddd, *J* = 14.1, 5.5, 2.5 Hz, 1H), 1.46 (d, *J* = 10.5 Hz, 1H), 1.30 (s, 3H), 1.28 (s, 3H), 1.27 (s, 3H), 1.02 (s, 3H), 0.99 (s, 3H); ^{13}C NMR (100 MHz, $CDCl_3$) δ 177.7, 172.1, 74.0, 72.0, 54.3, 46.1, 43.0, 40.5, 38.8, 38.6, 35.7, 34.9, 30.1, 30.0, 28.4, 28.0, 24.5, 24.3, 17.9; IR (thin film, NaCl) 3794, 2953, 2924, 2873, 1726, 1705, 1234, 1217, 1187, 1157, 1010, 931, 828, 758 cm^{-1}; HRMS (ESI-TOF) *m/z* calc'd for $[M-H]^-$ $C_{19}H_{29}O_5$ = 337.2015, found 337.2016.

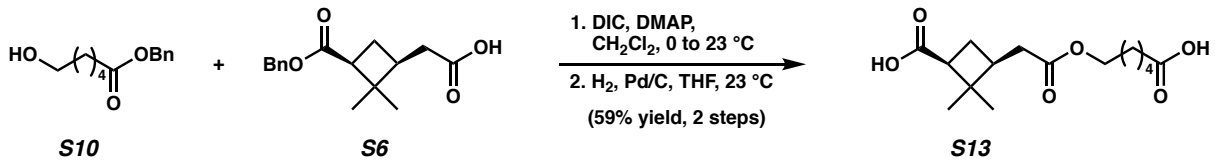

S10 *S6* *S13*

(1*S*,3*S*)-3-(2-((5-carboxypentyl)oxy)-2-oxoethyl)-2,2-dimethylcyclobutane-1-carboxylic acid (S13)

To a stirred solution of acid **S6** (25.0 mg, 0.0905 mmol, 1.0 equiv), alcohol **S10** (20.1 mg, 0.0905 mmol, 1.0 equiv), and DMAP (0.6 mg, 0.00453 mmol, 0.05 equiv) in CH_2Cl_2 (1.0 mL) at 0 °C was added DIC (14 μL, 0.0905 mmol, 1.0 equiv) dropwise. The mixture was stirred for 16 h and gradually allowed to warm to 23 °C, at which point TLC indicated complete consumption of **S6**.

The solution was diluted with EtOAc (10 mL) and H_2O (10 mL). The layers were separated and the aqueous layer was extracted with Et_2O (3 × 10 mL). The combined organic phases were washed with brine, dried over $MgSO_4$, and concentrated. The crude product was purified by flash chromatography (40–50% EtOAc/hexanes) to afford an intermediate triester as a colorless oil (29.0 mg, 0.0603 mmol, 67% yield).

In a 2-necked round bottom flask equipped with a 3-way valve at 23 °C, the intermediate triester (20.0 mg, 0.0416 mmol, 1.0 equiv) was dissolved in THF (2.1 mL) and to this solution was added Pd/C (10% w/w, 10 mg). The flask was evacuated and backfilled with N_2 (3×), then purged and backfilled with H_2 (3×). The suspension was stirred for 3 h at 23 °C under H_2 (1 atm, balloon), at which point TLC indicated complete consumption of the triester. The flask was evacuated and backfilled with N_2 (3×), then the suspension was diluted with EtOAc (10 mL), filtered through celite, and concentrated. The crude product was purified by flash chromatography (50–80% EtOAc/hexanes) to afford the title compound as a colorless oil (11.0 mg, 0.0366 mmol, 88% yield, 59% yield over two steps). $[\alpha]_D^{25} = -1.3°$ (*c* 1.0, $CHCl_3$); ^{1}H NMR (400 MHz, $CDCl_3$) δ 4.07 (t, *J* = 6.4 Hz, 2H), 2.79 (dd, *J* = 10.2, 7.8 Hz, 1H), 2.44 – 2.22 (m, 5H), 2.16 – 2.04 (m, 1H), 1.97 – 1.87 (m, 1H), 1.73 – 1.58 (m, 4H), 1.47 – 1.38 (m, 2H), 1.24 (s, 3H), 1.00 (s, 3H); ^{13}C NMR (100 MHz, $CDCl_3$) δ 179.4, 178.4, 172.9, 64.3, 46.2, 43.1, 38.5, 35.6, 33.9, 30.0, 28.4, 25.7, 24.5, 24.4, 17.7; IR (thin film, NaCl) 3801, 2352, 1725, 1704, 1416, 1255, 1234, 1219, 1204, 1187, 817, 682 cm^{-1}; HRMS (ESI-TOF) *m/z* calc'd for $[M-H]^-$ $C_{15}H_{23}O_6$ = 299.1495, found 299.1493.

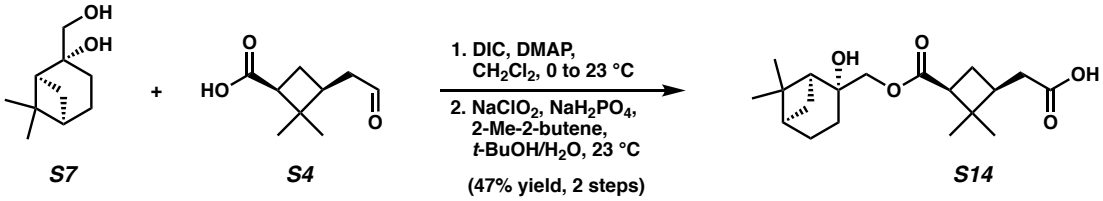

2-((1*S*,3*S*)-3-((((1*S*,2*R*,5*R*)-2-hydroxy-6,6-dimethylbicyclo[3.1.1]heptan-2-yl)methoxy)carbonyl)-2,2-dimethylcyclobutyl)acetic acid (S14)

To a stirred solution of aldehyde **S4** (50.0 mg, 0.294 mmol, 1.0 equiv), (+)-β-pinanediol (**S7**) (50.0 mg, 0.294 mmol, 1.0 equiv), and DMAP (2.0 mg, 0.0147 mmol, 0.05 equiv) in CH_2Cl_2 (3.0 mL) at 0 °C was added DIC (46 μL, 0.294 mmol, 1.0 equiv) dropwise. The mixture was stirred for 16 h and gradually allowed to warm to 23 °C, at which point TLC indicated complete consumption of **S4**. The solution was diluted with EtOAc (10 mL) and H_2O (10 mL). The layers were separated and the aqueous layer was extracted with Et_2O (3 × 10 mL). The combined organic phases were washed with brine, dried over $MgSO_4$, and concentrated. The crude product was purified by flash chromatography (30–50% EtOAc/hexanes) to afford an intermediate ester as a colorless oil (80.6 mg, 0.250 mmol, 85% yield).

To a stirred solution of the intermediate ester (30.0 mg, 0.0930 mmol, 1.0 equiv), NaH_2PO_4 (66.7 mg, 0.558 mmol, 6.0 equiv), and 2-Me-2-butene (789 μL, 7.44 mmol, 80.0 equiv) in t-BuOH/H_2O (5:1, 11 mL) at 23 °C was added $NaClO_2$ (25.3 mg, 0.279 mmol, 3.0 equiv) in one portion. The mixture was stirred for 2 h at 23 °C, at which point TLC indicated complete consumption of the ester. The t-BuOH was removed by rotary evaporation, and the remaining solution was diluted with EtOAc (10 mL) and H_2O (10 mL). The layers were separated and the aqueous layer was extracted with EtOAc (3 × 10 mL). The combined organic phases were washed with brine, dried

over $MgSO_4$, and concentrated. The crude product was purified by flash chromatography (20–50% EtOAc/hexanes) to afford the title compound as a colorless oil (17.3 mg, 0.0511 mmol, 55% yield, 47% yield over two steps). $[\alpha]_D^{25} = +11.2°$ (*c* 1.0, $CHCl_3$); ^1H NMR (400 MHz, $CDCl_3$) δ 4.11 (d, *J* = 11.2 Hz, 1H), 4.02 (d, *J* = 11.2 Hz, 1H), 2.79 (dd, *J* = 10.3, 7.8 Hz, 1H), 2.45 – 2.29 (m, 3H), 2.26 – 2.18 (m, 1H), 2.18 – 2.10 (m, 1H), 2.03 – 1.90 (m, 4H), 1.86 – 1.72 (m, 3H), 1.54 (d, *J* = 10.1 Hz, 1H), 1.24 (s, 6H), 0.96 (s, 3H), 0.95 (s, 3H); ^{13}C NMR (100 MHz, $CDCl_3$) δ 178.3, 173.0, 75.7, 71.4, 49.1, 46.4, 43.0, 41.0, 38.4, 38.2, 35.2, 30.2, 27.6, 27.5, 26.9, 24.7, 24.7, 23.4, 18.1; IR (thin film, NaCl) 3793, 2953, 2923, 2869, 1725, 1710, 1386, 1233, 1219, 1187, 1175, 918, 828, 759 cm^{-1}; HRMS (ESI-TOF) *m/z* calc'd for $[M–H]^-$ $C_{19}H_{29}O_5$ = 337.2015, found 337.2018.

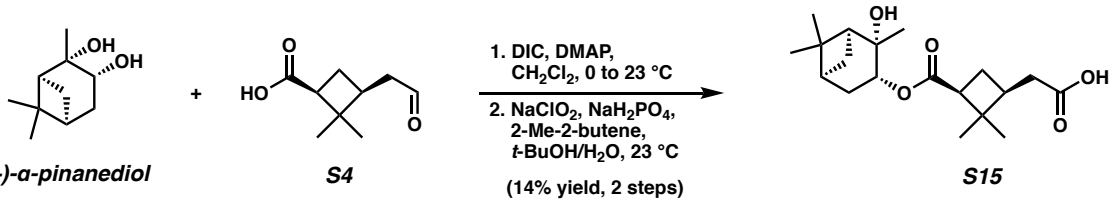

2-((1*S*,3*S*)-3-((((1*S*,2*S*,3*R*,5*S*)-2-hydroxy-2,6,6-trimethylbicyclo[3.1.1]heptan-3-yl)oxy)carbonyl)-2,2-dimethylcyclobutyl)acetic acid (S15)

Dimer ester **S15** was prepared from commercial (+)-α-pinanediol (99%, 99% ee, Sigma-Aldrich). To a stirred solution of aldehyde **S4** (50.0 mg, 0.294 mmol, 1.0 equiv), (+)-α-pinanediol (50.0 mg, 0.294 mmol, 1.0 equiv), and DMAP (2.0 mg, 0.0147 mmol, 0.05 equiv) in CH_2Cl_2 (3.0 mL) at 0 °C was added DIC (46 µL, 0.294 mmol, 1.0 equiv) dropwise. The mixture was stirred for 16 h and gradually allowed to warm to 23 °C, at which point TLC indicated complete consumption of **S4**. The solution was diluted with EtOAc (10 mL) and H_2O (10 mL). The layers were separated and the aqueous layer was extracted with Et_2O (3 × 10 mL). The combined organic phases were washed with brine, dried over $MgSO_4$, and concentrated. The crude product was purified by flash chromatography (20–40% EtOAc/hexanes) to afford an intermediate ester as a colorless oil (43.8 mg, 0.136 mmol, 46% yield).

To a stirred solution of the intermediate ester (20.0 mg, 0.0620 mmol, 1.0 equiv), NaH_2PO_4 (44.6 mg, 0.372 mmol, 6.0 equiv), and 2-Me-2-butene (526 µL, 4.96 mmol, 80.0 equiv) in t-BuOH/H_2O (5:1, 7.5 mL) at 23 °C was added $NaClO_2$ (16.9 mg, 0.186 mmol, 3.0 equiv) in one portion. The mixture was stirred for 2 h at 23 °C, at which point TLC indicated complete consumption of the ester. The t-BuOH was removed by rotary evaporation, and the remaining solution was diluted with EtOAc (10 mL) and H_2O (10 mL). The layers were separated and the aqueous layer was extracted with EtOAc (3 × 10 mL). The combined organic phases were washed with brine, dried over $MgSO_4$, and concentrated. The crude product was purified by flash chromatography (20–50% EtOAc/hexanes) to afford the title compound as a colorless oil (6.0 mg, 0.0177 mmol, 29% yield, 14% yield over two steps). $[\alpha]_D^{25} = –0.68°$ (*c* 0.83, $CHCl_3$); ^1H NMR (400 MHz, $CDCl_3$) δ 5.14 (dd, *J* = 9.6, 5.5 Hz, 1H), 2.83 (dd, *J* = 10.2, 7.8 Hz, 1H), 2.56 – 2.30 (m, 4H), 2.28 – 2.21 (m, 1H), 2.20 – 2.11 (m, 1H), 2.04 – 1.91 (m, 3H), 1.63 (ddd, *J* = 14.1, 5.5, 2.5 Hz, 1H), 1.47 (d, *J* = 10.5 Hz, 1H), 1.30 (s, 3H), 1.29 (s, 3H), 1.27 (s, 3H), 0.99 (s, 3H), 0.98 (s, 3H); ^{13}C NMR (100 MHz, $CDCl_3$) δ 177.8, 172.1, 74.0, 71.8, 54.2, 46.3, 43.0, 40.5, 38.8, 38.3, 35.3, 35.0, 30.3, 29.9, 28.5, 28.0, 24.7, 24.4, 17.9; IR (thin film, NaCl) 3812, 2952, 2352, 2339, 1712, 1254, 1238, 1219, 1187, 829, 668 cm^{-1}; HRMS (ESI-TOF) *m/z* calc'd for $[M–H]^-$ $C_{19}H_{29}O_5$ = 337.2015, found 337.2016.

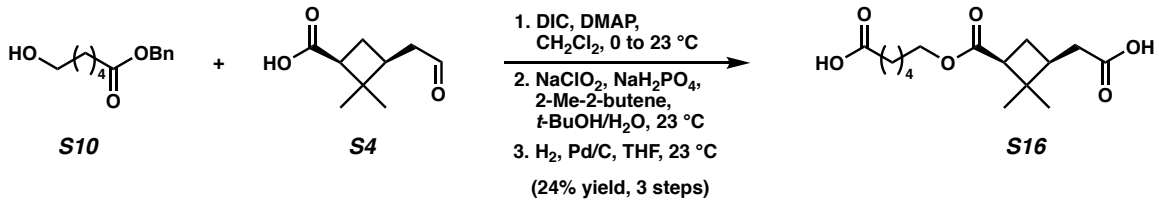

6-(((1*S*,3*S*)-3-(carboxymethyl)-2,2-dimethylcyclobutane-1-carbonyl)oxy)hexanoic acid (S16) To a stirred solution of aldehyde **S4** (28.0 mg, 0.165 mmol, 1.0 equiv), alcohol **S10** (36.6 mg, 0.165 mmol, 1.0 equiv), and DMAP (1.0 mg, 0.00825 mmol, 0.05 equiv) in CH_2Cl_2 (1.7 mL) at 0 °C was added DIC (26 µL, 0.165 mmol, 1.0 equiv) dropwise. The mixture was stirred for 16 h and gradually allowed to warm to 23 °C, at which point TLC indicated complete consumption of **S4**. The solution was diluted with EtOAc (10 mL) and H_2O (10 mL). The layers were separated and the aqueous layer was extracted with Et_2O (3 × 10 mL). The combined organic phases were washed with brine, dried over $MgSO_4$, and concentrated. The crude product was purified by flash chromatography (20–50% EtOAc/hexanes) to afford an intermediate diester as a colorless oil (31.6 mg, 0.0844 mmol, 51% yield).

To a stirred solution of the intermediate diester (16.0 mg, 0.0427 mmol, 1.0 equiv), NaH_2PO_4 (30.7 mg, 0.256 mmol, 6.0 equiv), and 2-Me-2-butene (363 µL, 3.42 mmol, 80.0 equiv) in t-BuOH/H_2O (5:1, 5.2 mL) at 23 °C was added $NaClO_2$ (11.6 mg, 0.128 mmol, 3.0 equiv) in one portion. The mixture was stirred for 2 h at 23 °C, at which point TLC indicated complete consumption of the diester. The t-BuOH was removed by rotary evaporation, and the remaining solution was diluted with EtOAc (10 mL) and H_2O (10 mL). The layers were separated and the aqueous layer was extracted with EtOAc (3 × 10 mL). The combined organic phases were washed with brine, dried over $MgSO_4$, and concentrated. The crude product was purified by flash chromatography (30–60% EtOAc/hexanes) to afford an intermediate diester acid as a colorless oil (8.0 mg, 0.0204 mmol, 48% yield).

In a 2-necked round bottom flask equipped with a 3-way valve at 23 °C, the intermediate diester acid (8.0 mg, 0.0204 mmol, 1.0 equiv) was dissolved in THF (1.0 mL) and to this solution was added Pd/C (10% w/w, 10 mg). The flask was evacuated and backfilled with N_2 (3×), then purged and backfilled with H_2 (3×). The suspension was stirred for 3 h at 23 °C under H_2 (1 atm, balloon), at which point TLC indicated complete consumption of the diester acid. The flask was evacuated and backfilled with N_2 (3×), then the suspension was diluted with EtOAc (10 mL), filtered through celite, and concentrated. The crude product was purified by flash chromatography (50–80% EtOAc/hexanes) to afford the title compound as a colorless oil (5.9 mg, 0.0197 mmol, 97% yield, 24% yield over three steps). $[\alpha]_D^{25}$ = +6.1° (*c* 0.50, $CHCl_3$); ^{1}H NMR (400 MHz, $CDCl_3$) δ 4.08 (qt, *J* = 11.0, 6.2 Hz, 2H), 2.74 (dd, *J* = 10.3, 7.8 Hz, 1H), 2.45 – 2.28 (m, 5H), 2.17 – 2.06 (m, 1H), 2.01 – 1.91 (m, 1H), 1.71 – 1.61 (m, 4H), 1.49 – 1.40 (m, 2H), 1.23 (s, 3H), 0.94 (s, 3H); ^{13}C NMR (100 MHz, $CDCl_3$) δ 179.5, 178.7, 173.0, 64.0, 46.4, 42.9, 38.2, 35.2, 33.9, 30.1, 28.5, 25.7, 24.5, 24.4, 17.8; IR (thin film, NaCl) 3550, 3278, 2957, 2925, 1729, 1707, 1687, 1638, 1233, 1179 cm^{-1}; HRMS (ESI-TOF) *m/z* calc'd for $[M–H]^-$ $C_{15}H_{23}O_6$ = 299.1495, found 299.1495.

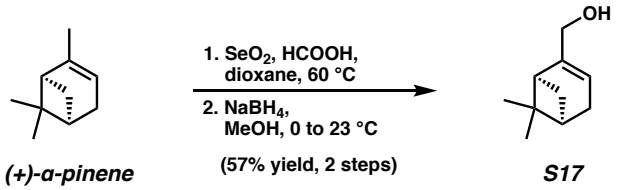

((1*S*,5*R*)-6,6-dimethylbicyclo[3.1.1]hept-2-en-2-yl)methanol ((+)-myrtenol, S17)
(+)-Myrtenol (**S17**) was prepared according to a modified literature procedure (*100*) from commercial (+)-α-pinene (98%, 89% ee, Sigma-Aldrich). To a stirred solution of (+)-α-pinene (5.83 mL, 36.7 mmol, 1.0 equiv) and HCOOH (2.08 mL, 55.1 mmol, 1.5 equiv) in dioxane (93 mL) at 23 °C was added SeO2 (4.07 g, 36.7 mmol, 1.0 equiv) in one portion. The mixture was heated to 60 °C and stirred for 24 h, at which point TLC indicated complete consumption of the starting material. The solution was diluted with saturated aqueous $NaHCO_3$ (200 mL) and EtOAc (200 mL). The layers were separated and the aqueous layer was extracted with EtOAc (3 × 150 mL). The combined organic phases were washed with brine, dried over $MgSO_4$, and concentrated to afford an intermediate aldehyde as an orange oil (3.86 g, 25.7 mmol, 70% yield) that was used in the next step without further purification.

To a stirred solution of the intermediate aldehyde (3.86 g, 25.7 mmol, 1.0 equiv) in MeOH (205 mL) at 0 °C was added $NaBH_4$ (1.95 g, 51.4 mmol, 1.4 equiv) in one portion. The mixture was stirred for 1 h and gradually allowed to warm to 23 °C, at which point TLC indicated complete consumption of the aldehyde. The mixture was quenched by addition of H_2O (100 mL) and diluted with EtOAc (150 mL) and H_2O (100 mL). The layers were separated and the aqueous layer was extracted with EtOAc (3 × 150 mL). The combined organic phases were washed with brine, dried over $MgSO_4$, and concentrated. The crude product was purified by flash chromatography (40% EtOAc/hexanes) to afford the title compound as a colorless oil (3.16 g, 20.8 mmol, 81% yield, 57% yield over two steps). ^{1}H NMR (600 MHz, $CDCl_3$) δ 5.47 (m, 1H), 3.99 (m, 2H), 2.45 – 2.38 (m, 1H), 2.35 – 2.21 (m, 2H), 2.17 – 2.08 (m, 2H), 1.30 (s, 3H), 1.18 (dd, J = 8.6, 1.2 Hz, 1H), 0.84 (s, 3H); ^{13}C NMR (100 MHz, $CDCl_3$) δ 147.9, 118.1, 66.2, 43.5, 41.1, 38.1, 31.8, 31.3, 26.3, 21.3. Spectral data are in good accordance with previously reported values (*100*).

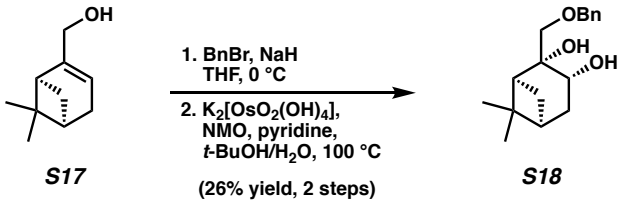

(1*S*,2*R*,3*R*,5*S*)-2-((benzyloxy)methyl)-6,6-dimethylbicyclo[3.1.1]heptane-2,3-diol (S18)
To a stirred solution of NaH (60% w/w dispersion in mineral oil, 1.66 g, 41.6 mmol, 2.0 equiv) in THF (60 mL) at 0 °C was added (+)-myrtenol (**S17**) (3.17 g, 20.8 mmol, 1.0 equiv) in one portion and the mixture was stirred for 1 h. Benzyl bromide (4.94 mL, 41.6 mmol, 2.0 equiv) was added dropwise and the mixture was stirred for an additional 2 h at 0 °C, at which point TLC indicated complete consumption of **S17**. The mixture was quenched by addition of saturated aqueous NH_4Cl (50 mL) and diluted with EtOAc (150 mL) and H_2O (150 mL). The layers were separated and the aqueous layer was extracted with EtOAc (3 × 150 mL). The combined organic phases were washed

with brine, dried over $MgSO_4$, and concentrated to afford an intermediate benzyl ether as a yellow oil (4.99 g, 20.6 mmol, 99% yield) that was used in the next step without further purification.

To a stirred solution of the intermediate benzyl ether (4.99 g, 20.6 mmol, 1.0 equiv), NMO (2.53 g, 21.6 mmol, 1.05 equiv), and pyridine (1.66 mL, 20.6 mmol, 1.0 equiv) in t-BuOH/H_2O (5:1, 18 mL) at 23 °C was added $K_2[OsO_2(OH)_4]$ (19.0 mg, 0.0515 mmol, 0.0025 equiv) in one portion. A reflux condenser was attached, the mixture was heated to 100 °C, and the mixture was stirred for 24 h at 100 °C, at which point TLC indicated complete consumption of the benzyl ether. The solution was cooled to 23 °C and diluted with saturated aqueous $NaHSO_3$ (30 mL) and EtOAc (30 mL). The layers were separated and the aqueous layer was extracted with EtOAc (3 × 50 mL). The combined organic phases were washed with brine, dried over $MgSO_4$, and concentrated. The crude product was purified by flash chromatography (35% EtOAc/hexanes) to afford the title compound as a white solid (1.51 g, 5.46 mmol, 27% yield, 26% yield over two steps). $[\alpha]_D^{25}$ = +2.9° (*c* 1.0, $CHCl_3$); ^{1}H NMR (400 MHz, $CDCl_3$) δ 7.38 – 7.27 (m, 5H), 4.63 – 4.51 (m, 2H), 4.16 (ddd, *J* = 9.4, 6.1, 0.9 Hz, 1H), 3.50 (dd, *J* = 9.2, 0.8 Hz, 1H), 3.37 (dd, *J* = 9.2, 0.8 Hz, 1H), 2.48 – 2.36 (m, 1H), 2.26 – 2.15 (m, 1H), 2.07 (t, *J* = 5.9 Hz, 1H), 1.91 (m, 1H), 1.66 (ddd, *J* = 13.9, 6.1, 2.3 Hz, 1H), 1.50 (d, *J* = 10.3 Hz, 1H), 1.23 (s, 3H), 0.83 (s, 3H); ^{13}C NMR (100 MHz, $CDCl_3$) δ 138.0, 128.7, 128.0, 127.9, 77.6, 75.3, 73.7, 66.4, 49.4, 40.8, 38.9, 36.9, 28.1, 28.1, 24.3; IR (thin film, NaCl) 3798, 3435, 2904, 2366, 1454, 1085 cm^{-1}; HRMS (FI) *m/z* calc'd for $[M]^{\bullet+}$ $C_{17}H_{24}O_3$ = 276.1725, found 276.1724.

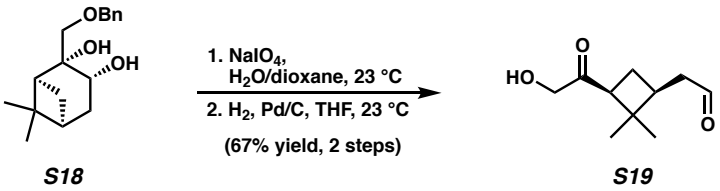

S18 ***S19***

2-((1*S*,3*S*)-3-(2-hydroxyacetyl)-2,2-dimethylcyclobutyl)acetaldehyde ((+)-*cis*-10-hydroxypinonaldehyde, S19)

To a stirred solution of diol **S18** (1.50 g, 5.43 mmol, 1.0 equiv) in H_2O/dioxane (1:3, 28 mL) at 23 °C was added $NaIO_4$ (4.65 g, 21.7 mmol, 4.0 equiv) in one portion. The mixture was stirred for 24 h at 23 °C, at which point TLC indicated complete consumption of **S18**. The solution was diluted with Et_2O (100 mL) and H_2O (100 mL). The layers were separated and the aqueous layer was extracted with Et_2O (3 × 100 mL). The combined organic phases were washed with brine, dried over $MgSO_4$, and concentrated to afford an intermediate benzyl ether aldehyde as a colorless oil (1.25 g, 4.56 mmol, 84% yield) that was used in the next step without further purification.

In a 2-necked round bottom flask equipped with a 3-way valve at 23 °C, the intermediate benzyl ether aldehyde (1.25 g, 4.56 mmol, 1.0 equiv) was dissolved in THF (46 mL) and to this solution was added Pd/C (10% w/w, 483 mg). The flask was evacuated and backfilled with N_2 (3×), then purged and backfilled with H_2 (3×). The suspension was stirred for 20 h at 23 °C under H_2 (1 atm, balloon), at which point TLC indicated complete consumption of the benzyl ether. The flask was evacuated and backfilled with N_2 (3×), then the suspension was diluted with EtOAc (40 mL), filtered through celite, and concentrated. The crude product was purified by flash chromatography (50–60% EtOAc/hexanes) to afford the title compound as a colorless oil (670 mg, 3.64 mmol, 80% yield, 67% yield over two steps). $[\alpha]_D^{25}$ = +7.9° (*c* 1.0, $CHCl_3$); ^{1}H NMR (400 MHz, $CDCl_3$) δ

9.74 (t, J = 1.2 Hz, 1H), 4.12 (q, J = 18.9 Hz, 2H), 3.21 – 3.08 (m, 1H), 2.91 (dd, J = 10.0, 7.6 Hz, 1H), 2.59 – 2.40 (m, 3H), 2.15 – 1.96 (m, 2H), 1.29 (s, 3H), 0.83 (s, 3H); ^{13}C NMR (100 MHz, $CDCl_3$) δ 207.9, 201.2, 68.8, 49.9, 45.2, 44.0, 36.2, 30.7, 22.4, 17.9; IR (thin film, NaCl) 3439, 2952, 1713, 1367, 1274, 1226, 1078 cm^{-1}; HRMS (FI) *m/z* calc'd for $[M]^{\bullet+}$ $C_{10}H_{16}O_3$ = 184.1099, found 184.1104.

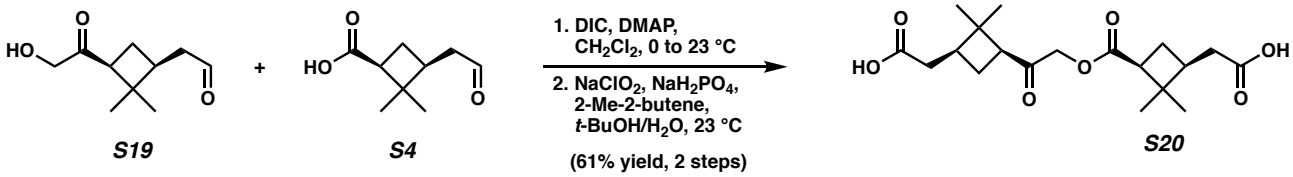

2-((1*S*,3*S*)-3-(2-(((1*S*,3*S*)-3-(carboxymethyl)-2,2-dimethylcyclobutane-1-carbonyl)oxy)acetyl)-2,2-dimethylcyclobutyl)acetic acid (S20)

To a stirred solution of aldehyde **S4** (277 mg, 1.63 mmol, 1.0 equiv), alcohol **S19** (300 mg, 1.63 mmol, 1.0 equiv), and DMAP (10.0 mg, 0.0815 mmol, 0.05 equiv) in CH_2Cl_2 (32.6 mL) at 0 °C was added DIC (255 μL, 1.63 mmol, 1.0 equiv) dropwise. The mixture was stirred for 16 h and gradually allowed to warm to 23 °C, at which point TLC indicated complete consumption of **S4**. The solution was diluted with EtOAc (50 mL) and H_2O (50 mL). The layers were separated and the aqueous layer was extracted with Et_2O (3 × 50 mL). The combined organic phases were washed with brine, dried over $MgSO_4$, and concentrated. The crude product was purified by flash chromatography (30–40% EtOAc/hexanes) to afford an intermediate ester as a colorless oil (454 mg, 1.35 mmol, 83% yield).

To a stirred solution of the intermediate ester (454 mg, 1.35 mmol, 1.0 equiv), NaH_2PO_4 (1.94 g, 16.2 mmol, 12.0 equiv), and 2-Me-2-butene (11.5 mL, 108 mmol, 80.0 equiv) in t-BuOH/H_2O (5:1, 170 mL) at 23 °C was added $NaClO_2$ (733 mg, 8.10 mmol, 6.0 equiv) in one portion. The mixture was stirred for 3 h at 23 °C, at which point TLC indicated complete consumption of the ester. The t-BuOH was removed by rotary evaporation, and the remaining solution was diluted with EtOAc (50 mL) and H_2O (50 mL). The layers were separated and the aqueous layer was extracted with EtOAc (3 × 50 mL). The combined organic phases were washed with brine, dried over $MgSO_4$, and concentrated. The crude product was purified by flash chromatography (30–40% EtOAc/hexanes; 1% AcOH). Residual AcOH was removed by rotary evaporation with added toluene to afford the title compound as a white solid (363 mg, 0.0985 mmol, 73% yield, 61% yield over two steps). $[\alpha]_D^{25}$ = –38.7° (*c* 0.08, $CHCl_3$); ^{1}H NMR (400 MHz, $CDCl_3$) δ 4.64 – 4.47 (m, 2H), 2.97 – 2.82 (m, 2H), 2.46 – 2.29 (m, 6H), 2.21 – 1.91 (m, 4H), 1.32 (s, 3H), 1.27 (s, 3H), 1.03 (s, 3H), 0.91 (s, 3H); ^{13}C NMR (100 MHz, $CDCl_3$) δ 202.0, 179.4, 179.3, 172.0, 68.2, 50.0, 46.0, 43.9, 43.2, 38.2, 38.0, 35.2, 35.0, 30.5, 30.1, 24.6, 22.4, 17.8, 17.5; IR (thin film, NaCl) 2915, 1708, 1457, 1416, 1168 cm^{-1}; HRMS (ESI-TOF) *m/z* calc'd for $[M–H]^-$ $C_{19}H_{27}O_7$ = 367.1757, found 367.1753.

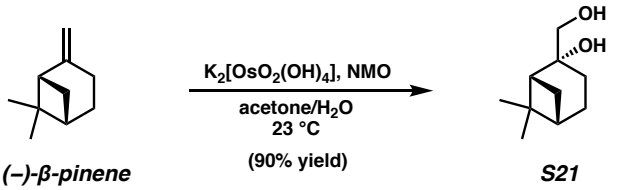

(1*R*,2*S*,5*S*)-2-(hydroxymethyl)-6,6-dimethylbicyclo[3.1.1]heptan-2-ol ((–)-β-pinanediol, S21) (–)-β-Pinanediol (**S21**) was prepared from commercial (–)-β-pinene (≥99%, 97% ee, Sigma-Aldrich). To a stirred solution of (–)-β-pinene (8.00 mL, 50.9 mmol, 1.0 equiv) and NMO (8.95 g, 76.4 mmol, 1.5 equiv) in acetone/H_2O (4:1, 100 mL) at 23 °C was added $K_2[OsO_2(OH)_4]$ (938 mg, 2.55 mmol, 0.05 equiv) in one portion. The mixture was stirred for 24 h at 23 °C, at which point TLC indicated complete consumption of the starting material. The mixture was quenched by addition of saturated aqueous $NaHSO_3$ (170 mL), stirred for an additional 30 min, then diluted with EtOAc (200 mL) and H_2O (200 mL). The layers were separated and the aqueous layer was extracted with EtOAc (3 × 200 mL). The combined organic phases were washed with brine, dried over $MgSO_4$, and concentrated. The crude product was purified by flash chromatography (65% EtOAc/hexanes) to afford the title compound as a white solid (7.76 g, 45.6 mmol, 90% yield). $[\alpha]_D^{25}$ –27.9° (*c* 0.90, $CHCl_3$); ^{1}H NMR (400 MHz, $CDCl_3$) δ 3.52 – 3.46 (m, 2H), 2.25 – 2.17 (m, 1H), 2.05 (t, *J* = 4.9 Hz, 1H), 1.98 – 1.88 (m, 2H), 1.83 – 1.66 (m, 3H), 1.46 (d, *J* = 10.2 Hz, 1H), 1.24 (s, 3H), 0.92 (s, 3H); ^{13}C NMR (100 MHz, $CDCl_3$) δ 77.2, 69.9, 48.5, 41.2, 38.3, 27.6, 27.4, 27.0, 24.8, 23.5; IR (thin film, NaCl) 3263, 2972, 2913, 2866, 1454, 1383, 1363, 1235, 1093, 1057, 1030 cm^{-1}; HRMS (FI) *m/z* calc'd for $[M]^{\bullet+}$ $C_{10}H_{18}O_2$ = 170.1307, found 170.1309.

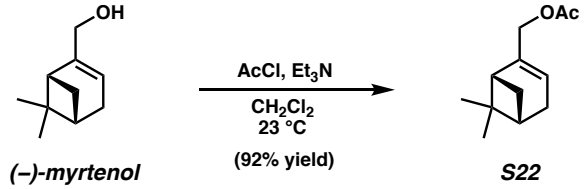

((1*R*,5*S*)-6,6-dimethylbicyclo[3.1.1]hept-2-en-2-yl)methyl acetate ((–)-myrtenyl acetate, S22) (–)-Myrtenyl acetate (**S22**) was prepared according to a modified literature procedure (*101*) from commercial (–)-myrtenol (95%, 95% ee, Sigma-Aldrich). To a stirred solution of (–)-myrtenol (5.00 mL, 31.3 mmol, 1.0 equiv) and Et_3N (6.55 mL, 47.0 mmol, 1.5 equiv) in CH_2Cl_2 (313 mL) at 23 °C was added AcCl (2.67 mL, 37.6 mmol, 1.2 equiv) in one portion. The mixture was stirred for 16 h at 23 °C, at which point TLC indicated complete consumption of the starting material. The solution was diluted with Et_2O (200 mL) and H_2O (200 mL). The layers were separated and the aqueous layer was extracted with Et_2O (3 × 200 mL). The combined organic phases were washed with brine, dried over $MgSO_4$, and concentrated. The crude product was purified by flash chromatography (2–5% Et_2O/hexanes) to afford the title compound as a colorless oil (5.64 g, 29.0 mmol, 93% yield). ^{1}H NMR (400 MHz, $CDCl_3$) δ 5.56 (tp, *J* = 2.9, 1.4 Hz, 1H), 4.44 (qq, *J* = 12.6, 1.6 Hz, 2H), 2.45 – 2.35 (m, 1H), 2.34 – 2.20 (m, 2H), 2.11 (dd, *J* = 5.6, 1.7 Hz, 2H), 2.05 (s, 3H), 1.29 (s, 3H), 1.18 (d, *J* = 8.7 Hz, 1H), 0.82 (s, 3H); ^{13}C NMR (100 MHz, $CDCl_3$) δ 171.2, 143.1, 121.6, 67.2, 43.7, 40.8, 38.2, 31.6, 31.4, 26.3, 21.2, 21.2. Spectral data are in good accordance with previously reported values (*101*, *102*).

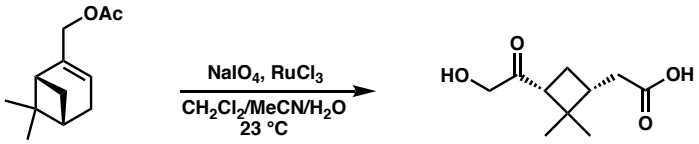

S22 *S23*

2-((1*R*,3*R*)-3-(2-hydroxyacetyl)-2,2-dimethylcyclobutyl)acetic acid ((−)-*cis*-10-hydroxypinonic acid, S23)

To a stirred solution of (−)-myrtenyl acetate (**S22**) (3.00 g, 15.4 mmol, 1.0 equiv) in CH_2Cl_2/MeCN/H_2O (2:2:3, 125 mL) at 23 °C was added $NaIO_4$ (13.2 g, 61.6 mmol, 4.0 equiv) followed by catalytic $RuCl_3$ hydrate (116 mg). After 24 h, TLC indicated complete conversion of S22 and the mixture was diluted with Et_2O (100 mL). The layers were separated and the aqueous layer was extracted with Et_2O (3 × 75 mL). The combined organic phases were filtered through celite and concentrated. The crude residue was dissolved in Et_2O (50 mL) and extracted with 10% aqueous Na_2CO_3 (3 × 75 mL). The aqueous phases were combined, acidified to pH 1 with concentrated H_2SO_4, and extracted with Et_2O (3 × 75 mL). The combined organic phases were washed with brine, dried over $MgSO_4$, and concentrated. The crude product was purified by flash chromatography (40–50% EtOAc/hexanes; 1% AcOH). Residual AcOH was removed by rotary evaporation with added toluene to afford the title compound as a white solid (919 mg, 4.59 mmol, 30% yield). $[\alpha]_D^{25}$ −59.2° (*c* 0.90, $CHCl_3$); ^{1}H NMR (400 MHz, $CDCl_3$) δ 4.22 – 4.03 (m, 2H), 2.89 (dd, *J* = 10.1, 7.6 Hz, 1H), 2.49 – 2.29 (m, 3H), 2.18 – 1.97 (m, 2H), 1.29 (s, 3H), 0.87 (s, 3H); ^{13}C NMR (100 MHz, $CDCl_3$) δ 207.9, 177.8, 68.8, 49.8, 44.0, 38.1, 34.7, 30.5, 22.5, 17.6; IR (thin film, NaCl) 2956, 2366, 1707, 1395, 1223, 1077 cm^{-1}; HRMS (ESI-TOF) *m/z* calc'd for $[M-H]^-$ $C_{10}H_{15}O_4$ = 199.0970, found 199.0971. Spectral data are in good accordance with previously reported values (*101*).

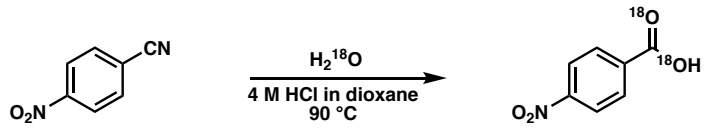

4-nitrobenzonitrile *S24*

4-nitrobenzoic-$^{18}O_2$ acid (S24)

4-nitrobenzoic-$^{18}O_2$ acid (**S24**) was prepared according to a modified literature procedure (*103*) from commercial 4-nitrobenzonitrile (98%, Fisher Scientific), $H_2{}^{18}O$ (98 atom % ^{18}O, Sercon Limited), and 4 M HCl in dioxane (Fisher Scientific). In a round bottom flask equipped with a rotary evaporator bump trap containing P_2O_5 (5.0 g), 4-nitrobenzonitrile (3.74 g, 25.2 mmol, 1.0 equiv) was heated to 50 °C for 18 h under vacuum. The dried 4-nitrobenzonitrile was transferred to a 20 mL Biotage® microwave vial, which was first flame dried under vacuum and allowed to cool to 23 °C under Ar. The vial was evacuated and backfilled with Ar (4×), and 4 M HCl in dioxane (10.1 mL, 40.4 mmol, 1.6 equiv) followed by $H_2{}^{18}O$ (1.00 mL, 55.5 mmol, 2.2 equiv) were added. The mixture was heated to 90 °C and stirred for 20 h, at which point TLC indicated complete consumption of the starting material. The solution was cooled to 23 ° C, $CHCl_3$ (15 mL) was added, and the precipitate was collected by vacuum filtration. The filter cake was washed with $CHCl_3$ (15 mL) and dried under vacuum to afford the title compound as a white solid (2.10 g, 12.3 mmol, 49% yield). ^{1}H NMR (400 MHz, CD_3OD) δ 8.33 (d, *J* = 8.9 Hz, 2H), 8.24 (d, *J* = 8.9 Hz, 2H); ^{13}C NMR (100 MHz, CD_3OD) δ 167.5, 152.0, 137.6, 131.9, 124.5. Spectral data are in good

accordance with previously reported values (*103*). ^{18}O incorporation was determined only for compound **S26**.

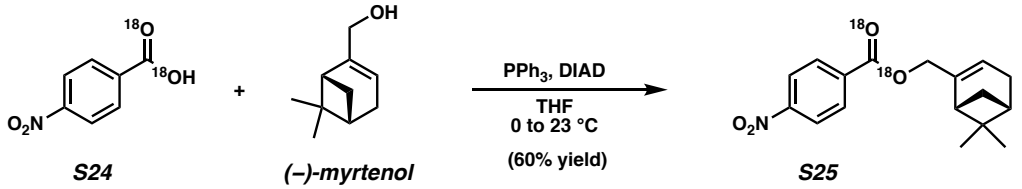

S24 *(–)-myrtenol* *S25*

((1*R*,5*S*)-6,6-dimethylbicyclo[3.1.1]hept-2-en-2-yl)methyl 4-nitrobenzoate-$^{18}O_2$ ((–)-myrtenyl 4-nitrobenzoate-$^{18}O_2$, S25)

(–)-Myrtenyl 4-nitrobenzoate-$^{18}O_2$ (**S25**) was prepared according to a modified literature procedure (*103*) from commercial (–)-myrtenol (95%, 95% ee, Sigma-Aldrich). To a stirred solution of 4-nitrobenzoic-$^{18}O_2$ acid (**S24**) (2.10 g, 12.3 mmol, 1.0 equiv), (–)-myrtenol (1.87 g, 12.3 mmol, 1.0 equiv), and PPh_3 (3.88 g, 14.8 mmol, 1.2 equiv) in THF (50 mL) at 0 °C was added DIAD (2.90 mL, 14.8 mmol, 1.2 equiv) dropwise. The mixture was stirred for 3 h and gradually allowed to warm to 23 °C, at which point TLC indicated complete consumption of **S24**. The solution was diluted with saturated aqueous $NaHCO_3$ (100 mL) and EtOAc (100 mL). The layers were separated and the aqueous layer was extracted with EtOAc (3 × 100 mL). The combined organic phases were washed with brine, dried over $MgSO_4$, and concentrated. The crude product was purified by flash chromatography (5–15% EtOAc/hexanes) to afford the title compound as a white solid (2.26 g, 7.40 mmol, 60% yield). ^1H NMR (500 MHz, $CDCl_3$) δ 8.32 – 8.26 (m, 2H), 8.22 – 8.16 (m, 2H), 5.69 (tt, *J* = 3.0, 1.5 Hz, 1H), 4.78 – 4.71 (m, 2H), 2.45 (dt, *J* = 8.7, 5.6 Hz, 1H), 2.40 – 2.27 (m, 2H), 2.22 (td, *J* = 5.6, 1.4 Hz, 1H), 2.18 – 2.12 (m, 1H), 1.31 (s, 3H), 1.24 (d, *J* = 8.7 Hz, 1H), 0.87 (s, 3H); ^{13}C NMR (100 MHz, $CDCl_3$) δ 164.7, 150.6, 142.5, 136.0, 130.8, 123.7, 122.9, 68.6, 43.9, 40.8, 38.3, 31.7, 31.5, 26.3, 21.3. Spectral data are in good accordance with previously reported values (*103*). ^{18}O incorporation was determined only for compound **S26**.

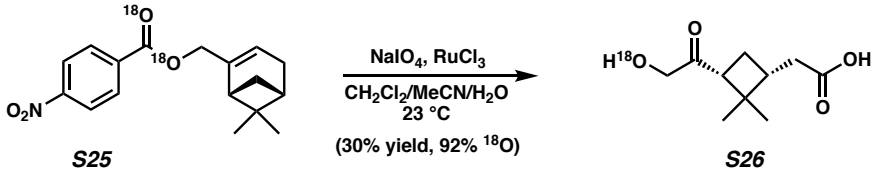

S25 *S26*

2-((1*R*,3*R*)-3-(2-hydroxyacetyl)-2,2-dimethylcyclobutyl)acetic-^{18}O acid ((–)-*cis*-10-hydroxypinonic-^{18}O acid, S26)

To a stirred solution of (–)-myrtenyl 4-nitrobenzoate-$^{18}O_2$ (**S25**) (2.20 g, 7.20 mmol, 1.0 equiv) in CH_2Cl_2/MeCN/H_2O (2:2:3, 63 mL) at 23 °C was added $NaIO_4$ (6.16 g, 28.8 mmol, 4.0 equiv) followed by catalytic $RuCl_3$ hydrate (55 mg). After 48 h, TLC indicated complete conversion of S25 and the mixture was diluted with Et_2O (50 mL). The layers were separated and the aqueous layer was extracted with Et_2O (3 × 40 mL). The combined organic phases were filtered through celite and concentrated. The crude residue was dissolved in Et_2O (25 mL) and extracted with 10% aqueous Na_2CO_3 (3 × 40 mL). The aqueous phases were combined, acidified to pH 1 with concentrated H_2SO_4, and extracted with Et_2O (3 × 40 mL). The combined organic phases were washed with brine, dried over $MgSO_4$, and concentrated. The crude product was purified by flash chromatography (40–70% EtOAc/hexanes; 1% AcOH). Residual AcOH was removed by rotary

evaporation with added toluene to afford the title compound as a white solid (436 mg, 2.16 mmol, 30% yield). $[\alpha]_D^{25} = -47.5°$ (*c* 0.50, $CHCl_3$); ^1H NMR (400 MHz, $CDCl_3$) δ 4.21 – 4.04 (m, 2H), 2.89 (dd, *J* = 10.1, 7.6 Hz, 1H), 2.49 – 2.30 (m, 3H), 2.17 – 1.98 (m, 2H), 1.29 (s, 3H), 0.87 (s, 3H); ^{13}C NMR (100 MHz, $CDCl_3$) δ 207.9, 177.9, 68.8, 49.8, 44.0, 38.1, 34.8, 30.5, 22.5, 17.6; IR (thin film, NaCl) 2954, 2366, 1706, 1399, 1218, 1025 cm^{-1}; HRMS (ESI-TOF) *m/z* calc'd for $[M-H]^-$ $C_{10}H_{15}{}^{18}O^{16}O_3$ = 201.1013, found 201.1012, 92.6% ^{18}O incorporation.

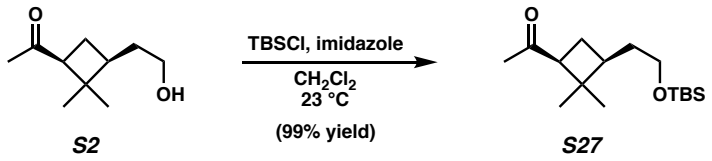

S2 ***S27***

1-((1*S*,3*S*)-3-(2-((*tert*-butyldimethylsilyl)oxy)ethyl)-2,2-dimethylcyclobutyl)ethan-1-one (S27)

To a stirred solution of alcohol S2 (1.50 g, 8.80 mmol, 1.0 equiv) and imidazole (2.40 g, 35.2 mmol, 4.0 equiv) in CH_2Cl_2 (88 mL) at 23 °C was added TBSCl (2.65 g, 17.6 mmol, 2.0 equiv) in one portion. The mixture was stirred for 16 h at 23 °C, at which point TLC indicated complete consumption of **S2**. The solution was diluted with Et_2O (100 mL) and H_2O (100 mL). The layers were separated and the aqueous layer was extracted with Et_2O (3 × 100 mL). The combined organic phases were washed with brine, dried over $MgSO_4$, and concentrated. The crude product was purified by flash chromatography (15% Et_2O/hexanes) to afford the title compound as a colorless oil (2.48 g, 8.72 mmol, 99% yield). $[\alpha]_D^{25} = +21.5°$ (*c* 0.80, $CHCl_3$); ^1H NMR (400 MHz, $CDCl_3$) δ 3.58 – 3.47 (m, 2H), 2.81 (dd, *J* = 9.9, 7.5 Hz, 1H), 2.03 (s, 3H), 2.00 – 1.93 (m, 1H), 1.92 – 1.80 (m, 2H), 1.59 – 1.51 (m, 1H), 1.45 – 1.34 (m, 1H), 1.27 (s, 3H), 0.88 (s, 9H), 0.85 (s, 3H), 0.03 (s, 6H); ^{13}C NMR (100 MHz, $CDCl_3$) δ 208.3, 61.7, 54.6, 43.5, 39.0, 33.4, 30.6, 30.3, 26.1, 23.3, 18.5, 17.5, –5.2; IR (thin film, NaCl) 2952, 2928, 2858, 1707, 1461, 1362, 1254, 1179, 1103 cm^{-1}; HRMS (FI) *m/z* calc'd for $[M]^{\bullet+}$ $C_{16}H_{32}O_2Si$ = 284.2172, found 284.2171.

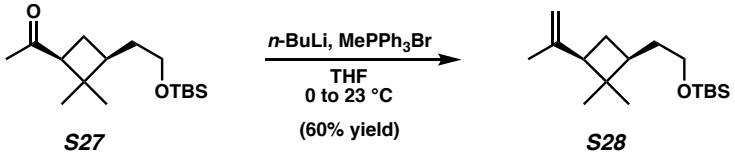

S27 ***S28***

***tert*-butyl(2-((1*S*,3*R*)-2,2-dimethyl-3-(prop-1-en-2-yl)cyclobutyl)ethoxy)dimethylsilane (S28)**

To a round bottom flask charged with $MePPh_3Br$ (2.51 g, 7.03 mmol, 2.0 equiv) and evacuated and backfilled with N_2 (3×) at 23 °C was added THF (35 mL). The solution was cooled to 0 °C, *n*-BuLi (2.5 M in THF, 2.81 mL, 7.03 mmol, 2.0 equiv) was added dropwise, and the solution was stirred for 10 min at 0 °C. Silyl ether **S27** (1.00 g, 3.51 mmol, 1.0 equiv) in THF (5.0 mL) was then added dropwise at 0 °C. The mixture was stirred for 12 h and gradually allowed to warm to 23 °C, at which point TLC indicated complete consumption of **S27**. The solution was diluted with Et_2O (50 mL) and H_2O (50 mL). The layers were separated and the aqueous layer was extracted with Et_2O (3 × 50 mL). The combined organic phases were washed with brine, dried over $MgSO_4$, and concentrated. The crude product was purified by flash chromatography (0–7% Et_2O/hexanes) to afford the title compound as a colorless oil (710 mg, 2.51 mmol, 71% yield). $[\alpha]_D^{25} = -18.3°$ (*c* 1.0, $CHCl_3$); ^1H NMR (600 MHz, $CDCl_3$) δ 4.78 (d, *J* = 2.0 Hz, 1H), 4.55 (d, *J* = 2.1 Hz, 1H), 3.54

(td, J = 6.9, 1.2 Hz, 2H), 2.33 (dd, J = 10.6, 7.0 Hz, 1H), 1.94 – 1.82 (m, 2H), 1.65 (s, 3H), 1.60 – 1.49 (m, 2H), 1.45 – 1.35 (m, 1H), 1.14 (s, 3H), 0.90 (s, 9H), 0.76 (s, 3H), 0.05 (s, 6H); ^{13}C NMR (100 MHz, $CDCl_3$) δ 145.9, 109.1, 62.1, 49.6, 41.6, 38.8, 33.7, 30.9, 26.5, 26.2, 23.2, 18.5, 16.5, –5.1; IR (thin film, NaCl) 2959, 1749, 1722, 1415, 1372, 1269, 1230, 1170, 1151, 1051 cm^{-1}; HRMS (FI) *m/z* calc'd for $[M]^{\bullet+}$ $C_{17}H_{34}OSi$ = 282.2379, found 282.2388.

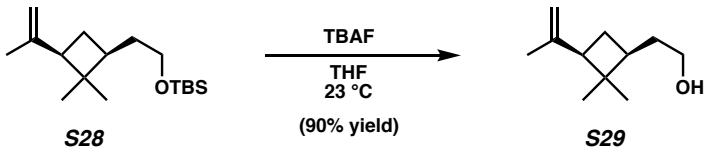

S28 ***S29***

2-((1*S*,3*R*)-2,2-dimethyl-3-(prop-1-en-2-yl)cyclobutyl)ethan-1-ol (S29)

To a stirred solution of silyl ether S28 (300 mg, 1.06 mmol, 1.0 equiv) in THF (11 mL) at 23 °C was added TBAF (1.0 M in THF, 1.59 mL, 1.59 mmol, 1.5 equiv) in one portion. The mixture was stirred for 16 h at 23 °C, at which point TLC indicated complete consumption of **S28**. The solution was diluted with Et_2O (30 mL) and H_2O (30 mL). The layers were separated and the aqueous layer was extracted with Et_2O (3 × 30 mL). The combined organic phases were washed with brine, dried over $MgSO_4$, and concentrated. The crude product was purified by flash chromatography (30% Et_2O/hexanes) to afford the title compound as a colorless oil (161 mg, 0.957 mmol, 90% yield). $[\alpha]_D^{25}$ = –22.6° (*c* 0.80, $CHCl_3$); ^{1}H NMR (400 MHz, $CDCl_3$) δ 4.78 (dt, J = 2.1, 1.4 Hz, 1H), 4.67 – 4.53 (m, 1H), 3.59 (td, J = 6.8, 1.0 Hz, 2H), 2.42 – 2.31 (m, 1H), 1.99 – 1.85 (m, 2H), 1.65 (dt, J = 1.5, 0.8 Hz, 3H), 1.63 – 1.52 (m, 2H), 1.49 – 1.39 (m, 1H), 1.15 (s, 3H), 0.77 (s, 3H); ^{13}C NMR (100 MHz, $CDCl_3$) δ 145.7, 109.3, 61.9, 49.6, 41.7, 38.7, 33.5, 30.8, 26.4, 23.2, 16.5; IR (thin film, NaCl) 3311, 3079, 2953, 2881, 1646, 1457, 1437, 1366, 1052 cm^{-1}; HRMS (FI) *m/z* calc'd for $[M]^{\bullet+}$ $C_{11}H_{20}O$ = 168.1514, found 168.1510.

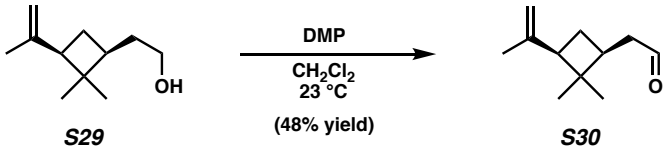

S29 ***S30***

2-((1*S*,3*R*)-2,2-dimethyl-3-(prop-1-en-2-yl)cyclobutyl)acetaldehyde ((+)-enal, S30)

To a stirred solution of alcohol S29 (420 mg, 2.50 mmol, 1.0 equiv) in CH_2Cl_2 (50 mL) at 23 °C was added DMP (2.12 g, 5.00 mmol, 2.0 equiv) in one portion. The mixture was stirred for 16 h at 23 °C, at which point TLC indicated complete consumption of **S29**. The solution was diluted with saturated aqueous $Na_2S_2O_3$ (25 mL), Et_2O (100 mL), and H_2O (60 mL). The layers were separated and the aqueous layer was extracted with Et_2O (3 × 50 mL). The combined organic phases were washed with brine, dried over $MgSO_4$, and concentrated. The crude product was purified by flash chromatography (10% Et_2O/hexanes) to afford the title compound as a colorless oil (200 mg, 1.20 mmol, 48% yield). ^{1}H NMR (500 MHz, $CDCl_3$) δ 9.73 (t, J = 2.0 Hz, 1H), 4.81 (dt, J = 2.0, 1.4 Hz, 1H), 4.56 (td, J = 1.9, 0.9 Hz, 1H), 2.49 – 2.42 (m, 2H), 2.39 – 2.28 (m, 2H), 2.08 – 1.98 (m, 1H), 1.66 (d, J = 0.7 Hz, 3H), 1.63 (d, J = 10.4 Hz, 1H), 1.19 (s, 3H), 0.78 (s, 3H); ^{13}C NMR (100 MHz, $CDCl_3$) δ 202.1, 145.0, 109.5, 49.6, 45.2, 41.9, 35.8, 30.5, 26.3, 22.9, 16.7. Spectral data are in good accordance with previously reported values (*94*).

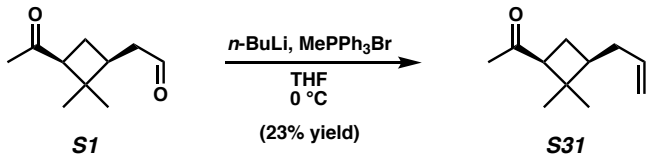

1-((1*S*,3*R*)-3-allyl-2,2-dimethylcyclobutyl)ethan-1-one ((+)-enone, S31)

To a round bottom flask charged with $MePPh_3Br$ (2.33 g, 6.53 mmol, 1.1 equiv) and evacuated and backfilled with N_2 (3×) at 23 °C was added THF (60 mL). The solution was cooled to 0 °C, *n*-BuLi (2.5 M in THF, 2.38 mL, 5.94 mmol, 1.0 equiv) was added dropwise, and the solution was stirred for 10 min at 0 °C. (+)-*cis*-Pinonaldehyde (**S1**) (1.00 g, 5.94 mmol, 1.0 equiv) in THF (25 mL) was then added dropwise at 0 °C. After 1 min, TLC indicated complete consumption of **S1**. The solution was diluted with Et_2O (100 mL) and H_2O (100 mL). The layers were separated and the aqueous layer was extracted with Et_2O (3 × 100 mL). The combined organic phases were washed with brine, dried over $MgSO_4$, and concentrated. The crude product was purified by flash chromatography (10% Et_2O/hexanes) to afford the title compound as a colorless oil (228 mg, 1.37 mmol, 23% yield). ^{1}H NMR (500 MHz, $CDCl_3$) δ 5.76 – 5.63 (m, 1H), 5.04 – 4.90 (m, 2H), 2.82 (dd, J = 9.9, 7.4 Hz, 1H), 2.12 – 2.06 (m, 1H), 2.03 (s, 3H), 2.01 – 1.80 (m, 4H), 1.29 (s, 3H), 0.87 (s, 3H); ^{13}C NMR (100 MHz, $CDCl_3$) δ 208.2, 136.9, 115.4, 54.4, 43.6, 41.6, 34.8, 30.7, 30.3, 23.2, 17.3. Spectral data are in good accordance with previously reported values (*94*).

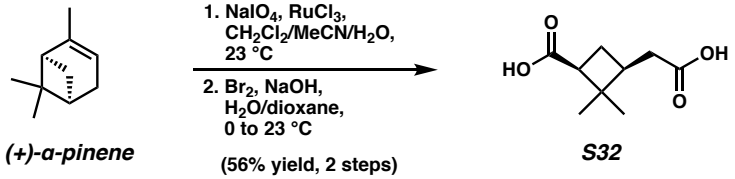

(1*S*,3*S*)-3-(carboxymethyl)-2,2-dimethylcyclobutane-1-carboxylic acid ((+)-*cis*-pinic acid, S32)

(+)-cis-Pinic acid (S32) was prepared previously (*34*) from commercial (+)-α-pinene (98%, 89% ee, Sigma-Aldrich). ^{1}H NMR (500 MHz, $CDCl_3$) δ 2.78 (dd, J = 10.3, 7.8 Hz, 1H), 2.44 – 2.30 (m, 3H), 2.16 – 2.09 (m, 1H), 1.97 – 1.89 (m, 1H), 1.24 (s, 3H), 1.01 (s, 3H); ^{13}C NMR (125 MHz, $CDCl_3$) δ 179.4, 179.1, 46.2, 43.1, 38.1, 35.3, 30.0, 24.4, 17.7.

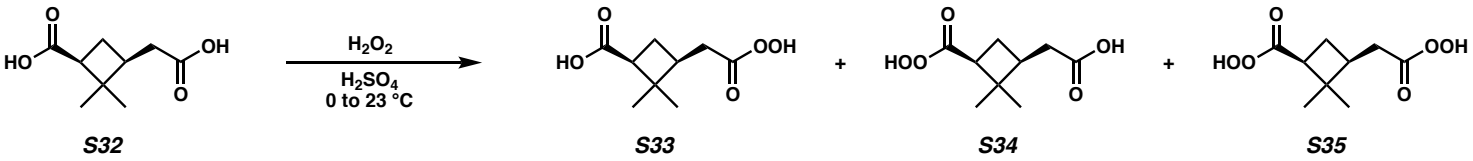

S32 *S33* *S34* *S35*

(1*S*,3*S*)-3-(2-hydroperoxy-2-oxoethyl)-2,2-dimethylcyclobutane-1-carboxylic acid (S33), 2-((1*S*,3*S*)-3-carboperoxy-2,2-dimethylcyclobutyl)acetic acid (S34), (1*S*,3*S*)-3-(2-hydroperoxy-2-oxoethyl)-2,2-dimethylcyclobutane-1-carboperoxoic acid (S35)

Peracids **S33**, **S34**, and **S35** were prepared according to a modified literature procedure (*104*) from (+)-cis-pinic acid (S32). To a stirred solution of (+)-cis-pinic acid (S32) (500 mg, 2.69 mmol, 1.0 equiv) in concentrated H_2SO_4 (610 μL) at 0 °C was slowly added H_2O_2 (50% w/w, 610 μL, 10.8 mmol, 4.0 equiv) dropwise. The mixture was stirred for 3 h and gradually allowed to warm to 23 °C. The solution was diluted with Et_2O (5 mL) and H_2O (5 mL). The layers were separated and the aqueous layer was extracted with Et_2O (3 × 5 mL). The combined organic phases were washed with brine, dried over $MgSO_4$, and concentrated to afford a mixture of (+)-*cis*-pinic acid (**S32**), (+)-*cis*-monoperoxypinic acid isomers (**S33** and **S34**), and (+)-*cis*-diperoxypinic acid (**S35**) as a yellow oil, verified by UPLC/(–)ESI-Q-TOF-MS (Fig. S11), that was used in subsequent experiments without further purification. HRMS (ESI-TOF) *m/z* calc'd for $[M–H]^-$ $C_9H_{13}O_5$ = 201.0763, found 201.0765 and $[M–H]^-$ $C_9H_{13}O_6$ = 217.0712, found 217.0703. Spectral data are in good accordance with previously reported values (*104*).

S6. NMR and IR Spectra

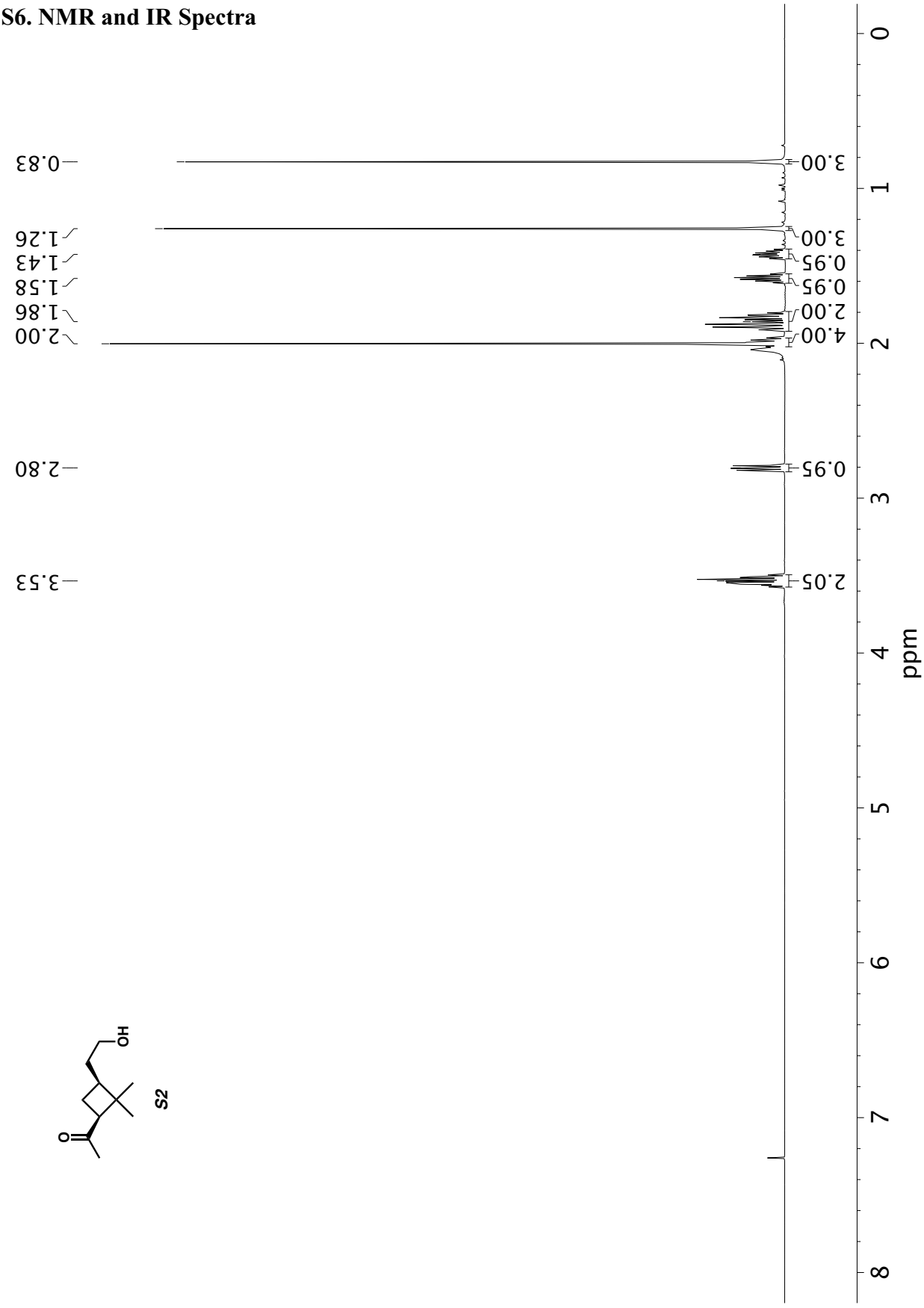

^{1}H NMR (600 MHz, $CDCl_3$) of compound **S2**.

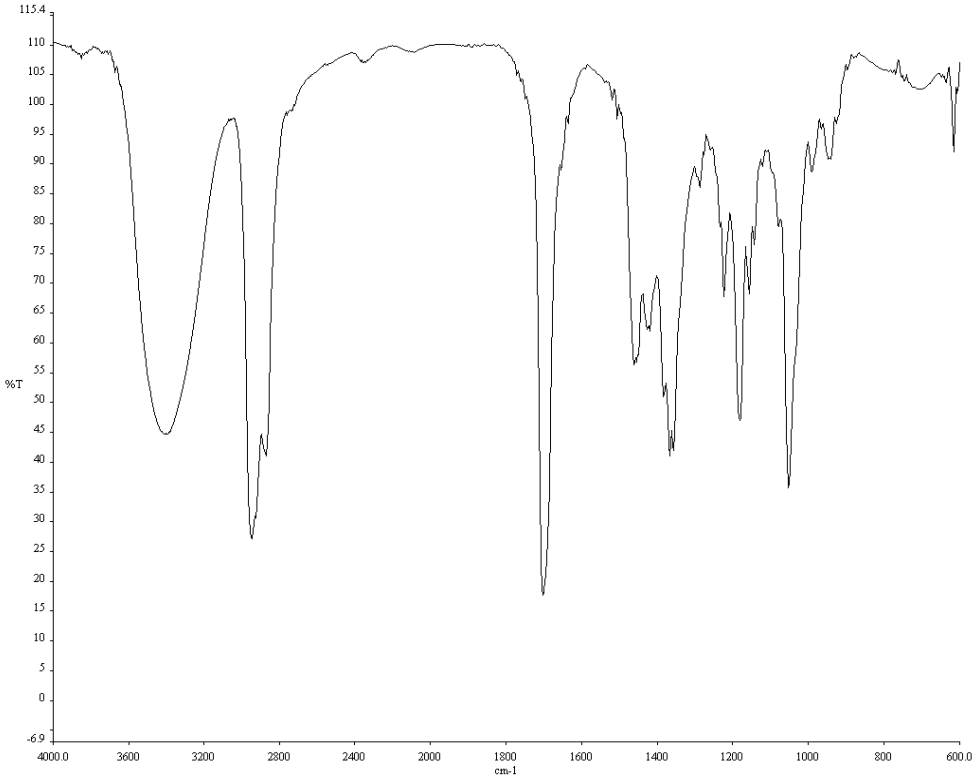

Infrared spectrum (thin film, NaCl) of compound **S2**.

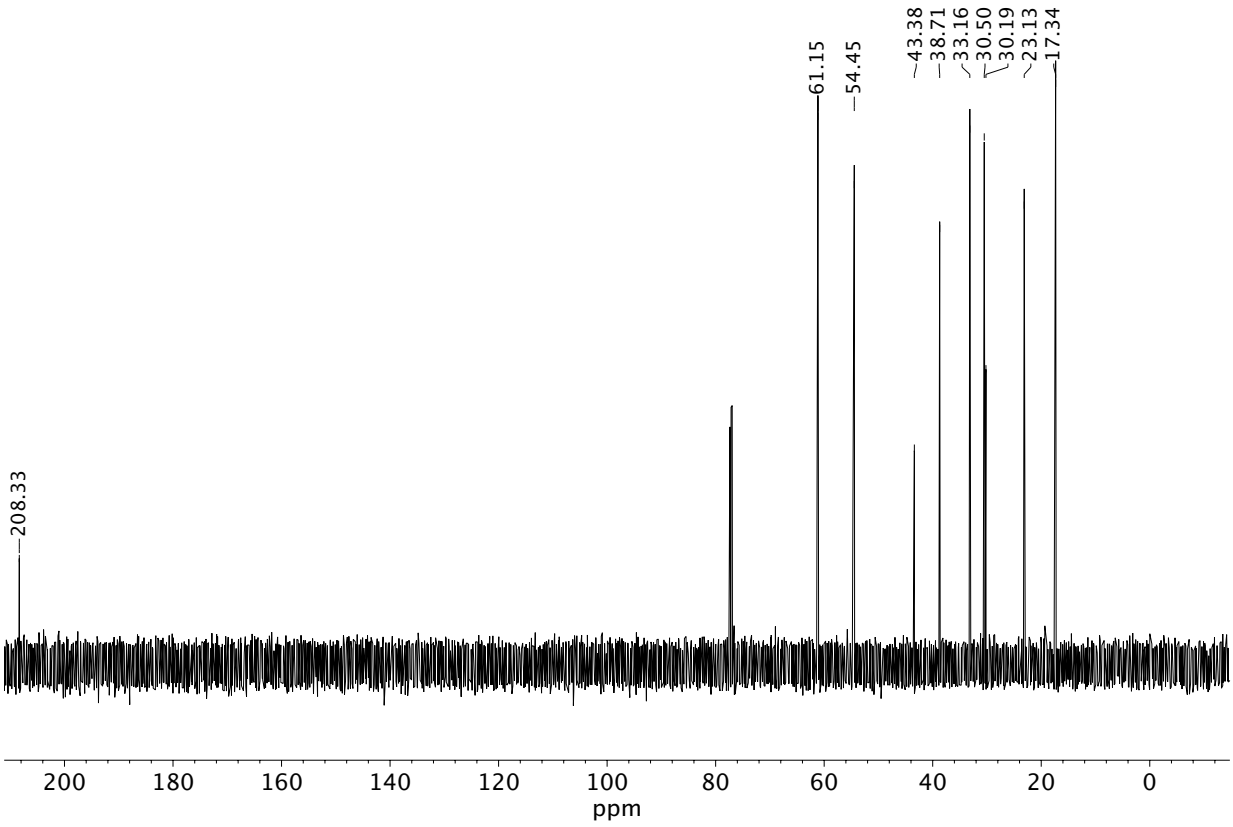

^{13}C NMR (151 MHz, $CDCl_3$) of compound **S2**.

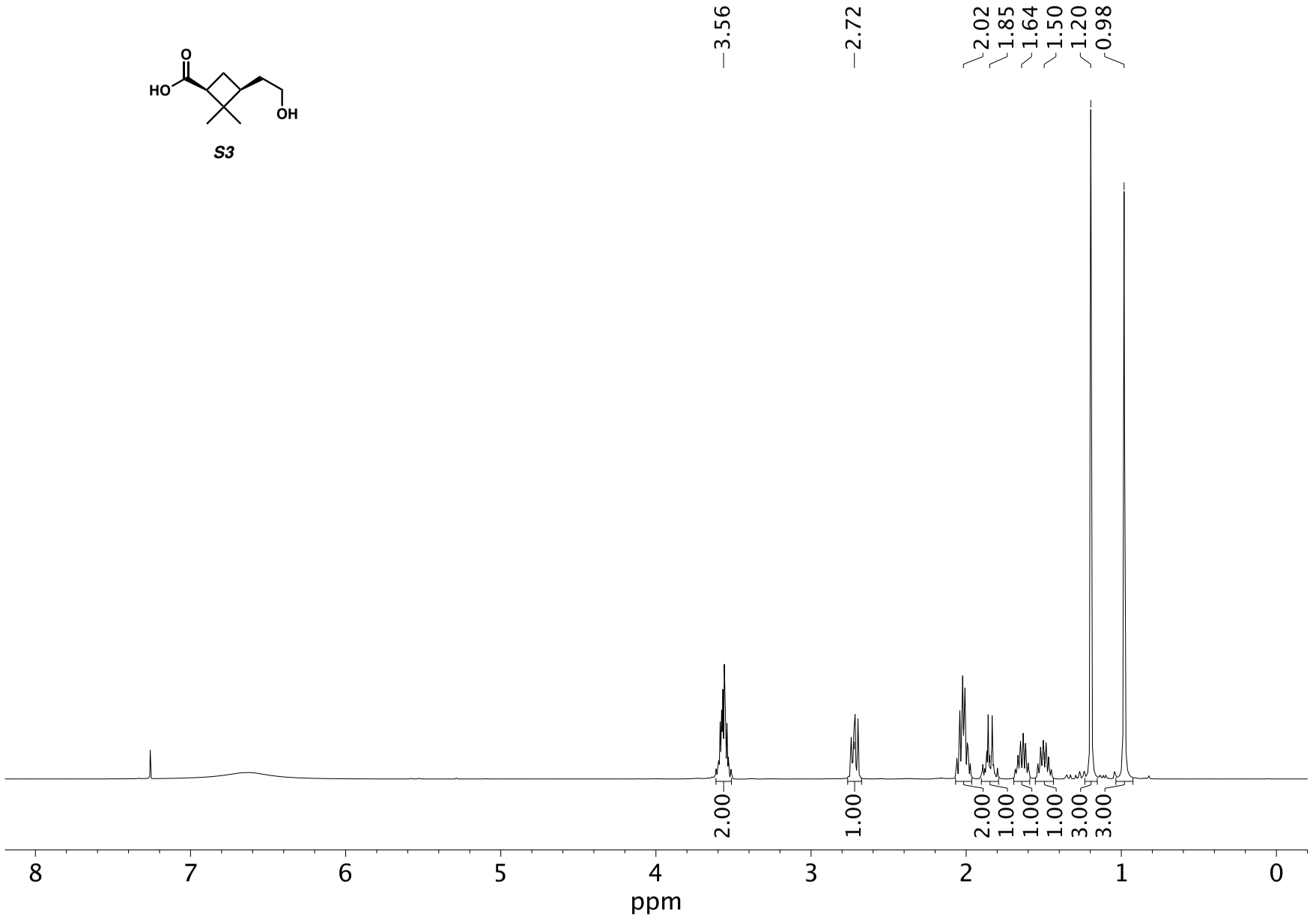

^{1}H NMR (400 MHz, $CDCl_3$) of compound **S3**.

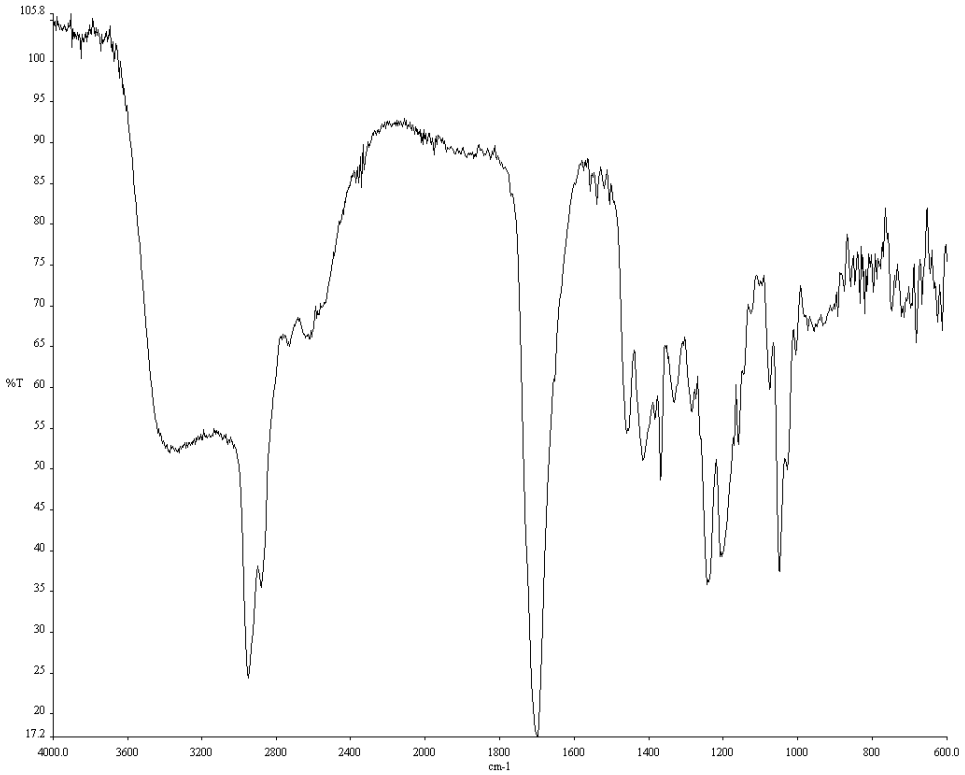

Infrared spectrum (thin film, NaCl) of compound **S3**.

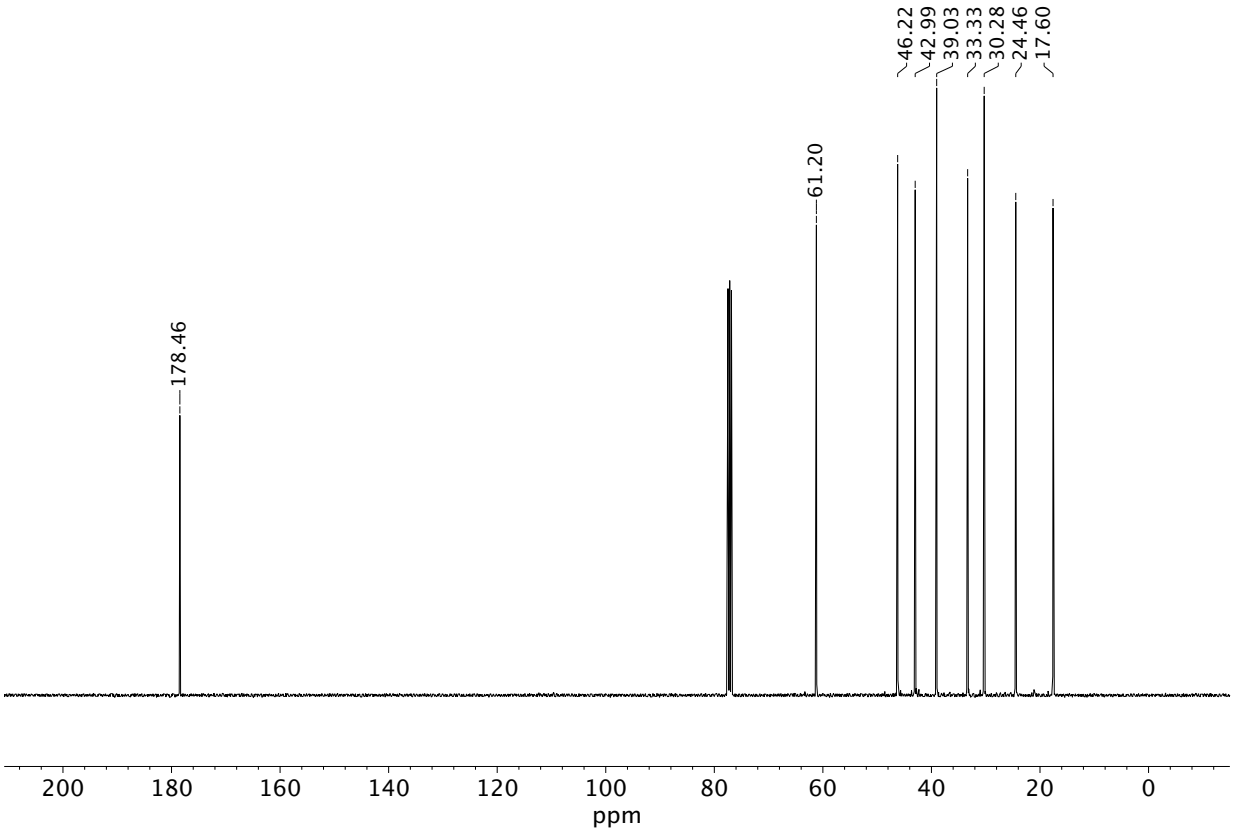

^{13}C NMR (100 MHz, $CDCl_3$) of compound **S3**.

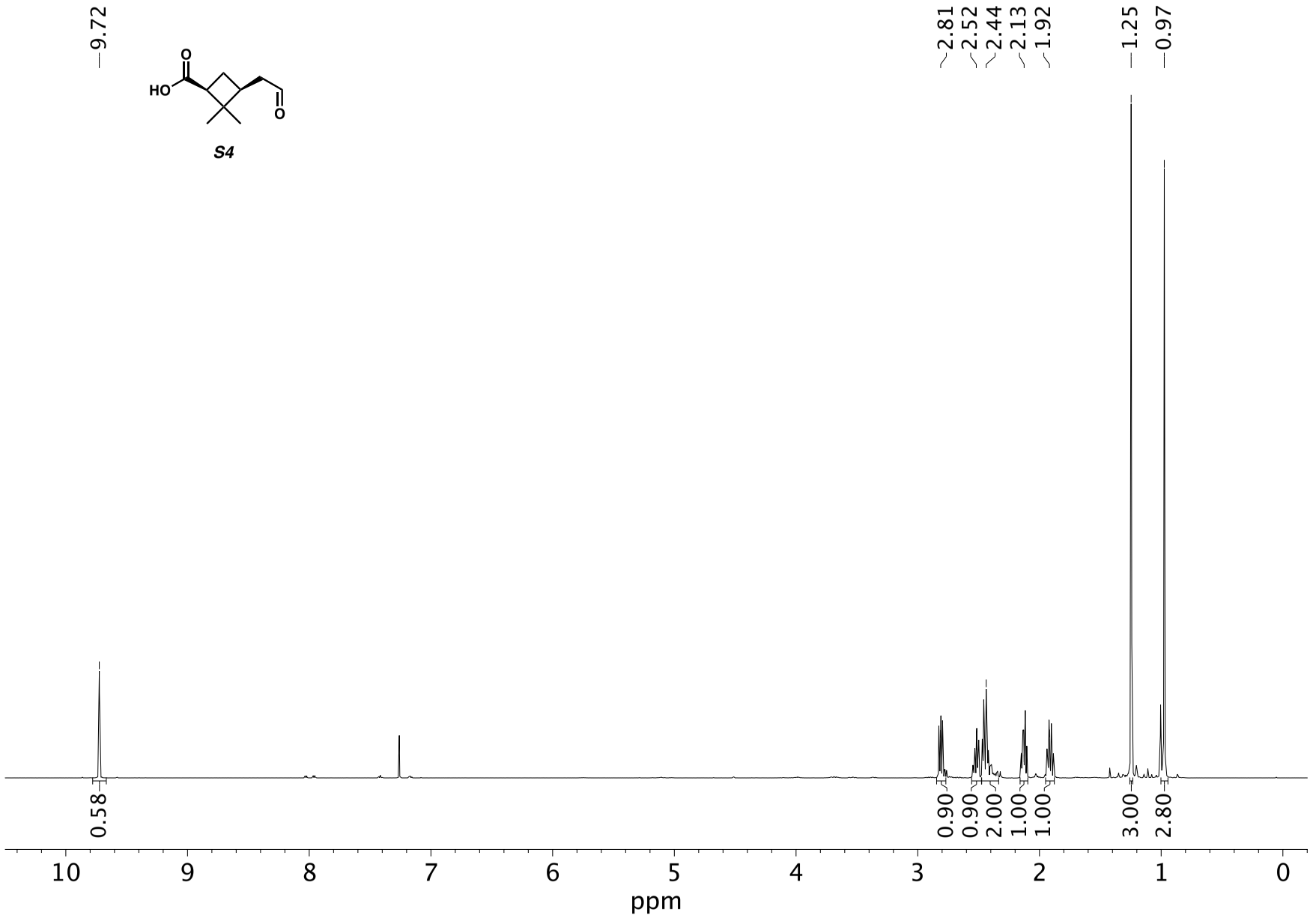

^{1}H NMR (600 MHz, $CDCl_3$) of compound **S4**.

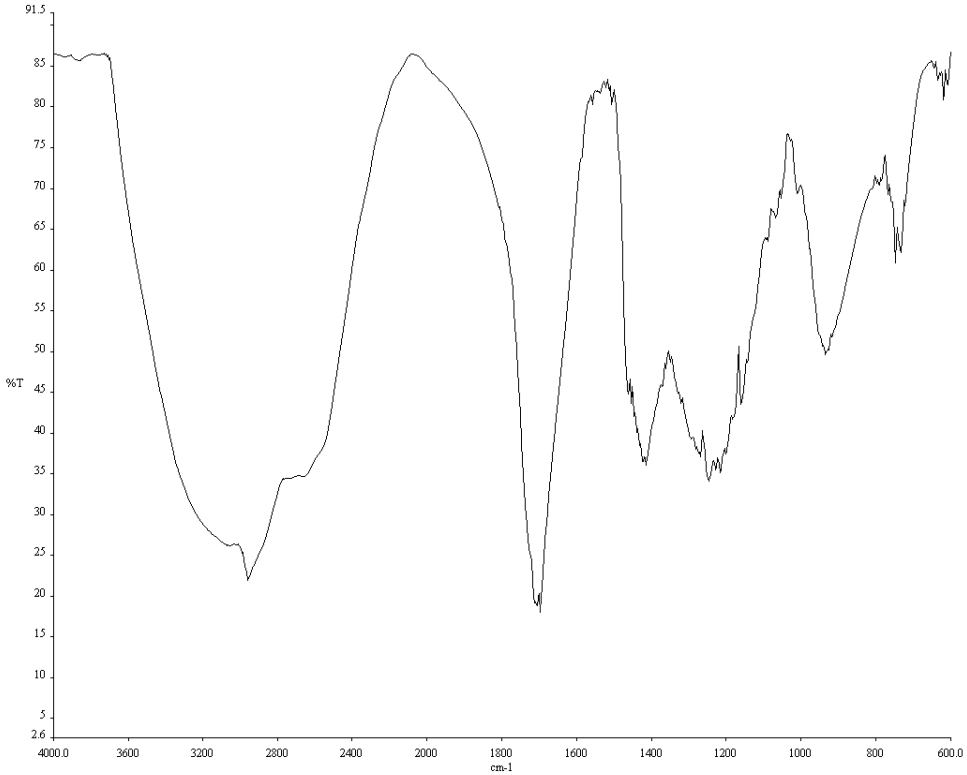

Infrared spectrum (thin film, NaCl) of compound **S4**.

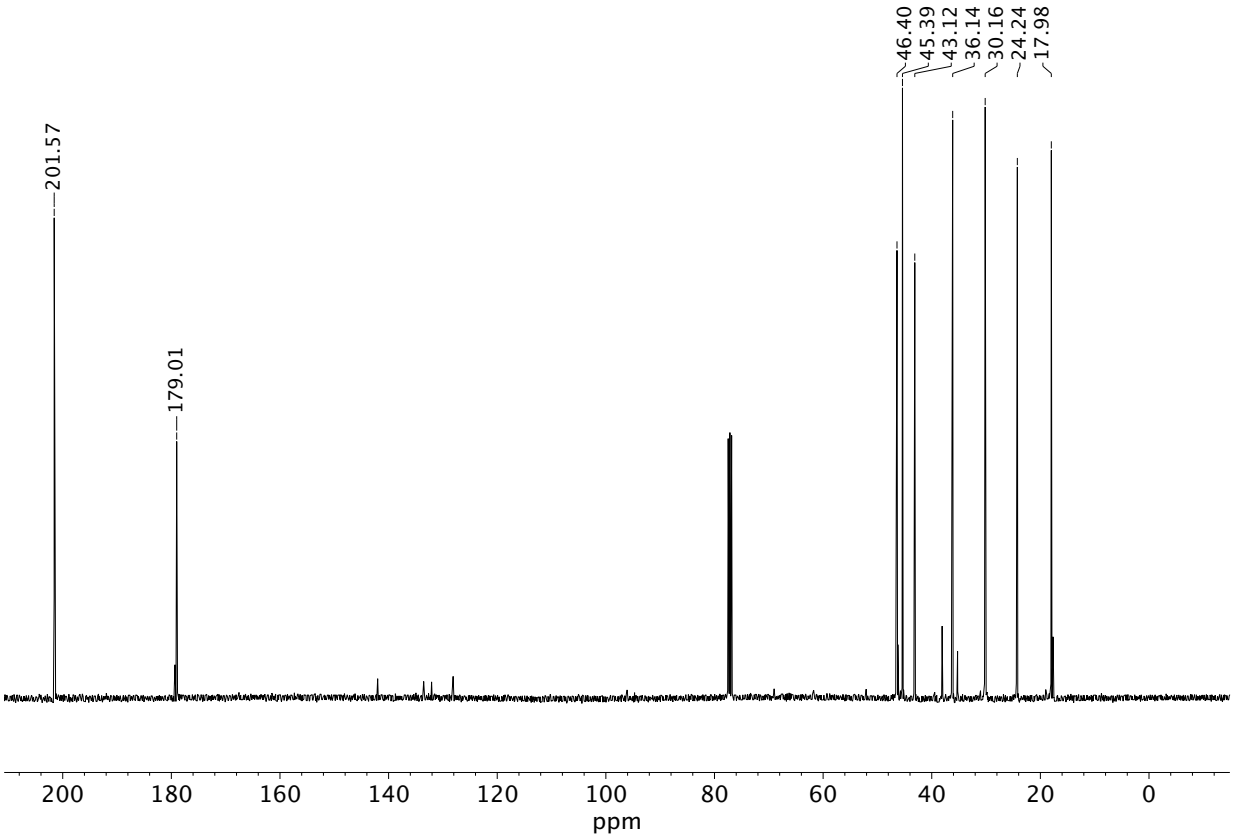

^{13}C NMR (100 MHz, $CDCl_3$) of compound **S4**.

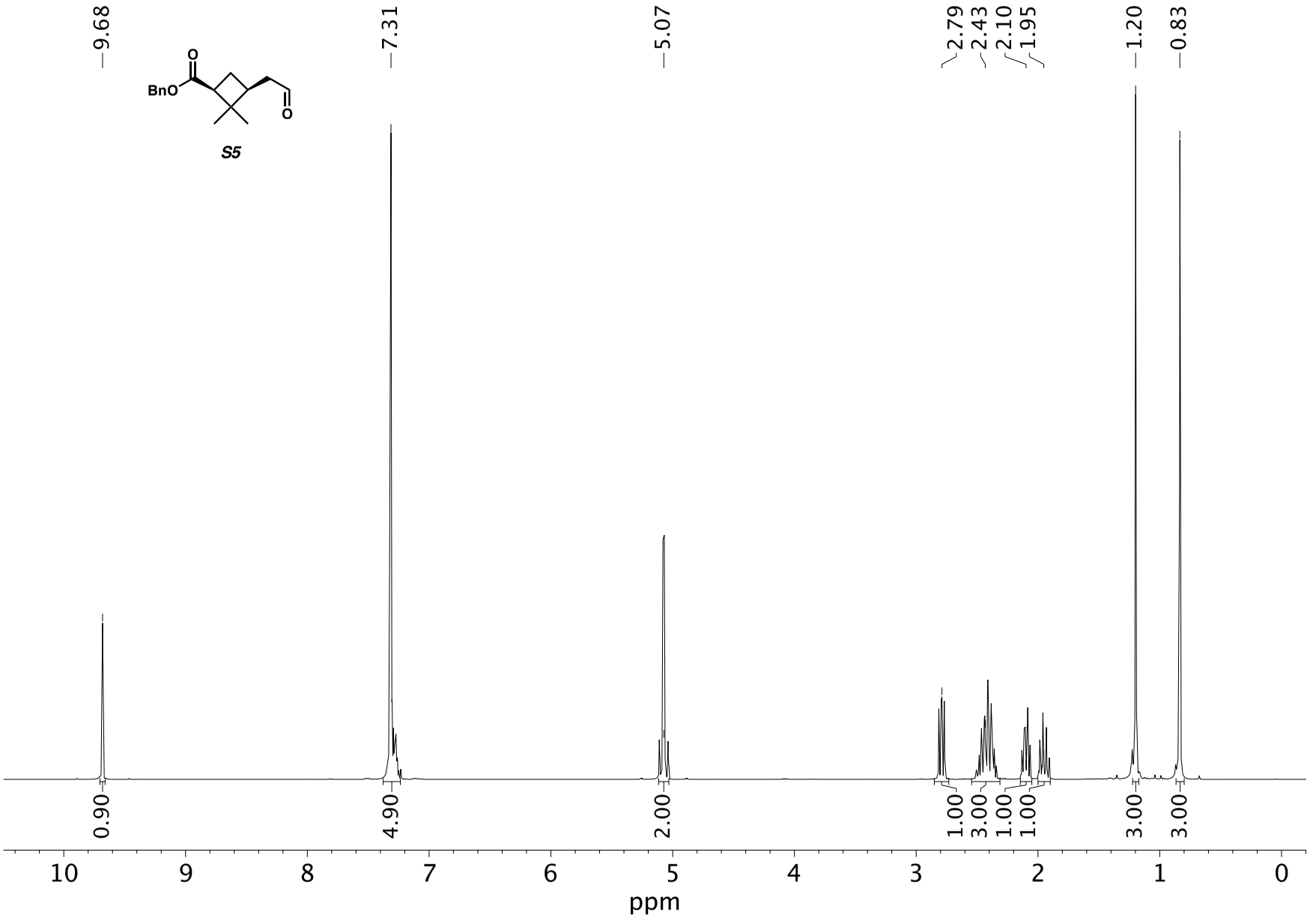

^{1}H NMR (400 MHz, $CDCl_3$) of compound **S5**.

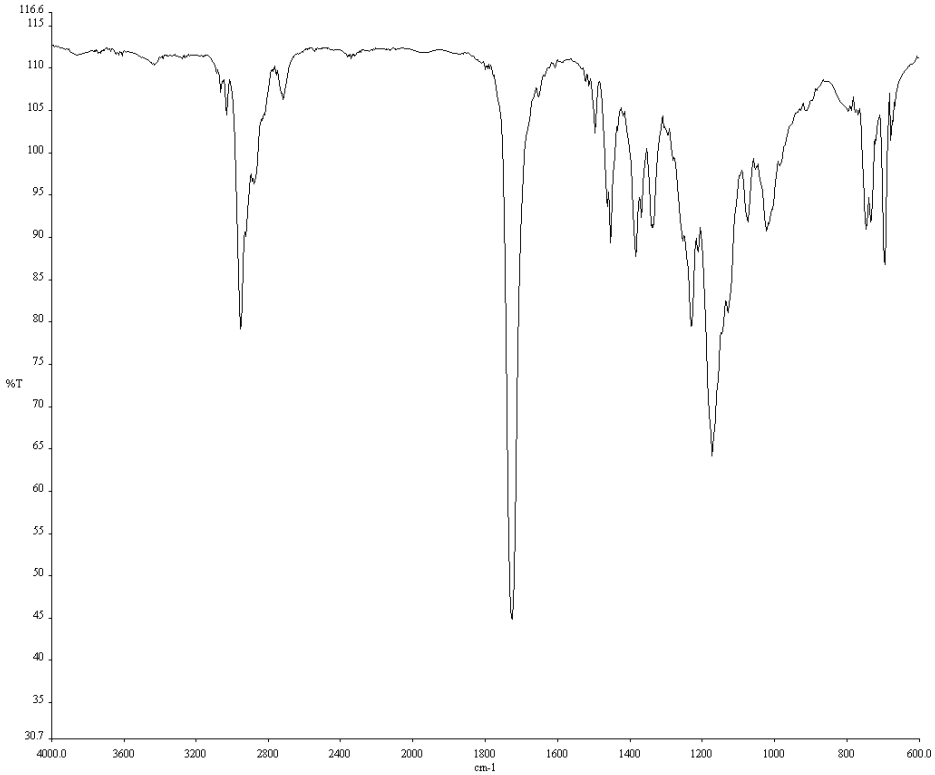

Infrared spectrum (thin film, NaCl) of compound **S5**.

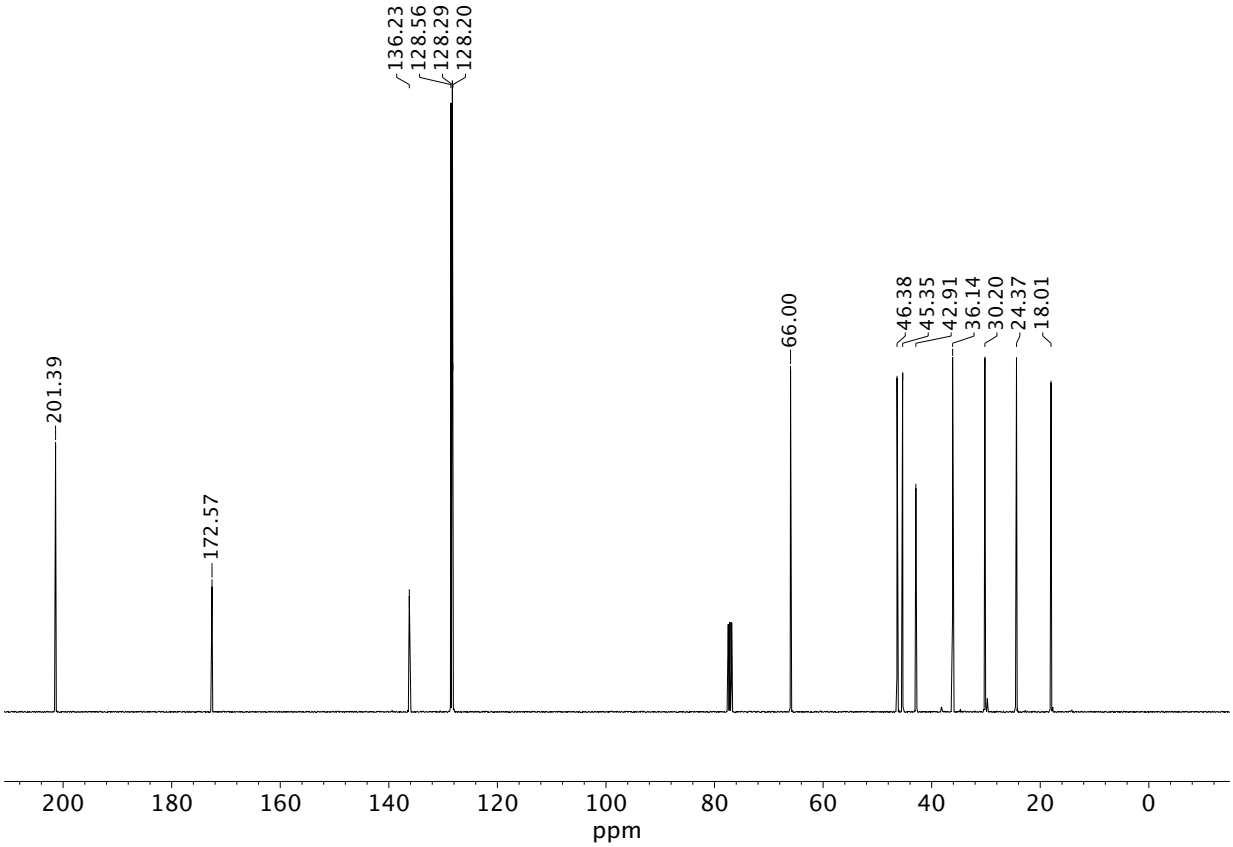

^{13}C NMR (100 MHz, $CDCl_3$) of compound **S5**.

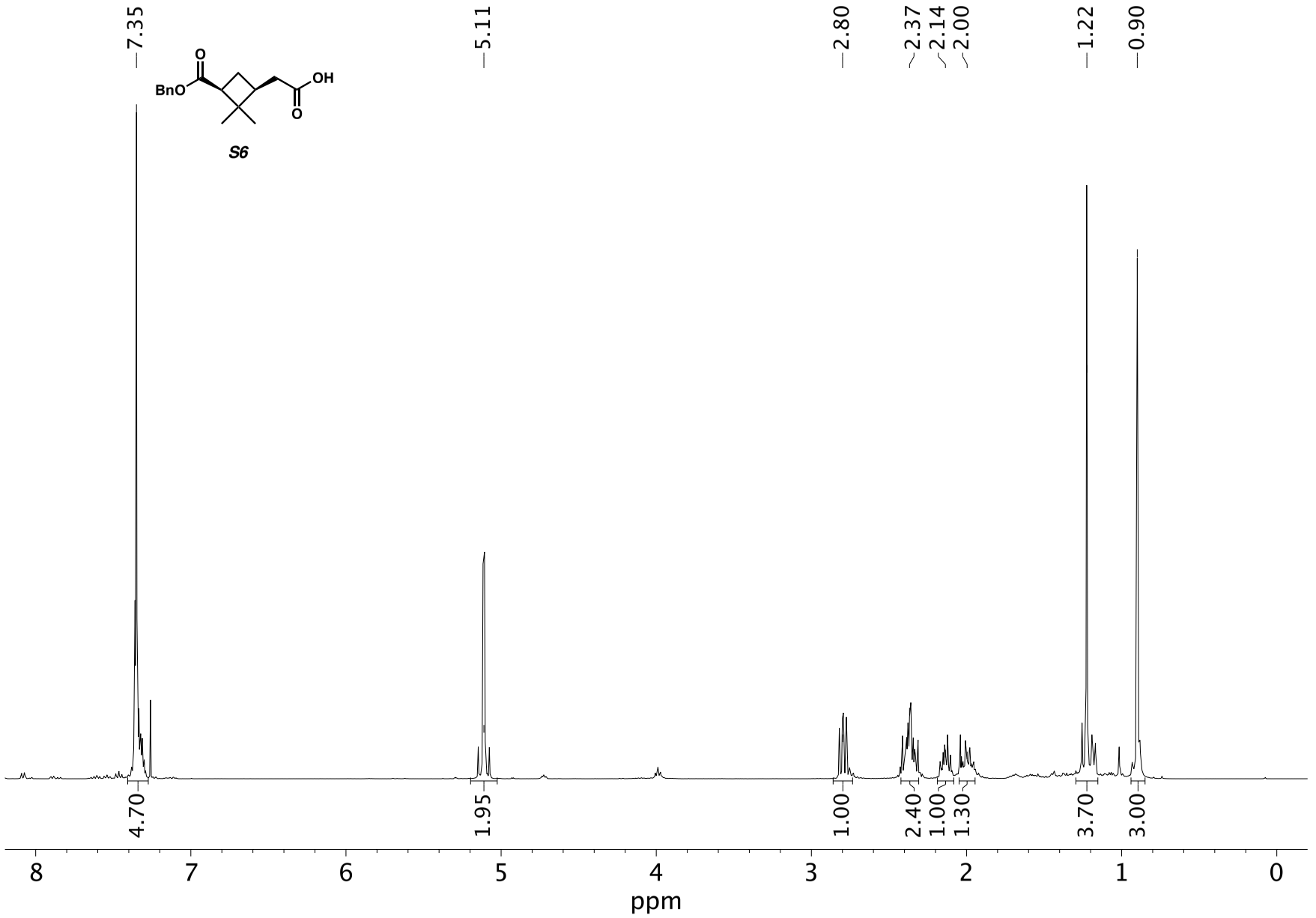

^{1}H NMR (400 MHz, $CDCl_3$) of compound **S6**.

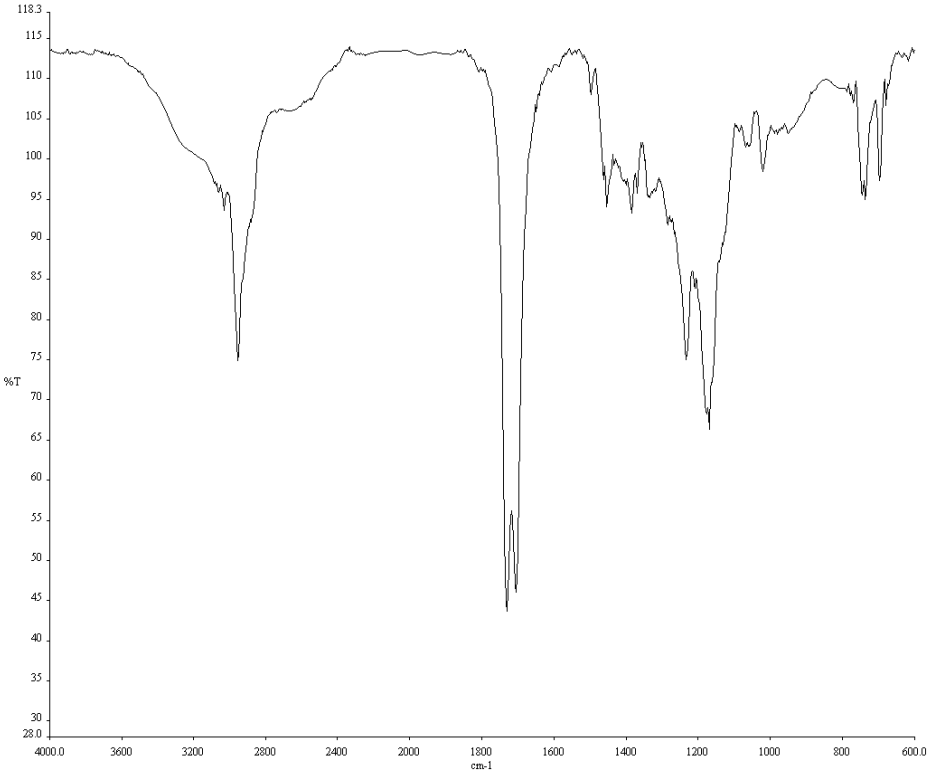

Infrared spectrum (thin film, NaCl) of compound **S6**.

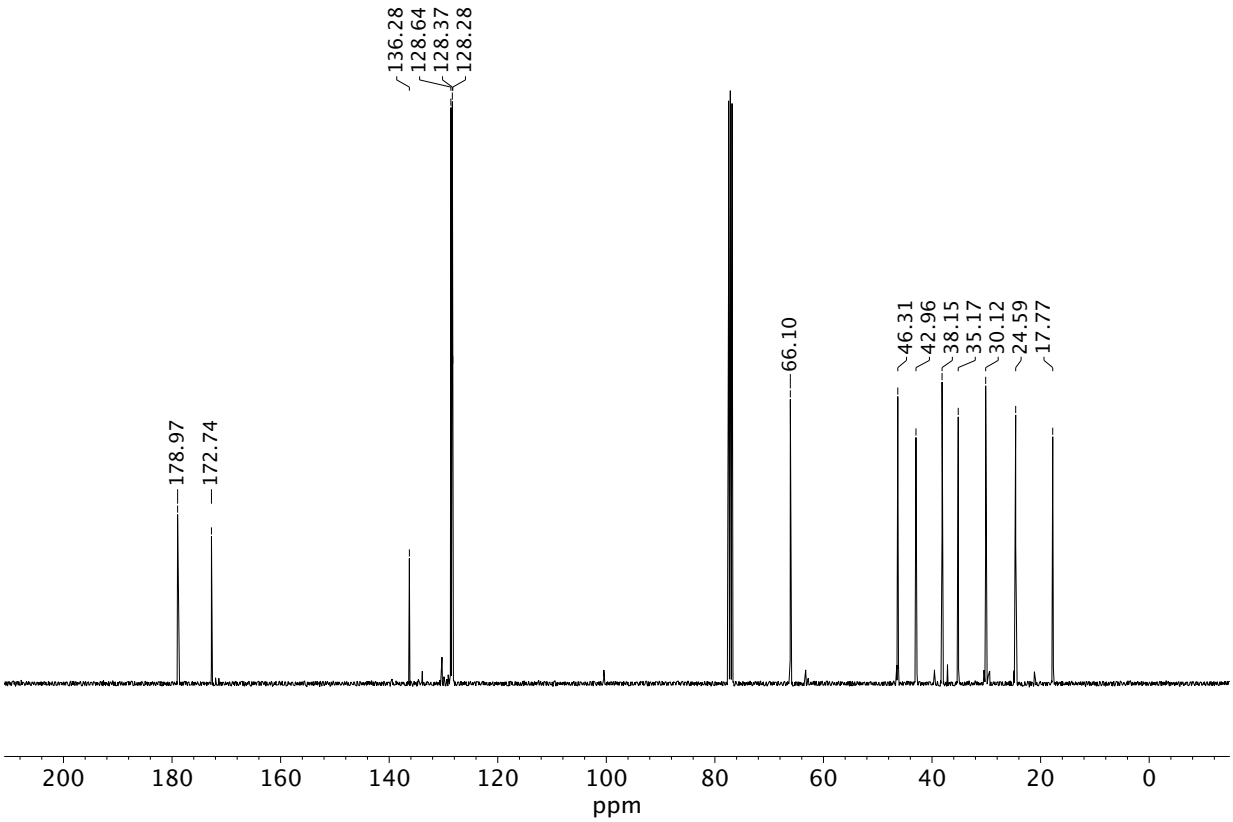

^{13}C NMR (100 MHz, $CDCl_3$) of compound **S6**.

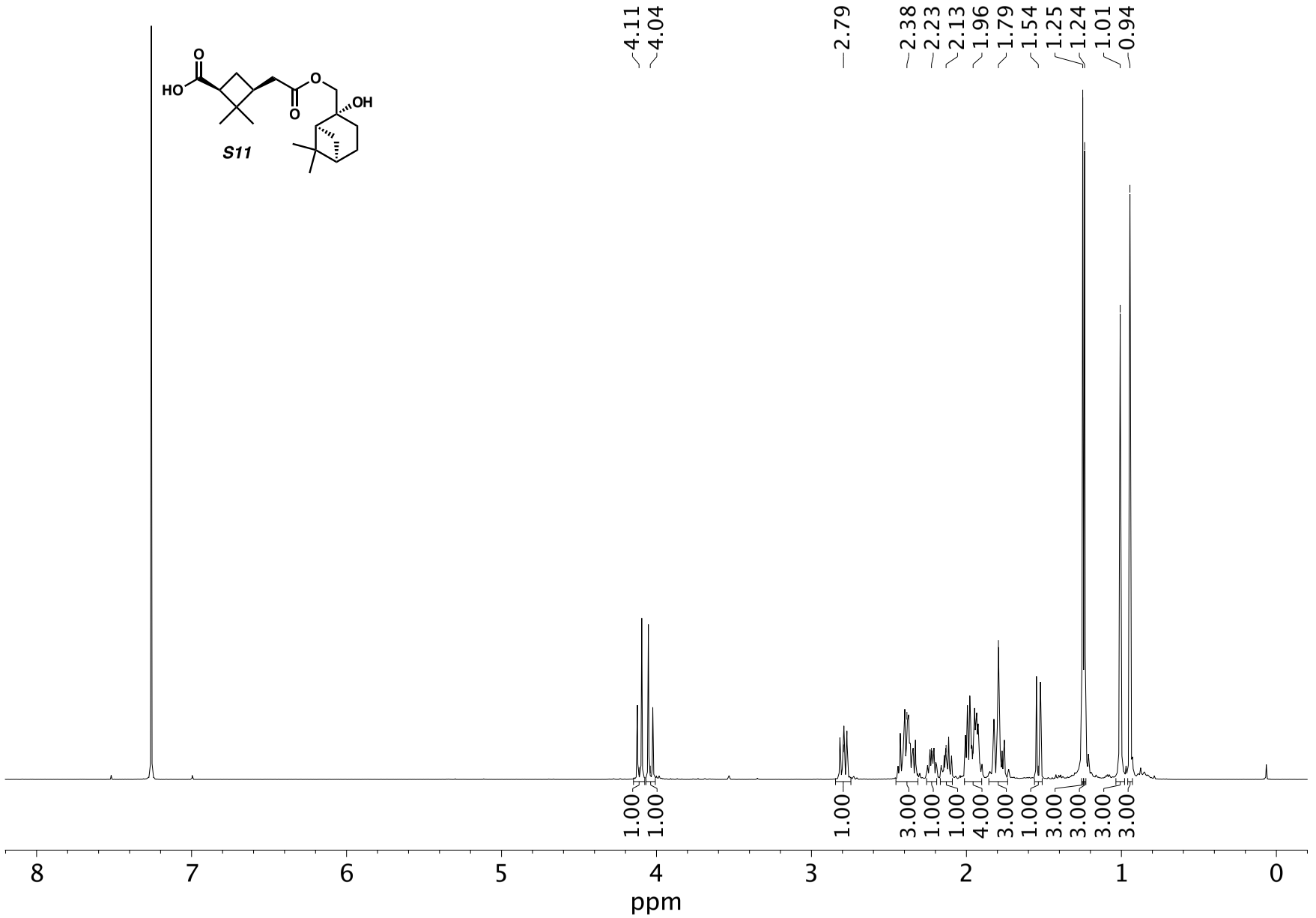

^{1}H NMR (400 MHz, $CDCl_3$) of compound **S11**.

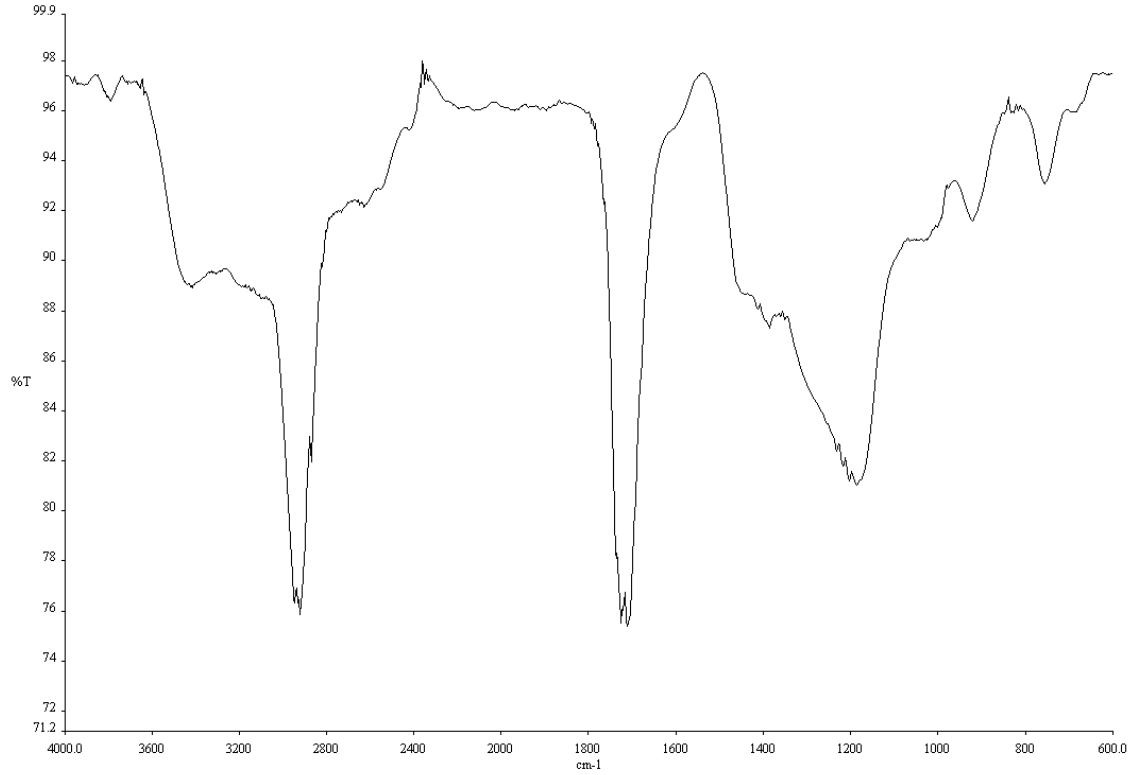

Infrared spectrum (thin film, NaCl) of compound **S11**.

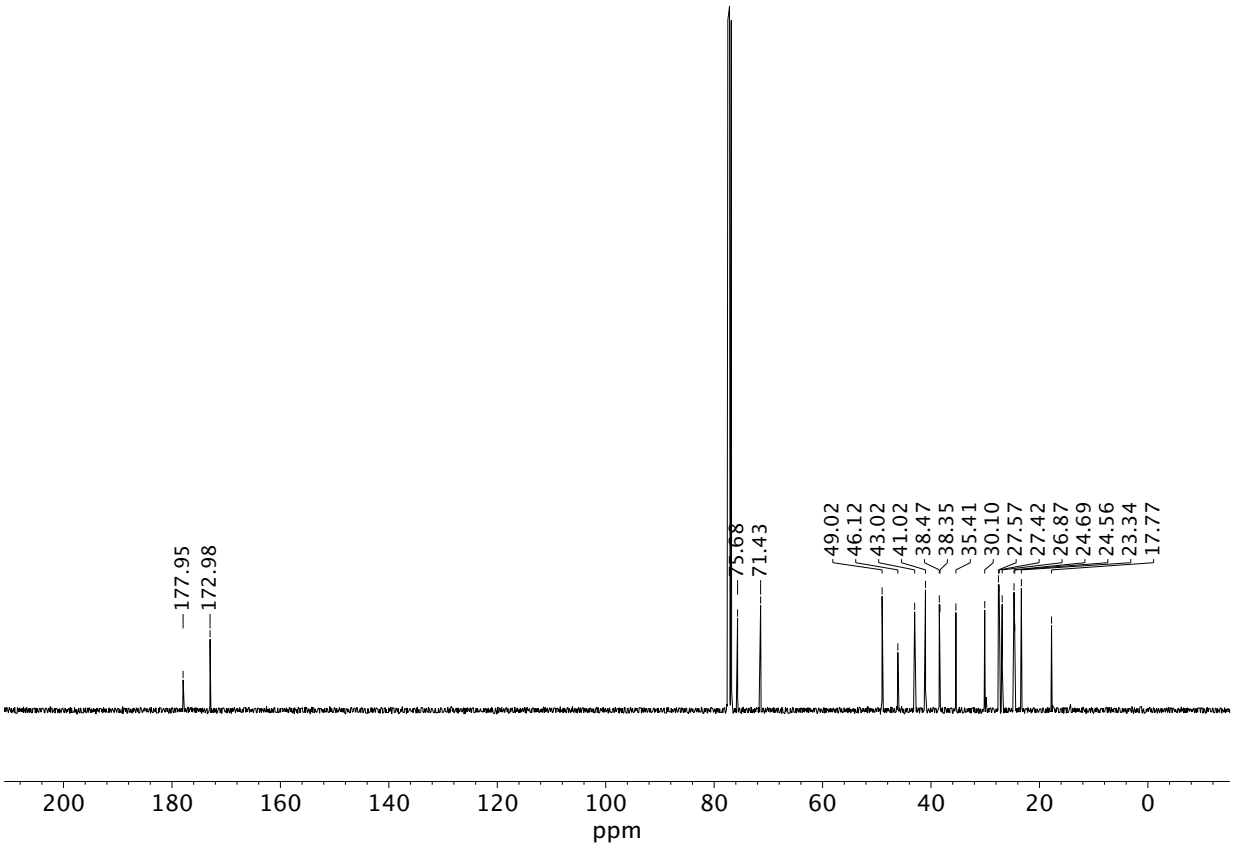

^{13}C NMR (100 MHz, $CDCl_3$) of compound **S11**.

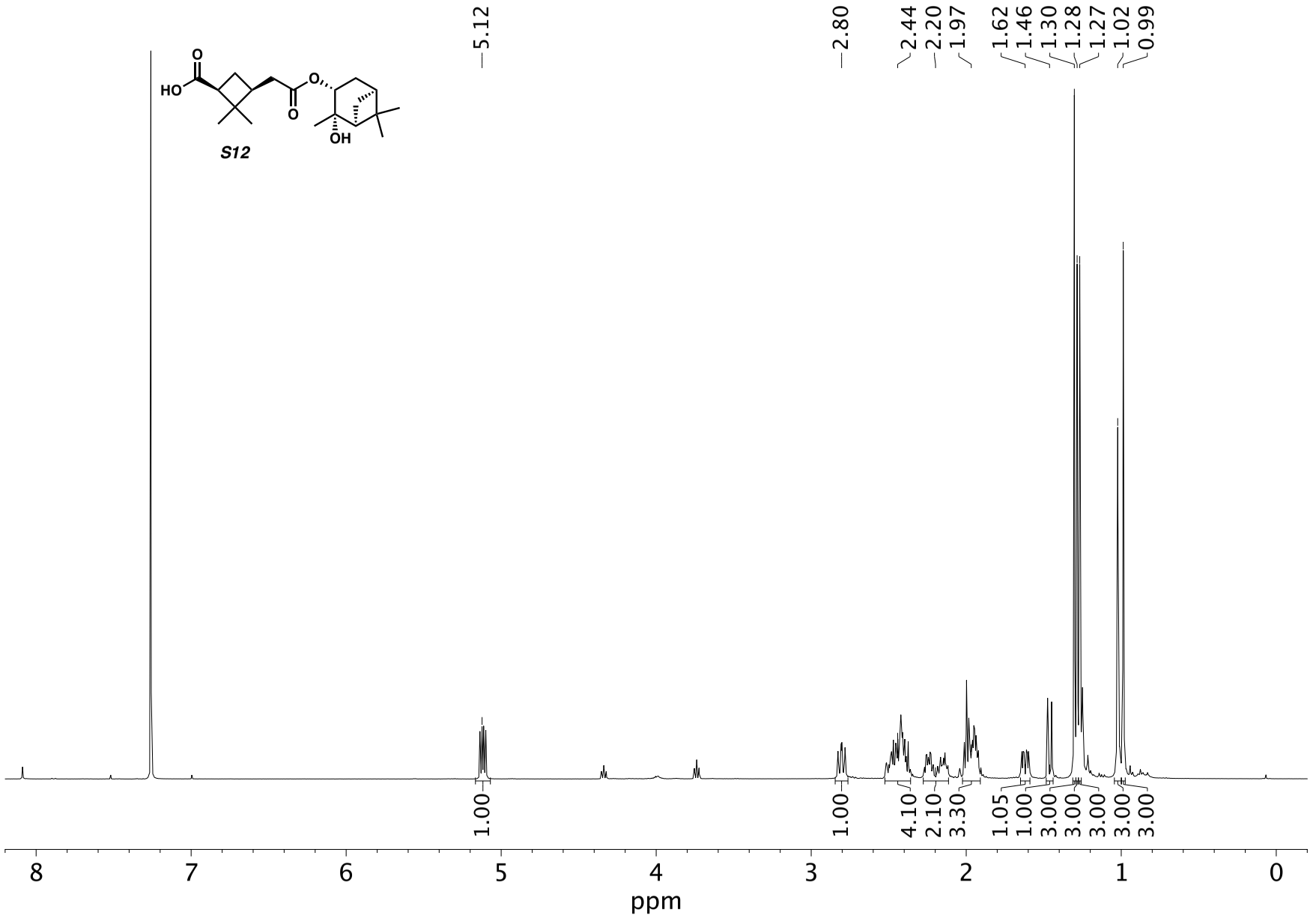

^{1}H NMR (400 MHz, $CDCl_3$) of compound **S12**.

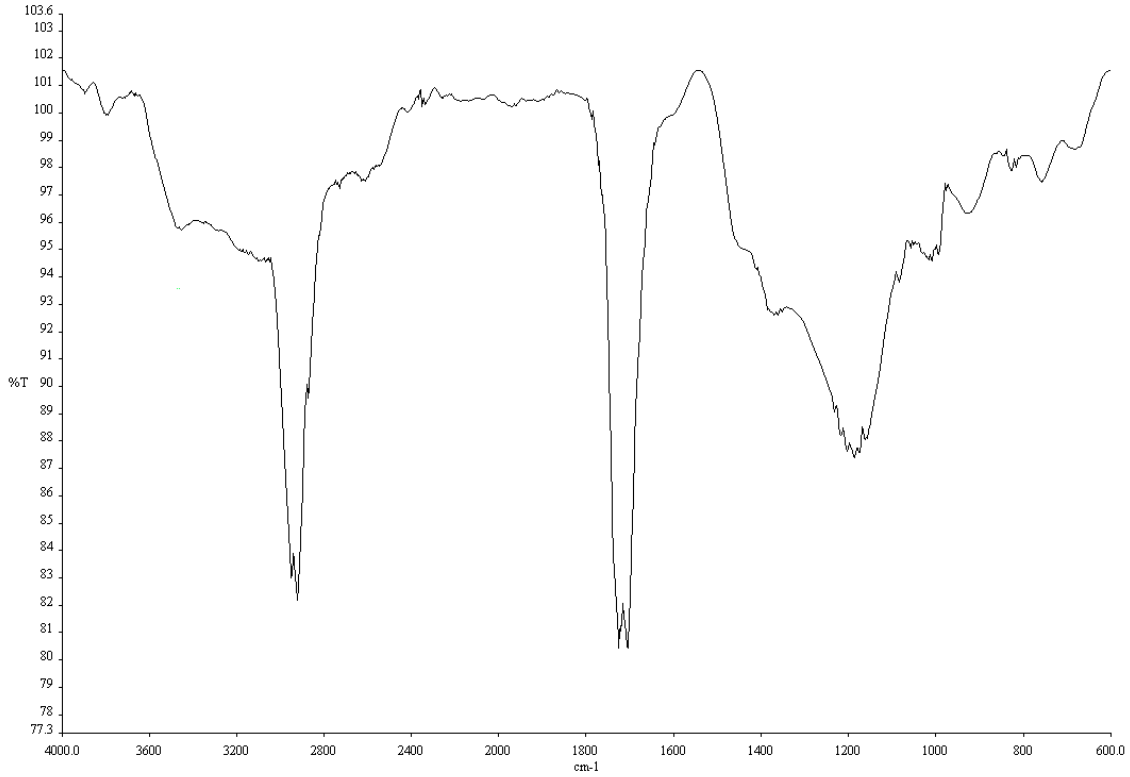

Infrared spectrum (thin film, NaCl) of compound **S12**.

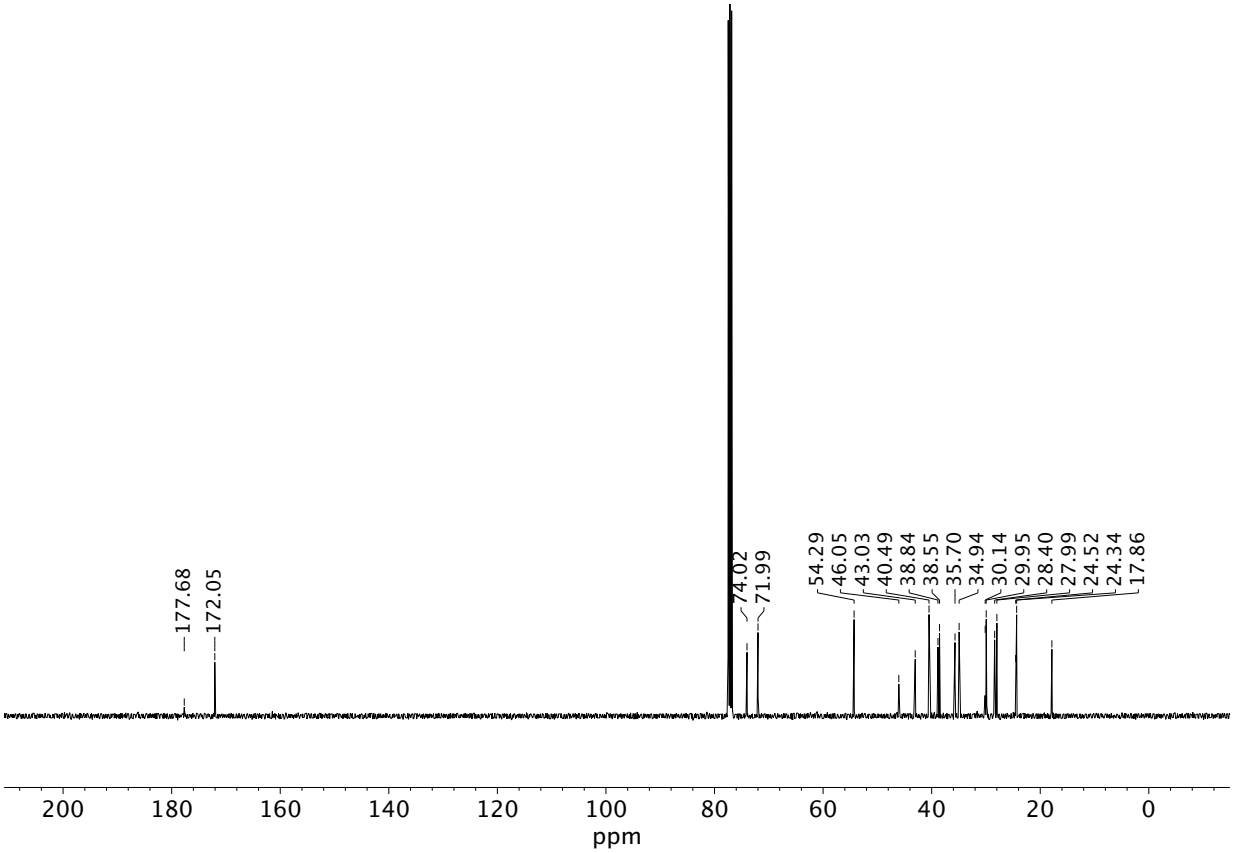

^{13}C NMR (100 MHz, $CDCl_3$) of compound **S12**.

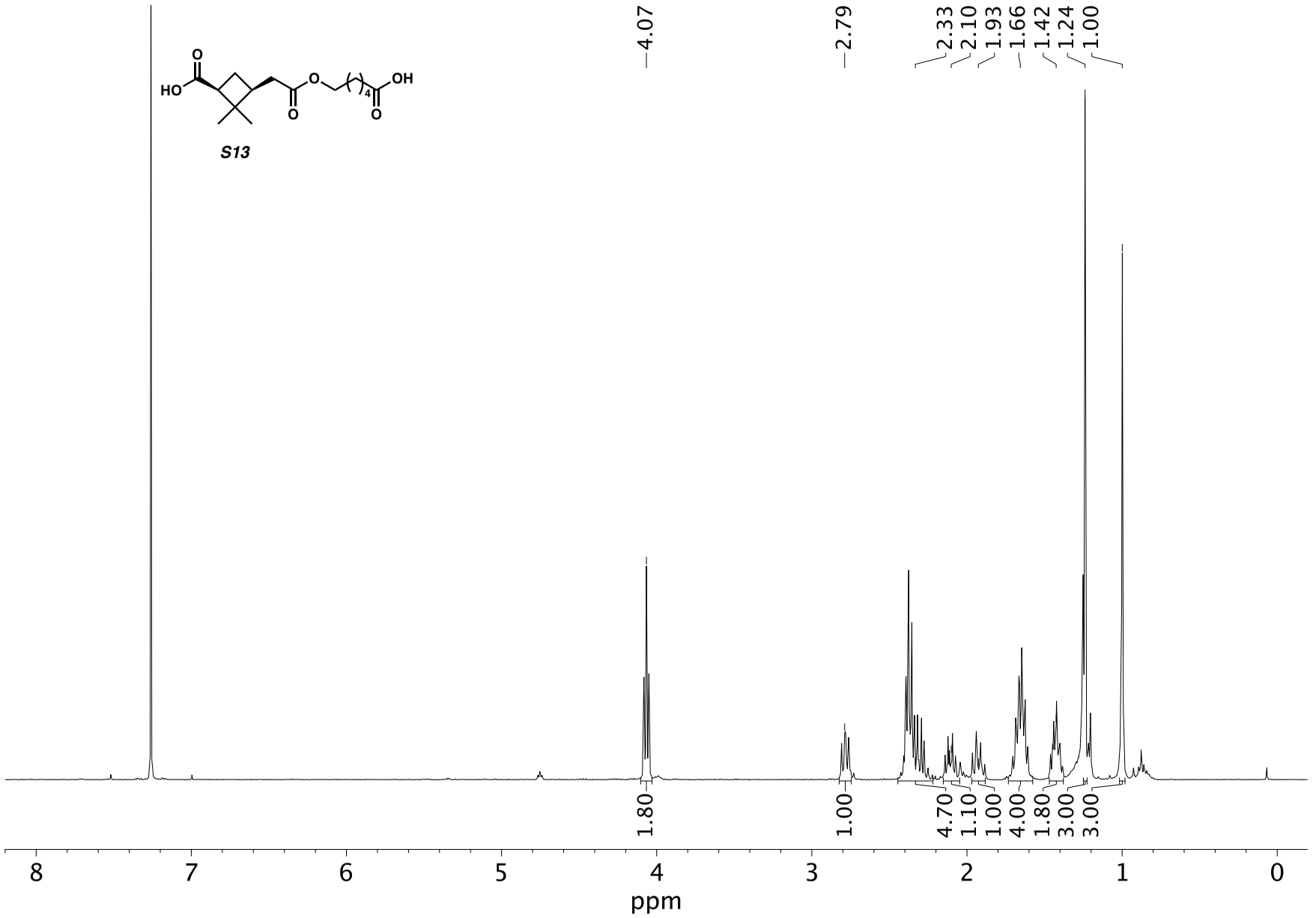

^{1}H NMR (400 MHz, $CDCl_3$) of compound **S13**.

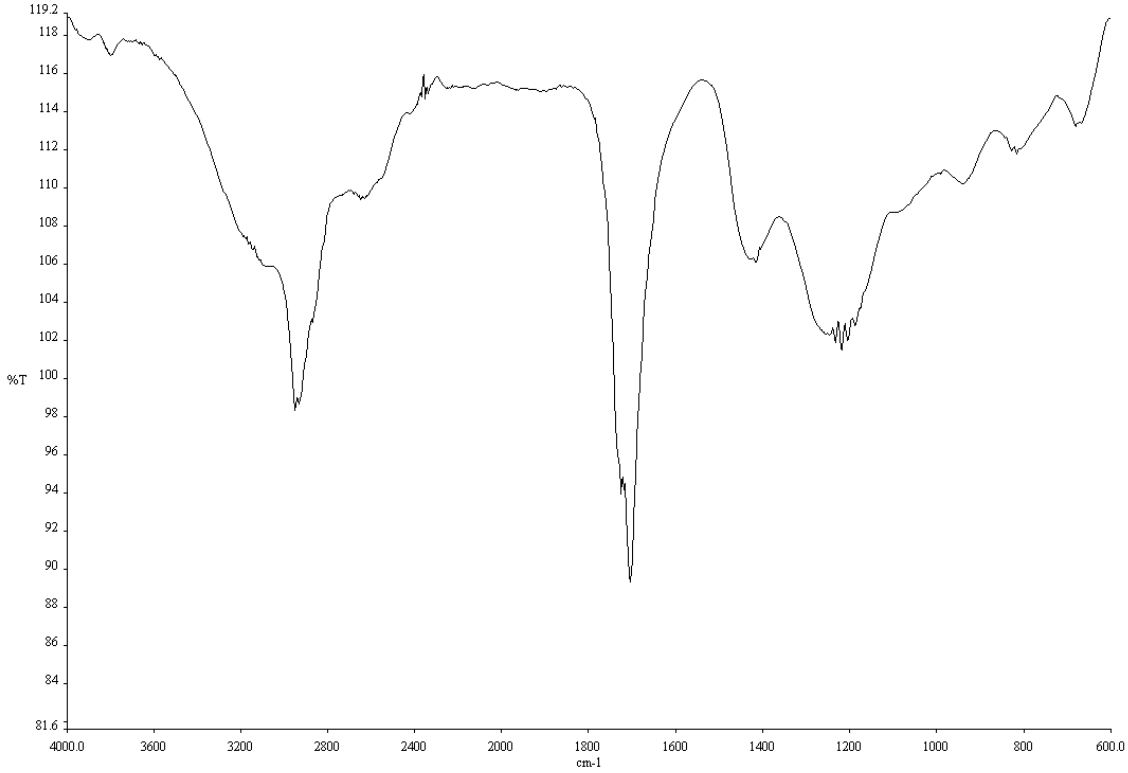

Infrared spectrum (thin film, NaCl) of compound **S13**.

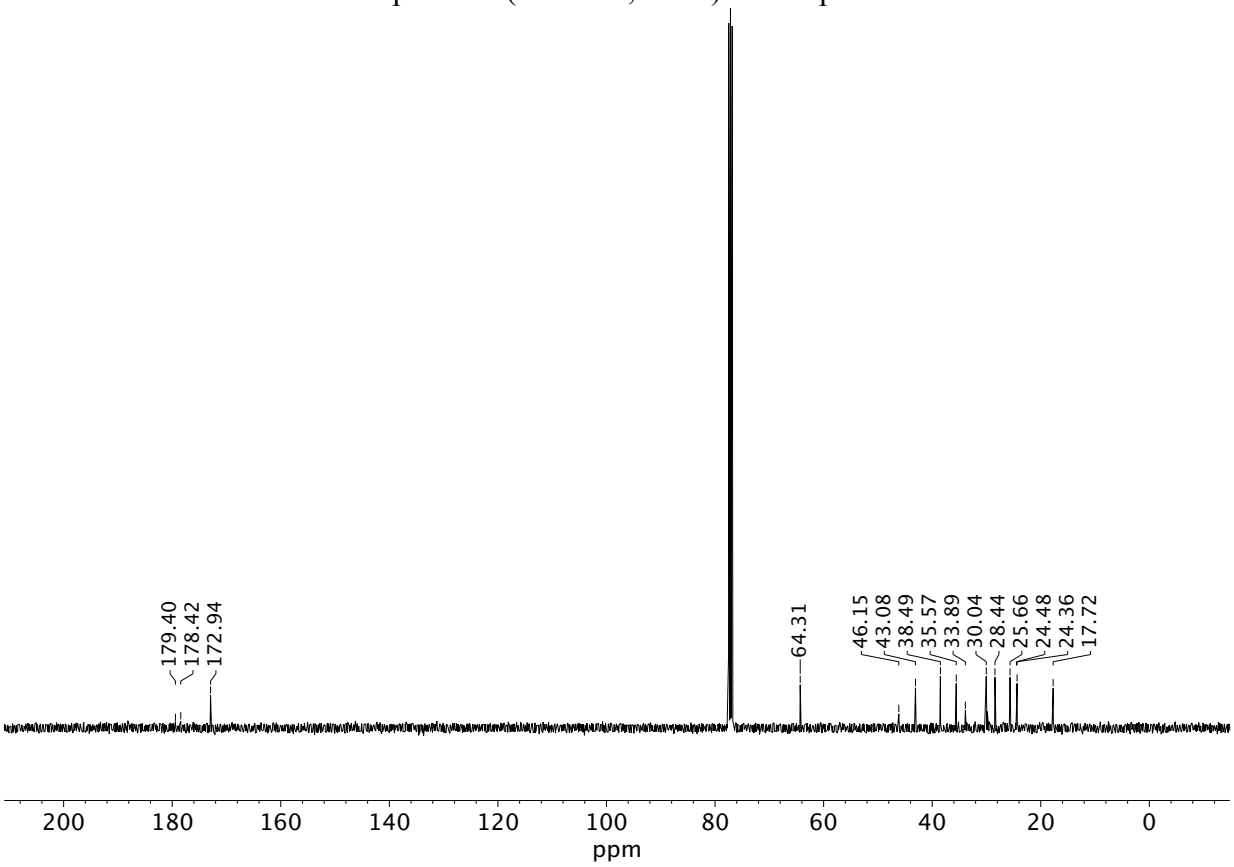

^{13}C NMR (100 MHz, $CDCl_3$) of compound **S13**.

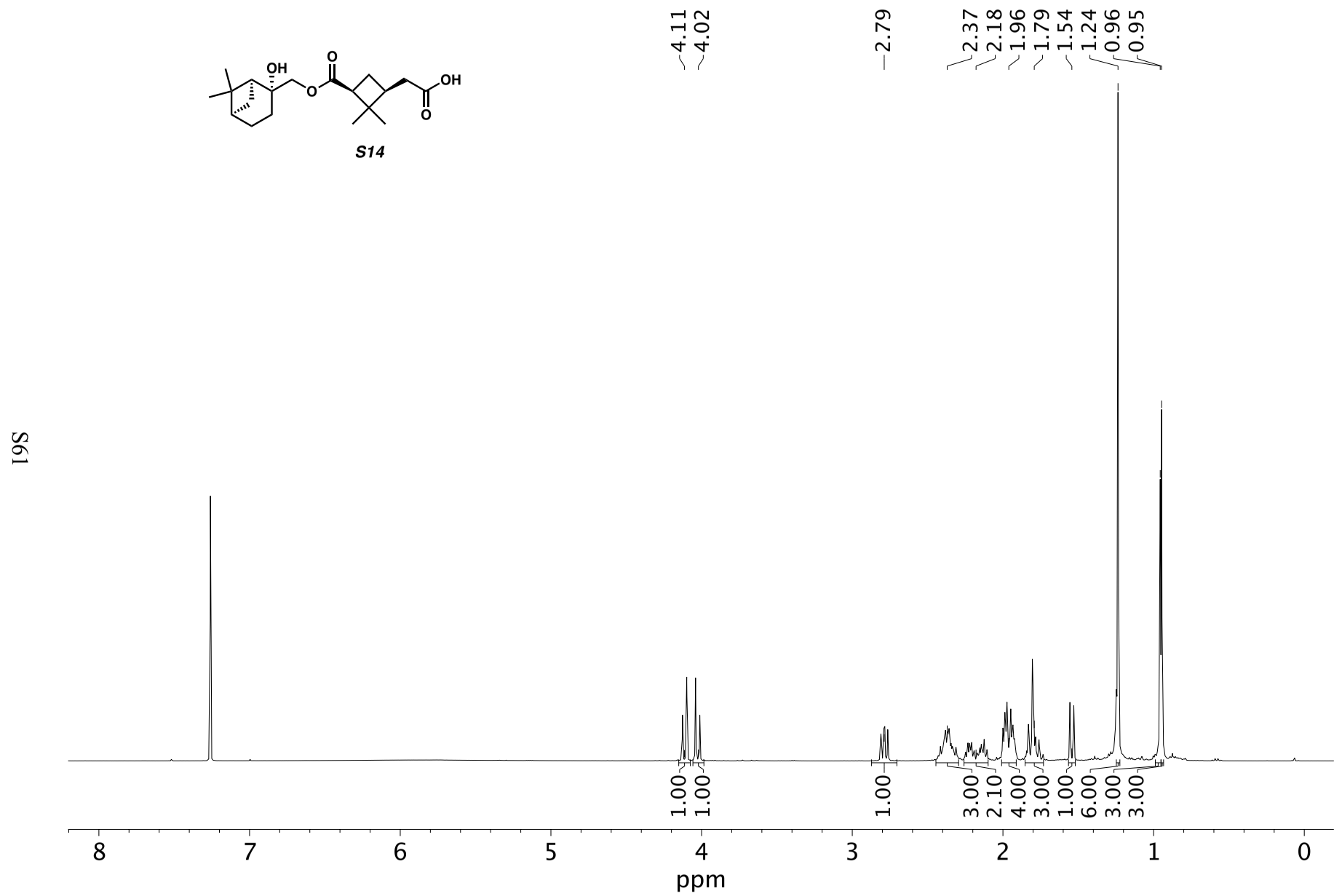

^{1}H NMR (400 MHz, $CDCl_3$) of compound **S14**.

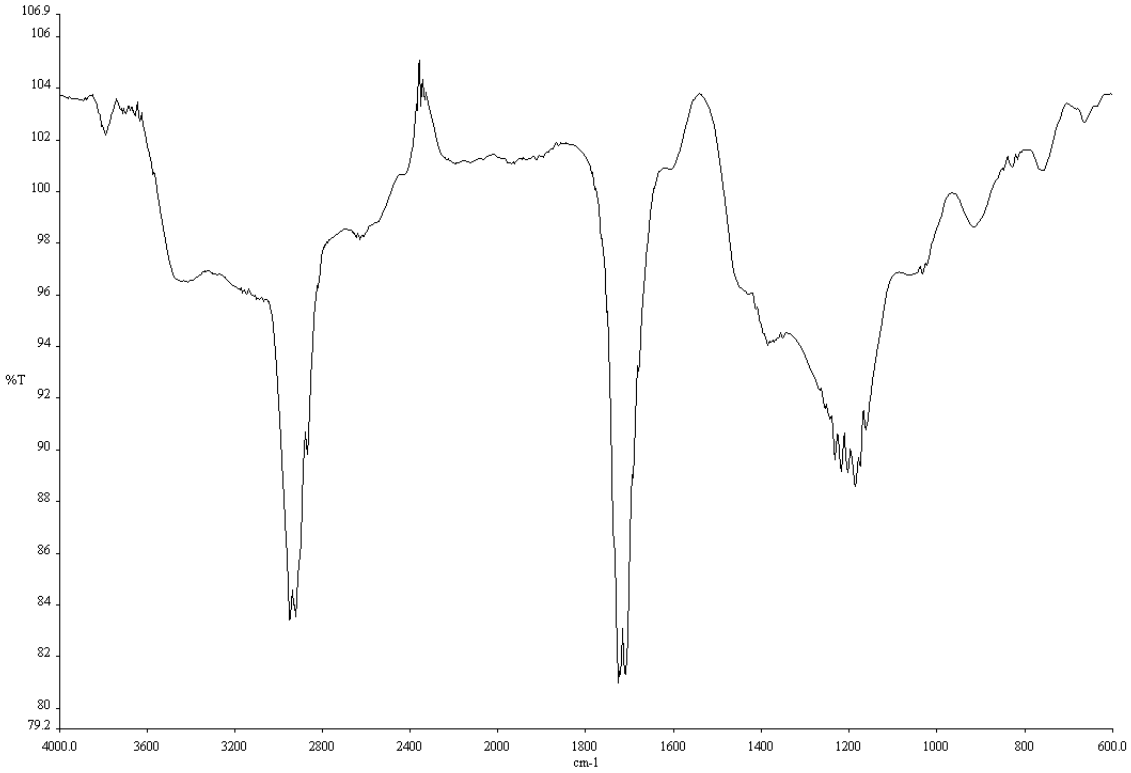

Infrared spectrum (thin film, NaCl) of compound **S14**.

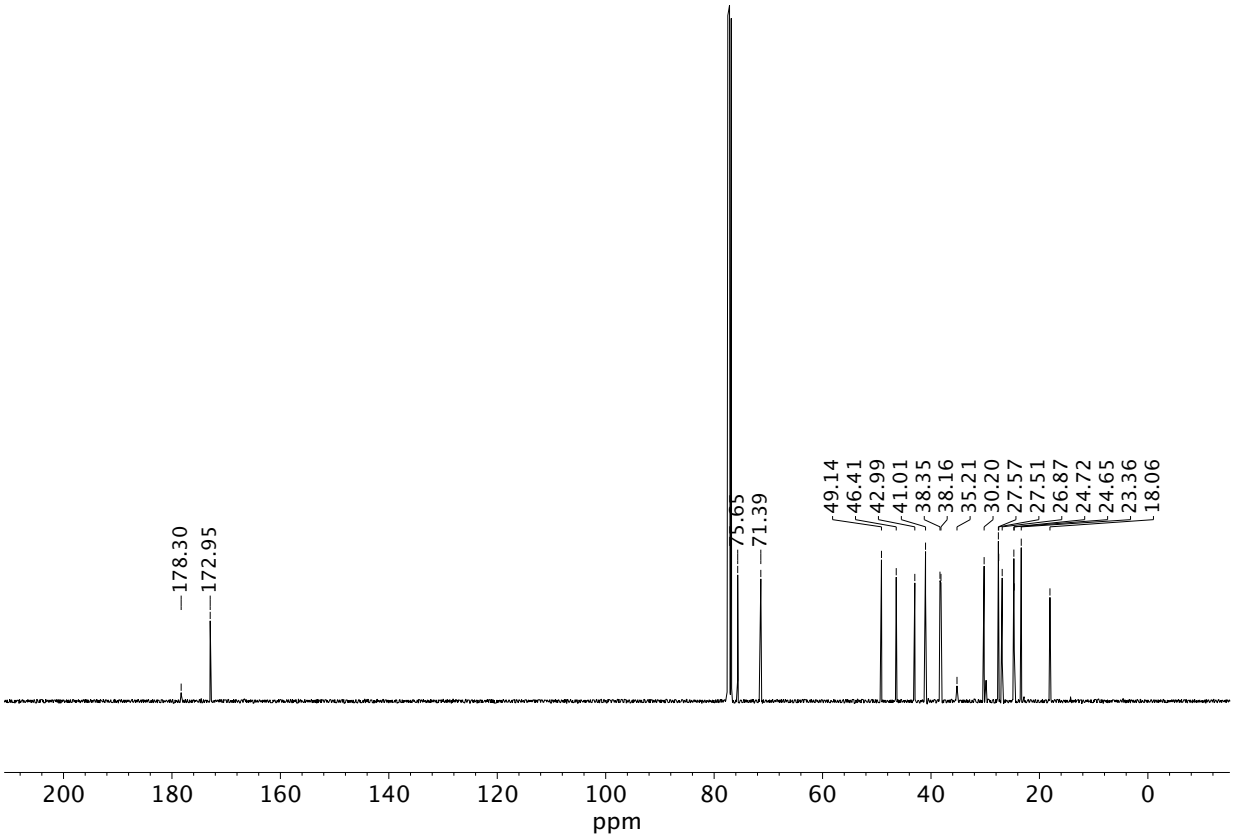

^{13}C NMR (100 MHz, $CDCl_3$) of compound **S14**.

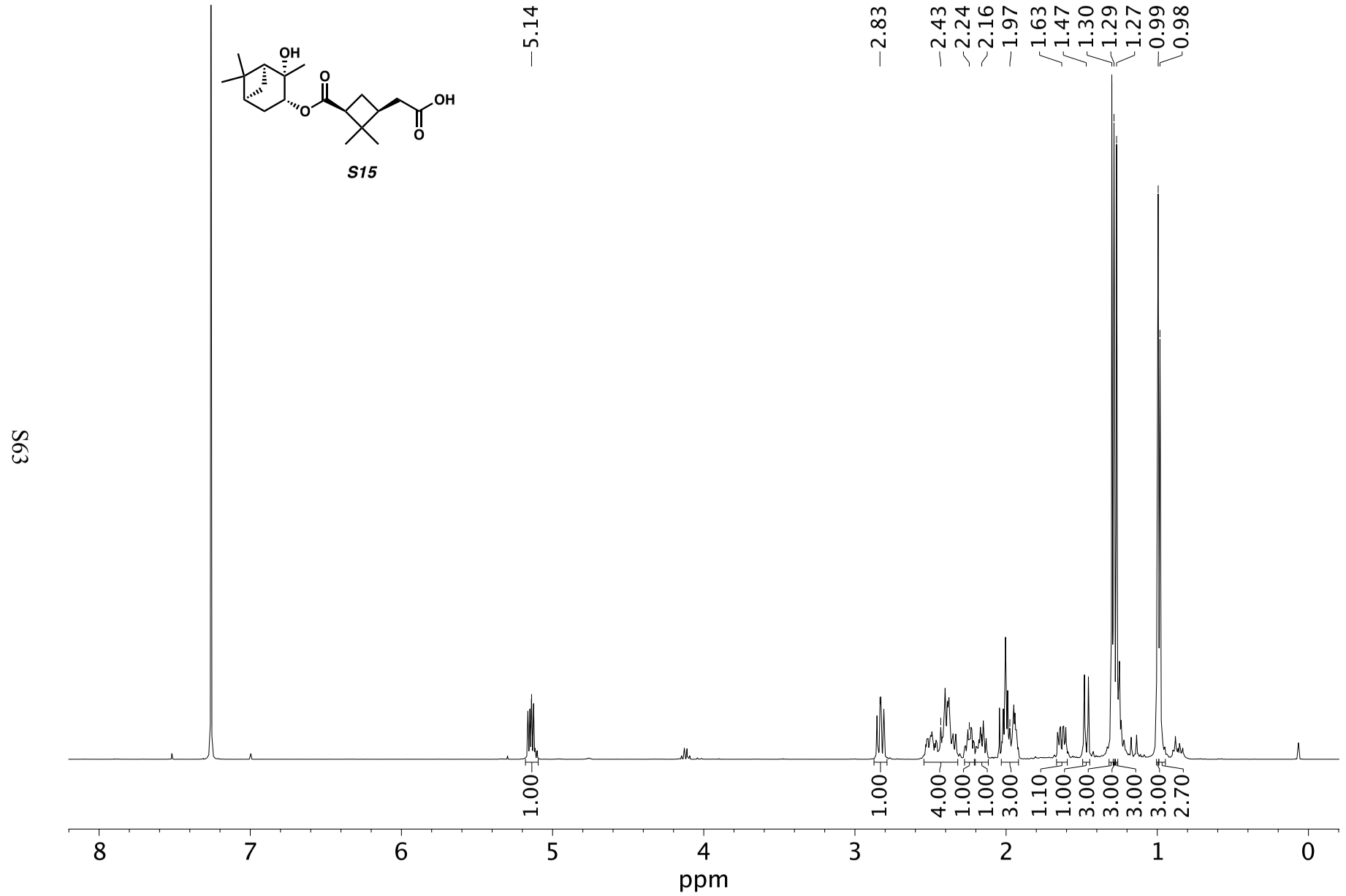

^{1}H NMR (400 MHz, $CDCl_3$) of compound **S15**.

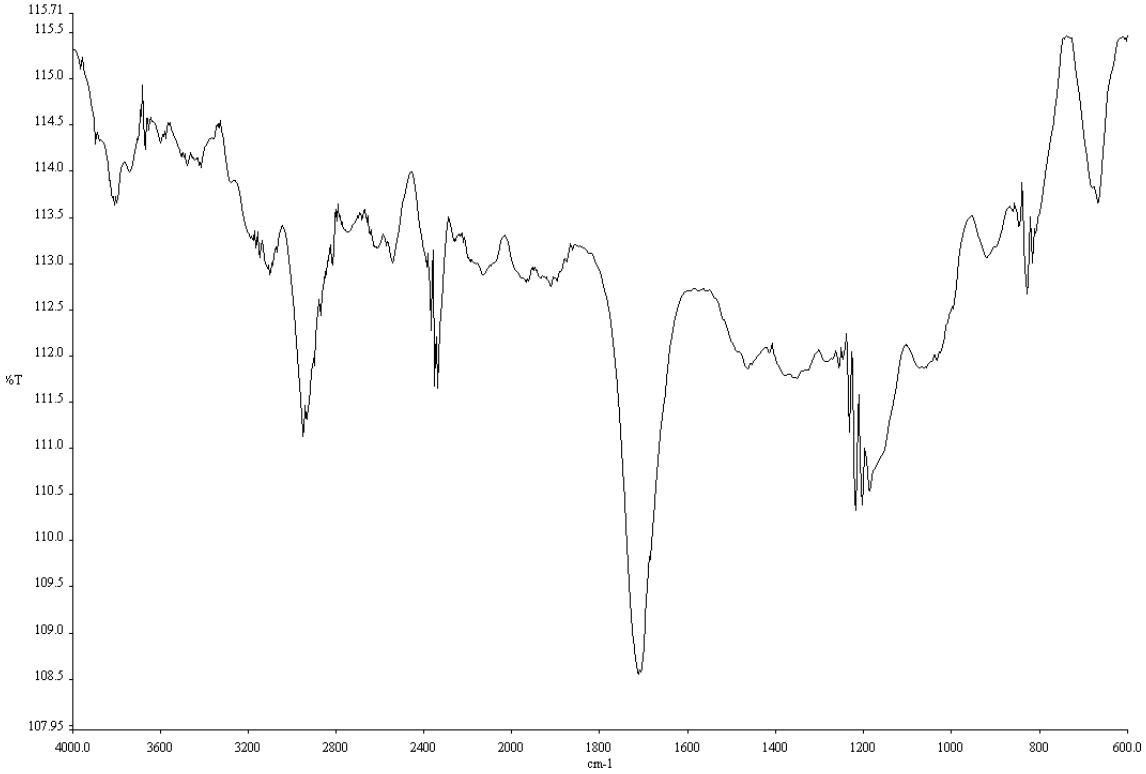

Infrared spectrum (thin film, NaCl) of compound **S15**.

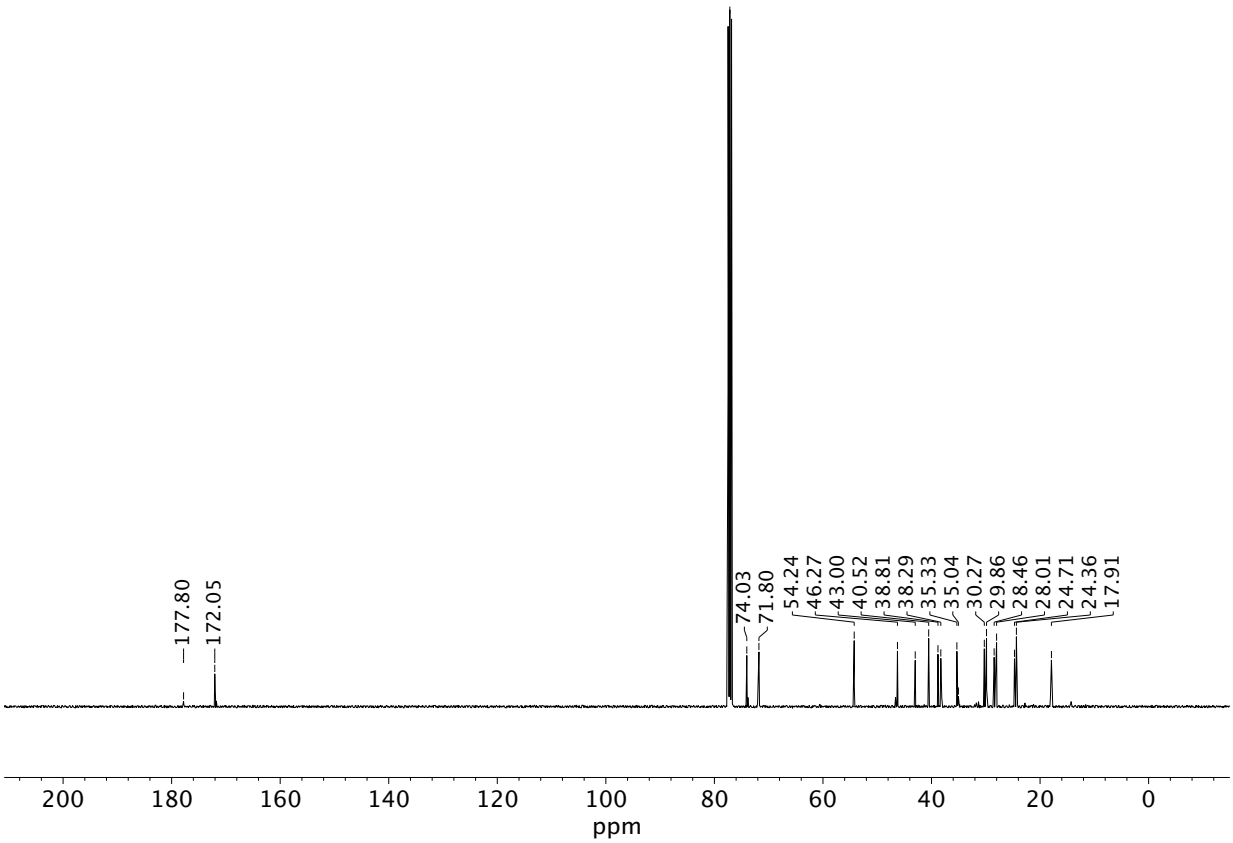

^{13}C NMR (100 MHz, $CDCl_3$) of compound **S15**.

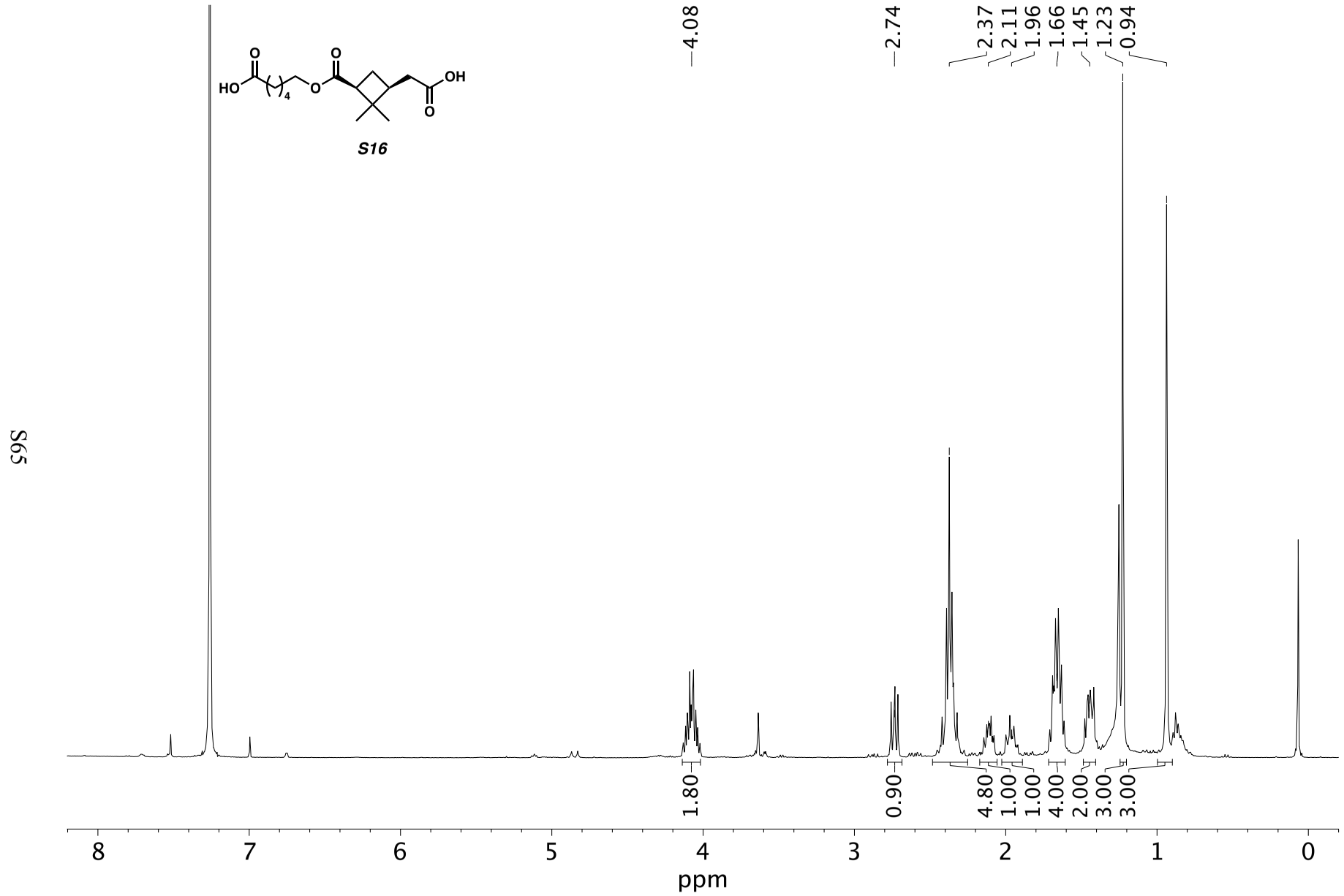

^{1}H NMR (400 MHz, $CDCl_3$) of compound **S16**.

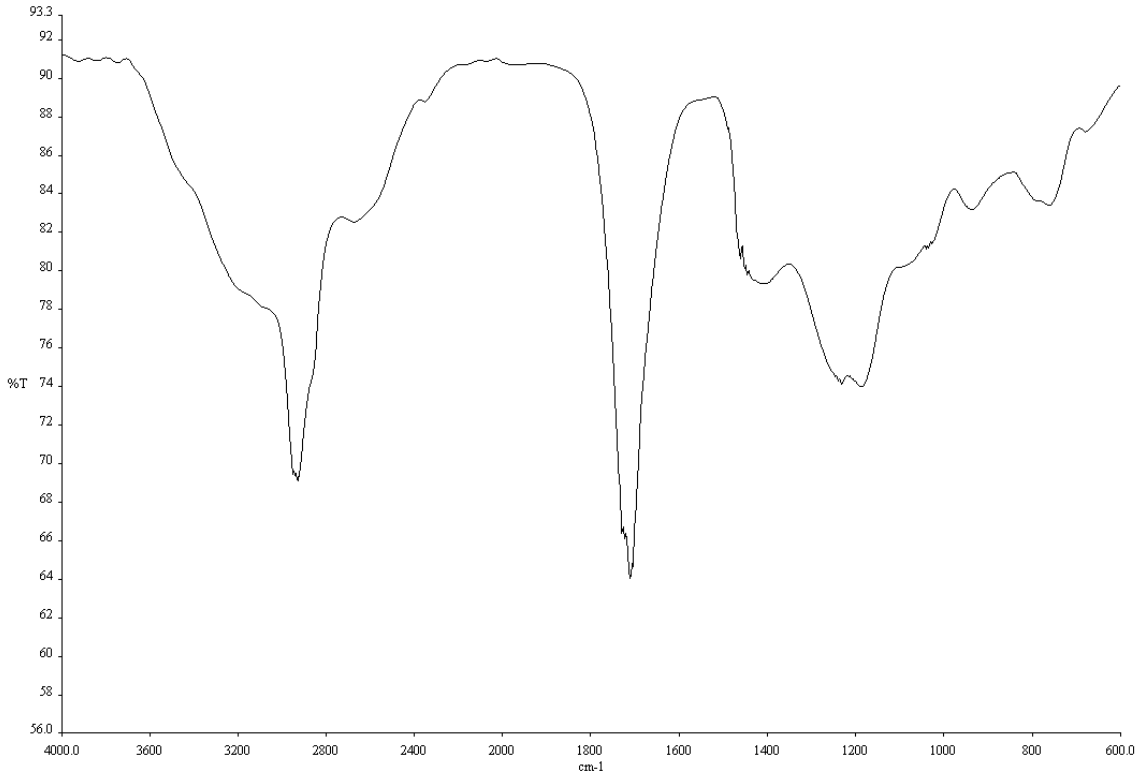

Infrared spectrum (thin film, NaCl) of compound **S16**.

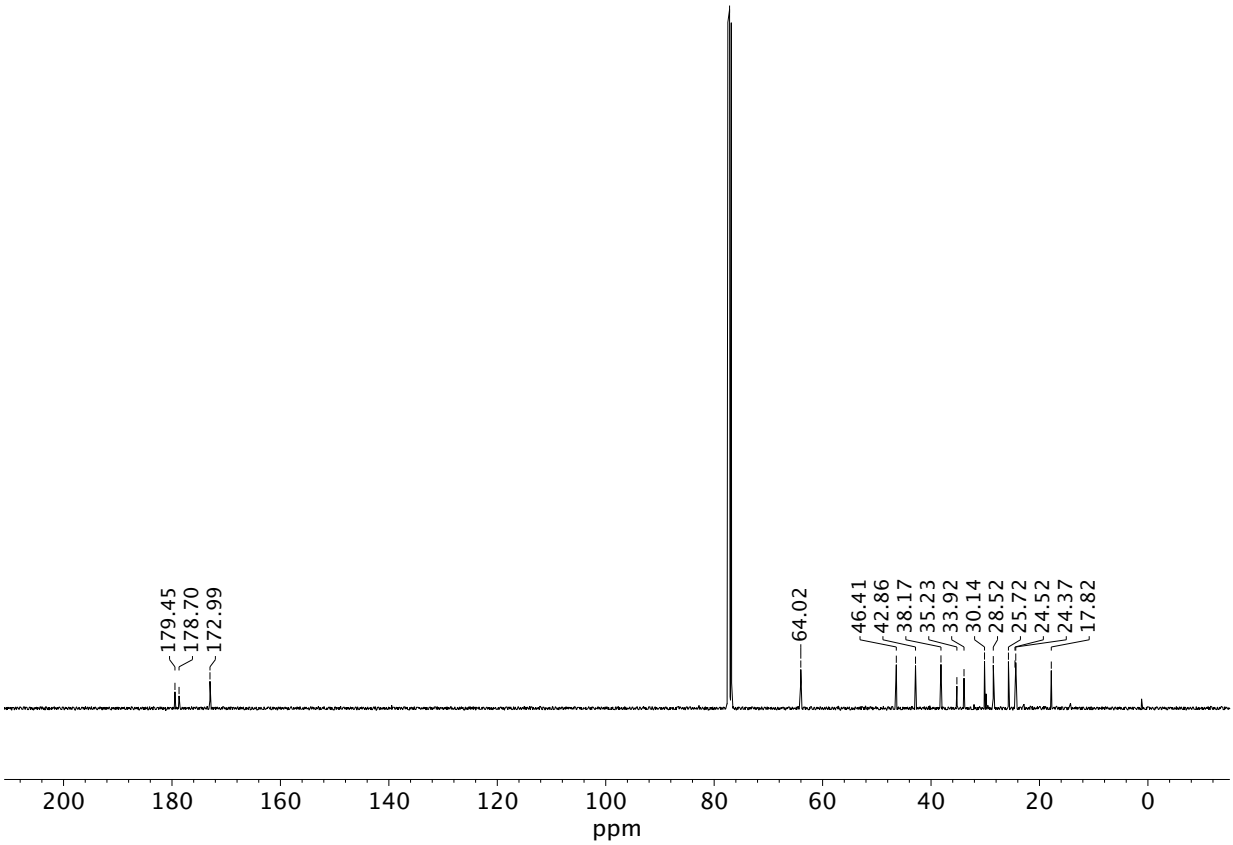

^{13}C NMR (100 MHz, $CDCl_3$) of compound **S16**.

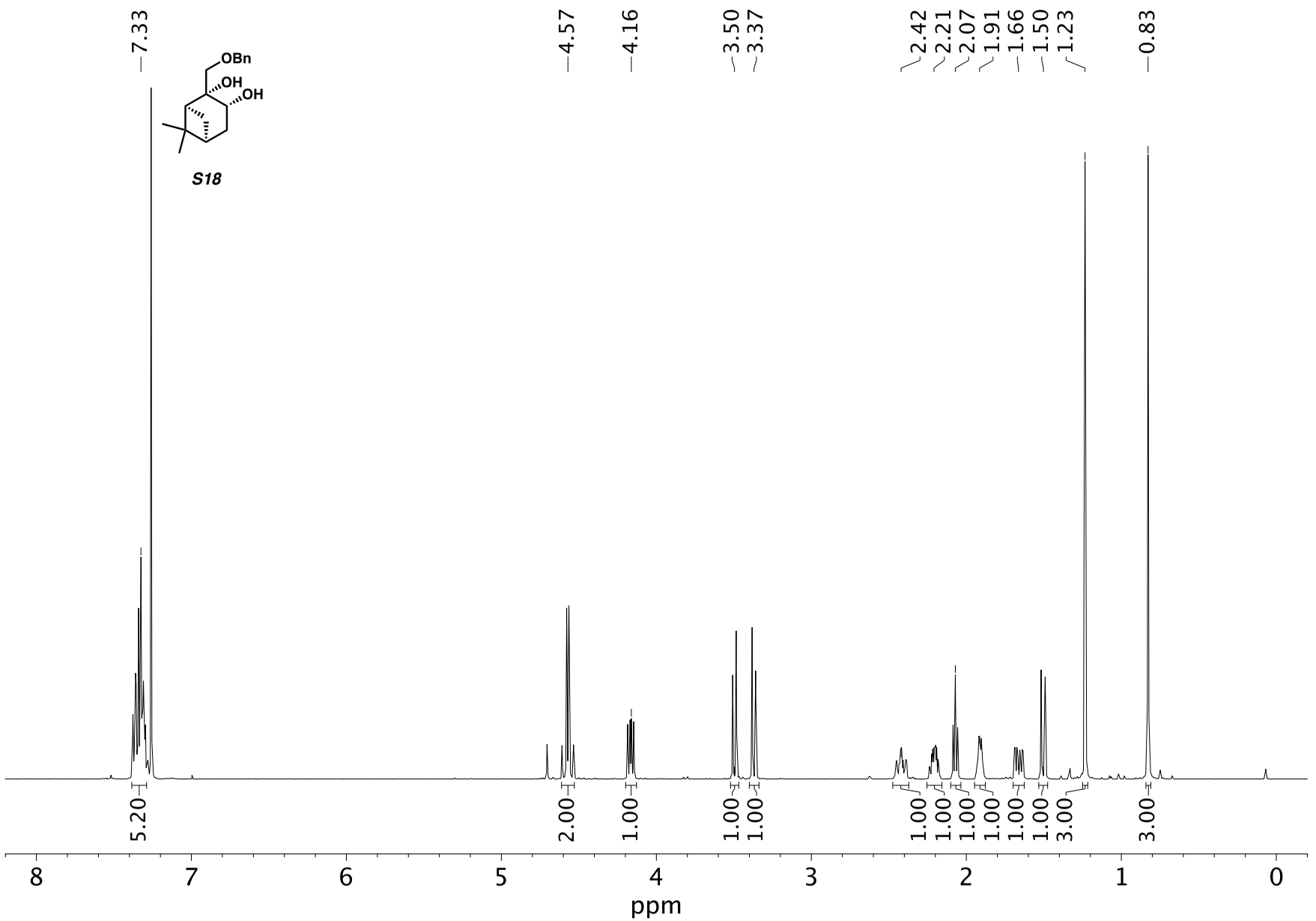

^{1}H NMR (400 MHz, $CDCl_3$) of compound **S18**.

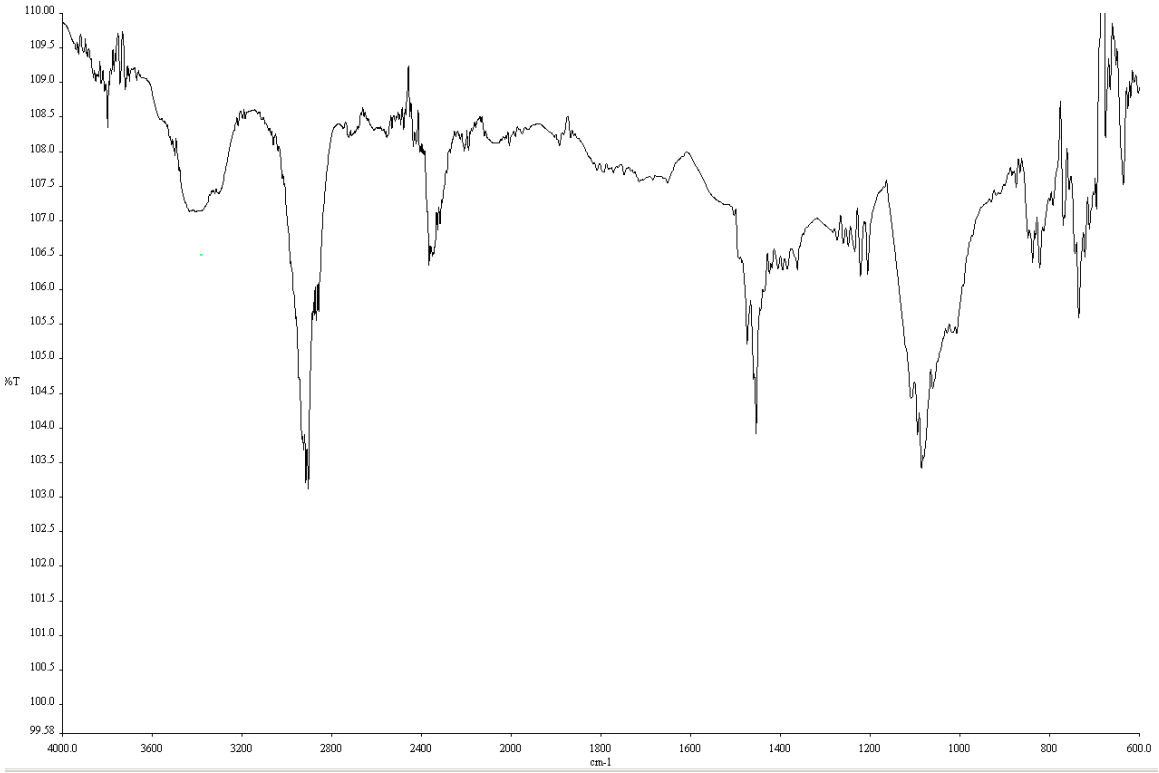

Infrared spectrum (thin film, NaCl) of compound **S18**.

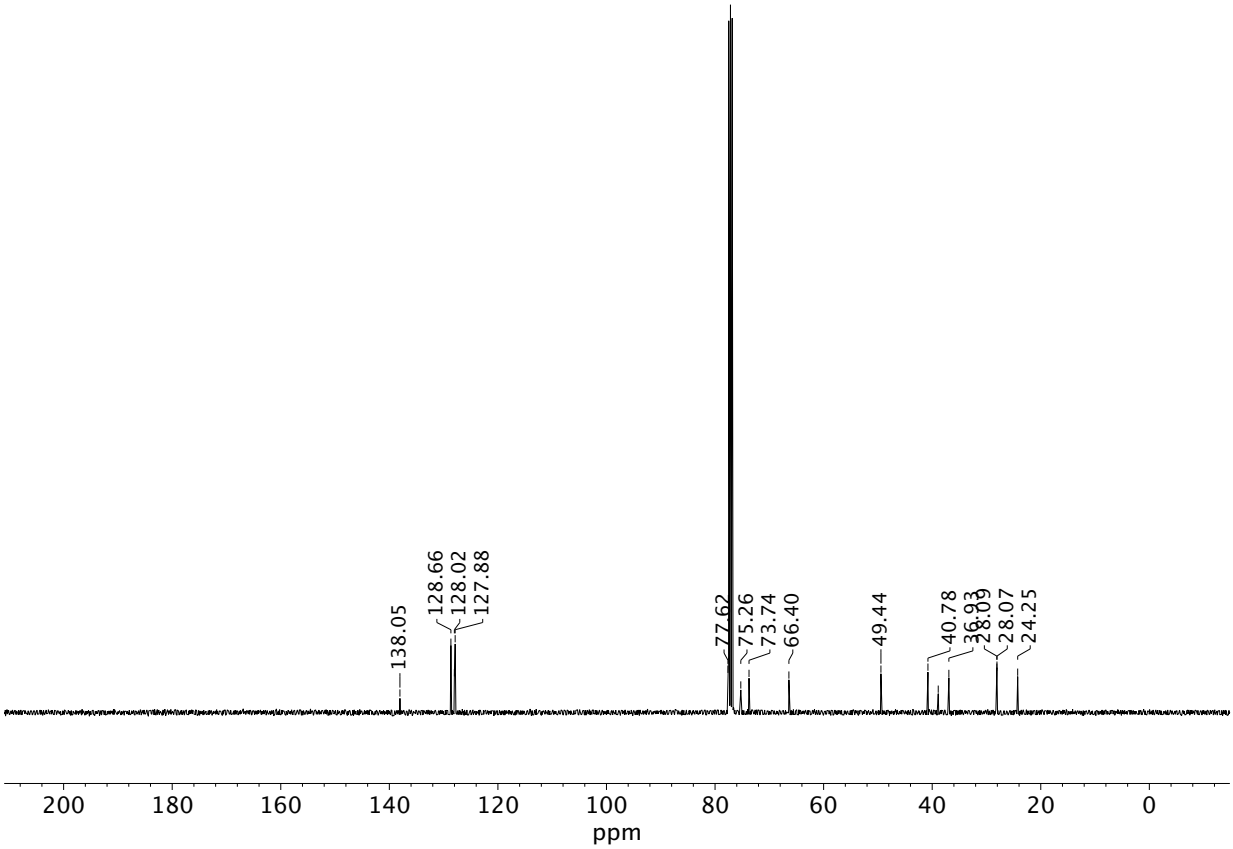

^{13}C NMR (100 MHz, $CDCl_3$) of compound **S18**.

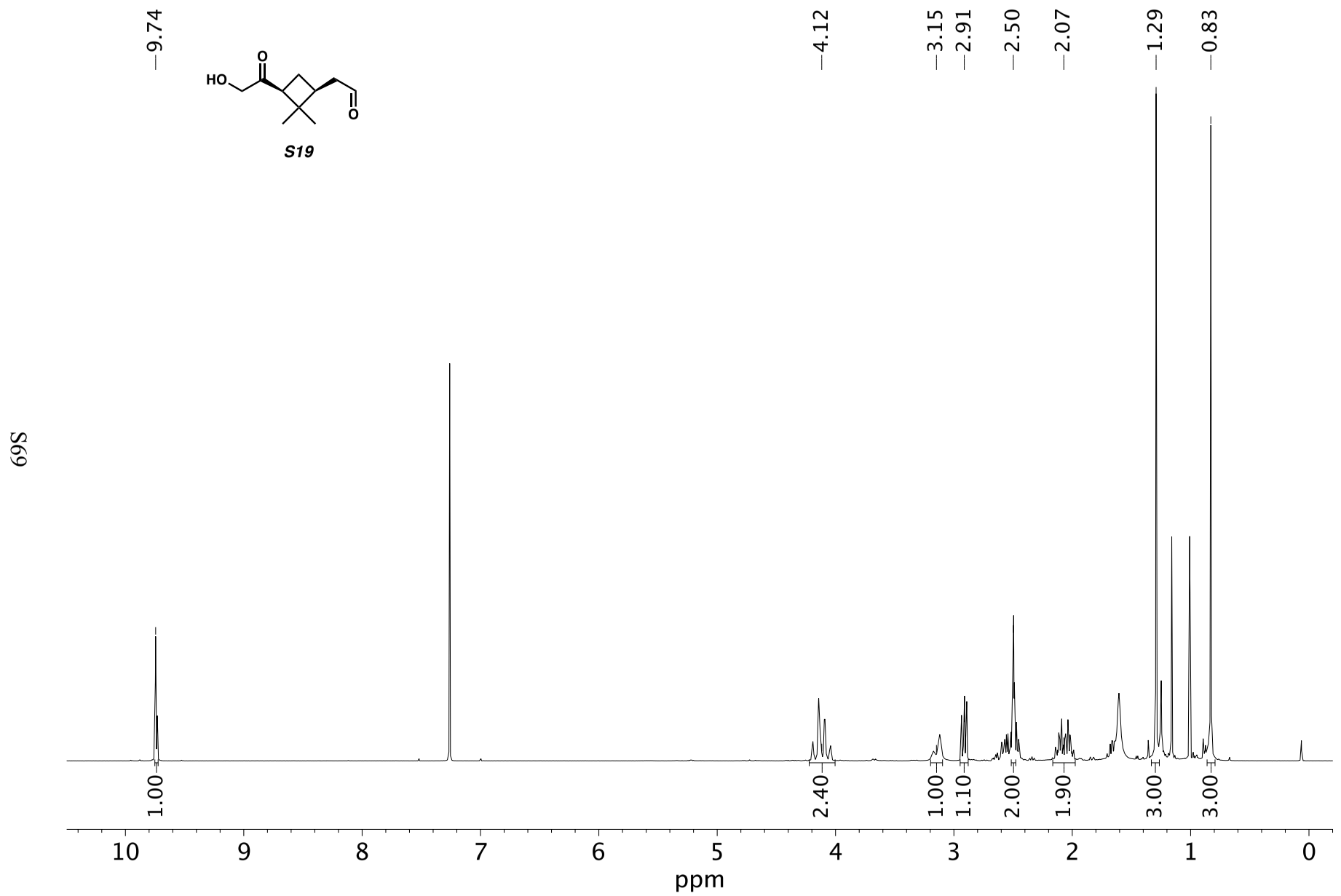

^{1}H NMR (400 MHz, $CDCl_3$) of compound **S19**.

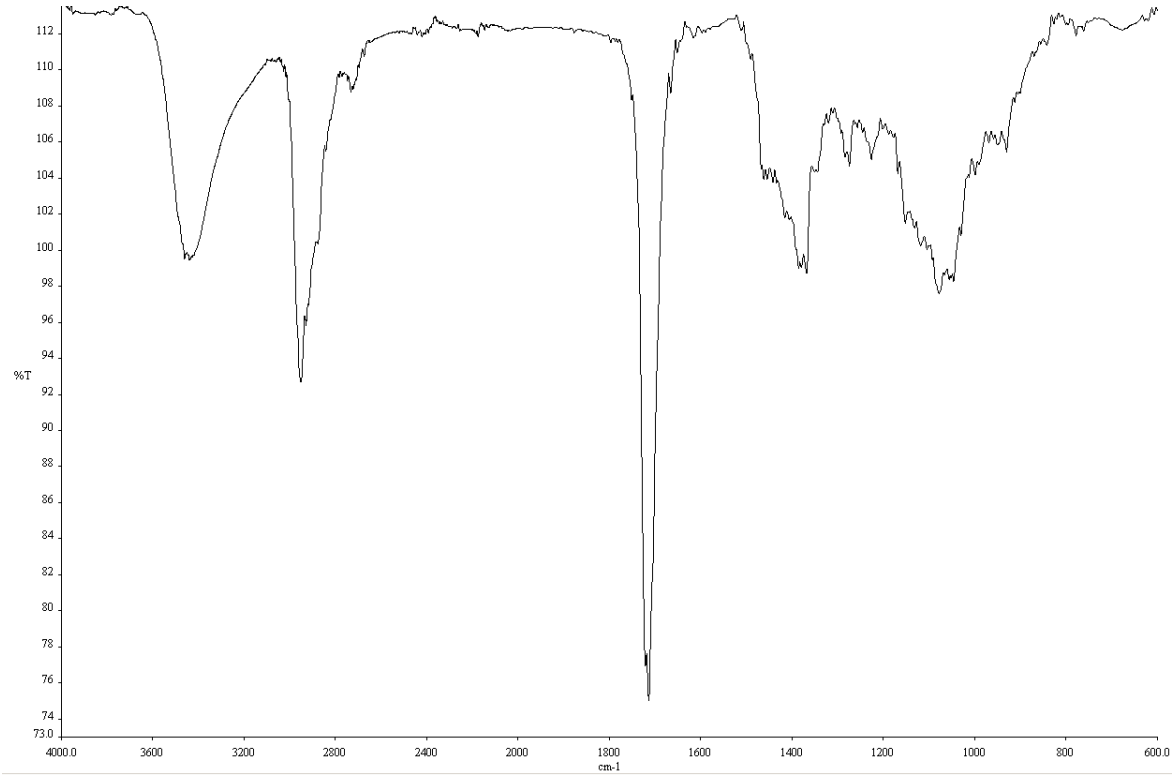

Infrared spectrum (thin film, NaCl) of compound **S19**.

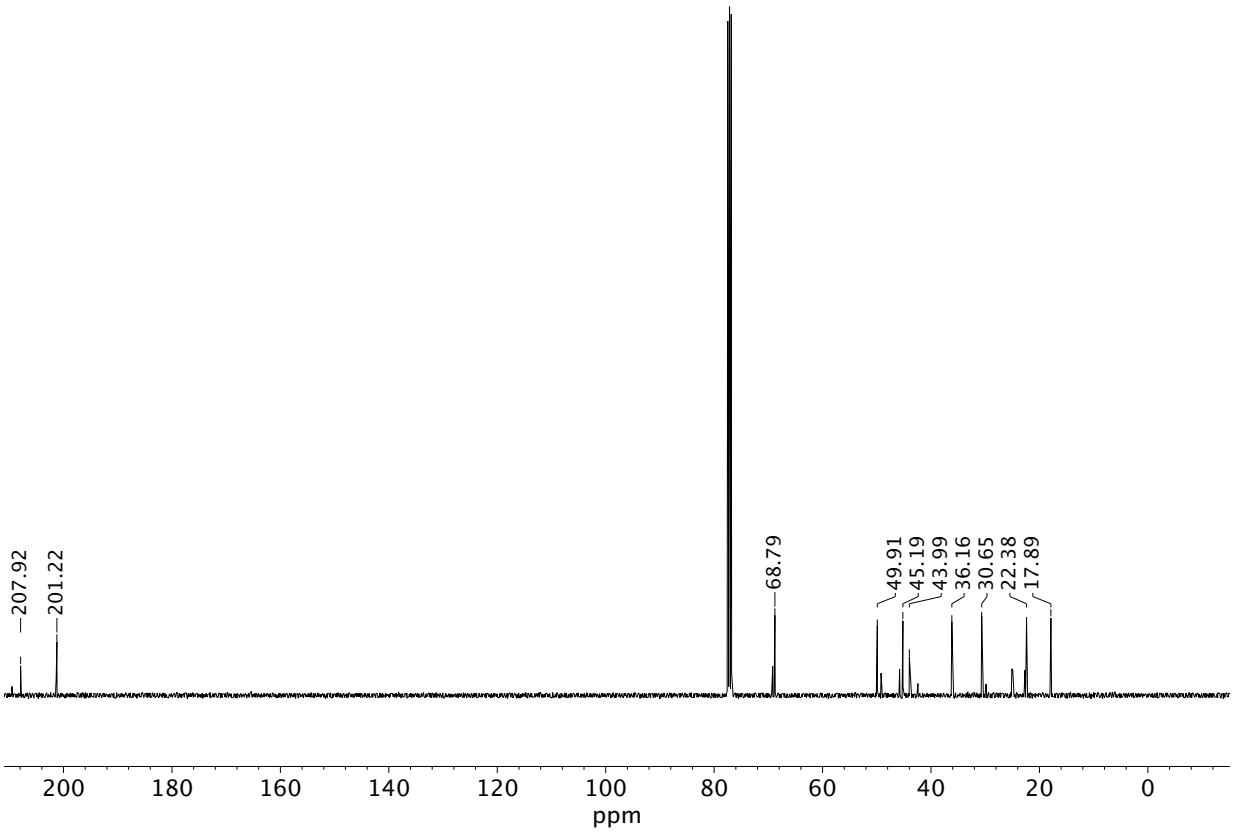

^{13}C NMR (100 MHz, $CDCl_3$) of compound **S19**.

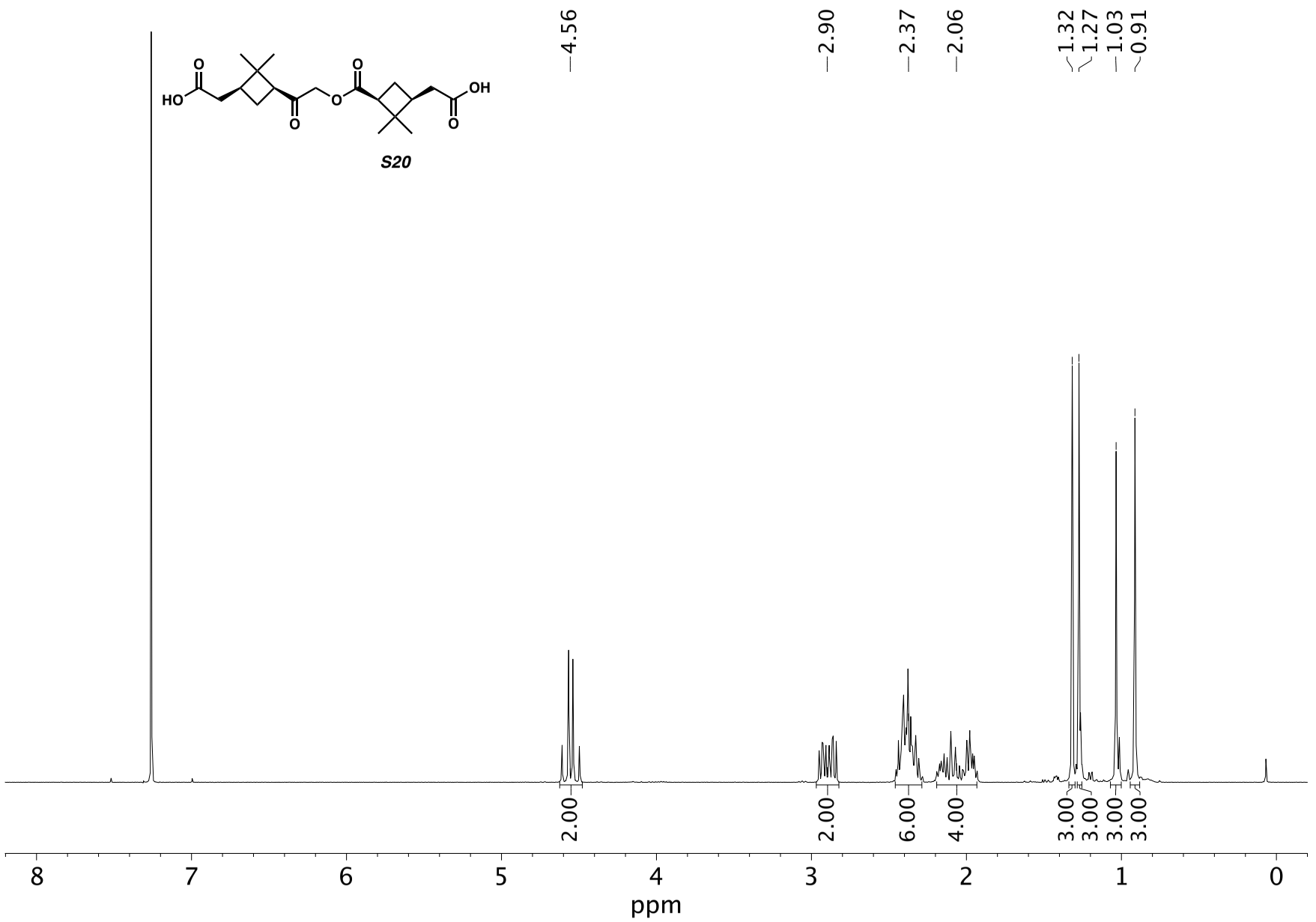

^{1}H NMR (400 MHz, $CDCl_3$) of compound **S20**.

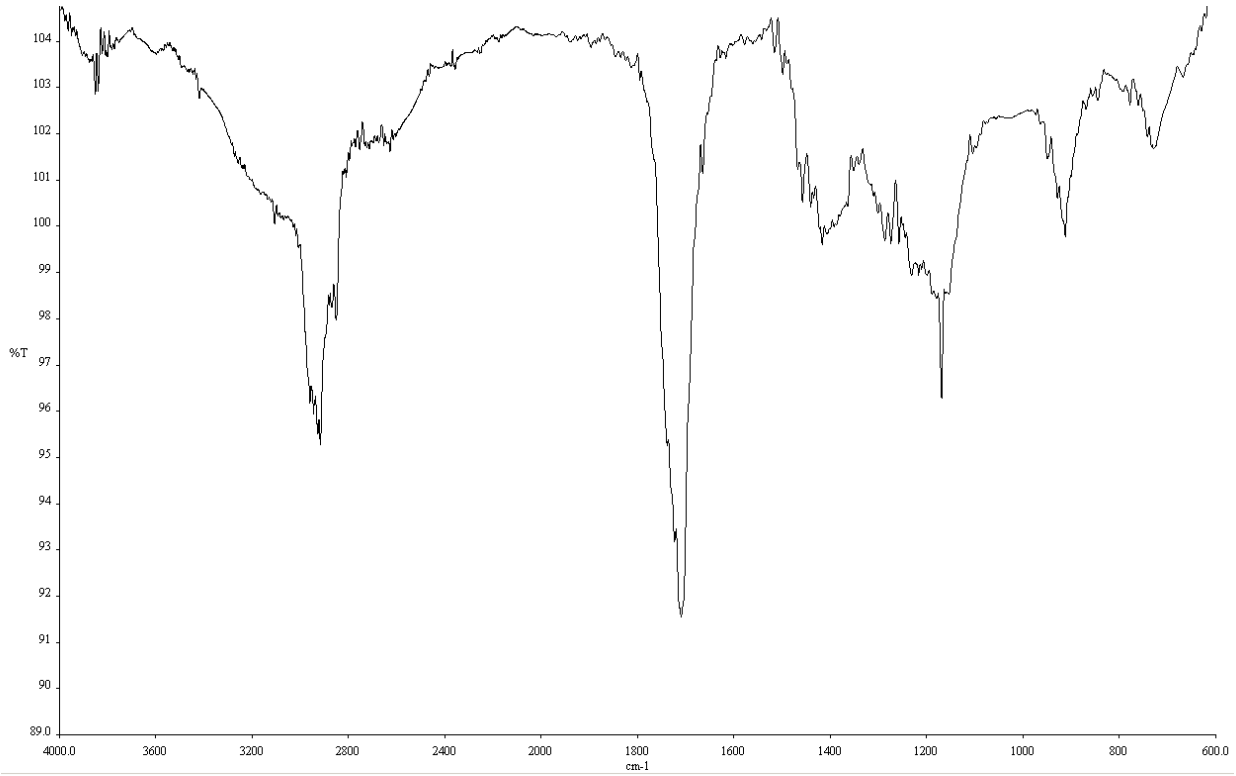

Infrared spectrum (thin film, NaCl) of compound **S20**.

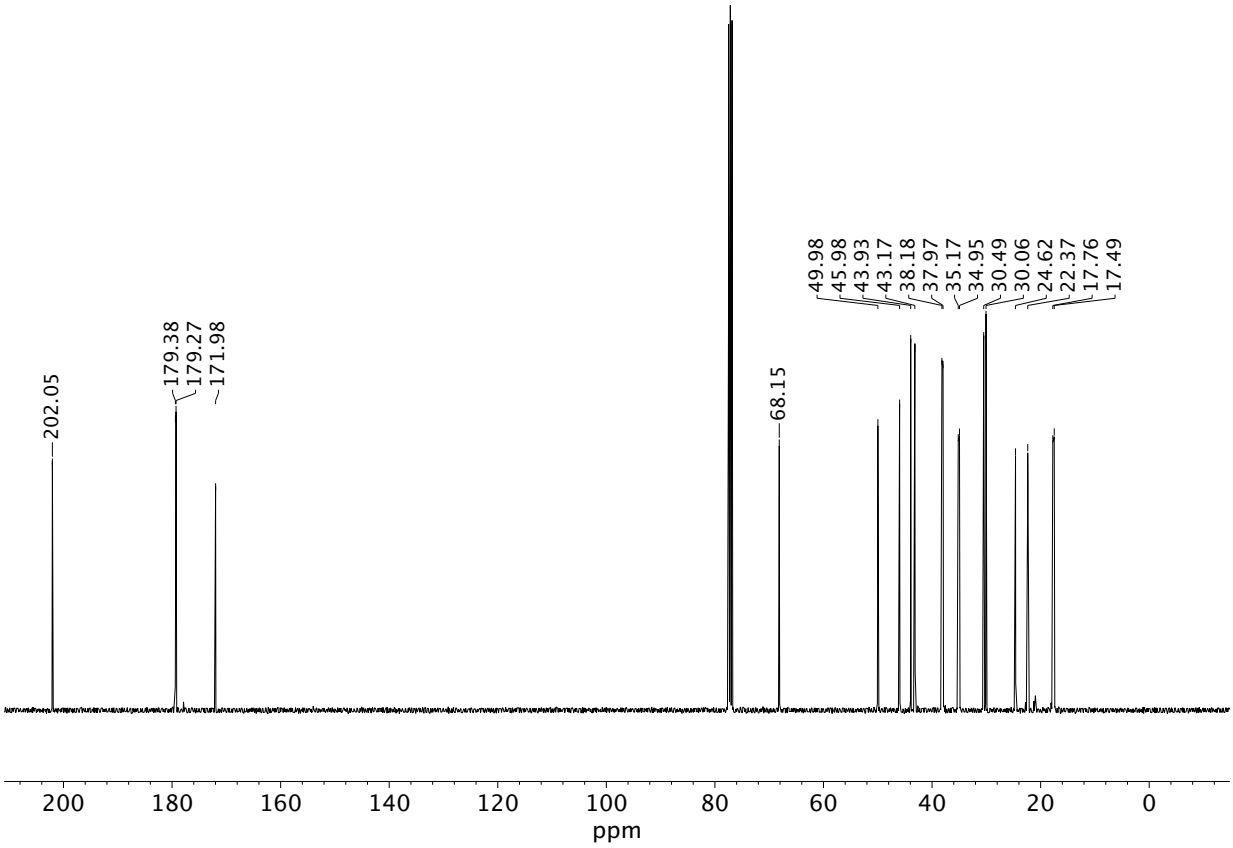

^{13}C NMR (100 MHz, $CDCl_3$) of compound **S20**.

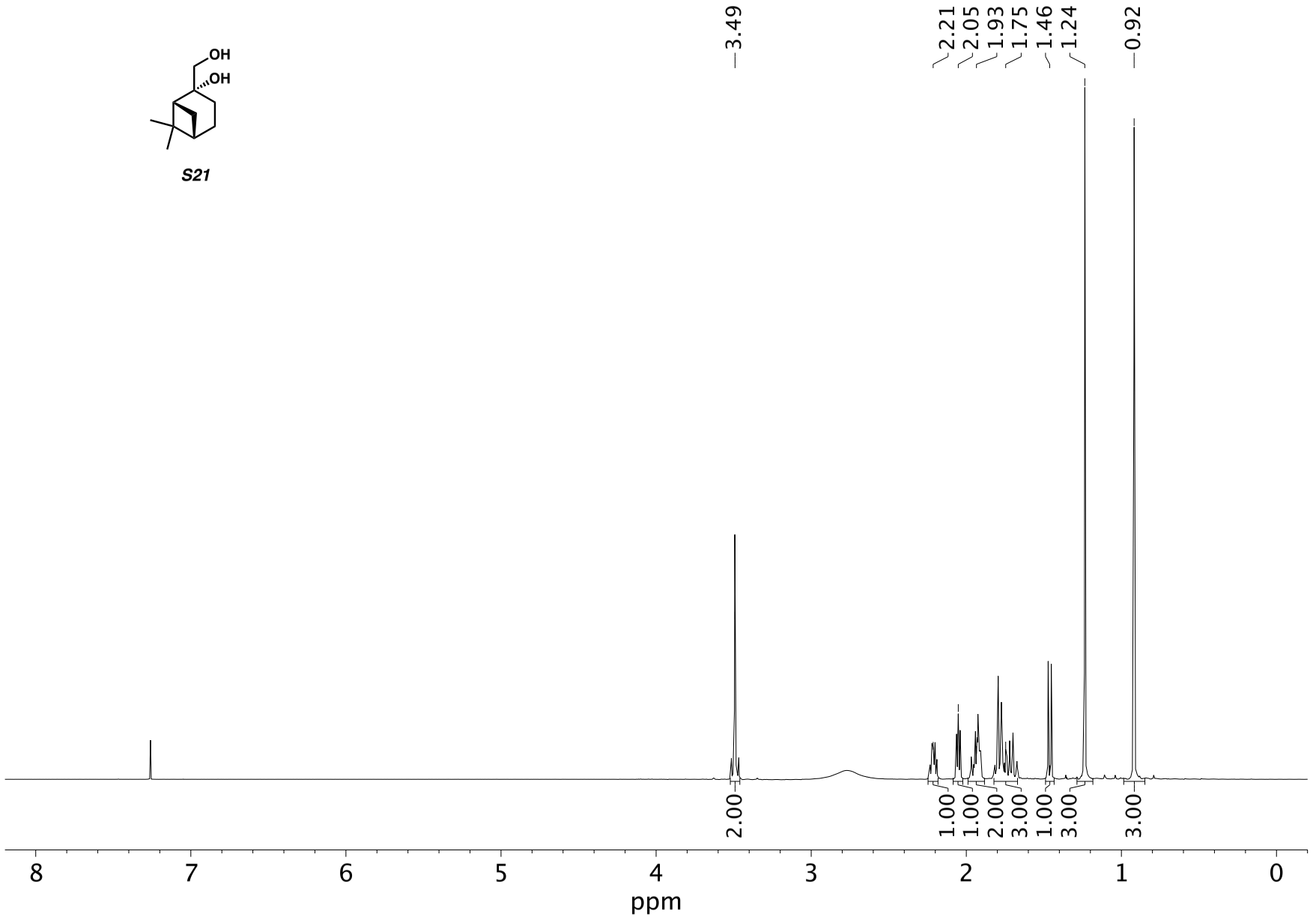

^{1}H NMR (400 MHz, $CDCl_3$) of compound **S21**.

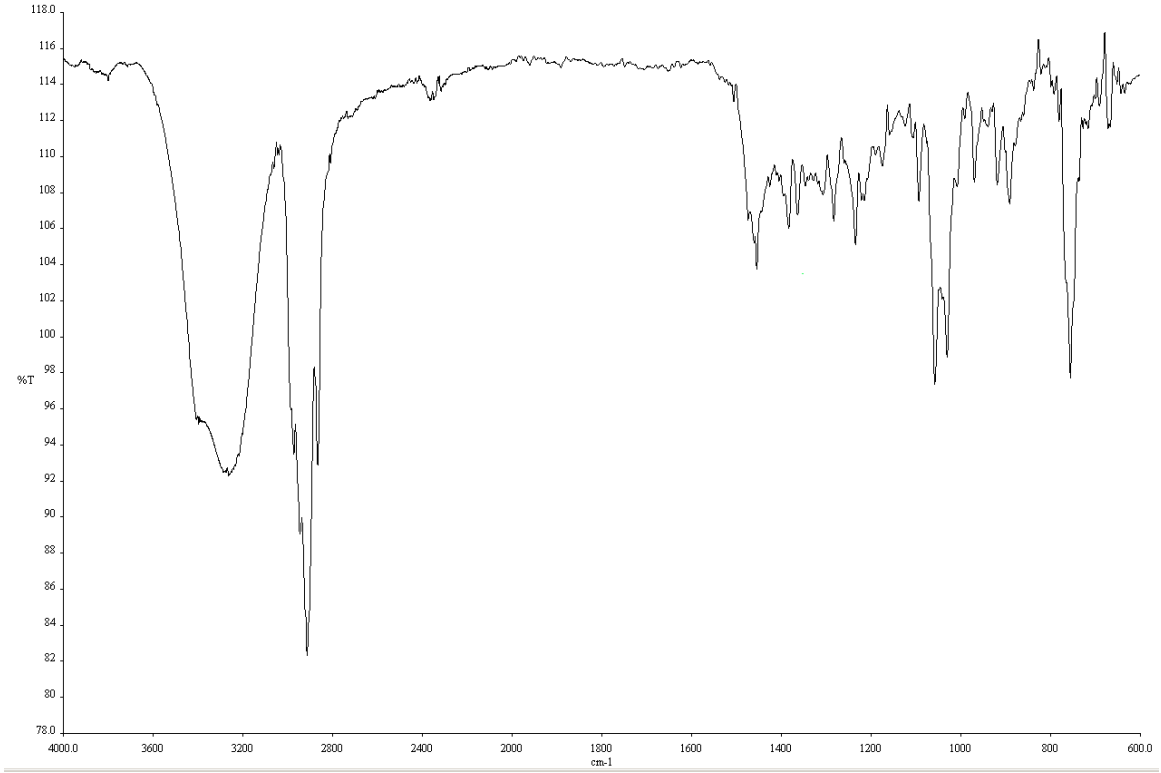

Infrared spectrum (thin film, NaCl) of compound **S21**.

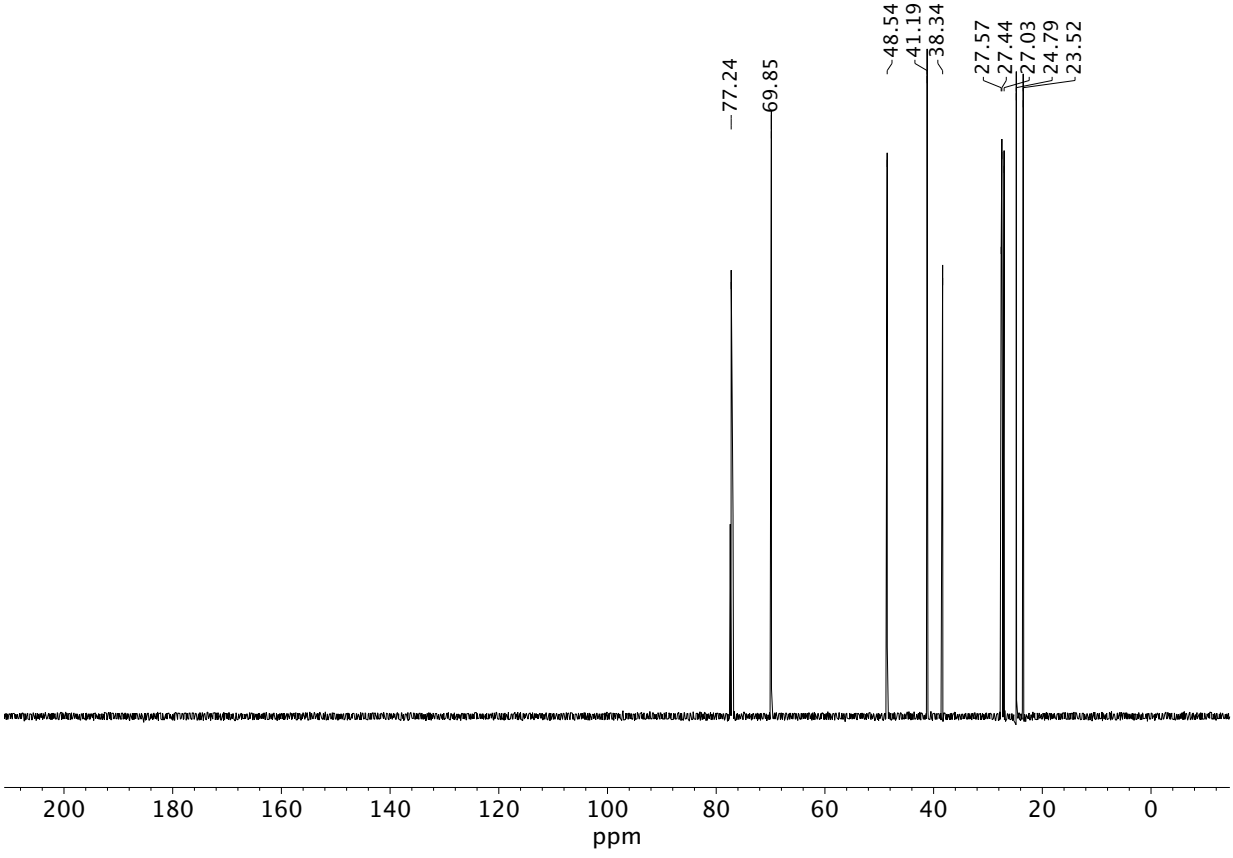

^{13}C NMR (100 MHz, $CDCl_3$) of compound **S21**.

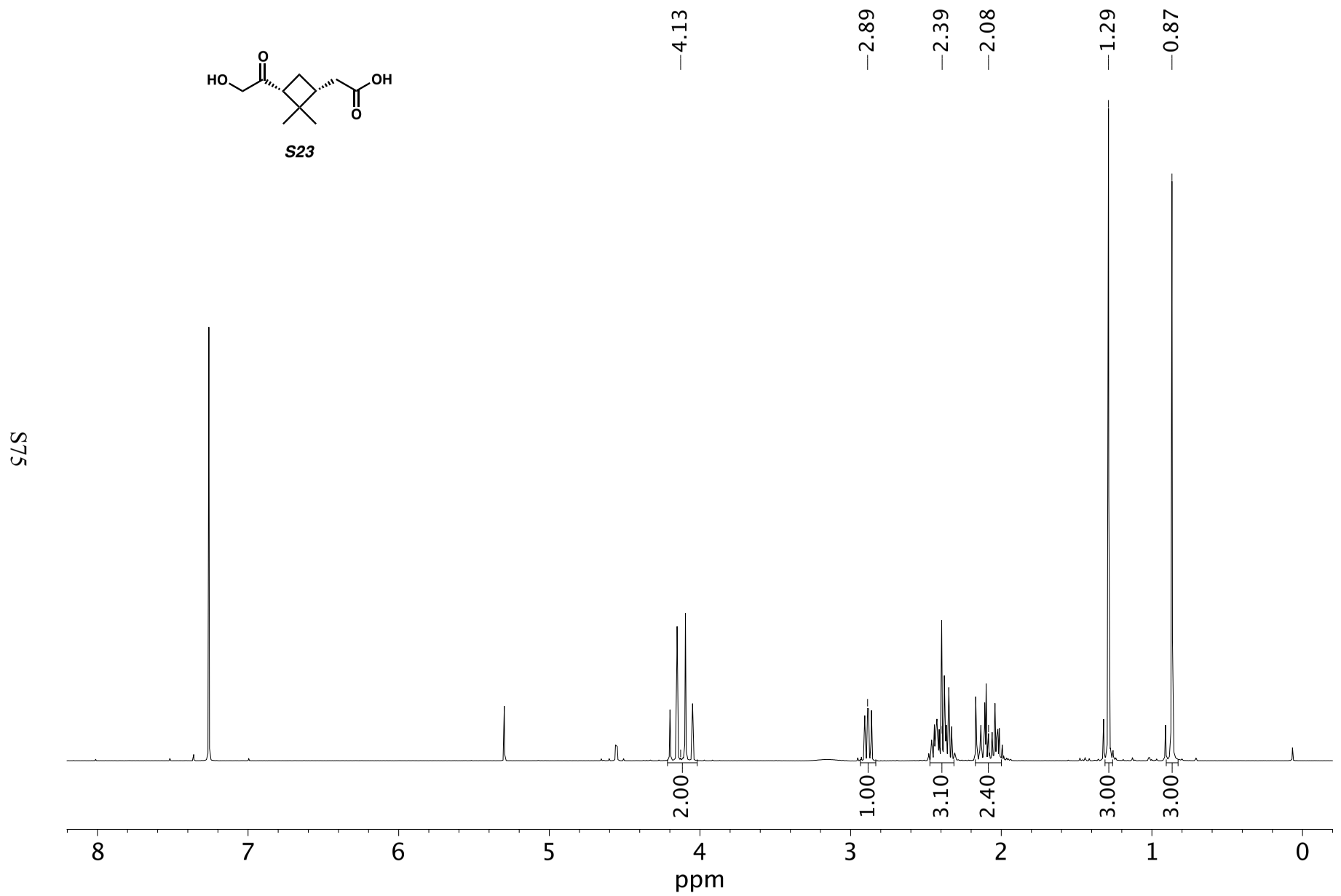

^{1}H NMR (400 MHz, $CDCl_3$) of compound **S23**.

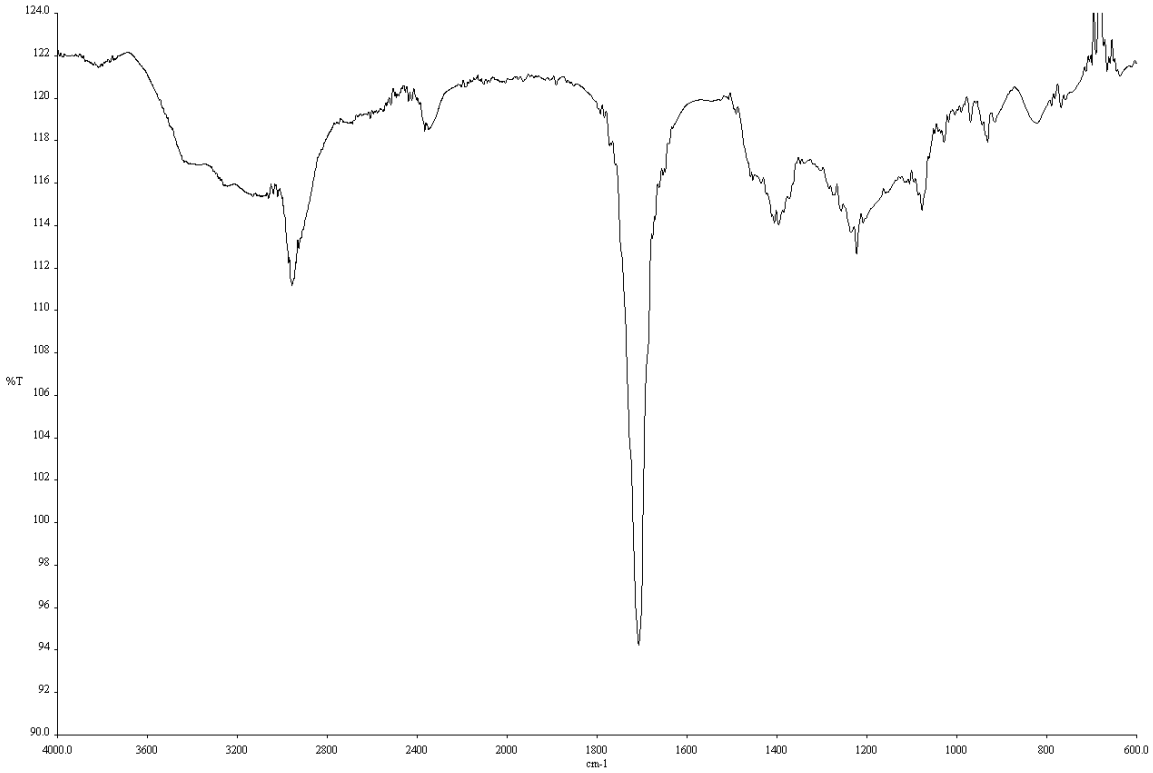

Infrared spectrum (thin film, NaCl) of compound **S23**.

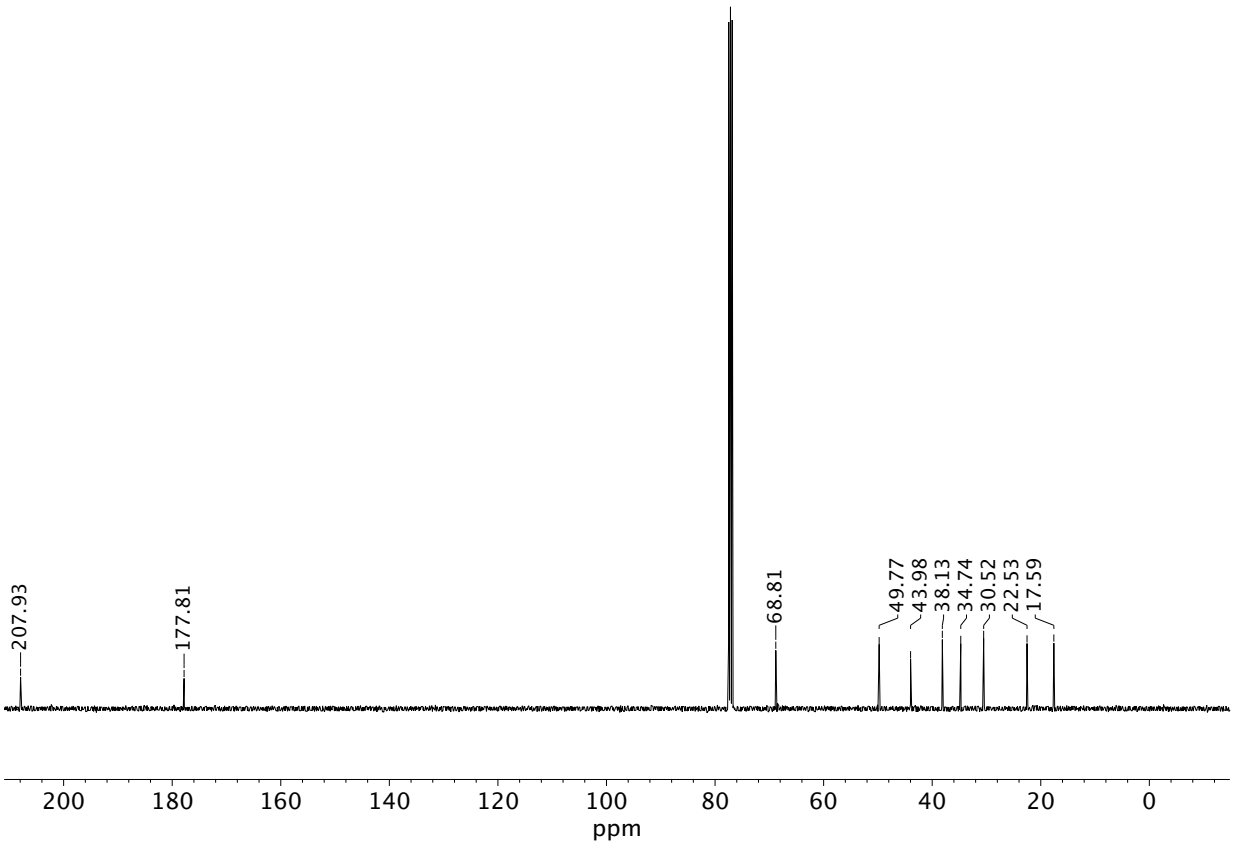

^{13}C NMR (100 MHz, $CDCl_3$) of compound **S23**.

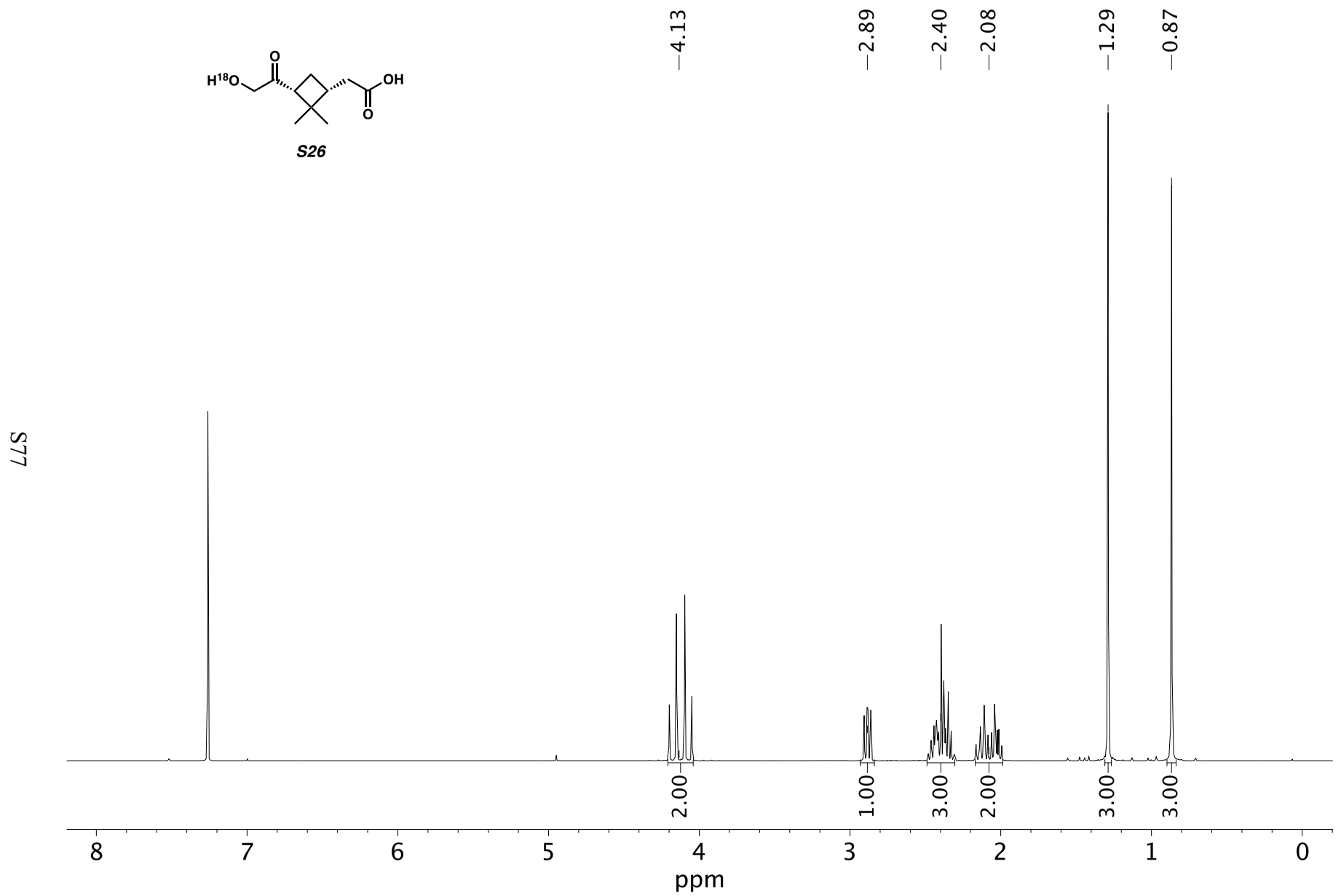

^{1}H NMR (400 MHz, $CDCl_3$) of compound **S26**.

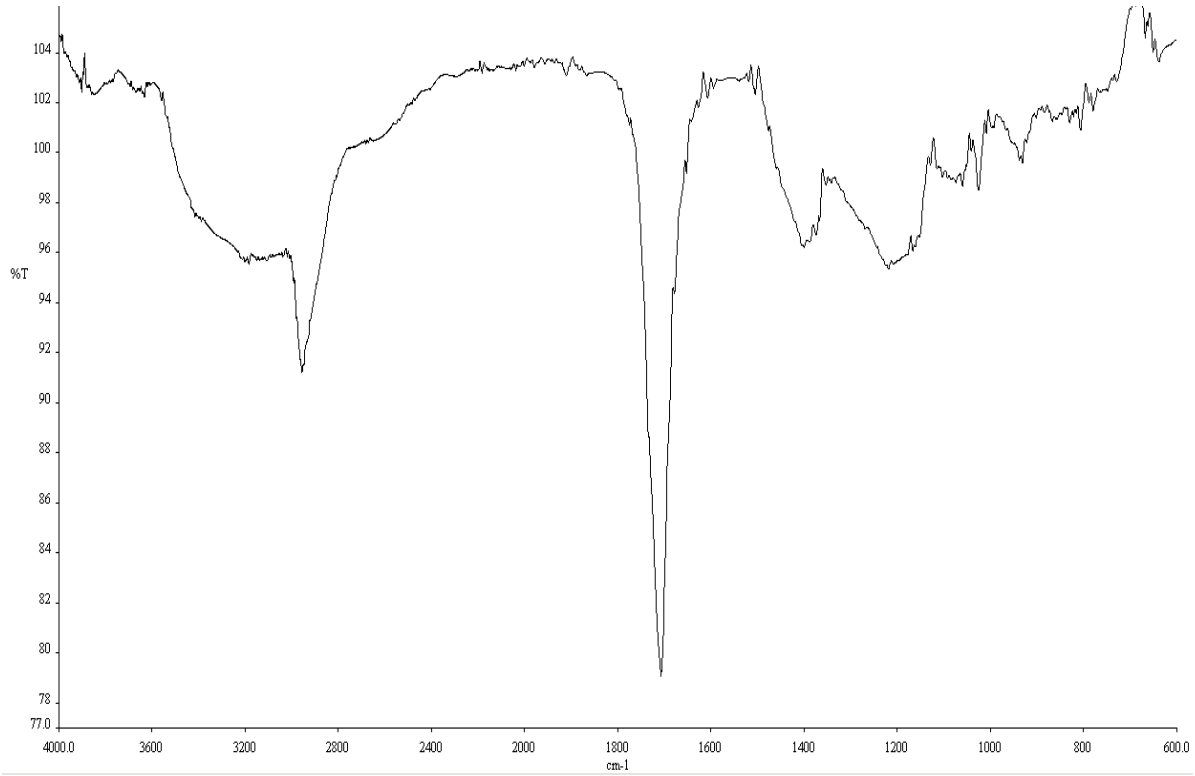

Infrared spectrum (thin film, NaCl) of compound **S26**.

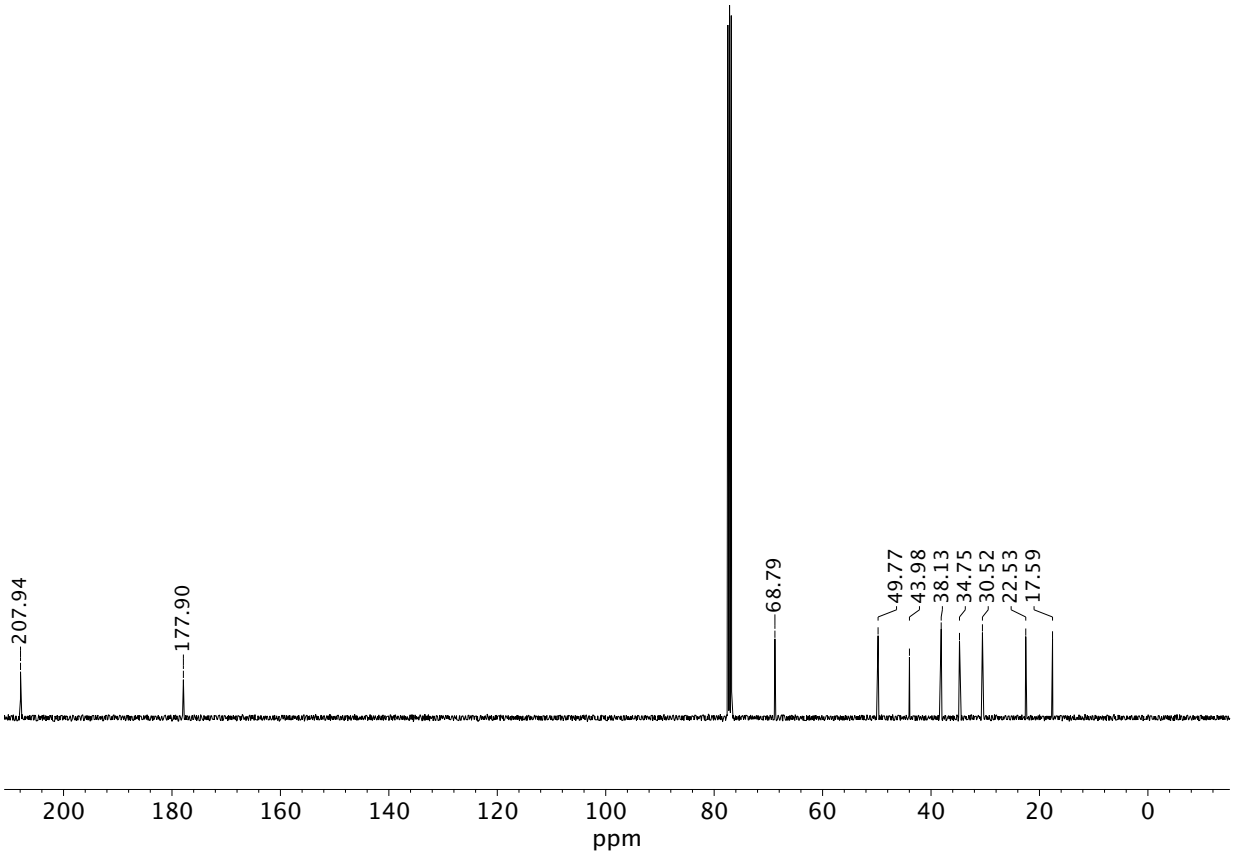

^{13}C NMR (101 MHz, $CDCl_3$) of compound **S26**.

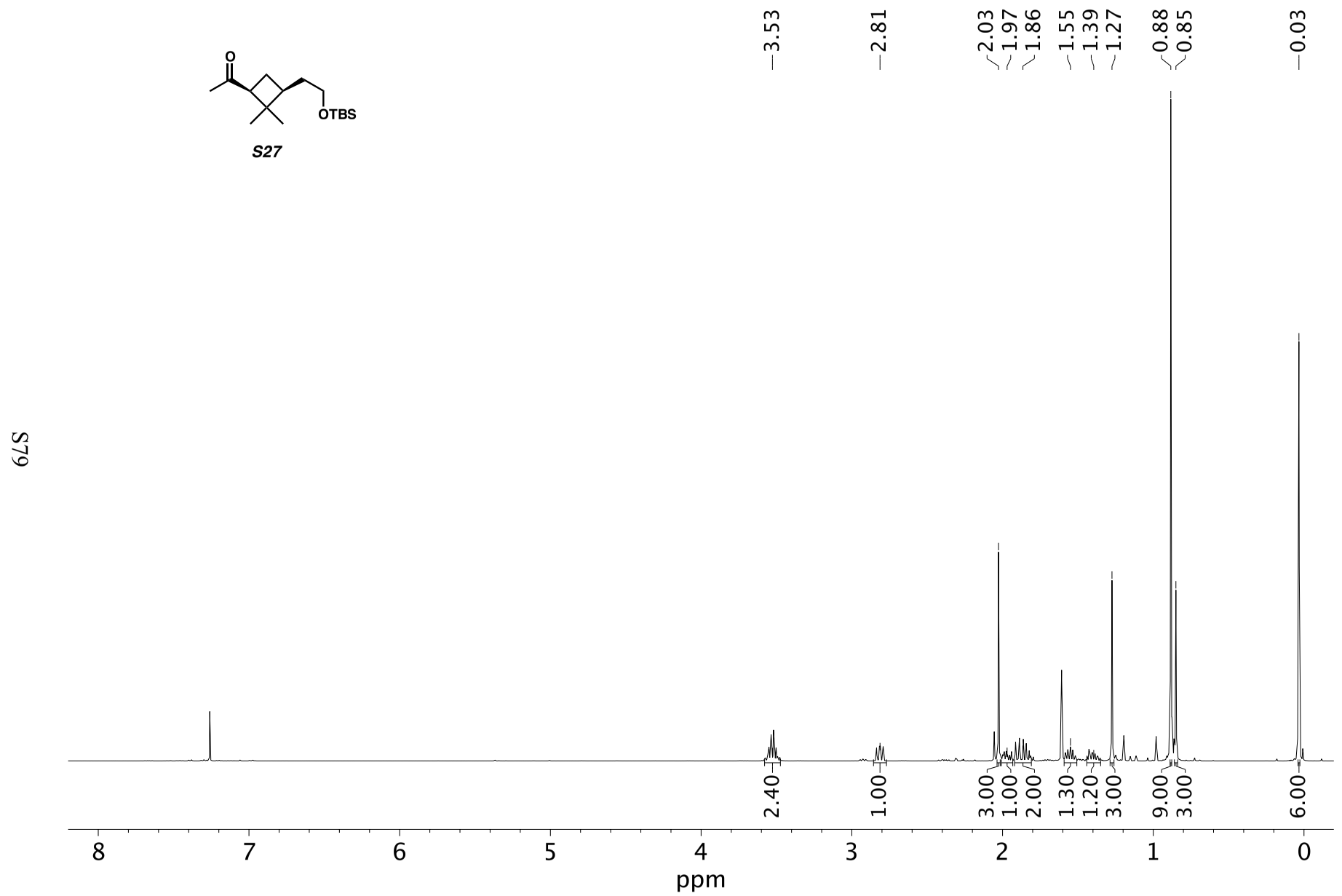

^{1}H NMR (400 MHz, $CDCl_3$) of compound **S27**.

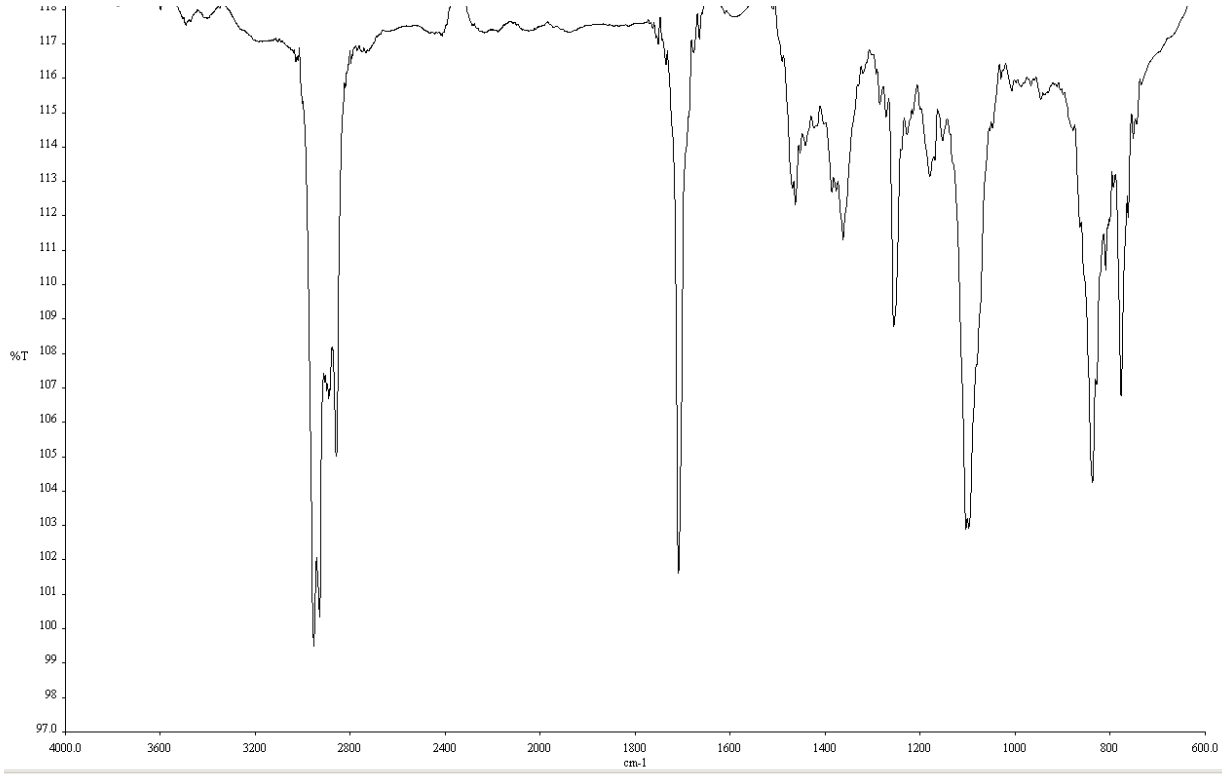

Infrared spectrum (thin film, NaCl) of compound **S27**.

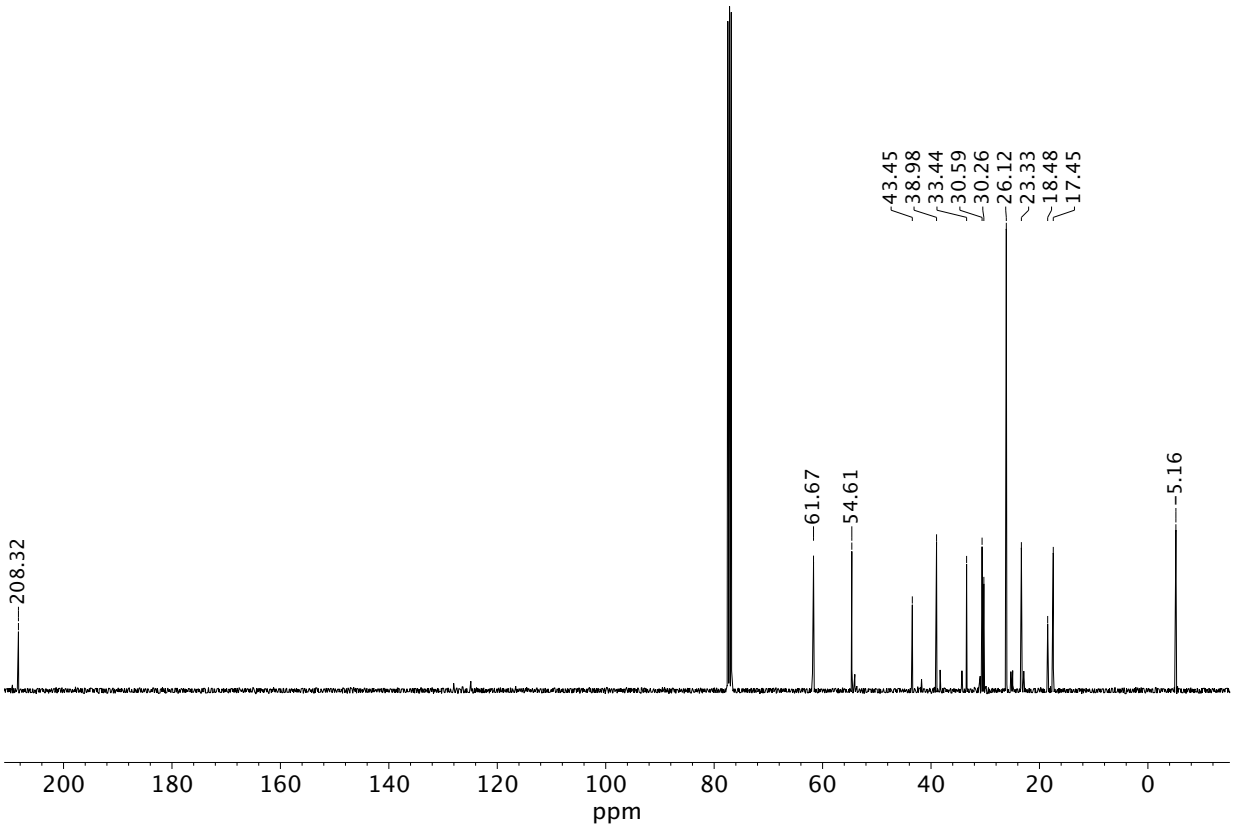

^{13}C NMR (101 MHz, $CDCl_3$) of compound **S27**.

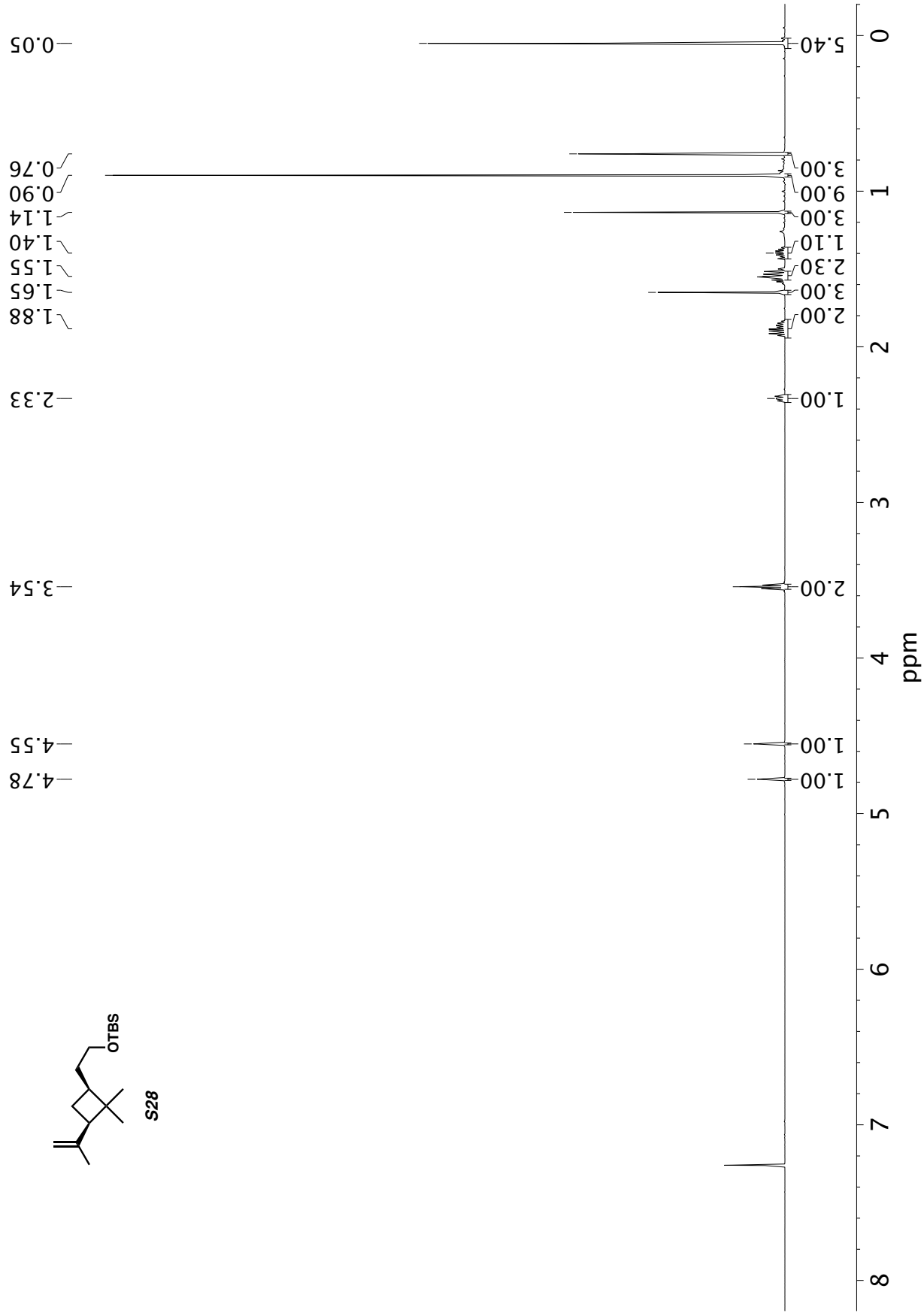

^{1}H NMR (600 MHz, $CDCl_3$) of compound **S28**.

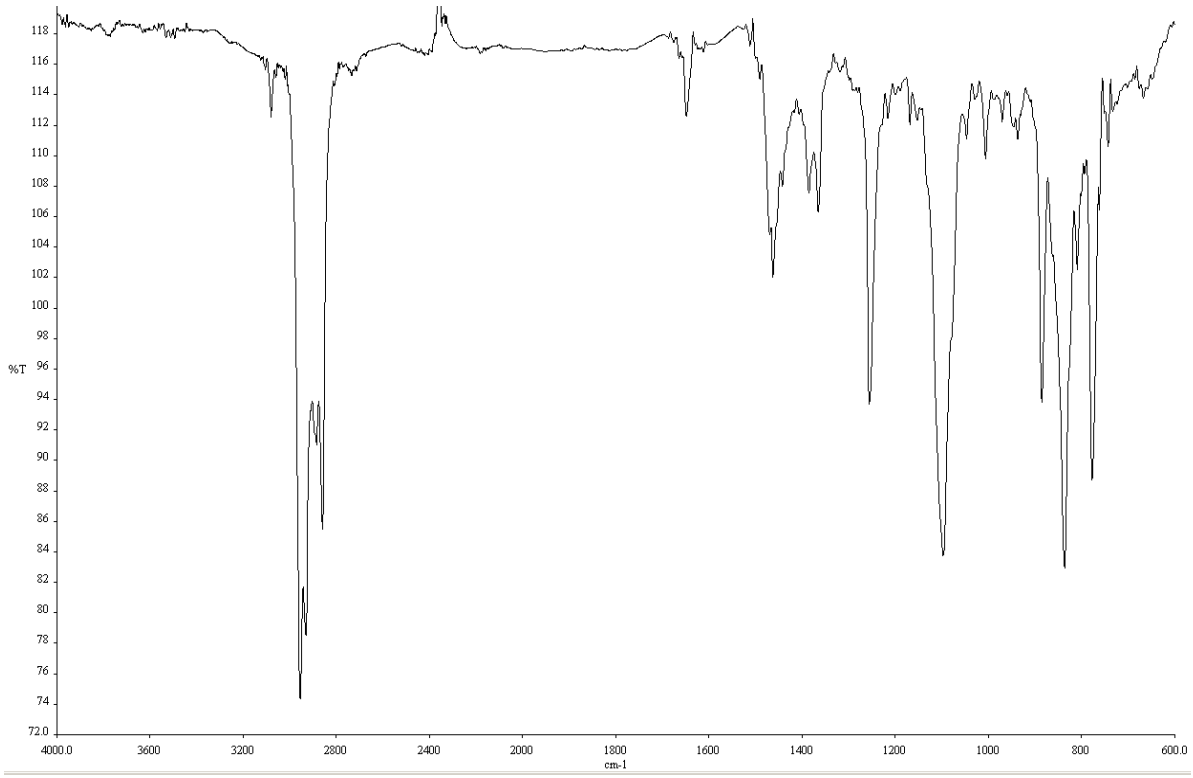

Infrared spectrum (thin film, NaCl) of compound **S28**.

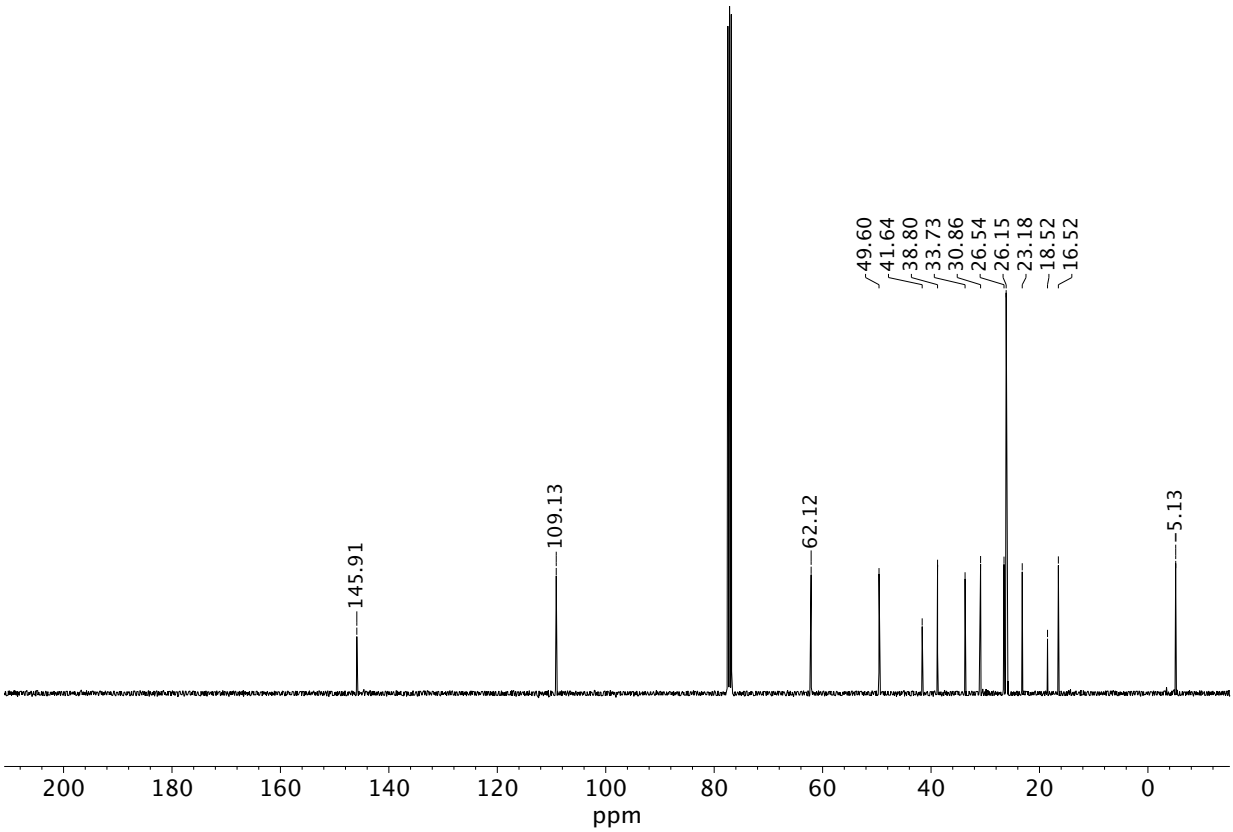

^{13}C NMR (101 MHz, $CDCl_3$) of compound **S28**.

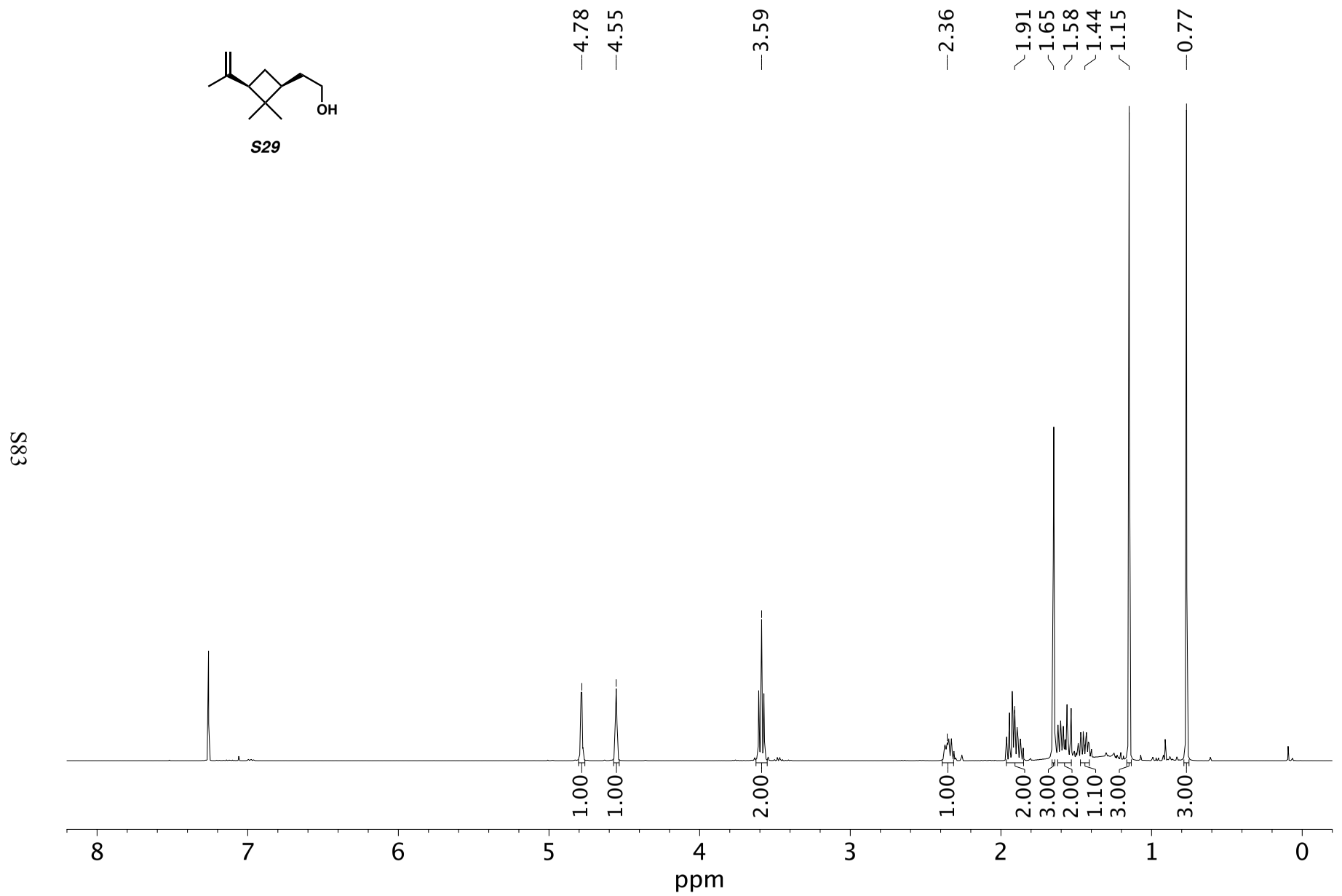

^{1}H NMR (400 MHz, $CDCl_3$) of compound **S29**.

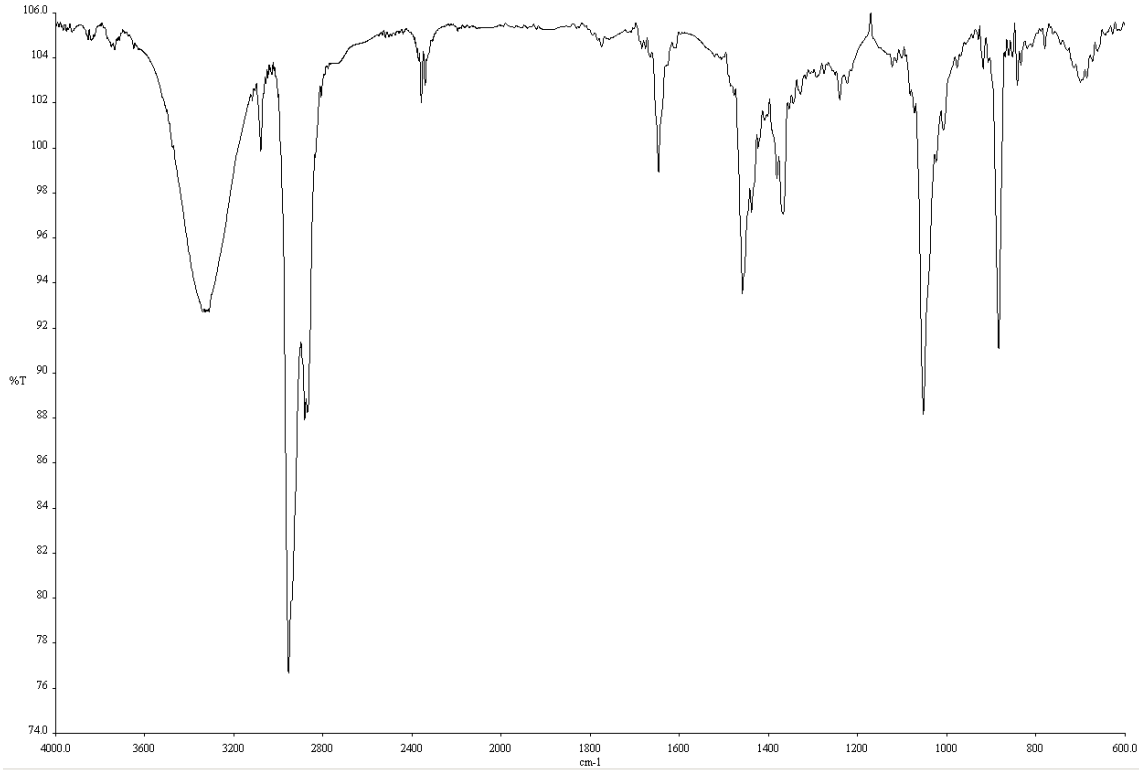

Infrared spectrum (thin film, NaCl) of compound **S29**.

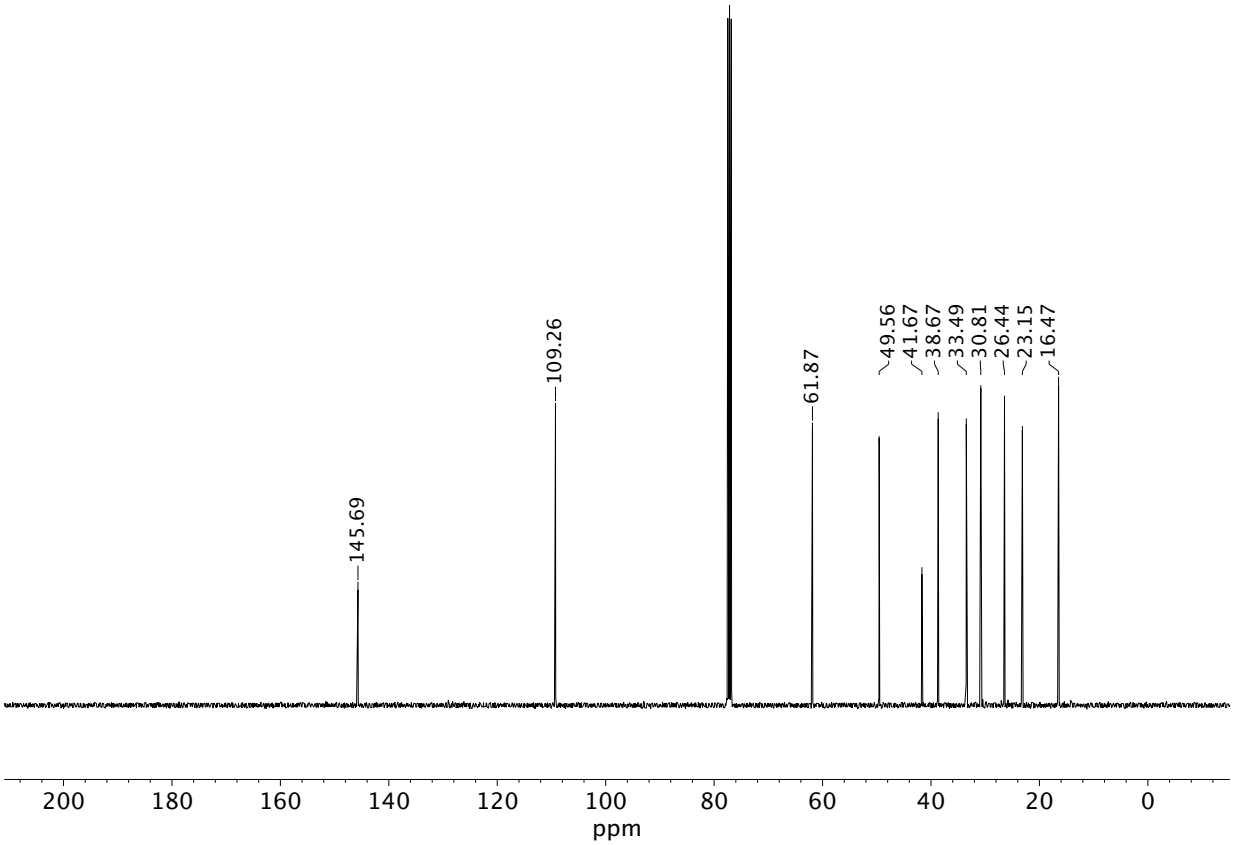

^{13}C NMR (101 MHz, $CDCl_3$) of compound **S29**.

S7. References

51. R. H. Schwantes, R. C. McVay, X. Zhang, M. M. Coggon, H. Lignell, R. C. Flagan, P. O. Wennberg, J. H. Seinfeld, "Science of the Environmental Chamber" in *Advances in Atmospheric Chemistry*, J. R. Barker, A. L. Steiner, T. J. Wallington, Eds. (World Scientific, Singapore, 2017; http://www.worldscientific.com/doi/abs/10.1142/9789813147355_0001), pp. 1–93.

52. S. M. Aschmann, J. Arey, R. Atkinson, OH radical formation from the gas-phase reactions of O_3 with a series of terpenes. *Atmos. Environ.* **36**, 4347–4355 (2002).

53. A. A. Presto, N. M. Donahue, Ozonolysis Fragment Quenching by Nitrate Formation: The Pressure Dependence of Prompt OH Radical Formation. *J. Phys. Chem. A*. **108**, 9096–9104 (2004).

54. Y. Ma, G. Marston, Multifunctional acid formation from the gas-phase ozonolysis of β-pinene. *Phys. Chem. Chem. Phys.* **10**, 6115 (2008).

55. T. L. Nguyen, J. Peeters, L. Vereecken, Theoretical study of the gas-phase ozonolysis of β-pinene ($C_{10}H_{16}$). *Phys. Chem. Chem. Phys.* **11**, 5643 (2009).

56. R. Atkinson, J. Arey, Atmospheric Degradation of Volatile Organic Compounds. *Chem. Rev.* **103**, 4605–4638 (2003).

57. E. Kwok, R. Atkinson, Estimation of hydroxyl radical reaction rate constants for gas-phase organic compounds using a structure-reactivity relationship: An update. *Atmospheric Environment*. **29**, 1685–1695 (1995).

58. J. D. Crounse, K. A. McKinney, A. J. Kwan, P. O. Wennberg, Measurement of Gas-Phase Hydroperoxides by Chemical Ionization Mass Spectrometry. *Anal. Chem.* **78**, 6726–6732 (2006).

59. J. M. St. Clair, D. C. McCabe, J. D. Crounse, U. Steiner, P. O. Wennberg, Chemical ionization tandem mass spectrometer for the *in situ* measurement of methyl hydrogen peroxide. *Review of Scientific Instruments*. **81**, 094102 (2010).

60. R. H. Schwantes, S. M. Charan, K. H. Bates, Y. Huang, T. B. Nguyen, H. Mai, W. Kong, R. C. Flagan, J. H. Seinfeld, Low-volatility compounds contribute significantly to isoprene secondary organic aerosol (SOA) under high-NO_x conditions. *Atmos. Chem. Phys.* **19**, 7255–7278 (2019).

61. R. Bahreini, M. D. Keywood, N. L. Ng, V. Varutbangkul, S. Gao, R. C. Flagan, J. H. Seinfeld, D. R. Worsnop, J. L. Jimenez, Measurements of Secondary Organic Aerosol from Oxidation of Cycloalkenes, Terpenes, and *m*-Xylene Using an Aerodyne Aerosol Mass Spectrometer. *Environ. Sci. Technol.* **39**, 5674–5688 (2005).

62. Q. G. J. Malloy, S. Nakao, L. Qi, R. Austin, C. Stothers, H. Hagino, D. R. Cocker, Real-Time Aerosol Density Determination Utilizing a Modified Scanning Mobility Particle Sizer—Aerosol Particle Mass Analyzer System. *Aerosol Sci. Technol.* **43**, 673–678 (2009).

63. J. E. Shilling, Q. Chen, S. M. King, T. Rosenoern, J. H. Kroll, D. R. Worsnop, P. F. DeCarlo, A. C. Aiken, D. Sueper, J. L. Jimenez, S. T. Martin, Loading-dependent elemental composition of α-pinene SOA particles. *Atmos. Chem. Phys.* **9**, 771–782 (2009).

64. H. Saathoff, K.-H. Naumann, O. Möhler, Å. M. Jonsson, M. Hallquist, A. Kiendler-Scharr, Th. F. Mentel, R. Tillmann, U. Schurath, Temperature dependence of yields of secondary organic aerosols from the ozonolysis of α-pinene and limonene. *Atmos. Chem. Phys.* **9**, 1551–1577 (2009).

65. P. Mikuška, Z. Večeřa, A. Bartošíková, W. Maenhaut, Annular diffusion denuder for simultaneous removal of gaseous organic compounds and air oxidants during sampling of carbonaceous aerosols. *Anal. Chim. Acta*. **714**, 68–75 (2012).

66. A. Mutzel, M. Rodigast, Y. Iinuma, O. Böge, H. Herrmann, An improved method for the quantification of SOA bound peroxides. *Atmos. Environ.* **67**, 365–369 (2013).

67. K. H. Møller, R. V. Otkjær, N. Hyttinen, T. Kurtén, H. G. Kjaergaard, Cost-Effective Implementation of Multiconformer Transition State Theory for Peroxy Radical Hydrogen Shift Reactions. *J. Phys. Chem. A*. **120**, 10072–10087 (2016).

68. T. A. Halgren, R. B. Nachbar, Merck molecular force field. IV. conformational energies and geometries for MMFF94. *J. Comput. Chem.* **17**, 587–615 (1996).

69. T. A. Halgren, Merck molecular force field. V. Extension of MMFF94 using experimental data, additional computational data, and empirical rules. *J. Comput. Chem.* **17**, 616–641 (1996).

70. Spartan'18 (2018), (available at https://www.wavefun.com/spartan).

71. M. J. Frisch, G. W. Trucks, H. B. Schlegel, G. E. Scuseria, M. A. Robb, J. R. Cheeseman, G. Scalmani, V. Barone, G. A. Petersson, H. Nakatsuji, X. Li, M. Caricato, A. V. Marenich, J. Bloino, B. G. Janesko, R. Gomperts, B. Mennucci, H. P. Hratchian, J. V. Ortiz, A. F. Izmaylov, J. L. Sonnenberg, Williams, F. Ding, F. Lipparini, F. Egidi, J. Goings, B. Peng, A. Petrone, T. Henderson, D. Ranasinghe, V. G. Zakrzewski, J. Gao, N. Rega, G. Zheng, W. Liang, M. Hada, M. Ehara, K. Toyota, R. Fukuda, J. Hasegawa, M. Ishida, T. Nakajima, Y. Honda, O. Kitao, H. Nakai, T. Vreven, K. Throssell, J. A. Montgomery Jr., J. E. Peralta, F. Ogliaro, M. J. Bearpark, J. J. Heyd, E. N. Brothers, K. N. Kudin, V. N. Staroverov, T. A. Keith, R. Kobayashi, J. Normand, K. Raghavachari, A. P. Rendell, J. C. Burant, S. S. Iyengar, J. Tomasi, M. Cossi, J. M. Millam, M. Klene, C. Adamo, R. Cammi, J. W. Ochterski, R. L. Martin, K. Morokuma, O. Farkas, J. B. Foresman, D. J. Fox, Gaussian 16 Rev. C.01 (2016).

72. A. J. Stone, Distributed multipole analysis, or how to describe a molecular charge distribution. *Chemical Physics Letters*. **83**, 233–239 (1981).

73. C. M. Breneman, K. B. Wiberg, Determining atom-centered monopoles from molecular electrostatic potentials. The need for high sampling density in formamide conformational analysis. *J. Comput. Chem.* **11**, 361–373 (1990).

74. T. Lu, F. Chen, Multiwfn: A multifunctional wavefunction analyzer. *J. Comput. Chem.* **33**, 580–592 (2012).

75. K. Fukui, The path of chemical reactions - the IRC approach. *Acc. Chem. Res.* **14**, 363–368 (1981).

76. S. M. Saunders, M. E. Jenkin, R. G. Derwent, M. J. Pilling, Protocol for the development of the Master Chemical Mechanism, MCM v3 (Part A): tropospheric degradation of non-aromatic volatile organic compounds. *Atmos. Chem. Phys.* **3**, 161–180 (2003).

77. L. Vereecken, J. Peeters, A theoretical study of the OH-initiated gas-phase oxidation mechanism of β-pinene ($C_{10}H_{16}$): first generation products. *Phys. Chem. Chem. Phys.* **14**, 3802 (2012).

78. J. Peeters, L. Vereecken, G. Fantechi, The detailed mechanism of the OH-initiated atmospheric oxidation of α-pinene: a theoretical study. *Phys. Chem. Chem. Phys.* **3**, 5489–5504 (2001).

79. M. S. Claflin, J. E. Krechmer, W. Hu, J. L. Jimenez, P. J. Ziemann, Functional Group Composition of Secondary Organic Aerosol Formed from Ozonolysis of α-Pinene Under High VOC and Autoxidation Conditions. *ACS Earth Space Chem.* **2**, 1196–1210 (2018).

80. L. Renbaum-Wolff, J. W. Grayson, A. P. Bateman, M. Kuwata, M. Sellier, B. J. Murray, J. E. Shilling, S. T. Martin, A. K. Bertram, Viscosity of *α*-pinene secondary organic material and implications for particle growth and reactivity. *Proc. Natl. Acad. Sci. U.S.A.* **110**, 8014–8019 (2013).

81. C. Kidd, V. Perraud, L. M. Wingen, B. J. Finlayson-Pitts, Integrating phase and composition of secondary organic aerosol from the ozonolysis of α-pinene. *Proc. Natl. Acad. Sci. U.S.A.* **111**, 7552–7557 (2014).

82. D. Thomsen, J. Elm, B. Rosati, J. T. Skønager, M. Bilde, M. Glasius, Large Discrepancy in the Formation of Secondary Organic Aerosols from Structurally Similar Monoterpenes. *ACS Earth Space Chem.* **5**, 632–644 (2021).

83. J. F. Hamilton, A. C. Lewis, J. C. Reynolds, L. J. Carpenter, A. Lubben, Investigating the composition of organic aerosol resulting from cyclohexene ozonolysis: low molecular weight and heterogeneous reaction products. *Atmos. Chem. Phys.* **6**, 4973–4984 (2006).

84. L. Xu, K. H. Møller, J. D. Crounse, R. V. Otkjær, H. G. Kjaergaard, P. O. Wennberg, Unimolecular Reactions of Peroxy Radicals Formed in the Oxidation of α-Pinene and β-Pinene by Hydroxyl Radicals. *J. Phys. Chem. A*. **123**, 1661–1674 (2019).

85. L. Müller, M.-C. Reinnig, K. H. Naumann, H. Saathoff, T. F. Mentel, N. M. Donahue, T. Hoffmann, Formation of 3-methyl-1,2,3-butanetricarboxylic acid via gas phase oxidation of pinonic acid – a mass spectrometric study of SOA aging. *Atmos. Chem. Phys.* **12**, 1483–1496 (2012).

86. S. Compernolle, K. Ceulemans, J.-F. Müller, EVAPORATION: a new vapour pressure estimation methodfor organic molecules including non-additivity and intramolecular interactions. *Atmos. Chem. Phys.* **11**, 9431–9450 (2011).

87. J. H. Kroll, J. H. Seinfeld, Chemistry of secondary organic aerosol: Formation and evolution of low-volatility organics in the atmosphere. *Atmospheric Environment*. **42**, 3593–3624 (2008).

88. Y. Ma, T. R. Willcox, A. T. Russell, G. Marston, Pinic and pinonic acid formation in the reaction of ozone with α-pinene. *Chem. Commun.*, 1328–1330 (2007).

89. Y. Ma, A. T. Russell, G. Marston, Mechanisms for the formation of secondary organic aerosol components from the gas-phase ozonolysis of α-pinene. *Phys. Chem. Chem. Phys.* **10**, 4294 (2008).

90. M. E. Jenkin, D. E. Shallcross, J. N. Harvey, Development and application of a possible mechanism for the generation of cis-pinic acid from the ozonolysis of α- and β-pinene. *Atmos. Environ.* **34**, 2837–2850 (2000).

91. S. Koch, R. Winterhalter, E. Uherek, A. Kolloff, P. Neeb, G. K. Moortgat, Formation of new particles in the gas-phase ozonolysis of monoterpenes. *Atmospheric Environment*. **34**, 4031–4042 (2000).

92. A. D. Castañeda, Z. Li, T. Joo, K. Benham, B. T. Burcar, R. Krishnamurthy, C. L. Liotta, N. L. Ng, T. M. Orlando, Prebiotic Phosphorylation of Uridine using Diamidophosphate in Aerosols. *Sci Rep*. **9**, 13527 (2019).

93. A. Bellcross, A. G. Bé, F. M. Geiger, R. J. Thomson, Molecular Chirality and Cloud Activation Potentials of Dimeric α-Pinene Oxidation Products. *J. Am. Chem. Soc.* **143**, 16653–16662 (2021).

94. Z. Zhao, W. Zhang, T. Alexander, X. Zhang, D. B. C. Martin, H. Zhang, Isolating α-Pinene Ozonolysis Pathways Reveals New Insights into Peroxy Radical Chemistry and Secondary Organic Aerosol Formation. *Environ. Sci. Technol.* **55**, 6700–6709 (2021).

95. K. S. Docherty, W. Wu, Y. B. Lim, P. J. Ziemann, Contributions of Organic Peroxides to Secondary Aerosol Formed from Reactions of Monoterpenes with O_3. *Environ. Sci. Technol.* **39**, 4049–4059 (2005).

96. G. McFiggans, T. F. Mentel, J. Wildt, I. Pullinen, S. Kang, E. Kleist, S. Schmitt, M. Springer, R. Tillmann, C. Wu, D. Zhao, M. Hallquist, C. Faxon, M. Le Breton, Å. M. Hallquist, D. Simpson, R. Bergström, M. E. Jenkin, M. Ehn, J. A. Thornton, M. R. Alfarra, T. J. Bannan, C. J. Percival, M. Priestley, D. Topping, A. Kiendler-Scharr, Secondary organic aerosol reduced by mixture of atmospheric vapours. *Nature*. **565**, 587–593 (2019).

97. J. N. Moorthy, N. Singhal, K. Senapati, Oxidative cleavage of vicinal diols: IBX can do what Dess–Martin periodinane (DMP) can. *Org. Biomol. Chem.* **5**, 767–771 (2007).

98. M. Gomes, O. A. C. Antunes, Upjohn catalytic osmium tetroxide oxidation process: Diastereoselective dihydroxylation of monoterpenes. *Catalysis Communications*. **2**, 225–227 (2001).

99. C. Samorì, H. Ali-Boucetta, R. Sainz, C. Guo, F. M. Toma, C. Fabbro, T. da Ros, M. Prato, K. Kostarelos, A. Bianco, Enhanced anticancer activity of multi-walled carbon nanotube–methotrexate conjugates using cleavable linkers. *Chem. Commun.* **46**, 1494–1496 (2010).

100. H.-X. Liu, H.-B. Tan, M.-T. He, L. Li, Y.-H. Wang, C.-L. Long, Isolation and synthesis of two hydroxychavicol heterodimers from Piper nudibaccatum. *Tetrahedron*. **71**, 2369–2375 (2015).

101. F. Fache, O. Piva, P. Mirabel, First synthesis of hydroxy-pinonaldehyde and hydroxy-pinonic acid, monoterpene degradation products present in atmosphere. *Tetrahedron Letters*. **43**, 2511–2513 (2002).

102. P. A. Procopiou, S. P. D. Baugh, S. S. Flack, G. G. A. Inglis, An Extremely Powerful Acylation Reaction of Alcohols with Acid Anhydrides Catalyzed by Trimethylsilyl Trifluoromethanesulfonate. *J. Org. Chem.* **63**, 2342–2347 (1998).

103. R. H. Beddoe, D. C. Edwards, L. Goodman, H. F. Sneddon, R. M. Denton, Synthesis of ^{18}O-labelled alcohols from unlabelled alcohols. *Chem. Commun.* **56**, 6480–6483 (2020).

104. S. S. Steimer, A. Delvaux, S. J. Campbell, P. J. Gallimore, P. Grice, D. J. Howe, D. Pitton, M. Claeys, T. Hoffmann, M. Kalberer, Synthesis and characterisation of peroxypinic acids as proxies for highly oxygenated molecules (HOMs) in secondary organic aerosol. *Atmos. Chem. Phys.* **18**, 10973–10983 (2018).